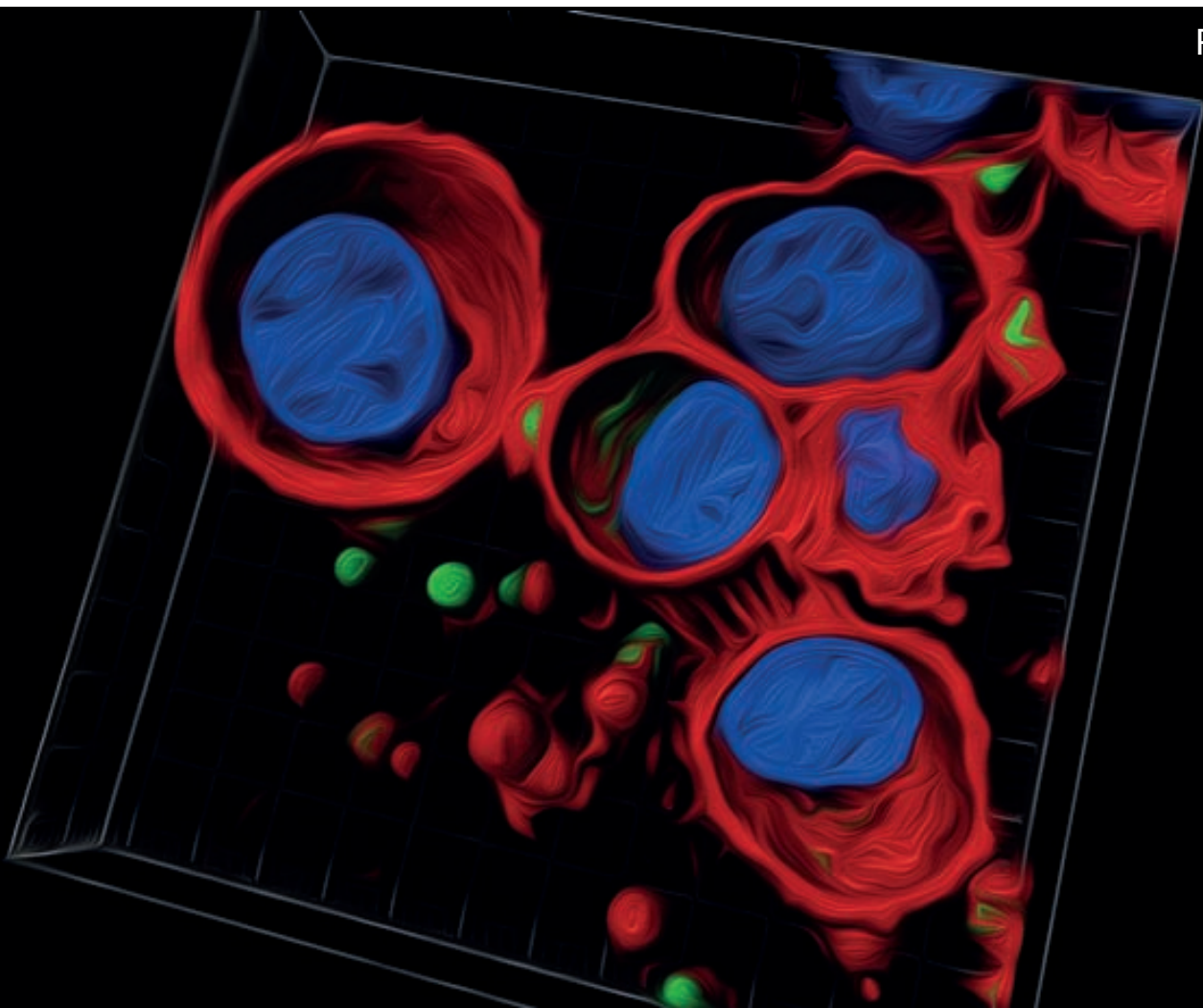


De novo design of self-assembling protein nanoparticles towards the gene therapy of colorectal cancer

Ugutzu Unzueta Elorza

PhD Thesis
2013



Programa de doctorat en Biotecnologia

De novo design of self-assembling protein nanoparticles towards the gene therapy of colorectal cancer

Tesi doctoral

2013

Departament de Genètica i Microbiologia

Facultat de Biociències



**Memòria presentada per Ugutz Unzueta Elorza
per optar al grau de doctor en Biotecnologia
per la Universitat Autònoma de Barcelona.**

Ugutz Unzueta Elorza

Vist i plau dels directors de la tesi:

Antonio Villaverde Corrales

Esther Vázquez Gómez

Neus Ferrer Miralles

Aquest treball ha estat realitzat principalment a l'Institut de Biotecnologia i de Biomedicina, Vicent Villar i Palasí, sota la direcció dels doctors/es: Antonio Villaverde Corrales, Esther Vázquez Gómez i Neus Ferrer Miralles. Una part però ha estat duta a terme a la Universitat degli studi di Napoli Federico II sota la supervisió de la doctora Maria Luisa Tutino.



Contents

Contents

Contents	1
Introduction	5
1. Cancer	8
1.1 Colorectal cancer	10
2. Nanoparticles in the context of nanomedicine	12
2.1 Targeted nanoparticles.....	13
2.2 Physico-Chemical properties (size).....	14
2.3 Current state of nanoparticles in medicine	18
2.4 Controlling nanoparticle size	21
2.5 Biocompatibility	22
2.6 Protein nanoparticles	24
3. Gene therapy	29
3.1 Gene therapy approaches in cancer.....	30
3.2 Gene therapy vectors	32
3.3 Protein-only gene therapy vectors	35
4. Protein-only gene therapy in colorectal cancer	36
4.1 CXCR4 receptor	36
4.2 Target genes in colorectal cancer	39
5. Overview	41
Objectives	43
Results	47
Paper 1.....	49
Paper 2.....	61
Paper 3.....	71
Discussion	93
1. Construction and intracellular trafficking of self-assembling protein nanoparticles.	95
2. <i>In vivo</i> biodistribution and stability of cell-targeted, self-assembling protein nanoparticles.	99
3. Self-assembling protein nanoparticles towards the gene therapy in colorectal cancer.	103

Contents

Conclusions	109
Annex	113
Annex 1 (Manuscript 1)	115
Annex 2 (Manuscript 2)	137
Annex 3 (Manuscript 3)	157
Annex 4 (Reference 370)	175
Annex 5 (European patent)	187
Annex 6 (Reference 177)	191
Annex 7 (Other publications)	209
References	211
Acknowledgements	239



Introduction

Human health is a permanent matter of concern of mankind during all its history. Thousands of years ago, in the prehistoric era, humans already used plants, animal body parts or minerals in order to treat diseases. However, Hippocrates is considered the father of medicine since he established it as a profession for the first time and introduced the rational approach on medicine declaring that diseases are something natural and not divine¹.

The modern medicine began at the end of the 18th century when Edward Jenner developed the first vaccine to protect people against the smallpox virus and Robert Koch postulated the relationships between some diseases and microorganisms². After that, medicine has progressed so fast leading to really great medical advances. Some of the most relevant events in human history that has led to current medical level have been microbiology studies and bacterial vaccine development by Louis Pasteur³, discovery of penicillin by Alexander Fleming⁴, discovery of the DNA structure by Watson and Crick⁵ and subsequent DNA recombinant technologies development in the late 20th century⁶ among others.

Furthermore, apart from that significant medical progress, development of new technologies such as Nanotechnology at the end of the 20th century has led to the huge development of new scientific disciplines as modern Biotechnology and nanomedicine. Nanomedicine is a recent biomedical field that has appeared as a consequence of the application of the nanotechnologies in medicine. Nanotechnology can offer an enormous range of nanomaterials or molecular tools for diagnosis and therapy.

Even though modern medicine has achieved stellar successes over the last few years, some important milestones have been elusive. For instance, current medicine needs to make drugs more efficient in order to reduce therapeutic doses and associated toxicity. Thus, one of the biggest challenges of the current medicine is targeted drug delivery of conventional and innovative drugs, including nucleic acids for which nanomedicine offers promise. In addition, nanomedicine has also many other applications apart of this mentioned above. For example, Quantum dots have been recently developed for nanoscale cell imaging and cellular tracking and gold coated nanoshells have been also used for nanoparticle-mediated laser surgery^{7, 8}. Moreover it has become a very promising approach for the diagnose and treatment of many molecular diseases as cancer among others⁹.

1. Cancer

Cancer is a somatic genetic disease generated by a stepwise acquisition of genetic mutations at multiple sites during usually long periods of time. Those mutations confer growing advantages over normal cells by the loss of the cell cycle control that make those cells grow without control, converting the normal tissue into clinically detectable lesions¹⁰.

The transformation of normal cells into malignant cancer cells is usually driven by the activation of dominant oncogenes or the loss of recessive tumor suppressor gene functions¹¹. In this multistep process, in which the mutation progression sequence seems not to be very relevant, cells gain growing advantages progressively in each step of the succession of changes, converting them from normal cells into malignant cancer cells¹¹.

It is suggested that 6 essential physiological alterations are needed to convert normal cells in malignant growing cells (Figure 1). Each of those changes allow cells to overcome the different anticancer defense systems posed by normal cells and tissues¹⁰.

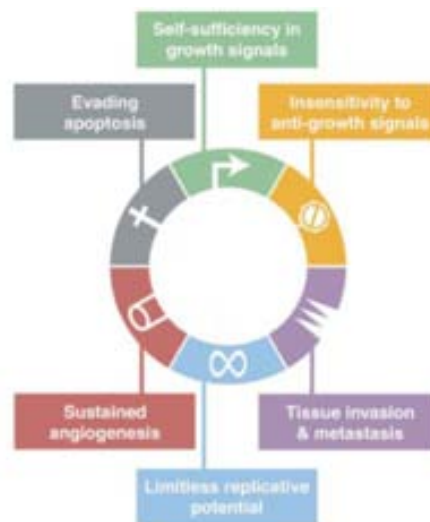


Figure 1. Acquired capacities of cancer cells in tumor development. (Modified from Hanahan D. *et. al*, 2000)

Cancer research is one of the mayor medical needs of the present world since cancers as a whole, represents the second cause of mortality after cardiovascular diseases with 7.6 million (13%) of deaths from a total of 58 million worldwide according to 2008 World Health Organization (WHO) report. Moreover, it is estimated that in the next few decades, this incidence will rise up to 45% due to the increasing exposure to environmental carcinogens and the progressive aging of the population¹².

The most common cancer types among the worldwide population are: lung cancer (representing 18% of cancer deaths), stomach cancer (9.6%), liver cancer (9.1%), colorectal cancer (8%) and breast cancer (6%). Thus, research on these types of cancer is a priority of the public health system.

Few medical advances in cancer therapy have been achieved in the last 50 years. Nowadays, a significant proportion of cancers can be cured by current therapies such as surgery, chemotherapy or radiotherapy, but still the diagnose at early stage of the disease is crucial for patients' survival.

Existing therapies fail in their effectiveness since their systemic administration and strong adverse secondary effects against normal cells and tissues firmly limit their administrable dose. Thus, more effective drugs are needed showing lower toxicity, better pharmacokinetic and pharmacodynamic properties and higher therapeutic activity. In this context, the development of targeted drug delivery systems is a promising strategy to overcome the limitations that conventional therapies currently offer.

Targeted therapy should allow acting specifically against cancer cells, dramatically reducing undesired effects over normal cells. Moreover, the enhancement of the therapeutic activity not only reduces the therapeutic dose, but it also allows the simultaneous administration of more than one drug to search for synergistic therapeutic effects. Those therapies usually act against proteins or genes that are directly implicated in the tumorigenic process. Thus, understanding the molecular basis of cancer is imperative for the rational design of those therapies¹³.

There are many targeted drug therapies that have been already tested. Most of them are based on small molecule inhibitors and monoclonal antibodies. Those drugs show some limitations since small molecules can freely diffuse and therefore are not specific enough. In addition, monoclonal antibodies can only be used to target proteins exposed in cell surface and while the majority of cancer molecular targets are intracellular, they usually are not efficiently internalized. Some of those tested drugs act against proteins encoded by mutated genes in cancer as Trastuzumab (herceptin)¹⁴⁻¹⁶, Imatinib (Gleevec)¹⁷⁻²⁰, Gefitinib (Iressa) and Erlotinib²¹⁻²⁷ or Cetuximab^{28, 29}. Some of them as Bevacizumab, are angiogenesis inhibitors³⁰⁻³² and some of them just try to induce cell death³³⁻³⁵. Even though those therapies have prolonged patient's survival in general, they still fail to cure most of patients with advanced stages of the illness.

Introduction

1.1 Colorectal cancer

Colorectal cancer is the third most common cancer type and the fourth cause of cancer death in the world. However, in developed countries, it becomes the second most common cancer. The average 5-year survival is around 60% in the USA and around 40% in less developed countries³⁶.

This type of cancer usually starts in the colonic sub-mucosal compartment and it can be relatively easily removed by conventional surgery if it is diagnosed in the first stages of the disease. However, metastatic foci can be found in 25% of the recently diagnosed colon cancers cases being the first cause of mortality with a 5-years life survival of less than 10%. The main metastatic foci in human colon cancer are lymphatic nodes, liver, lungs and peritoneum³⁷⁻³⁹.

Being one of the most studied cancer models, colon cancer is the tumor type in which histopathological and mutational progression that converts normal colon cells into malignant tumoral cells is better known. It has been observed in a statistically significant number of cases that the tumoral process follows the same mutational progression in those genes that are essential for the cellular proliferation control as it is shown in the model presented by Kinzler & Vogelstein in 1996³⁹ (Figure 2). This model has been recently updated considering new findings regarding hypermethylations in promoter regions of genes implicated in cell apoptosis and reparation of somatic mutations, inhibiting their expression^{40, 41}.

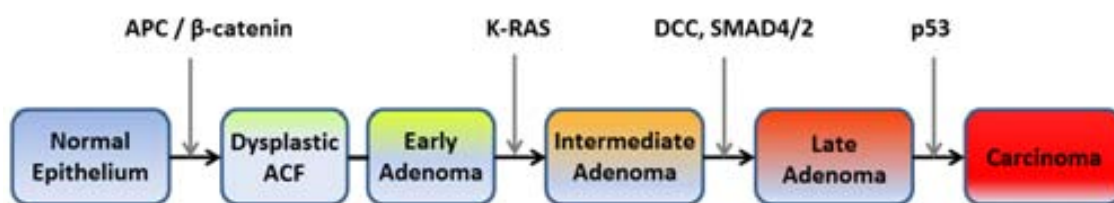


Figure 2. Mutational progression model in colorectal cancer proposed by Kinzler & Vogelstein in 1996.

The process described above is the most common way colon cancer is generated. However, alternative ways have been also described as the hereditary nonpolyposis colon cancer (HNPCC) in which mismatch reparation genes (mainly *MLH1*, *MSH2* and *MSH6*) are mutated^{42, 43} or MYH associated polyposis in which the process starts when both copies of the base excision repair gene (*MYH*) are mutated^{44, 45}.

In colon cancer, as in some other cancers, the most important therapeutic targets have already been identified. In 40% of the cases, mutations in *K-RAS* oncogene can be detected, being the most frequent mutations *K-RasVal12*, *K-RasAsp13* and *K-RasAsp12*⁴⁶. This gene not only is involved in tumorigenic process but it also participates in angiogenesis and metastasis formation⁴⁷⁻⁵⁰. However, mutations in other genes that are also implicated in metastatic and angiogenic process as *BRAF*,

MMP9 or *VEGF* can be found in many cases⁵¹⁻⁵⁴. Many superficial cell receptors can be also found overexpressed in colorectal cancer cells. However, two of those receptors have been found to be especially involved in metastatic process, namely the CXCR4 chemoquine receptor and CD44 receptor. The presence of those overexpressed receptors, have been directly correlated with invasiveness and metastatic phenotype in colorectal cancer⁵⁵⁻⁵⁷.

Nowadays, surgery is still the only effective treatment in both primary colon cancer and metastatic colon cancer³⁶. 5-fluorouracil based co-adjuvant chemotherapy after primary tumor radical resection is a very effective therapy in patients with no metastatic tumors. In the cases where metastatic foci have already appeared, the application of new chemotherapeutic compounds as Oxaliplatin or Irinotecan have slightly improved patient survival⁵⁸.

Current therapies still only offer global patient survival of around 40-60%, mainly because of the appearance of local recurrences and metastatic foci in many of the treated patients. Recent studies in the application of new targeted therapeutic vectors as antibodies, small molecules or nanoparticles for gene therapy combined with the conventional chemotherapy treatment have shown to be very interesting approaches being significantly more effective than the conventional chemotherapy alone^{15, 59}.

Thus, since the therapeutic targets in colon cancer have already been perfectly identified (Table 1), the main problem for the effectiveness of the current therapies are the huge limitations that the currently available vectors have. Therefore, since colon cancer is one of the most frequent tumor types worldwide, there is a huge social demand to research and develop new therapeutic vectors that improve their capacity not only to target specifically cancer cells but more specially to avoid the generation of metastatic foci.

Therapeutic targets in colorectal cancer	
Oncogenes and tumor supressor genes:	K-Ras, C-myc, p53, DCC, SMAD4, NM23, B-Raf
Apoptosis and survival related factors:	BCL-2, BAX, Survivin, Telomerase
Growth factor and receptors:	TGF- α , TGF- β CTGF, HER-2/NEU, EGFR, C-MET
Replication error reparation genes:	MSH2, MLH1
Angiogenic factors:	VEGF, Endoglin (CD105), HIF, SCF, SDF-1
Cicling dependent kinase inhibitors:	P27, P21, P16
Adhesion molecules:	CD44, E-Cadherine, ICAM-1
Invasivity implicated factors:	MMP, TIMPUPA,
Proliferation factors:	K1-67, MIB1, PCNA, β -Catenina
Antitumor vaccines:	TAA, CEA
Hipemetilation epigenetic factors:	DNMT1
Immunostimulation factors:	IL-12, FLT3L, α -Interferon, TRAIL
Chemotherapy resistance conferring factors:	MDR1
Propharmacologic therapy:	Cytosine Deaminase / 5-fluorocytosine...

Table 1. Therapeutic targets identified in colorectal cancer.

2. Nanoparticles in the context of nanomedicine.

Nanomedicine involves any medical application of nanoscale materials, compounds or technologies. However, one of the most currently promising approaches within nanomedicine and innovative medicines is the targeted drug and nucleic acid delivery (Figure 3).

Nanoparticle-driven targeted delivery allows the directed transport and specific release of the therapeutic components in the desired cells or tissues, therefore increasing local drug concentration and reducing potential off-target side effects^{60, 61}. In addition, the association of the nanoparticle with the therapeutic compounds can change their pharmacokinetic profile increasing their half life in the target site⁶². Conventional therapies are still far from being effective in many pathologies since their lack of specificity and its associated systemic toxicity strongly limit administrable therapeutic dose. Moreover, conventional therapies usually use standardized treatment procedures for specific pathologies without taken into account that in some cases the molecular bases causing the disease can considerably differ among different affected individuals. In this context, targeted drug or nucleic acid delivery not only overcomes those toxicity limitations but it also allows the application of personalized therapies⁶³.

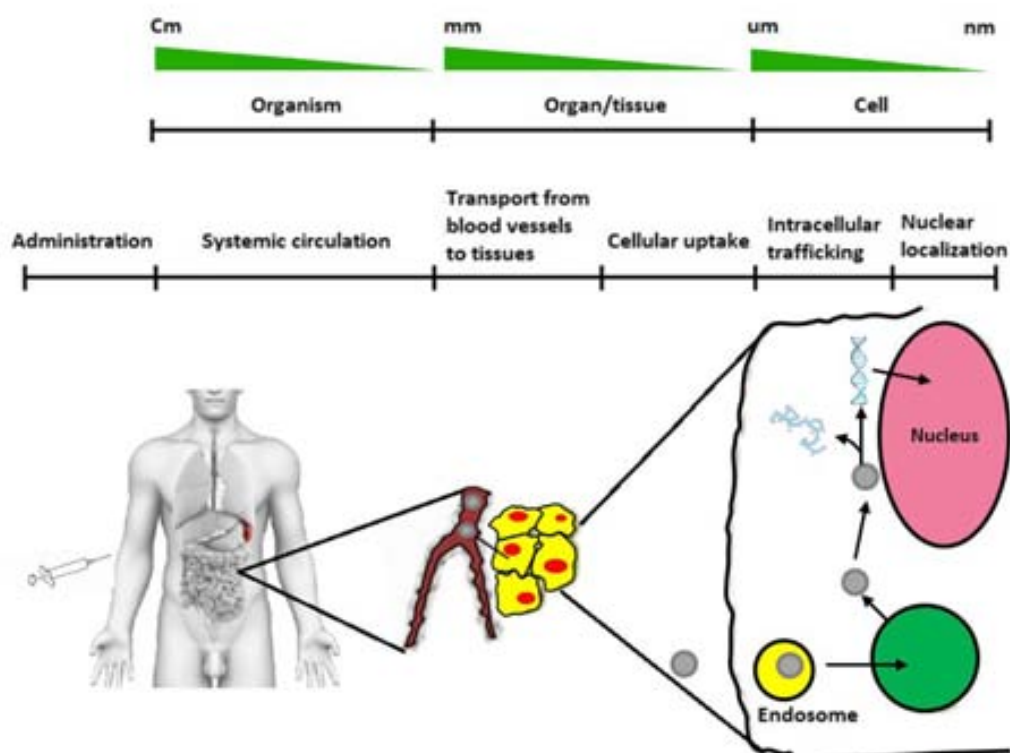


Figure 3. Targeted delivery of nanostructured materials at different biological scales.

2.1 Targeted nanoparticles

Many approaches are being developed for specific cellular targeting in order to rationally define the biodistribution of engineered nanoparticles. However, three predominant strategies have been used to achieve it, classified as passive targeting, active nonselective targeting and active selective targeting.

The first strategy is only relevant in oncology applications and it is based on the nanoparticle accumulation in tumors by the enhanced permeability retention effect. This effect consists in the passive accumulation of nanoparticles in tumoral tissue since the underdeveloped tumor vasculature allows molecules of certain size range to cross tumor capillaries and accumulate in that tissue (Figure 4). Moreover, the lack of efficient lymphatic draining allows nanoparticles to remain in tumor site^{64, 65}.

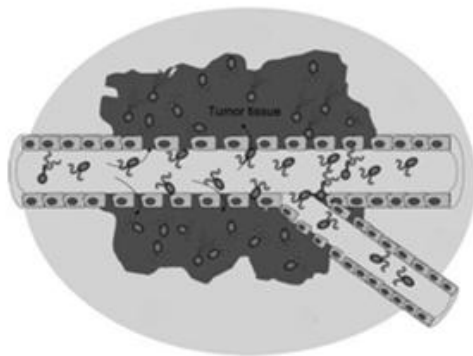


Figure 4. Enhanced permeability retention effect. Circulating nanoparticles passively accumulate in solid tumor tissue by hyperpermeable tumor vasculature. (Modified from Cho K. *et al*, 2008)

Active targeting strategies are based on the presence of specific ligands on the nanoparticles surface. Two different approaches have been described depending on the selectivity of the used ligands. In nonselective targeting, ligands that recognize usually overexpressed receptors in target cells are used and although good cell targeting can be achieved by this strategy, it doesn't completely avoid off-target effects since generally those receptors can also be found expressed in normal cells. However, in selective targeting, ligands that recognize receptors exclusively expressed in target cells are used, completely avoiding thus any off-target effect⁶⁶.

Thus, for a correct cellular targeting, it is necessary to carefully study and identify overexpressed or exclusively expressed cell surface receptors or antigens in target cells in order to add a specific ligand on engineered nanoparticles.

Organelle specific targeting is also a very important issue since the effectiveness of any engineered nanoparticle will strongly depend on their capacity to reach and release the therapeutic agent in the subcellular compartment where the action has to be done. For example, any nanoparticle transporting nucleic acids as therapeutic agents for targeted gene therapy will imperatively need to reach cell nucleus if they are transporting an expressible DNA molecule, but they will only need to reach cells cytoplasm if the transported nucleic acid is a siRNA molecule. Moreover, any nanoparticle internalized by clathrin-dependent endocytosis pathway that lacks

Introduction

endosomal escape ability will inevitably be degraded in cell lysosomes⁶⁶ (Figure 5). Thus, it is imperative to develop appropriate tools for nanoparticles targeting into the proper subcellular compartments. In this context, many organelle targeting tools are currently emerging for targeted delivery to cellular cytosol^{67, 68}, nucleus⁶⁹⁻⁷¹, mitochondria^{72, 73}, peroxisomes⁷⁴ and lysosomes⁷⁵.

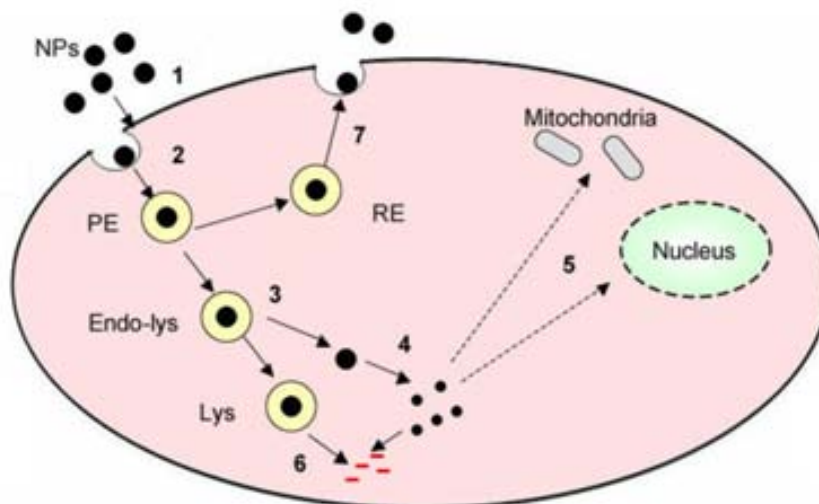


Figure 5: Schematic representation of steps involved in cytosolic and organelle specific delivery of nanoparticles (NPs). 1) cell membrane-nanoparticles association. 2) NPs internalization by endocytosis. 3) Endosomal escape of NPs. 4) NPs/therapeutic agent release in cytoplasm. 5) Cytosolic transport to target organelle. 6) NPs degradation either in lysosomes or cytoplasm. 7) Exocytosis of NPs. PE: Primary endosomes, Endo-Lys: Endo-lysosomes, Lys: lysosomes, RE: Recycling endosomes. (Modified from Vasir JK *et al.* 2007).

Receptor-mediated targeting has been generally considered as a very promising approach since its efficacy has been usually easy to demonstrate *in vitro*. However, some *in vivo* experiments performed using radiolabeled antibodies have shown that only 0,01% of the administrated dose reached target cells⁷⁶. Those results suggest that since receptor mediated targeting potential has been widely demonstrated, other nanoparticle's properties have to be very carefully taken into account to allow those nanoparticles to overcome all the biological barriers they will find in their journey from the administration site to the target cells in an *in vivo* system.

2.2 Physico-Chemical properties (size)

In nanomedicine, a wide spectrum of nanomaterials is available, each of them offering different physico-chemical properties. In the rational design of nanoparticles, those physico-chemical properties as nanoparticle size, shape, surface charge or mechanical properties have to be very carefully selected since they are very important determinants of the nanoparticle functionality. Among all those parameters, nanoparticle size is one of the most relevant properties in nanomedicine and more specially in targeted drug and nucleic acid delivery⁷⁷. Size not only has a very important role in how the nanoparticle is biodistributed in human body, but it also determines

the biological effects that those particles have over the target cells in terms of interactions, internalization, intracellular trafficking or even in terms of toxicity and immunogenicity⁷⁸. Even though some studies have shown that nanoparticle shape can also very strongly determine nanoparticle biodistribution and internalization, optimum parameters for engineered nanoparticles have yet to be determined^{66, 79}. Furthermore, selected administration pathway and target tissue localization have to be very carefully studied in order to choose the appropriate nanoparticle⁸⁰.

Effects of size have already been extensively studied with spherical nanoparticles from what general trends have been noted. Circulating nanoparticles under normal circumstances are typically removed by reticuloendothelial system (RES), by Kupffer cells in liver, by renal clearance at kidney or by mechanical filtration in spleen. Nanoparticles smaller than 5nm usually are rapidly cleared from the circulation by renal clearance⁸¹ while nanoparticles bigger than 200nm could be cleared by spleen since spleen fenestration are typically between 200-500nm in width. RES removal however, is dictated by the opsonization process that occurs when nanoparticles contact with blood plasma, so large particles can more easily be cleared by this system since they show bigger opsonization capacity⁶⁶.

When brain cells have to be targeted, only nanoparticles smaller than 15nm efficiently cross the blood brain barrier (BBB). However, targeted nanoparticles up to 100nm will be able to reach brain cells although their uptake efficiency will exponentially decrease with size⁷⁸. The appropriate nanoparticle size for lymphatic node targeting strongly depends on the chosen administration pathway. While nanoparticles up to 80nm will be able to reach lymphatic nodes by subcutaneous administration, only nanoparticles between 6-34nm in size will be able to reach it by intrapulmonary administration^{82, 83}. Alternatively, bigger intravenously administered nanoparticles could indirectly be targeted to lymph nodes attached to circulating leucocyte surface⁸⁴. Liver can easily be targeted by intravenous administration but only nanoparticles smaller than 100nm will cross liver fenestrae and reach hepatocytes since bigger nanoparticles are usually taken up by Kupffer cells^{78, 85}. Finally, lungs can also be targeted either by direct inhalation or by intravenous administration. It has been seen that nanoparticles larger than 200 nm in diameter usually get physically trapped in alveolar capillaries when they are intravenously administered⁸⁶. Moreover, by inhalatory administration pathway, particles even bigger than 5µm can be effectively administered⁸⁷ (Table 2).

Introduction

Target organ	Partice size	Surface property	Comments
Brain	5-100 nm: uptake efficiency decreases exponentially with size.	Lipophilic moieties and neutral charge enhance brain uptake	Leukocytes can take up nanoparticles in circulation and then carry them to disease site in the brain.
Lung	>200 nm: particles are trapped in lung capillaries	Positive surface charge	Inhaled particles of large size (>5µm) are also retained in the lung.
Liver	<100 nm to cross liver fenestrae and target hepatocytes >100 nm particles will be taken up by Kupffer cells	No specificity needed	Lipids tend to accumulate in the liver
Lymph nodes	6-34 nm: intrapulmonar administration. 80 nm: Subcutaneous administration.	Non-cationic, non-pegylated and sugar-based particles	200nm particles in circulation can be taken up by leukocytes and trafficked to lymph nodes.

Table 2. Organ specific targeting: general considerations for nanoparticle delivery to specific organ.

Once administered and target cells have been reached, the way those nanoparticles interact and the effects they cause on them seems to be again strongly dependent of nanoparticle size. Recent studies on ligand/receptor-mediated nanoparticle internalization have shown that nanoparticles of sizes ranging between 25-50nm are the most efficiently internalized. Out of this range, internalization efficiency is considerably reduced showing higher cell membrane accumulation pattern⁸⁸.

In ligand/receptor binding and internalization process, the number of superficially exposed ligands and the ligand/receptor dissociation constant are key parameters in order to achieve good interaction pattern and to induce particle internalization. Those two parameters are directly dependent of nanoparticle size, since the ligand absorption capacity at nanoparticle surfaces is directly proportional to their size, whereas the ligand/receptor dissociation constant is inversely proportional to the nanoparticle size. In this context, very small nanoparticles show low ligand density in their surfaces and a elevate dissociation constant. Since the internalization process is very dependent on the cells wrapping time, small molecules may not remain attached enough time to the cell surface during the internalization process. On the contrary, very big nanoparticles show very high ligand density presented on their surfaces and a low dissociation constant. This makes those nanoparticles to strongly attach saturating available local and distant receptors, and consequently limiting considerably cell wrapping capacity^{89, 90}. Thus, the optimal nanoparticle size for ligand/receptor mediated internalization process has been suggested to be around 25-50nm. The nanoparticles with an optimal size present an appropriate dissociation constant that allow them to be attached to the receptors enough time and also show a good superficial ligand density to correctly attach to more than one adjacent receptor. This combination allows a correct and efficient cell wrapping process (Figure 6)⁸⁸.

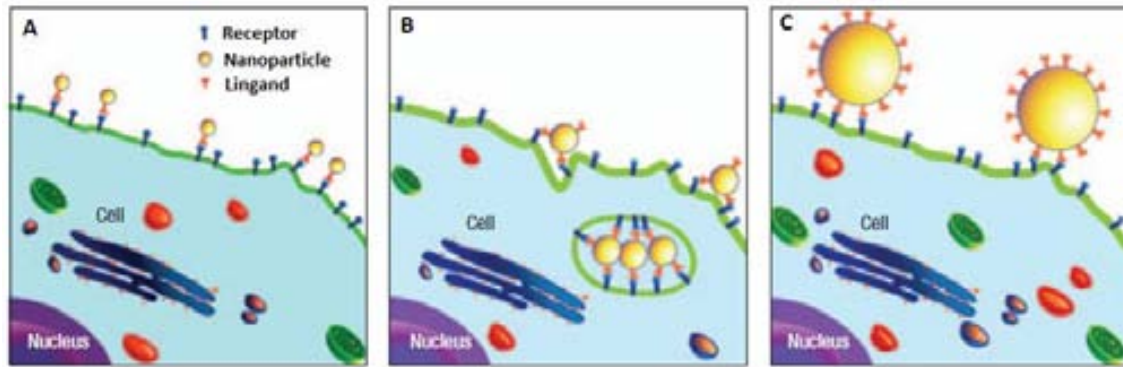


Figure 6. Ligand-receptor binding mediated nanoparticle internalization. A: Small size nanoparticle, B: optimal size nanoparticles, C: Big size nanoparticles. (Modified from Jiang *et. al.* 2008)

Different cell internalization pathways have been described in mammalian cells including clathrin dependent endocytosis, caveolae mediated endocytosis, micropinocytosis, macropinocytosis or even phagocytosis among others. All of them use very different cellular uptake mechanisms for particle internalization and although the majority of receptor-ligand complexes usually enter cells by clathrin mediated endocytosis, once again, nanoparticle size seems to play an important role determining the pathway that cell will use for their internalization⁹¹⁻⁹³.

Recent studies performed with microspheres of different size have shown that nanoparticles smaller than 200nm are usually internalized by clathrin dependent endocytosis. However it seems that nanoparticles between 200-500nm preferentially use caveolae mediated endocytosis progressively tending to use this pathway as the size become bigger⁹⁴. This resulted somewhat surprising since caveolae have been described to generate vesicles of around 55-65nm⁹². Nanoparticles of bigger sizes have been described to preferentially enter cells by macropinocytosis or phagocytosis⁹².

In some therapies, reaching cell nucleus is imperative for the therapeutic action as it has been mentioned above. Nuclear pore complex size is around 55Å so nanoparticles bigger in size than 40 kDa (10-30 nm) will not be able to go inside by passive diffusion. Nuclear transport of larger nanoparticles will necessarily require an active transport mechanism^{92,95}.

Finally, nanoparticle potential toxicity and immune system activation have been also related with nanoparticle size. Big nanoparticles are recognized more easily by the complement system since their bigger surface allows higher extend of opsonization.⁹⁶ It has also been reviewed that some nanoparticles, as quantum dots, show multiple factor depending cell toxicity in which one of the determining key parameter is the nanoparticle size⁹⁷.

2.3 Current state of nanoparticles in medicine

In the last decades, several nanoparticles have successfully been generated and introduced in the market for the treatment of several pathologies as cancer or infectious diseases among others (Figure 7).



Figure 7. Development of nanoparticle therapeutics during the last five decades. EPR: Enhanced permeability and retention, BBB: Blood-brain barrier, FDA: US Food and Drug Administration, PEG: Polyethylene glycol, PLA: Polylactic acid. (Adapted from Petros *Et. al.* 2010)

Many different nanomaterials have been used for the development of those nanoparticles including materials of biological, organic and inorganic origins. Those nanoparticles can generally be classified in 5 different groups including lipids, proteins, polymers, metals and carbon derivatives (Table 3).

Building block	Nano-scale vehicles	Uses
Polymers	Core-shell nanoparticles, nanogels and polymer micelles	Well-characterized, biocompatible and modular delivery vehicles.
Lipids	Liposomes, lipoplexes, micelles and filomicelles.	Effectively delivers water-soluble and -insoluble drugs.
Metals	Gold nanorods, gold nanoparticles, iron-oxide nanoparticles and quantum dots.	Thermoablative therapies and imaging agents for diagnosis.
Carbon	Carbon nanotubes, nanodiamonds and graphene.	Near infrared emissions allow for tissue-transparent imaging for diagnosis and tracking.
Biologicals	Viruses, nucleic acid nanoparticles and protein nanoparticles.	Viruses deliver a non-covalently bound payload without loss from passive diffusion.

Table 3. Nanoparticles building materials and their general uses.

Even though many types of nanoparticles are currently available, most of the approved and clinically used nanoparticles are still only lipids and polymers since they were the first ones being developed and they offer interesting properties as the possibility to be functionalized with cell specific ligands, their degradability in specific conditions and their high drug transporting capacity. However, nanoparticles that have been developed more recently, offer new properties that open a wide range of new possibilities for the future of nanomedicine⁹⁸.

Lipids are small organic molecules that have the ability to self-assemble in well-organized vesicles as lipid bilayers, liposomes or micelles and are able to transport high quantities of hydrophobic and hydrophilic drugs physically trapped inside the nanoparticles. They can be functionalized with cell specific ligand in order to confer them specific targeting^{99, 100} and they can also be made pH and temperature sensitive in order to confer them the ability to release transported drug in target cells at the moment that particles are exposed to specific conditions¹⁰¹⁻¹⁰³.

Polymers, ranging from dendrimers¹⁰⁴ to nanogels¹⁰⁵, represent a heterogeneous group of materials for the construction of nanoparticles. Those particles not only transport therapeutic agents physically trapped inside the particles, but also chemically conjugated to their surface. One of the most promising advances in this kind of nanoparticles is the recent use of PLGA-based biodegradable polymers that are generated with FDA approved material for drug incorporation¹⁰⁶. Dendrimers have been widely studied since the classical PAMAN dendrimers family appeared many years ago^{98, 104}. They have also been functionalized with specific ligands¹⁰⁷ and some studies have shown their ability to cross biological barriers¹⁰⁸. Other widely used agents are self-assembling cyclodextrin-based polymers¹⁰⁹. However, the polyethylene glycol (PEG) polymer, which has been described to enhance solubility, plasma stability and reduce immunogenicity, is the most widely studied polymer so far by its multiple benefits⁶⁶.

Metal derived nanoparticles have been generated using different materials including gold, silver, silica, iron oxides or quantum dots. Among gold particles, small size gold

Introduction

nanoparticles (5-10nm), gold nanorods and gold nanoshells have been generated⁹⁸. They can be functionalized either to bind specific ligands or therapeutic drugs but they have been mostly used for thermoablative therapies since they efficiently respond to near infra-red light (NIR) liberating heat energy in target cells¹¹⁰⁻¹¹². Very interesting approaches have been performed with iron oxide nanoparticles since they can also be used for thermoablative therapies and their magnetic properties allow directing a specific localization by manipulating magnets¹¹³⁻¹¹⁵. Silica-based nanoparticles are also being currently developed but only few studies have been performed yet¹¹⁶. Quantum dots are small semiconductor crystals of around 1-100nm in size that are generally composed by a cadmium selenide (CdSe) core coated with ZnS or CdS layer to protect them from photooxidation. Being very useful either for diagnose or for therapy, they are one of the most studied nanoparticles currently¹¹⁷. These nanoparticles can also be functionalized for specific cell targeting¹¹⁸.

Many carbon-derived nanoparticles have been developed as carbon spheres of around 100-150nm named buckysomes¹¹⁹, carbon nanotubes¹²⁰ or nanodiamonds¹²¹ among which carbon nanotubes have been the most widely studied¹²². Some studies have recently suggested that carbon nanotubes can pierce the cell membranes and directly be translocated to the cytosol, although this issue remains unclear^{123, 124}.

Protein-only nanoparticles have been developed for nanomedical purposes and more especially for targeted drug and nucleic acid delivery¹²⁵. The most studied protein nanoparticles are classified as virus like particles (VLP) and artificial viruses. VLPs are natural self-assembling constructs consisting on non-replicative viral capsids generated by recombinant technologies and lacking the viral genome. They have been used as safe viral vaccines and they can also act as protein cages transporting therapeutic compounds to their natural target cells^{126, 127}. Artificial viruses however, are manmade nanoparticles that mimic properties of natural viruses in terms of targeting and intracellular trafficking. Protein only artificial viruses can also be functionalized with therapeutic agents for targeted therapy and in some cases the protein itself could perform the therapeutic action¹²⁸⁻¹³⁰. In 2005, the first protein based nanoparticle (Abraxane) consisting of albumin bound to paclitaxel, was approved by the FDA for the treatment of metastatic breast cancer¹³¹.

Nanoparticles created by combinations between different types of nanomaterials have also shown to have very interesting properties and in many cases to have considerably improved nanoparticles performance. Some already developed combinations include peptide activated metal nanoparticles¹³², metal-polymer hybrids¹³³, metal-lipid hybrids¹³⁴ or polymer-lipid hybrids¹³⁵.

2.4 Controlling nanoparticle size

Architectural design of nanomaterial structure is essential to reach the full potential of materials. Very different synthesis processes have been used to produce nanoparticles and there is consensus on the fact that resultant physico-chemical properties are determinants of their potential success in nanomedicine. However, being a critical parameter, size cannot be rationally controlled by current nanofabrication procedures, with few exceptions.

Gold and silver nanoparticles are usually generated by simple chemical reaction processes, in which size can be controlled by changing the chemical components ratios in the reaction. Gold nanoparticles are generated mixing chloroauric acid with citric acid at different ratios to obtain 10nm, 20nm and 40nm nanoparticles. Moreover, nanoparticles smaller than 10nm have been also generated using sodium borohydride as reducing agent. Silver nanoparticles of different sizes have also been created by mixing silver nitrate and sodium borohydride at different ratios⁸⁸.

Successful application of iron oxide nanoparticles depends on their size, and different synthesis methods including aqueous co-precipitation, microemulsion and thermal decomposition have been described, that allows controlling the size of generated nanoparticles. Aqueous co-precipitation consists in the precipitation of Fe^{2+} and Fe^{3+} ions in aqueous salt solutions. Although nanoparticle size can be controlled through the use of different salts, pH reaction and $\text{Fe}^{2+}/\text{Fe}^{3+}$ ratios, achieving a narrow size distribution is still a challenge. Microemulsion offers a better size control and higher monodisperse size distribution. Nanoparticle size depends on the generated microemulsion size and this can be easily controlled by changing the water/surfactant/oil ratios. However, this method is very difficult to scale up due to the high amounts of oils and surfactants that are required. Finally, thermal decomposition is based on the decomposition of iron precursors as $\text{Fe}(\text{CO})_5$ under high temperatures and produce highly monodisperse nanocrystals. However, the hydrophobic surface that those nanoparticles show, strongly limits their biomedical application because of their low biocompatibility¹³⁶.

Silicon nanoparticles size can be also rationally controlled just by changing chemical reaction conditions. A recent work has shown a simple approach for the mesoporous monodisperse silica nanospheres production with adjustable size. They show how nanoparticles between 50 and 100nm with high monodisperse size distribution can be easily achieved just by increasing the reaction temperature from 40° to 80°. Mesoporous pore size can be also controlled in a range between 2.8nm to 4nm just by the variation of the subsequent hydrothermal treatment temperature from 100° to 130°¹³⁷.

Introduction

Particle replication in non-wetting templates (PRINT) is a newly developed nanoparticle manufacturing technique based in the use of templates that allow the production of highly monodisperse size tunable nanoparticles. This manufacturing process has been commonly used in the electronic industry for the preparation of nanosized particles of a particular size and architecture and it has now been applied to the generation of a variety of nanomaterials^{66, 138}. Some hydrogel based polymeric nanoparticles created by this production technique have been recently used for gene silencing assays¹³⁹.

The use of compressed and supercritical fluids is another recently described promising technology for the production of size controlled nanoscale particles. The most relevant properties of this technique include the production of highly homogeneous nanoparticles and its batch to batch reproducibility. Those properties together with its high scalability, confers to the generated nanoparticles a great commercial potential. This technology has already been used for some liposomes and polymeric nanoparticle generation¹⁴⁰.

Proteins are usually produced in biological systems, and although protein production is very well known, the mechanisms that drive the formation of protein nanoparticles remains unclear. Some naturally self-assembling protein structures have been already observed and studied such as viral capsids or bacterial subcellular organelles as carboxisomes among others. Based on those structures, some size defined self-assembling nanoparticles have been created including virus like particles (VLPs)¹²⁶ or icosahedral protein cages recently named encapsulins¹⁴¹.

2.5 Biocompatibility

Nanomedicine needs proper nanoparticles to reach the full therapeutic potential. Many different nanoparticles have been generated since this technology begun, but not all of them have proved suitable in the field. There are five key parameters that any nanopharmaceutical agent should fulfill for its successful application: degradability, low toxicity, high specificity, high efficiency and the capacity to deliver multiple therapeutic agents. In this context, some promising nanoparticles have been tested showing really good results in preclinical studies and potentially having all the required properties. However there is still a great concern about the biosafety of most of the developed nanoparticles. All medicines must display an acceptable risk-benefit relation with respect to its proposed use. Thus, biocompatibility and low toxicity profiles are imperative requisites for any particle used in medicine and it is still one of the main reasons why most of these therapies are not approved for clinical uses.

Targeted drug delivery claims to reduce the transported drug systemic toxicity avoiding non desired off-target effects. However the potential toxicity produced by the

used nanoparticles has sometimes been overlooked and it should be very carefully studied.

In first place, nanodrugs should be biodegradable and many of the used materials, despite having a natural origin, are poorly degraded by human enzymes. Moreover, chemical functionalization could convert degradable materials into effectively non-biodegradable⁹⁸. In this context, non-biodegradable or slowly degradable nanoparticles can progressively accumulate in the body (in lysosomes) after high dose or chronic administrations if they are not correctly removed by the renal system. Lysosomal accumulation is well known in the context of lysosomal diseases. Intracellular vacuolation has also been reported with some pegylated nanoparticles in animal models. Thus, if non-biodegradable nanoparticles have to be used, renal and hepatobiliar elimination should at least be confirmed at early stages⁹⁸.

Immunotoxicity is also a matter of concern since the introduced nanoparticles could be recognized by the immune system and generate non desirable strong immune responses. Thus, the antigenicity and potential activation of the complement system have to be checked. The use of appropriate preclinical models is also essential since some cases have been reported in which nanoparticles showed an excellent performance in mouse models and resulted to have severe toxic effects in clinical trials¹⁴². Infusion reactions have been clinically observed after intravenous administration of some nanosize particles as liposomes and there have also been reported complement activation cases by dendrimers, liposomes and PEG containing nanoparticles¹⁴³⁻¹⁴⁶.

Finally, the introduction of novel biodegradable materials and functionalization linkers, produces new metabolites never seen before in the human body as a consequence of the metabolic degradation of those nanoparticles. The potential toxicity that those new metabolites could have in the human body is completely unknown⁹⁸.

Fullerenes and other carbon derivatives as the well characterized carbon nanotubes for example, have proved very interesting tools for biomedical applications. However, many concerns about their potential risks for human health have been reported. Their bioaccumulation and the oxygen species formation at high concentrations may cause inflammation and genetic damages. Thus, apparently its potential risk could be dose-dependent^{147, 148}.

Toxicology of metal derived nanoparticles has also been widely studied¹⁴⁹. Gold nanoparticles are generally considered as nontoxic, but size dependent cytotoxicity has been reported in a case in which small gold nanoparticles (1.4nm) induced cell death by oxidation stress and mitochondrial damage¹⁵⁰. On the other hand, silver has generally been shown to be cytotoxic¹⁵¹. Iron oxide nanoparticles are generally classified as biocompatible without showing severe toxic effects neither *in vitro* nor *in*

Introduction

vivo^{149, 152}. However, some concerns remain in the use of iron based particles since adverse effects of iron overload and iron induced free radical generation are well documented such as the iron induced neurotoxicity^{153, 154}. Toxicity of crystalline silica is also well known but little has been investigated about mesoporous silica nanoparticles toxicity¹⁵⁵. Nonporous and porous silica nanoparticles have been reported to be hemolytic in concentration and size dependent manner. However, mesoporous nanoparticles have been described to be less hemolytic being the pore structure the critical determinant of the hemolysis¹⁵⁶. Finally, quantum dots are one of the most widely studied metal derived nanoparticles and since heavy metal's toxicity is very well documented, many concerns still remain about their potential toxicity^{157, 158}. Quantum dots toxicity has been reported to be size, charge and surface coating dependent^{159, 160}.

Polymers are usually non-biodegradable materials and among polymeric nanoparticles, dendrimers are the most polemic ones since some chemistry used in their generation has shown to have unacceptable toxicity¹⁴⁹. Cationic dendrimers have proved more toxic than anionic ones and several different toxic effect have been reported including cell disruption by membrane pore formation, apoptosis induction by mitochondrial dysfunction or hemolytic and cytotoxic effects¹⁶¹⁻¹⁶³. Lipid and protein nanoparticles have been generally considered less toxic and more biocompatible than polymers as their biological origin make them usually highly biodegradable.

Considering all the reported toxicity problems, the development of good performing, safe and biocompatible nanoparticles is still a very important challenge of nanomedicine and more efforts need to be done to dissipate any remaining concerns about the potential of targeted delivery approaches in this context.

2.6 Protein nanoparticles

Proteins are biological molecules consisting of one or more aminoacidic chains that perform an enormous amount of different activities in living organisms. They are considered complex nanoparticles since their size range from few nanometers to hundreds of nanometers when supramolecular interactions occur as in the case of viral capsids. Since they participate in virtually every process within cells, they have been widely used as therapeutic components from the beginning of medicine. With the development of nanomedicine, protein nanoparticles have generated high expectations because of their potential applicability especially in targeted drug and nucleic acid delivery. Although some negative effects have been reported in some cases as immune and inflammatory reactions, their biodegradability, low toxicity, high functionality and their tuneability have made protein nanoparticles very promising tools in nanomedicines. Moreover they can be used not only as vehicles for targeted drug and nucleic acid delivery, but also by themselves as therapeutic molecules. Being

their most promising properties biocompatibility and targeting capacity, many efforts are being made for the development of protein nanoparticles.

Proteins are generated in biological expression systems. Many microorganisms of different origins as bacteria, yeast, insect cells and mammalian cells have been widely used for recombinant protein production each of them having different production mechanisms. Bacteria are usually the first option since they offer the most cost-effective production processes being *Escherichia coli* the most widely used and best characterized microorganism¹⁶⁴. The approval in the early 80s of the commercial use of recombinant human insulin produced in *E. coli* by the FDA represented an inflexion point in the development of protein based therapeutics¹⁶⁵. However, many eukaryotic proteins cannot be correctly produced in bacterial expression systems since prokaryotic microorganisms are not able to produce post-traslational modifications, strongly compromising the protein folding process. In this context, yeast is the simplest eukaryotic organism that can be used for recombinant protein production, being the most commonly used hosts *Pichia pastoris* and *Saccharomyces cerevisiae*. However, some proteins also fail to be produced in that system since the glycosylation patterns of yeast are different from higher eukaryotes¹⁶⁶. Insect cells have been also used for recombinant protein production using baculovirus expression system. This system has become an interesting alternative since those cells are able to produce more complex post-traslational modification and high expression levels can be obtained in a cost-effective process¹⁶⁷. However, mammalian cell lines are sometimes the only choice for the expression of difficult to express proteins, especially for highly glycosylated ones. Proteins are usually soluble and active when are produced in this system, but the production cost is still very high and production processes usually get long time^{168, 169}. Besides the biological systems mentioned before, cell-free protein production systems have also been developed where transcription and translation reactions are carried out *in vitro*. However, this system is not generally used for nanoparticles generation since they still show important limitations¹⁷⁰.

The first developed protein nanoparticles generally consisted of regular drug-loaded protein units usually targeted against a specific cell or tissue. Since albumin-based nanoparticles were reported in 1972, many interesting results have been achieved using this approach, being in fact an albumin-based drug the first protein nanoparticle approved by the FDA for human clinical use^{131, 171}. However, more sophisticated approaches are being developed, based on multifunctional proteins and self-assembling proteins.

Multifunctional proteins

The development of genetic engineering techniques has allowed the creation of new proteins or the modification of existing ones with the aim of obtaining new proteins with the desired functions. In this context, multifunctional proteins are manmade

Introduction

engineered chimerical proteins that incorporate different selected protein functional domain from different origins and usually in the same polypeptide chain to provide the required activities. They are considered artificial viruses since they try to mimic virus properties in terms of cell targeting and intracellular trafficking. For the proper design and generation of those multifunctional proteins, the modules that will be part of the protein have to be carefully selected. There are several biological barriers that a protein-only nanoparticle has to overcome to successfully get into the target cells from the administration site. Thus, since several protein motifs have been described to overcome each of those barriers, the incorporation of those modules and the order that they will have in the polypeptide chain will be key determinants in the successful performance of the protein nanoparticles. The functional protein segments that are usually incorporated in these nanoparticles include protein domains conferring systemic stability, nucleic acid or drug interaction, cell targeting and internalization, endosomal escape, cytosolic mobility, nuclear localization or blood brain barrier crossing abilities (Figure 8)^{172, 173}. Many prototypes able to deliver DNA or molecules in cell cultures but also in specific cells in living organisms have already been described¹²⁹.

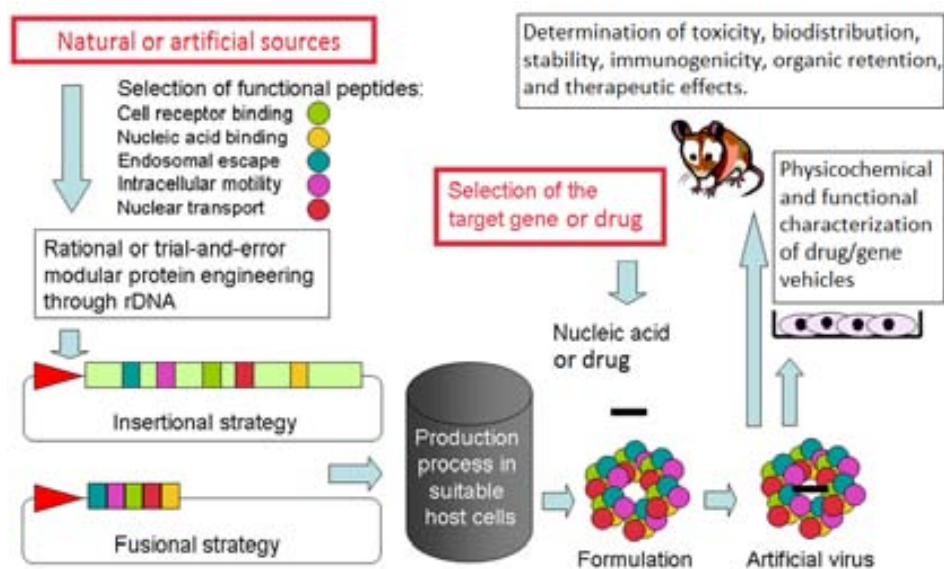


Figure 8. Therapeutic multifunctional proteins design and generation schematic process (Modified from Vazquez E. *et. al*, 2009).

Self-assembling proteins

Only when a protein is able to organize into a supramolecular structure we may talk of protein nanoparticles. Self-assembling proteins spontaneously cross-interact to form ordered structures, usually of nanoscale sizes. It has been widely documented that those protein structures are stabilized by weak non-covalent interactions as hydrophobic interactions, electrostatic interactions or Van der Waals forces¹⁷⁴⁻¹⁷⁶.

Apart from those protein-protein interactions, nucleic acid-peptide interactions have also been described to strongly influence in nanoparticle architecture¹⁷⁷. However, really little is known about the protein properties and processes that drive and control the self-assembling ability of any protein in regularly structured nanoparticles of a specific size. Some natural self-assembling proteins have been described and successfully imitated for nanomedical purposes. Among them, we can find monomers of viral capsids and non-viral self-assembling proteins that generate protein oligomers and subcellular organelles as carboxisomes. Different protein nanoparticles as virus-like particles (VLPs), amyloid fibers or bacterial micro-compartments (BMCs) have been generated based on those previously mentioned self-assembling natural proteins in order to achieve highly regular and monodisperse nanosize protein nanocarriers. VLPs are self-assembling, non-replicative and therefore non-pathogenic viral capsids ranging from 20 to 100nm, usually generated by the recombinant expression of viral capsid proteins¹⁷⁸. Although they lack the viral genome, they still conserve viral properties as the cellular tropism and uptake and intracellular trafficking, making them an appropriate tool for drug delivery and gene therapy^{126, 127, 179}. Since the first DNA packaging and transduction using mouse polyomavirus (MPyV) was described in 1983¹⁸⁰, VLPs of many different viruses have been generated¹⁸¹⁻¹⁸⁸. Some VLPs have already been used for directed delivery in biomedical applications and although they are considered biologically safe nanostructures since they are not infectious and do not replicate, immune inflammatory responses especially when repeated administrations are needed can be observed¹⁸⁹. Based on some bacterial micro-compartments, the recently named encapsulins have been generated. They consist of self-assembling polyhedral protein structures of around 100-150nm that imitate those subcellular organelles. They can be functionalized with specific ligands and be filled with therapeutic molecules to use them as nanocarriers for targeted delivery¹⁴¹. Amyloid proteins based particles have been also generated but far from generating highly regular nanoparticles, amorphous particles have been obtained^{190, 191}.

Our group has an extensive expertise in the design, production and characterization of protein nanoparticles. We have studied and generated several multifunctional proteins for biomedical applications following different production strategies. Aris *et al.* generated multifunctional proteins following insertional mutagenesis in which different functional domains were introduced in permissive sites of a beta-galactosidase protein. They were later successfully used in *in vivo* assays for targeted gene therapy approaches in mice with a brain ischemia model^{192, 193}. Smaller multifunctional proteins have been more recently generated by our group just by producing chimerical proteins with different functional domains one beside another and they have successfully been used in *in-vitro* assays^{177, 194}. Although very interesting results have been obtained with these protein nanoparticles, rational particle size control remains elusive. We have also generated and studied different bacterial inclusion bodies which are nanoscale regular insoluble protein aggregates generated

Introduction

during bacterial protein production process. Although they have also been used as protein nanoparticles for nanomedical purposes ¹⁹⁵⁻¹⁹⁷, their architecture cannot be neither rationally controlled.

In summary, protein nanoparticles have shown to be very promising tools for nanomedicine. Many interesting results have been obtained using this type of particles and their well characterized biosafety and biosecurity have made them appropriate tools for cell therapy. Nanoparticle size has been widely discussed above to be a crucial property for their functionality *in vivo*. Although many protein nanoparticles with appropriate size range have been already generated, no one has been able to rationally control their size yet. Thus, there is a huge necessity to study and understand which are the properties that drive the self-assembling capacity of those proteins into discrete particles of defined and desired size, in order to get the full potential of protein nanoparticles.

3. Gene therapy

The development of recombinant DNA techniques has made it possible to rationally manipulate DNA sequences, allowing the massive study of genes and the better understanding of the genetic causes implicated in many diseases. These discoveries have opened new possibilities for the development of new and innovative medicines useful for gene therapy.

Gene therapy consists in the treatment of different diseases at genetic level by the introduction of nucleic acids into affected cells. The therapeutic effect can be achieved either by the overexpression of a delivered gene to increase the amount of a therapeutic protein or by a controlled downregulation of a cellular gene with deleterious effects. It appears as very promising strategy since gene therapy not only can be used for the treatment of genetic diseases but it also can be used for the treatment of many other non-genetic pathologies. Knowing the molecular bases involved in a specific pathology enables the design of gene therapy approaches for its treatment. In this context, current mayor targets for gene therapy include different types of cancer and in decreasing percentages monogenic, cardiovascular, infectious and neurological diseases among others (Figure 9)¹⁷².

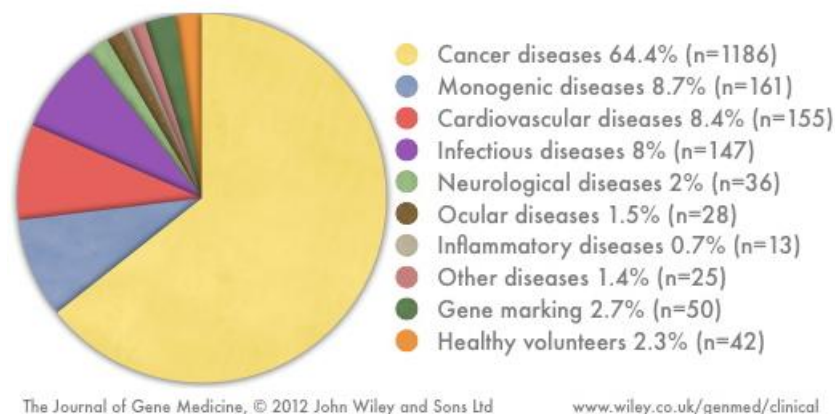


Figure 9. Gene therapy target diseases in current clinical trials (2012; John Wiley and Sons Ltd).

Human cancer has generated special interest in public health because its high incidence, mortality rate and low efficiency of conventional therapies. Although conventional therapy side effects can be dramatically reduced by specific targeting, drug therapy still shows high toxicity and most of molecular targets are not easily accessible. In this context, the use of targeted nanoconjugates for nucleic acid delivery in cancer treatments is an attractive alternative. Furthermore, gene therapy provides the possibility to perform personalized treatments where different nucleic acids can be delivered to target cells depending on the molecular bases involved in each individual cancer case. Moreover, different molecular targets can be also treated at the same time to obtain synergistic effects¹⁷².

Introduction

3.1 Gene therapy approaches in cancer

Many different gene therapy approaches have been currently developed which can be classified in five major groups including gene correction therapy, enzyme/prodrug therapy, immuno-gene therapy, drug resistance gene therapy and chemo-gene therapy.

Gene correction therapy

Gene correction therapy corresponds to the classical gene therapy approaches in which genetic anomalies, responsible for the pathology, are corrected usually by the replacement of an inactivated tumor suppressor gene or by the down-regulation of an activated oncogene.

Any protein, whose activity is required for tumor generation, progression and spread or just contributes to the tumor phenotype maintenance, is a putative target to be downregulated by interfering RNAs (iRNAs). However, usually the most significant antitumoral effect is achieved by the knockdown of those genes mutated in the first stages of the tumorigenic multistep process or those involved in the tumor phenotype maintenance. Small interfering (siRNA) molecules are the most used iRNA molecules in this kind of treatments since their inhibitory efficacy has been widely described and their specificity is so high that they are able to distinguish single-base mutated oncogenes from the wild type genes, considerably reducing possible side effects^{50, 172, 198-200}. In this context, different approaches have been followed to inhibit Ras family of proteins, mutated in about 30% of human tumors²⁰¹.

Tumor suppressor genes are involved in cell cycle control by inducing cell cycle arrest and/or apoptosis. Restoration of tumor suppressor genes is another interesting strategy where mutated or inactivated gene activity is replaced by a correct copy of that gene²⁰². Among them, *P53* gene is one of the most important and widely studied tumor suppressor genes, since mutations in this gene have been found in 40% of human cancers^{203, 204}. *P53* is responsible for the detection of DNA damages followed by repair initiation or apoptosis induction. Many approaches have been already performed in which *P53* gene has been transferred to tumor cells²⁰⁴. Promising expectations have been generated on this strategy since successful cell arrest and apoptosis induction has been observed in some of those experiments^{205, 206}. Expression of other transferred tumor suppressor genes as *RB* or *BRCA-1* among others have also been tested for their antitumor activity^{204, 207}.

Enzyme / prodrug therapy

Enzyme-prodrug therapy, also known as suicide gene therapy, is a two-step process consisting in the transference of a prodrug converting enzyme gene (suicide gene) to target cancer cells and the following administration of a low toxic inactive prodrug.

Once the administered prodrug reaches enzyme expressing cancer cells, is metabolized and converted to a cytotoxic drug, limiting this way its toxic effects to only those tumor cells where suicide gene has previously integrated. Moreover, one of the major advantages of this type of therapy is the so-called “bystander effect” in which the expressed enzyme or the active cytotoxic drug are able to pass between adjacent cells by cellular gap junctions allowing the ablation of the entire tumor although not all the tumor cells have been transfected with the suicide gene^{208, 209}. The most used suicide gene prodrug combinations include the Thymidine kinase gene that transforms the non-toxic ganciclovir into a cytotoxic form by its phosphorylation, or the cytosine deaminase gene that transforms non-toxic 5-fluorocytosine molecules into the widely used chemotherapeutic drug 5-fluorouracil, among others (Table 4)^{210, 211}. Double enzyme/prodrug therapy approaches have also been tested in some cancers where combined suicide genes have been transfected to cancer cells showing better performance than single gene therapy²¹².

Enzyme	Inactive prodrug	Active metabolite	Mechanism of action
Thymidine kinase	Ganciclovir	Ganciclovir triphosphate	Inhibition of DNA polymerase.
Cytosine deaminase	5 Fluorocytosine	5 Fluorouracil	Inhibition of thymidylate synthase.
Thymidine phosphorylase	5'-deoxy-5-fluorouridine	5 Fluorouracil	Inhibition of thymidylate synthase.
Nitro-reductase	CB1954	Bifunctional alkylating agent	Formation of DNA cross links.

Table 4. Enzyme-Prodrug gene therapy.

Immunogene therapy

Tumor cells are usually recognized and destroyed by CD8⁺ T lymphocytes and natural killer cells. However, many tumors have successfully evaded immune system because of the poor antigenicity of tumor antigens, the lac of MHC molecules and the secretion of immunosuppressive factors²¹³. The induction of tumor antigen recognition by immune system is an interesting approach that is being currently studied. Gene transference and overexpression of immune cytokines and chemokines in cancer cells can induce tumoral antigens recognition and the consequent tumor cell destruction by the immune system. A number of studies have already been performed using such approaches, yielding some promising results²¹⁴⁻²¹⁷.

Drug resistance therapy

Drug resistance gene therapy is still only a potential and experimental gene therapy approach. It consists in conferring higher drug resistance capacity to those cells and tissues that are more vulnerable to drug toxicity in order to higher drug doses be tolerated. The main limiting factor for patient’s chemotherapy is the bone narrow toxicity. In this context, multiple drug resistance gene (*MDR1*) has been described that

Introduction

transferred to bone marrow cells might confer them resistance to some alkanoids, anthrocyclins and paclitaxel²¹⁸⁻²²⁰.

Chemo-gene therapy

Chemo-gene therapy combines conventional chemotherapy treatments with the transference of a gene that enhances drug sensitivity of tumor cells. The synergistic effect obtained by the combination of both therapies confers much higher antitumor efficacy. Many different combinations have been already tested in which really interesting synergistic effects have been observed²²¹⁻²²⁵.

3.2 Gene therapy vectors

Two different methods have been developed for gene transfer into target cells. The first method (*in vivo*) consists in *in vivo* transfer of exogenous nucleic acids by local or systemic administration, while in the second method (*ex vivo*), nucleic acids are transferred *in vitro* to cultured patient cells and later reintroduced into patients. In both cases, targeted vector, charged with the corresponding nucleic acids, is generally required and although different types of vectors have been developed for their use in gene therapy, all of them can be classified in two groups: viral and non-viral vectors.

Viral vectors

Viruses, being strict intracellular parasites, are natural vectors for cell targeted nucleic acid delivery. In this context, genetically modified viruses that lack their infective and replication potential and incorporate the therapeutic genes in their genome have been generated for their use as gene therapy vectors. Those vectors exploit viral natural abilities such as cell specific binding and uptake, genetic cargo delivery in cell nucleus or genomic integration in some cases, resulting in extremely efficient vehicles for targeted nucleic acid delivery.

Since the first human gene therapy trial using a retrovirus vector was performed in 1989²²⁶, a variety of viral families have been engineered including retroviruses, lentiviruses, adenoviruses or adeno-associated viruses. All of them offer different properties regarding cell tropism, integration ability and quiescent cell infection capacity. Permanent gene expression can be achieved in target cells using integrative viruses while only transient gene expression can be obtained with non-integrative viral vectors^{218, 227}. However, the random integration of viral genomes can generate severe side effects in target cells by insertional mutagenesis^{228, 229}. In this context, although most of the gene therapy vectors under current investigation correspond to viral vectors, many concerns about their biosafety still remain²³⁰. Strong inflammation immune responses have been described²³¹⁻²³³ and reported cases in which successfully treated patients developed leukemia being fatal in one patient, resulted in an inflexion point regarding viral vectors biosafety consideration^{234, 235}.

Thus, even though viral vectors have widely demonstrated their extremely efficient performance for gene therapy approaches (It has been recently approved the first viral gene therapy treatment in the European Union²³⁶), their high associated immune toxicity and unmet biosafety aspects, are still generally unacceptable and imposes the huge necessity for the development of more safe gene therapy vectors.

Non-viral vectors

Non-viral gene therapy vectors include all those currently available nanoparticles able to specifically bind and deliver nucleic acid molecules into target cells (Figure 10). Many nanoparticles have been already developed for gene therapy applications showing high cell specificity and good transfection efficiency being the most used ones, cationic lipids, polymers and protein nanoparticles among other^{128, 237}. All the currently available nanoparticles have been widely discussed in previous sections of this introduction.

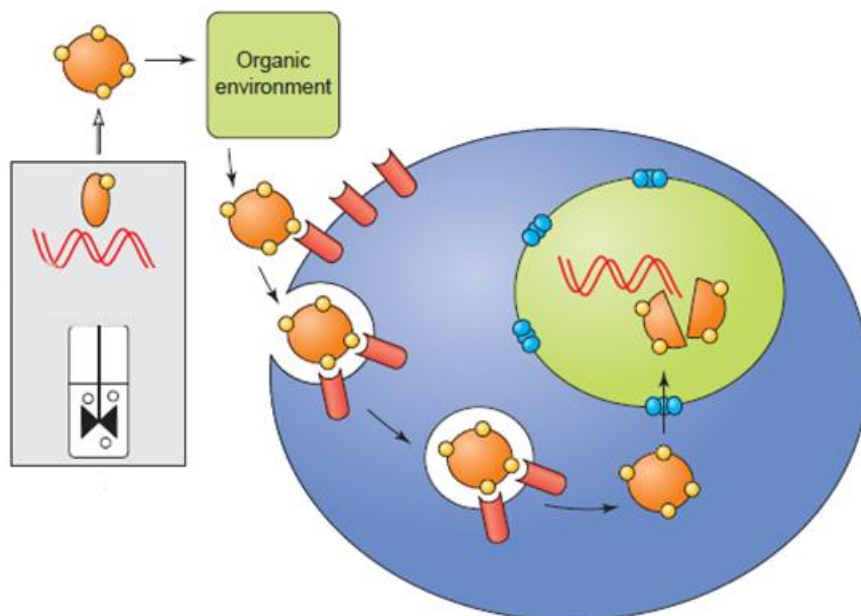


Figure 10. Formulation and activities of non-viral gene therapy vectors. Produced non-viral vector is properly formulated with an adequate therapeutic nucleic acid. The final particle has to successfully recognize target cell, be efficiently internalized and deliver transported nucleic acid in the appropriate subcellular compartment. (Modified from Aris A. *et al* 2004).

Non-viral gene therapy vectors represent a feasible alternative to those risky but extremely efficient viral vectors, since they generally show higher biosafety and lower toxicity profiles. However, they still have some drawbacks such as lower transfection efficacy and low transient gene expression levels^{130, 238}. It has been described that 10^6 naked DNA plasmid molecules are needed to efficiently transform a single cell; from

Introduction

them, only 10^2 to 10^4 will reach cell nucleus²³⁹. Moreover, the transference need to be very fast since plasmidic DNA is highly sensitive to cytoplasmatic calcium dependent nucleases having a half live of only 50-90min²⁴⁰. Thus, improvement of nucleic acid delivery efficiency of those vectors is one of the mayor challenges for this type of therapy. Nevertheless, some cases where lower transgene expression for the therapeutic action is more desirable have also been described²⁴¹.

After more than three decades of research and hundreds of clinical trials performed, only four products have been marketed for their clinical use in human patients and although most of the gene therapy particles under study correspond to viral vectors (Figure 11), only a adeno-associated viral vector engineered to express lipoprotein lipase in muscle cells (Glybera) has been recently approved for its use in western countries^{236, 242}. A replication deficient adenoviral vector transfecting *P53* gene (Gendicine) has been also approved for its use exclusively in China²⁴³. Non-viral gene therapy products currently available in Europe and USA include Vitravene, an antisense oligonucleotide complementary to one of cytomegalovirus early genes²⁴⁴ and Macugen, a synthetic pegylated oligonucleotide that specifically binds vascular endothelial growth factor gene^{245, 246}. Thus, although they show lower transfection efficiency than viral vectors and less clinical trials have been performed, most of the marketed gene therapy products in Europe and USA still correspond to non-viral approaches supporting the idea that they represent more reliable alternative at this moment.

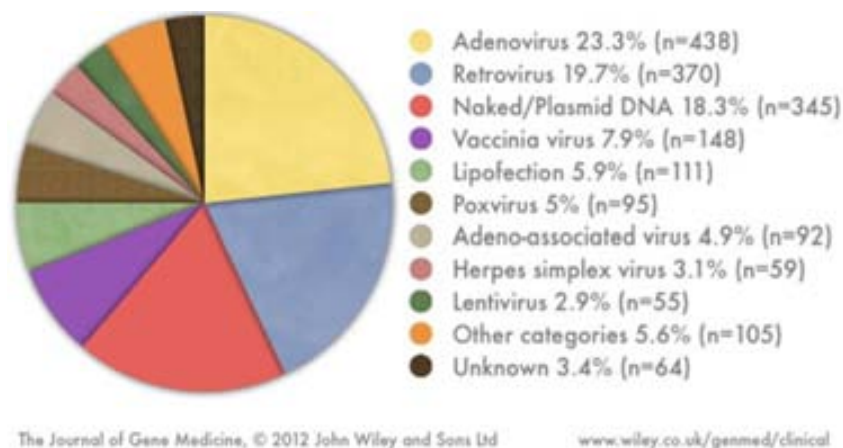


Figure 11. Gene therapy vectors used in clinical trials. (2012; John Wiley and Sons Ltd)

Since biosafety is currently the mayor concern regarding gene therapy approaches, huge efforts are being made on enhancing biological efficiency of non-viral vectors. Although the science of non-viral vector gene therapy is still in its infancy all available data suggest that they will represent the long-term future of gene therapy. Thus, future science directions should go in the development of more efficient and better performing non-viral gene therapy vectors.

3.3 Protein-only gene therapy vectors

Non-viral gene therapy nanoparticle vectors usually are named as artificial viruses since they mimic viral particles in their composition, size and biological activities. For their successful application, those particles need to have some abilities as nucleic acid binding, specific cell recognition and uptake, endosomal escape and nuclear transport for expressible DNA. Although different nanomaterials have been used for their generation¹²⁸, protein-only artificial viruses show very promising properties for their application in current nanomedicines as gene therapy regarding biocompatibility.

VLPs have successfully been used for nucleic acid transference using papillomavirus and polyomavirus proteins²⁴⁷. However, since VLPs of only a limited number of viral families can be efficiently produced, their applicability in gene therapy is strongly limited. As a different approach, multifunctional protein nanoparticles have been also produced for nucleic acid delivery without necessarily mimicking viral capsids. Most of those particles have been generated following genetic engineering techniques and reproducing a modular structure that combines different functional domains conferring all necessary biological activities for their successful application^{128, 129}. Different multifunctional proteins have been already tested for their use in gene therapy approaches²⁴⁸⁻²⁵² and although some immunological responses can be observed specially after repeated administrations, the possibility of selecting human protein carriers or human functional domains can considerably minimize this effect¹²⁹.

Since our group has wide expertise in the generation and use of this type of multifunctional protein-only nanoparticles for gene therapy approaches with successful results^{129, 169, 172, 173, 177, 192-194, 253-258}, we focused our research on the generation of new multifunctional protein vectors applicable to different therapeutic models and specifically in this project to be used in colon cancer.

4. Protein-only gene therapy in colorectal cancer

Being the third most common type of cancer, many efforts have been made for the development of efficient therapeutic processes for the successful treatment of colorectal cancer. However, the overall five-year survival rate for colon cancer is 60 percent using current therapies, being mortality related to the appearance of metastatic foci. Current genotoxic treatments have a systemic toxicity that prevent from using higher doses, and attempting to target the drug to cancer cells with antibodies have not improved much the prognosis of these patients due to the low penetrability into the tumor. Therefore, there is an urgent necessity of therapies targeted to metastatic cancer cells. In this context, target-specific gene therapy appears as a very promising tool for the development of much more effective treatments. This innovative approach allows the targeted performance of therapeutic nucleic acids in cancer cells specifically acting over desired molecular targets in a personalized way and dramatically reducing non desired off-target toxic effects. Moreover, the possibility to act over those molecular targets directly involved in metastatic processes opens a wide spectrum of new possibilities to overcome the current main milestone in colon cancer. For the development of those therapeutic actions, multifunctional protein nanoparticles appear as one of the most promising gene therapy vectors due to their high biocompatibility, low toxicity and easy tuneability, advantages that make them very appropriate for targeted nucleic acid delivery approaches.

The successful application of those nanoparticles strongly depends on their correct targeting, so the identification and incorporation of appropriate peptide ligands that specifically recognize cell surface receptors on colon cancer cells, is completely imperative. Different cell surface receptors have been described to be overexpressed in colonic tumor cells such as VEGFR, CXCR4, CD44 or EGFR, among others. However, CXCR4 is the one that has generated most interest since it is specifically involved in metastatic processes and it is therefore associated to bad prognosis²⁵⁹. Furthermore, being also one of the HIV co-receptors, CXCR4 blockers have been widely studied. Thus, the highly available knowledge and its direct implication in tumoral and metastatic processes make CXCR4 an appropriate target molecule for the specific cell recognition of gene therapy vectors in colorectal cancer.

4.1 CXCR4 receptor

CXCR4 has been described to be the only chemokine receptor essential for life. It is expressed in many different human cells and tissues such as lymphocytes, neurons, thymus or lung among other, and it has been found to be overexpressed in many human cancer cells including colon cancer. Among its main functions are the intracellular signaling and bidirectional migration (chemotaxia), playing an important

role in hematopoietic cell homing and gastrointestinal vascularization. Since its activation induces the production of VEGF, which is an angiogenesis stimulator, and also MMP9, which is involved in extracellular matrix degradation, CXCR4 is directly involved in metastatic processes and its overexpression in tumor cells has been related to bad prognosis^{57, 260}.

Only one natural ligand recognizing the CXCR4 receptor has been described in human body: The CXCL12 chemokine. However, other peptidic ligands also specifically recognizing the CXCR4 receptor have been described in other organisms (table 5)²⁶¹.

Ligand	Amino acid sequence	IC ₅₀ (nM)	Internalization described
CXCL12 α (SDF1 α)	KPVSLSYRCPCRFFESHVARANVKHLKILNTPNCALQ IVARLKNNNRQVCIDPKLKWIQEYLEKALN	3.6	Yes
V3	CTRPNNNTRKSIHIGPGRAFYTTEIICDIRQAHC	N/A	No
vCCL2	LGASWHRPDKCCLGYQKRPLPQVLLSSWYPTSQLCS KPGVIFLTKRGRQVCADKSKDWVKKLMQQLPVTA	5.8	No
V1 (1-21 vCCL2)	LGASWHRPDKCCLGYQKRPLP	190	Yes
T22	RRWCYRKCYKGYCYRKCR	5.1	No
ALX40-4C (9R)	RRRRRRRRR	N/A	Yes

Table 5. Binding affinity of CXCR4 ligands. IC₅₀: Inhibition of ligand binding to CXCR4.

CXCL12 (SDF1)

CXCL12, also known as SDF1, is the only natural ligand of CXCR4 in human body. It is a highly basic alpha chemokine and it is implicated in chemotaxis processes and B-cell maturation acting as pre-Bcell growth stimulatory factor. Six different isoforms only differing in their C-terminal ends have been described but the most used and studied one corresponds to the CXCL12 α isoform (SDF1 α)^{261, 262}. CXCL12 interacts with the CXCR4 receptor by different protein regions in a two-step mechanism^{263, 264} and it has been observed that the ligand-receptor interaction efficiently induces the complex internalization by an endocytic pathway²⁶⁵. Many CXCL12 protein derivatives have also been generated and described to specifically bind to CXCR4 receptor but most of them have shown to have lower receptor affinity than the natural ligand^{261, 266, 267}.

V3 peptide

HIV interacts with human lymphocyte CD4 and CXCR4 receptors using envelope protein gp120. It is known that the V3 domain of gp120 specifically interacts with CXCR4 receptor and it has also been described that this interaction occurs at the same place where CXCL12 protein interacts^{261, 268}. Since HIV is extremely efficient infecting human cells, this protein appears as very promising ligand for CXCR4 targeting. However, it has been described that the receptor affinity of isolated V3 peptide is not as high as the natural ligand. Some V3 peptide derivatives have also been generated but they have not shown better receptor affinity²⁶¹.

Introduction

vCCL2 and V1peptide

Viral macrophage inflammatory protein II (vMIPII) also known as vCCL2, is a viral chemokine produced by the herpes virus simple 8 that has been described to interact with many human alpha and beta chemokine receptors including CXCR4. Although it shows very high affinity for CXCR4 receptor, its low specificity strongly compromises its targeted delivery applicability. However, some vCCL2 derivatives have been developed showing better CXCR4 specificity among which the named V1 peptide appears as one of the most interesting one^{261, 269}.

V1 peptide corresponds to the first 21 amino acids of the vCCL2 chemokine and although its affinity is considerably lower, it only recognizes the CXCR4 receptor. Moreover, it has been described that V1 peptide-receptor interaction induces ligand-receptor complex internalization²⁷⁰.

T22 protein

Polyphemusin II is a basic protein extracted from horseshoe crabs' blood that has been described to specifically interact with CXCR4 receptor. Among their derivatives, T22 protein appears as the most promising protein for CXCR4 targeting since it shows 200 times higher receptor affinity.

T22 protein has been created by the introduction of three amino acid mutations in polyphemusin II protein (Tyr5, Lys7 and Tyr12) that increases protein global positive charge enhancing electrostatic interaction between protein and the CXCR4 receptor. The protein specifically interacts with the N-terminus and two first extracellular loops of the receptor where protein's Tyr-Arg-Lys motives appear to be key structures in the interaction. However, no ligand-receptor complex internalization has been described yet. Some T22 protein derivatives, that have achieved higher receptor affinity by the introduction of synthetic amino acids, have been also described. However, the presence of synthetic amino acids, limit their productivity in biological systems^{261, 271}.

ALX40-4C protein (R9)

The R9 peptide, which is generated by just 9 arginines and which is also named as ALX40-AC protein, have been reported to electrostatically interact with the CXCR4 receptor. However, this protein have been also described to act as cell penetrating peptide (CPP) and shown to unspecifically interact with other cell surface molecules^{172, 261, 272, 273}.

In order to select the most appropriate ligand for the successful and efficient cell targeting of gene therapy vectors, two major properties have to be taken into account. The affinity is the most important property since the higher the affinity is, the lower the administrated dose will be and consequently this decreases potential toxicity. By the other hand, previous ligand-receptor complex internalization studies are another important parameter to be considered since the uptake of the targeted vector is an indispensable step for the successful application of these therapies. Thus, these two properties, among others, are important to be considered for the final design of a specific vector for gene therapy.

4.2 Target genes in colorectal cancer

Selecting an appropriate target gene, results as important as achieving a good cell-specific targeting for the success of gene therapy in colorectal cancer. Being one of the most frequent and studied tumor types, all the therapeutic targets have already been perfectly identified, so the most appropriate target gene has to be selected in each individual case depending on the tumor genotype in order to design a personalized gene therapy treatment. In this context, *K-Ras* gene appears as one of the most important therapeutic target for gene therapy treatments in colorectal cancer, since it has been found to be mutated in about 40% of all the reported cases^{46, 274}.

K-Ras

Ras gene superfamily codifies for small GTPase proteins implicated in the regulation of many cellular processes. Three different *Ras* alleles have been identified including *H-Ras*, *K-Ras* and *N-Ras*. Being one of the most common mutations in human cancers, *K-Ras*, which has been described to be directly implicated in many intracellular signaling pathways such as MAPK, PI3 kinase, Phospholipase C and Ral pathways, is one of the most widely studied oncogenes (Figure 12). Specifically, it has been found to be mutated in 40% of total colon cancer cases being the most common mutations *K-RasVal12*, *K-RasAsp12* and *K-RasVal13*. Those mutations constitutively activate *K-Ras* protein by the inactivation of its intrinsic GTPase activity, strongly affecting those cellular functions controlled by this protein such as cell proliferation (stimulation), cellular mobility, cell apoptosis (inhibition) and cytoskeleton organization^{46, 274, 275}.

In this context, mutations in *K-Ras* gene have been directly related with aggressive and metastatic behavior of tumor cells. Moreover it has also been described that mutations in *K-Ras* are associated to resistance to some chemotherapeutic agents such as 5-Fluorouracil²⁷⁵.

Thus, the targeted nucleic acid delivery for the downregulation of *K-Ras* gene with deleterious effects appears as a very promising therapeutic approach for the successful treatment of metastatic colon cancer patients, even more with the fact that we can

Introduction

improve specificity by interfering just the mutated gene without affecting the wild type transcribed in non-tumoral cells⁵⁰.

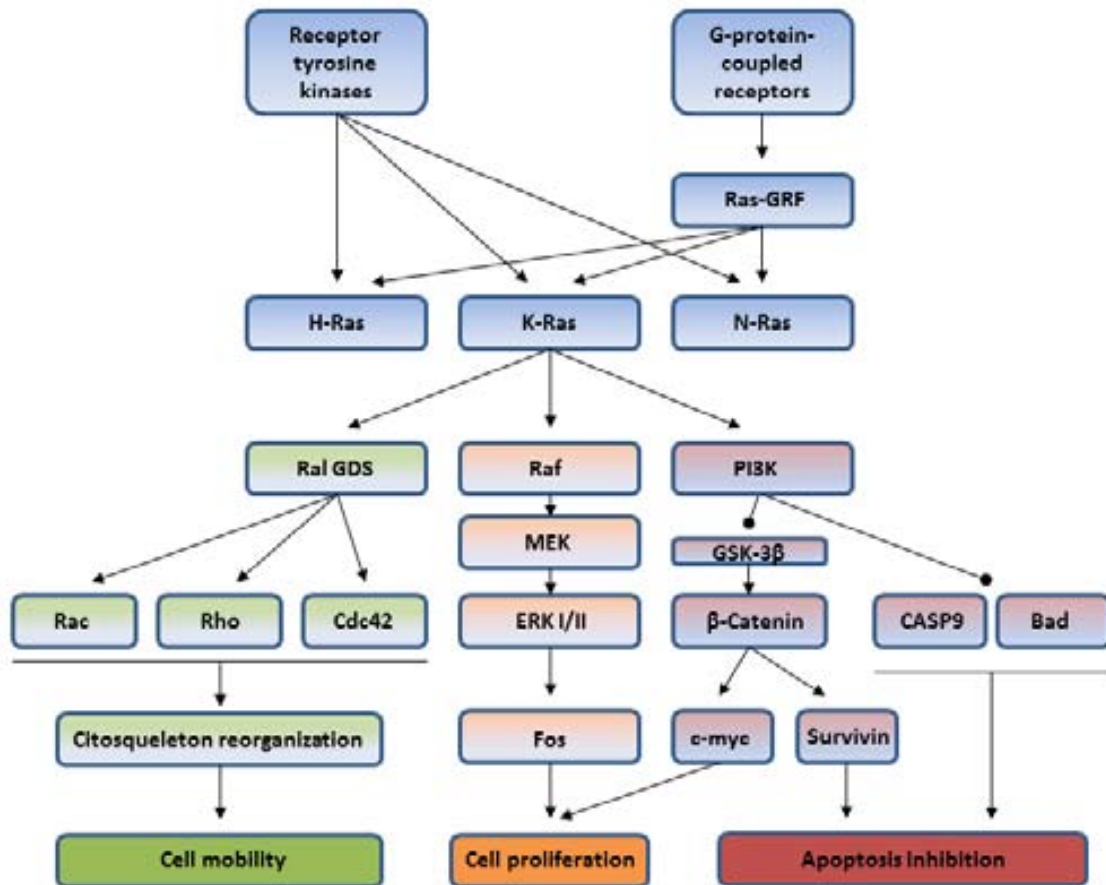


Figure 12. K-Ras oncogene signaling pathway (Adapted from 05210-Kanehisa labs. and Chapman 2002)

5. Overview

Cancer is ranked as the second leading cause of death worldwide. Consequently there is a huge necessity of finding more effective cancer therapies. Currently available cancer therapies, far from being effective, present high systemic toxicity and low patient survival rates being the main mortality cause the appearance of metastatic foci, especially in colon cancer. Thus, improving cell specificity and avoiding metastases generation are the mayor challenges for future cancer therapies. In this context, gene therapy appears as very promising alternative therapy since cell targeted personalized therapies can be performed with low systemic toxicity. Since biosafety is the current mayor concern in this type of therapies, multifunctional proteins appear as the most promising gene therapy vectors because of their high biocompatibility and biosafety, low toxicity and really complete tuneability. The necessity of adequate nanoparticle size for their efficient biodistribution and delivery has been widely discussed in this introduction. It is important in this context, to study and understand which are the factors that drive the self-assembling capacity of proteins in particles of defined size distribution, in order to rationally get the full potential of those nanoparticles for their subsequent application in colorectal cancer gene therapy. For this purpose, CXCR4 receptor has been proposed as the most appropriate cell-targeting molecule for the efficient delivery in colorectal metastatic cells, and *K-Ras* oncogene downregulation has been claimed to be the most effective therapeutic action not only for the treatment of solid tumors but more specially to avoid the metastatic foci appearance.

Thus, we think that the design, generation and characterization of multifunctional proteins with the adequate nanoparticle size for the efficient and specific delivery of drugs or nucleic acids (e.g. mutated *K-ras* allele-specific therapeutic siRNA molecules) in CXCR4 overexpressing colon cancer cells, may result an important turning point in the successful application of non-viral gene therapy treatments in metastatic colon cancer.



Objectives

The aim of this study is to engineer protein-protein interactions in recombinant proteins for the construction of functional protein-based nanoparticles and to determine the suitability of self-assembled entities as nanomedical tools for targeted nucleic acid delivery in metastatic colorectal cancer. In this regard, this work has been firstly focused on the identification and characterization of architectonic peptidic tags to induce the self-assembling of functionalized protein monomers into size compatible nanoscale entities. Then, the applicability of this type of particles for the appropriate tumor specific biodistribution and the subsequent therapeutic nucleic acid delivery in a metastatic colorectal cancer model has been extensively analyzed. In order to reach these goals, we planned the following objectives:

1. To explore the possibility of effectively controlling the self-assembly of protein nanoparticles by the incorporation of selected functional modules acting as architectonic tags.
2. To analyze the intracellular trafficking and stability of self-assembled protein nanoparticles when they are exposed to cultured cells.
3. To construct CXCR4+ cell-targeted self-assembling protein nanoparticles and assess their biodistribution in a metastatic colorectal cancer murine model.
4. To determine the stability of the supramolecular complexes *in vivo*.
5. To characterize the DNA condensation and protection capacity of nucleic acid binding domains in self-assembled protein nanoparticles for their use as artificial viruses.
6. To determine the suitability of generated artificial viruses as targeted nucleic acid delivery vectors for gene therapy approaches.



Results

Paper 1**Non-amyloidogenic peptide tags for the regulatable self-assembling of protein-only nanoparticles.**

Ugutz Unzueta, Neus Ferrer-Miralles, Juan Cedano, Xu Zikung, Mireia Pesarrodona, Paolo Saccardo, Elena García-Fruitós, Joan Domingo-Espín, Pradeep Kumar, Kailash C. Gupta, Ramón Mangues, Antonio Villaverde, Esther Vazquez.

Biomaterials, 33, 8714-8722, 2012

Controlling the size of generated nanoparticles has been extensively proven to be an important requisite for their successful application in nanomedicine. In this work, we explore the possibility of effectively modulating the protein monomers self-assembling by the incorporation of peptidic architectonic tags in order to regulate the formation of protein nanoparticles of the optimal size for a correct *in vivo* biodistribution. For that, different arginine-rich and other cationic peptides have been tested for their ability to induce the self-assembling of monomeric building blocks in monodisperse, protein-only nanoparticles when they are incorporated to His-tagged proteins. We have deeply examined in this study the role of cationic peptides and poly-histidine as an architectonic tag pair.

We have observed how the combination of cationic peptides and hexa-histidine tail fused to the amino and carboxy termini respectively, can induce the self-assembling of different proteins in nanoparticles whose properties can be regulated by pH during the particle formation. Moreover, the obtained results suggest that the cationic nature of the tag may determine its architectonic potential and influence the size of the resulting construct. Additionally, we have provided evidences to prove that the architectonic properties of the tag pair are supported by electrostatic interactions between protein monomers driven by the cationic tag primarily, and subsidiarily, by the hexa-histidine tail when it gets protonated at slightly acidic pHs.

Thus, the incorporation of this architectonic tag pair to different protein species acting as monomers opens up the possibility of effectively controlling their self-assembling potential for the generation of size compatible protein-only nanoparticles.



Non-amyloidogenic peptide tags for the regulatable self-assembling of protein-only nanoparticles

Ugutzu Unzueta^{a,b,c}, Neus Ferrer-Miralles^{a,b,c}, Juan Cedano^d, Xu Zikung^{a,b,c}, Mireia Pesarrodonà^{a,b,c}, Paolo Saccardo^{a,b,c}, Elena García-Fruitós^{a,b,c}, Joan Domingo-Espín^{a,b,c}, Pradeep Kumar^e, Kailash C. Gupta^f, Ramón Mangues^g, Antonio Villaverde^{a,b,c,*}, Esther Vazquez^{a,b,c}

^a Institut de Biotecnologia i de Biomedicina, Universitat Autònoma de Barcelona, Bellaterra, 08193 Barcelona, Spain

^b Departament de Genètica i de Microbiologia, Universitat Autònoma de Barcelona, Bellaterra, 08193 Barcelona, Spain

^c CIBER de Biotecnologia, Biomateriales y Nanomedicina (CIBER-BBN), Bellaterra, 08193 Barcelona, Spain

^d Laboratory of Immunology, Regional Norte, Universidad de la República, Gral. Rivera 1350, Salto 50.000, Uruguay

^e CSIR, Institute of Genomics and Integrative Biology, University Campus, Mall Road, Delhi 110007, India

^f CSIR, Indian Institute of Toxicology Research, Mahatma Gandhi Marg, Lucknow 226001, Uttar Pradesh, India

^g Grup d'Oncogènesi i Antitumoral, Institut de Recerca, Hospital de la Santa Creu i Sant Pau, Barcelona, Spain

ARTICLE INFO

Article history:

Received 31 July 2012

Accepted 15 August 2012

Available online 3 September 2012

Keywords:

Nanoparticles

Artificial viruses

Peptide tags

Protein engineering

Cationic peptides

Electrostatic interactions

ABSTRACT

Controlling the self-assembling of building blocks as nanoscale entities is a requisite for the generation of bio-inspired vehicles for nanomedicines. A wide spectrum of functional peptides has been incorporated to different types of nanoparticles for the delivery of conventional drugs and nucleic acids, enabling receptor-specific cell binding and internalization, endosomal escape, cytosolic trafficking, nuclear targeting and DNA condensation. However, the development of architectonic tags to induce the self-assembling of functionalized monomers has been essentially neglected. We have examined here the nanoscale architectonic capabilities of arginine-rich cationic peptides, that when displayed on His-tagged proteins, promote their self-assembling as monodisperse, protein-only nanoparticles. The scrutiny of the cross-molecular interactivity cooperatively conferred by poly-arginines and poly-histidines has identified regulatable electrostatic interactions between building blocks that can also be engineered to encapsulate cargo DNA. The combined use of cationic peptides and poly-histidine tags offers an unusually versatile approach for the tailored design and biofabrication of protein-based nano-therapeutics, beyond the more limited spectrum of possibilities so far offered by self-assembling amyloidogenic peptides.

© 2012 Elsevier Ltd. All rights reserved.

1. Introduction

Viral capsid proteins self-assemble as complex, highly symmetric particles that act as natural cages for the cell-targeted delivery of their genomes. The tailored construction of virus-inspired complexes is a promising route to drug delivery [1–7]. Being devoid of any infectious material, “artificial viruses” [8] do not show the undesired biological side effects associated to administration of viruses in viral gene therapy [9]. In this context, virus-like particles (VLPs), microbial organelles, [10], multifunctional proteins [11] and a spectrum of diverse vesicular materials are under development as carriers for therapeutic nucleic acids or

conventional drugs. Many functional peptides have been identified from nature or selected by directed molecular evolution as ligands for cell surface receptors, membrane-active peptides and nuclear localization signals [4–6,12]. When conveniently pooled, these tag-mediated activities confer virus-like properties to the resulting multifunctional entities. In protein-only vehicles, all these domains can be covalently combined in single chain molecules that constitute the monomeric building blocks [11]. However, peptides enabling their holding proteins to organize as nanosized particles have so far been unidentified. The so-called self-assembling peptides, that might have been potentially promising for nanoparticle generation, are in general amyloidogenic protein segments that form fibers, membranes or hydrogels [13,14]. When used in fusion proteins, these peptides induce protein aggregation [15,16], being useless as tags for nanoparticle formation. Therefore, promoting the assembling of a selected protein as nanoparticles is so far excluded from rational engineering.

* Corresponding author. Institut de Biotecnologia i de Biomedicina, Universitat Autònoma de Barcelona, Bellaterra, 08193 Barcelona, Spain.

E-mail addresses: antoni.villaverde@uab.cat, prof.avillaverde@gmail.com (A. Villaverde).

We have very recently described that a nine-arginine peptide (R9), when displayed on the surface of a recombinant, His-tagged GFP, promotes the self-assembly of the whole fusion protein as regular nanoparticles of about 20 nm in diameter [17]. These constructs efficiently penetrate cultured mammalian cells by an endocytic pathway [18], cross the nuclear membrane, accumulate in the nucleus and allow the expression of a carried transgene [17]. The formation of these supramolecular complexes is completely distinguishable from unspecific protein aggregation [7,19,20]. Cationic peptides, including poly-arginines of different lengths, are well known by their membrane-crossing and DNA-condensation abilities, and widely used in gene therapy and more generally in drug delivery [5,6,12,21]. However, if showing a general applicability, such a newly described architectonic ability would be specially promising for the easy engineering of protein nanoparticles formed by specific proteins with desired biological activities.

To explore the possibility of effectively controlling the assembly of protein nanoparticles, we have examined here the role of cationic peptides and poly-histidines as an architectonic tag pair. These agents, upon incorporated into monomeric building blocks, synergistically cooperate in promoting nanoparticle formation by balancing, in a regulatable way, protein–protein and protein–DNA interactions. The potential of the ‘nano-architectonic tag’ concept is discussed here in the context of the design of smart, protein-based particles by conventional genetic engineering.

2. Materials and methods

2.1. Protein design and gene cloning

Several derivatives of R9–GFP–H6 containing decreasing numbers of arginine residues were constructed in house by site directed mutagenesis of the parental clone, by replacing these residues by glycines and alanines to keep the length of the peptide tag constant (Table 1). The new constructs R7–GFP–H6, R6–GFP–H6 and R3–GFP–H6 were efficiently produced in *Escherichia coli* Rosetta from the vector pET21b (Novagen 69744-3). Nine additional derivatives of GFP–H6 containing diverse amino terminal peptides of variable amino acid sequence, length and charge (Table 2), were designed in-house, provided by Genent (Regensburg, Germany) or GenScript (Piscataway, USA), and produced from pET22b in *Escherichia coli* Origami B (BL21, OmpT⁻, Lon⁻, TrxB⁻, Gor⁻ (Novagen)) and the related strain BL21(DE3) for characterization.

2.2. Protein production and purification

Bacterial cells carrying the appropriate plasmid vectors were grown in shaker flask in Luria–Bertani (LB) medium containing 34 µg/ml chloramphenicol, 12.5 µg/ml tetracycline (strain resistance) and 100 µg/ml ampicillin (vector resistance) at 37 °C to $A_{550} = 0.5–0.7$. Recombinant gene expression was induced overnight at 20 °C by 0.1 mM isopropyl-β-D-thiogalactopyranoside (IPTG). Cell cultures were then centrifuged for 45 min (5,000g at 4 °C) and resuspended in Tris buffer (Tris 20 mM pH 8.0, NaCl 500 mM, Imidazol 10 mM) in the presence of EDTA-Free protease inhibitor (Complete EDTA-Free; Roche). The cells were then disrupted at 1100 psi using a French Press (Thermo FA-078A).

Table 1

Peak size (in nm) of Rn–GFP–H6 nanoparticles in low salt and high salt buffers. The occurrence of larger soluble particles and their size is also indicated. Relevant properties of the cationic tag are also depicted.

Tag name	Sequence	Size in low salt buffer ^a (larger particles)/PDI	Size in high salt buffer ^b (larger particles)/PDI	Number of arginines
R9	RRRRRRRR	23.0/0.2	20.4/0.3	9
R7	RRRGRRRR	37.9/0.2	6.5/0.5	7
R6	RARGRRRR	15.5 (827.1)/0.7	8.5/0.4	6
R3	RARGGGGA	14 (240.9, 526.9)/0.7	7.0/0.7	3

PDI: polydispersion index.

^a Tris–dextrose.

^b Tris–NaCl.

Proteins were purified by 6×His-tag affinity chromatography using HiTrap Chelating HP 1 ml columns (GE healthcare) by ÄKTA purifier FPLC (GE healthcare). Filtered cell extracts were loaded onto the HiTrap column after insoluble cell fraction separation by centrifugation (15,000g at 4 °C). The column was washed with Tris 20 mM, 500 mM NaCl, 10 mM Imidazole, pH 8.0. Proteins were eluted with a high imidazole content buffer (Tris 20 mM pH 8.0, 500 mM NaCl, 500 mM Imidazol) in a linear gradient. The recombinant protein production has been performed in the Protein Production Platform (CIBER-BBN-UAB) (<http://bbn.ciberbbn.es/programas/plataformas/equipamiento>).

After purification, selected protein fractions were dialyzed overnight at 4 °C. Protein stability had been previously tested in several buffers from which the most appropriate regarding protein stability were selected in a per case basis. Low salt buffers were carbonate buffer (166 mM NaHCO₃, pH 7.4), Tris dextrose (20 mM Tris 500 mM + 5% dextrose pH 7.4) and PBS glycerol (140 mM NaCl, 7.5 mM Na₂HPO₄, 2.5 mM NaH₂PO₄ + 10% glycerol pH 7.4). The high salt buffer was always Tris–NaCl (20 mM Tris 500 mM NaCl pH 7.4). Proteins were finally aliquoted in small samples (30 µl) after 0.22 µm pore membrane filtration. Proteins were characterized by mass spectrometry and N-terminal sequencing and their amounts determined by Bradford's assay [22].

2.3. Fluorescence determination and dynamic light scattering (DLS)

Protein fluorescence was determined by Cary Eclipse Fluorescence Spectrophotometer (Variant) at detection wavelength of 510 nm by using an excitation wavelength of 450 nm. Volume size distribution of nanoparticles and monomeric GFP fusions were determined by dynamic light scattering at 633 nm (Zetasizer Nano ZS, Malvern Instruments Limited, Malvern, UK).

2.4. Transmission electron microscopy (TEM)

For transmission electron microscopy, proteins purified as described above were diluted to 0.2 mg/ml, deposited onto carbon-coated grids and contrasted by the evaporation of 1 nm platinum layer. These samples were observed in a Hitachi H-7000 transmission electron microscope.

2.5. Determination of protein physicochemical properties

Protein physicochemical properties including molecular weight, isoelectric point, aliphatic index, hydrophobicity and stability index were determined in silico by ‘ProtParam’ software (ExPASy). Protein solubility was determined by conventional western-blot analysis from whole cell extracts using Quantity One software (Bio-Rad), upon estimation of soluble and insoluble protein fractions. Bands corresponding to the recombinant protein were revealed with a commercial monoclonal antibody that recognizes the C-terminal His-tag (GE Healthcare), using dilutions of GFP–H6 as a reference. Protein charge and accessible surface were calculated from model structures. PDB2PQR was used to calculate protein protonation states to infer electrostatic charge at a particular pH [23], and solvent accessible surface areas were calculated by means of the Pops algorithms [24].

2.6. Modeling protein monomers and protein–DNA interactions

Homology models of the protein models were generated using Modeller [25], PyMol [26] and Swiss-PdbViewer [27]. The quality and stereochemical properties of the models were evaluated using Vadar [28]. The electrostatic interactions between the R9–GFP–H6 monomer and double stranded DNA were explored at acidic pH by using Haddock [29]. After obtaining the solution, a molecular dynamics was performed through NAMD [30] to minimize the energy of the system and to obtain the sequence of frames. The resulting movie was generated using VMD [31].

2.7. Cell culture and transfection and confocal microscopy

HeLa (ATCC-CCL-2) cells were cultured in MEM (GIBCO, Rockville, MD) supplemented with 10% Fetal Calf Serum (GIBCO) and incubated at 37 °C and 5% CO₂. For confocal analysis, cells were grown on Mat-Teck culture dishes and processed as described [17]. For the analysis of cell transfection, cells were exposed to R9–GFP–H6 nanoparticles combined with pDNA 3.1 encoding the td Tomato gene. Red fluorescence in cells was analyzed on a FACS Calibur system (Becton Dickinson) after detachment with 0.5 mg/ml trypsin. DNA retardation assays were carried out according to previously reports [32]. Detailed protocols can be found elsewhere [17,18].

2.8. Statistic analysis

Mean data, standard deviations and errors were calculated by Microsoft Office Excel 2003 (Microsoft). Pair-wise correlations, regressions and statistical significances were calculated by Sigmaplot 10.0. All the potential parametric correlations were analyzed by a linear regression statistic assay.

Table 2

Peak size (in nm) of peptide tagged GFP–H6 nanoparticles in low salt and high salt buffers. The occurrence of larger soluble particles and their size is also indicated. Relevant properties of the respective building blocks are also listed.

Peptide name	Sequence	Reference	Size in low salt buffer (larger particles)/PDI	Size in high salt buffer ^c (larger particles)/PDI	Number of arginines	Number of positively charged residues (arg + lys)
T22	RRWCYRKYRGYCYRKR	[73]	35.3/0.4 ^a	10.92/0.4	5	8
CXCL12	KPVLSYRCPFRFFESHVARANVKHL KILNTPNCALQIVARLKNNNRQVCIDP KIKWIQEYLEKALN	[74]	145.6/0.4 ^a	14.6/0.2	5	12
vCCL2	LGASWHRPDKCCLGYQKRPLPQVLL SSWYPTSQKCSKPGVIFLTKRGRQV CADKSKDWVKKLMQQLPVT A	[75]	46.24 (342.1)/0.2 ^a	83.3/0.2	4	12
V1	LGASWHRPDKCCLGYQKRPLP	[76]	9.4 (227.0)/0.4 ^a	8.0 (20)/0.3	2	4
Angiopep-2	TFYGGSRGKRNNFKTEEY	[77]	5.8/0.5 ^b	nd	2	4
Seq-1	KYLAYPDSVHIW	[78]	5.9/0.6 ^b	nd	0	1
Laminin 5alpha peptide A5G27	RLVSYNGIFFLK	[79]	26.2/0.4 ^b	nd	1	2
Fibronectin peptide I	KNNQKSEPLIGRKKK	[80]	4.0/0.6	nd	1	5
Fibronectin peptide V	WQPPRARI	[80]	4.1/0.8	nd	2	2

PDI: polydispersion index.

^a PBS–glycerol.

^b Carbonate.

^c Tris–NaCl.

3. Results

3.1. Mapping the architectonic abilities of poly-arginines

While His-tagged GFP is exclusively found in a disassembled monomeric form (of around 5 nm), the addition of the cell-penetrating poly-arginine (R9) peptide at the amino terminus promoted the spontaneous organization of R9–GFP–H6 as building blocks of regularly sized nanoparticles of around 20 nm [17]. To map the architectonic properties of poly-arginines we constructed a series of arginine-based tags (Rn) with a decreasing number of arginine residues, to evaluate if they retained the ability to promote protein self-assembling. Soluble versions of R7–GFP–H6, R6–GFP–H6 and R3–GFP–H6 were all found in the form of relatively monodispersed nanoparticulate entities of sizes ranging from 14 nm (R3–GFP–H6) to 38 nm (R7–GFP–H6, Table 1). This was indicative that a lower number of arginine residues (3) were already able to promote self-assembling of the monomers as protein-only nanoparticles. However, R3–GFP–H6 and R6–GFP–H6 showed secondary peaks of larger sizes (Table 1 and Figure 1), indicative of structural instability. On the other side, when Rn–GFP–H6 fusions were dialyzed against a high salt buffer upon purification, these proteins (at exception of R9–GFP–H6) did not form nanoparticles (Table 1). These data demonstrated the electrostatic nature of the protein–protein interactions supporting their self-assembling, that were much stronger when promoted by the highly cationic peptide R9, resulting in the formation of tightly assembled, highly stable particles.

3.2. Architectonic properties of non poly-arginine cationic peptides

To discriminate between a potential specific role of arginine residues and a generic influence of the cationic nature of the tag, in promoting ordered monomer self-assembling, other protein segments with unrelated amino acid sequences and lengths were fused to the amino terminus of GFP–H6 and challenged for nanoparticle formation. Four ligands of the cell surface cytokine receptor CXCR4 (T22, V1, CXCL12 and vCCL2), three ligands of CD44 (the fibronectin segments I and V, and the laminin 5alpha peptide A5G27), and the membrane-active peptides Seq-1 and Angiopep-2 (Table 2) were incorporated as N-terminal GFP–H6 fusions. Among them, T22, in form of T22–GFP–H6, had been

recently observed as tending to form regular oligomers [33]. Interestingly, most of these peptides enabled GFP–H6 to form stable nanoparticles of different sizes, ranging from around 20 to 150 nm (Table 2, Fig. 2a, and Supplementary Fig. S1). Again, a high salt content in the buffer tended to minimize particle formation and to reduce the resulting size of the complexes (Table 2). This was especially evident in the case of CXCL12-empowered constructs, for which size dropped from 145 to 15 nm (Fig. 2a, Table 2). On the other hand, the addition of V1 resulted in a mixed population of monomers and nanoparticles, the last fraction being reduced by high salt content (Fig. 2a). However, even in a high salt buffer, V1-empowered particles organized as regular entities of 8 and 20 nm, whose occurrence was fully confirmed by TEM (Fig. 2b). In fact, the larger CXCL12- and V1-empowered particles observed in absence of salt (see Fig. 2b) seemed to be due to clusters of smaller particles. Such a hierarchic supramolecular organization was not so apparent in T22–GFP–H6, in which different sized but tight nanoparticles were observed in both high and low salt buffers (Fig. 2b), indicative of architectonic robustness. Angiopep-2, Seq-1 and the fibronectin peptides I and V failed in promoting assembling of their respective functionalized monomers (Table 2, Supplementary Fig. S1).

At that point, we wanted to explore any potential parameter of the tags that might be determinative of nanoparticle formation and size. We unsuccessfully explored dependences between diverse biochemical properties of the peptides and of full fusion proteins (including length, molecular mass, hydrophobicity, aliphatic index and accessibility to the solvent) with particle size (not shown). However, the formation of nanoparticles was slightly but clearly influenced by the number of arginine residues of the amino terminal tag, in the border of the statistic significance (Fig. 3). While considering the total number of positively charged amino acids (lysines and arginines), the significance of the dependence dramatically increased (Fig. 3). In these plots, the highly unstable construct CXCL12–GFP–H6 is shown but the data was excluded from the analysis because of the instability of the assembled construct as discussed above (Fig. 2a, Table 2). As a control, no relationship between the total length of the tag and nanoparticle size was observed (Fig. 3). These data clearly supported the concept that not arginines as specific amino acids but the whole cationic nature of the tag determined its architectonic potential and influenced the size of the resulting constructs.

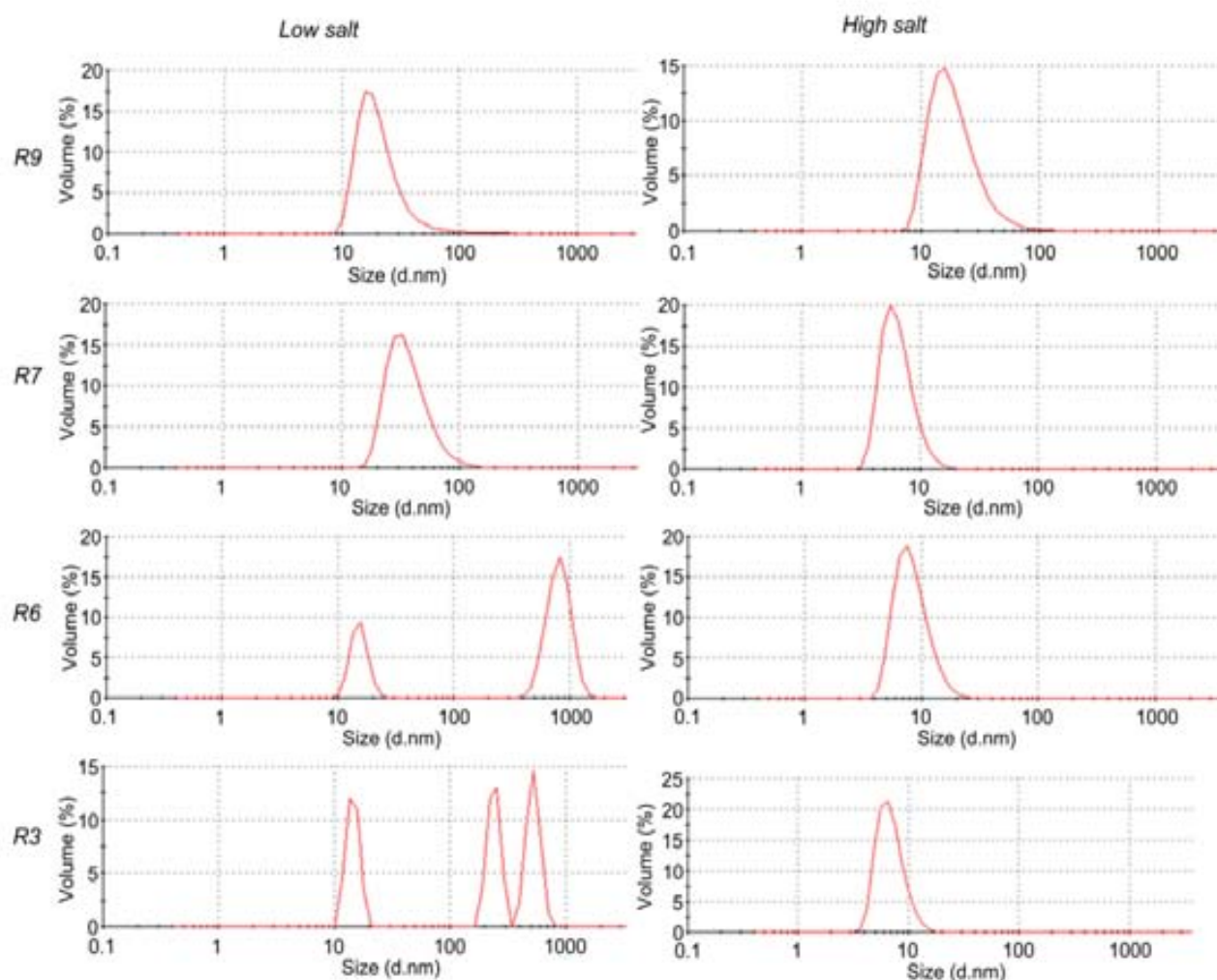


Fig. 1. Size distribution of GFP–H6 monomers tagged with amino terminal arginine-rich peptides (Table 1). Upon purification, proteins were dialyzed against PBS–glycerol (low salt buffer) or Tris–NaCl (high salt buffer). All the constructs were fluorescent.

3.3. Regulatable functional properties of poly-histidines in protein-only nanoparticles

Once confirmed the structural potential of cationic peptides, we also wanted to explore if poly-histidines would contribute to the supramolecular organization of tagged building blocks, apart from their utility as protein purification tags and as endosomolytic agents in drug delivery [34]. We suspected a role of H6 since the pKa of the imidazole group of histidines is 6.10, and its charge, at difference of poly-arginines (pKa of 12.48), is expected to be unstable at pH close to neutral. In this regard, several functional properties of R9–GFP–H6 nanoparticles were highly dependent on pH. Indeed, cell penetrability of R9–GFP–H6 was optimal at pH 5.8 and progressively decreased at higher pH (Fig. 4a), suggesting a gradual inactivation of R9 activities under alkaline media. At pH 4, the protein precipitated and remained externally attached to the plasma membrane, showing poor internalization. When analyzed by DLS (Fig. 4b), the size of R9–GFP–H6 particles remained constant at pH values between 5.8 and 10 (17–20 nm), and marginally increased up to 35 nm at pH 4 (some aggregation was observed at pH 4 and 10). When R9–GFP–H6 was combined with plasmid DNA at pH 5.8 and further exposed to cultured mammalian cells, about 50% of the population expressed the transgene (Fig. 4c). However, this value dropped to about 3% at pH 4 and to even lower

values at neutral and basic pH, indicating pH-dependent functional variability and probably structural rearrangements of the polyplexes. Interestingly, the differential effectiveness of the polyplexes in transfection experiments that were all performed in MEM culture media at neutral pH indicated that the specific properties of the nanoparticles reached at different pHs are stable and did not revert when further incubated under physiological conditions.

On the other hand, the ability of R9–GFP–H6 nanoparticles to bind DNA was null at neutral and basic pH, clear at pH 5.8 and maximal at pH 4 (Fig. 4d). These data suggested that at pH over 6.1, H6 having no charge, R9 might be overtitrated by electrostatic protein–protein interactions, rendering the tag unavailable for other activities such as cell penetration and DNA binding. Below pH = 6.1, protonation of histidines would enable H6 for protein–protein and protein–DNA contacts, releasing R9 for plasma membrane translocation, DNA loading and efficient transgene delivery and expression. At pH 4, protein denaturation and aggregation is expected to eclipse the enhanced cross-molecular abilities of H6.

3.4. Architectonic potential of poly-histidines

The above data suggested cross-molecular reactivity of H6. However, no architectonic abilities of poly-histidines regarding

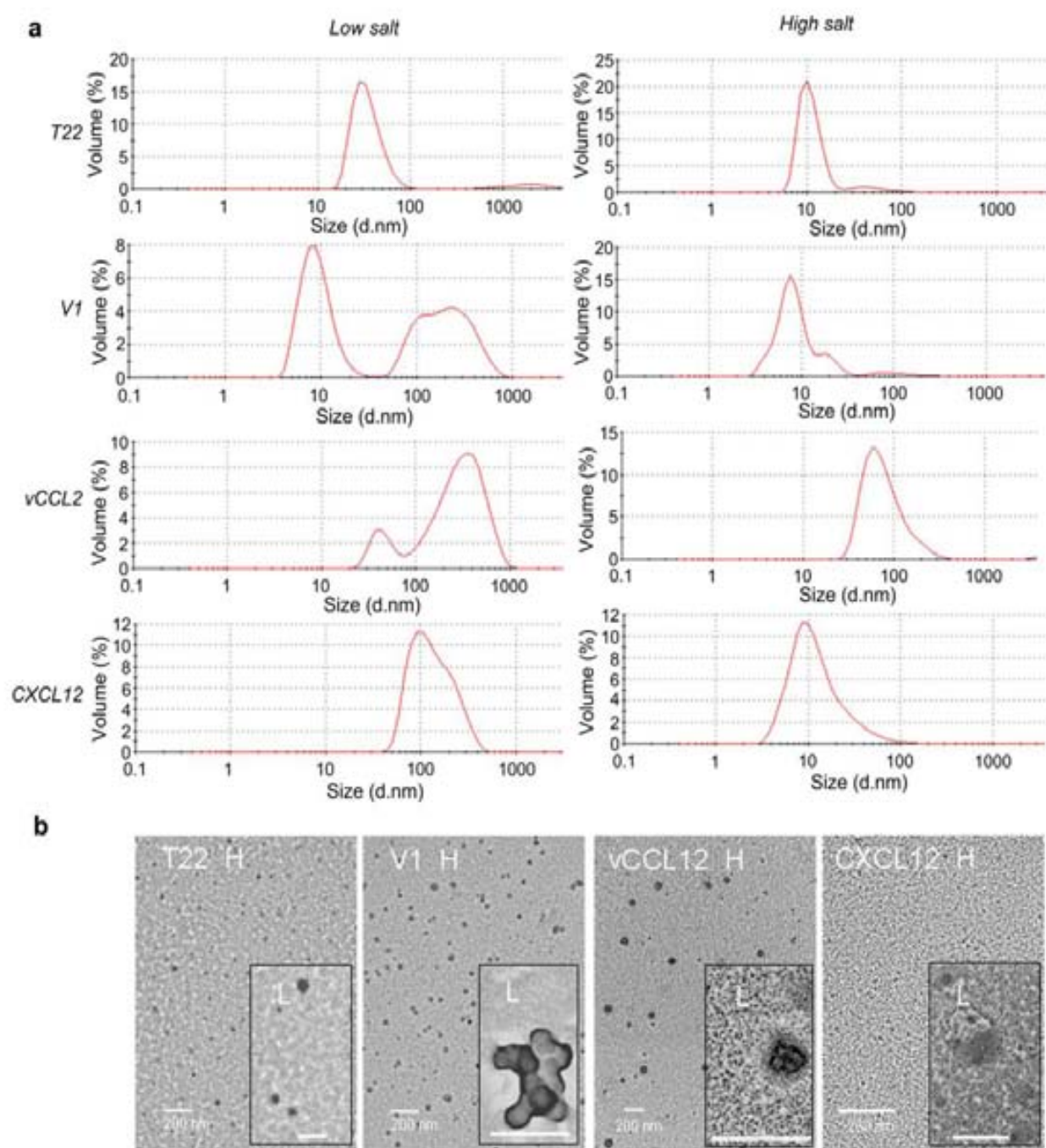


Fig. 2. Architecture of GFP-derived nanoparticles empowered with different amino terminal cationic peptides (Table 2). Upon purification, proteins were dialyzed against PBS-glycerol (low salt buffer) or Tris-NaCl (high salt buffer). (A) Size distribution of the resulting GFP-H6 constructs monitored by DLS. (B) TEM micrographs of these particles formed in either high salt (H) or low salt (L) buffers. All the constructs were fluorescent.

nanoparticle formation had been so far reported. Therefore, the potential assembling of GFP-H6 (lacking any amino terminal cationic peptide) was explored at different pHs. At pH 7 and 8, size of GFP-H6 peaked at around 5 nm (Fig. 5a), a value compatible with monomer size (at pH 10 the protein fully precipitated; not shown). However, at pH 5.8, a minor but regular size up-shift was observed, that was more even pronounced at pH 4. Also, under acidic conditions, a minor but significant fraction of GFP-H6 organized as regular particles of about 22 nm. On the other hand, with protonated H6 tails, GFP-H6 was able to bind DNA at pH 4 (although not at 5.8, Fig. 5b and Supplementary Video S1). These

data confirmed that charged H6 was able to promote, as suspected, stable protein-protein and protein-DNA interactions. In R9-GFP-H6, showing a marked dipolar charge distribution (Fig. 5c), H6 intervened in nanoparticle formation by promoting electrostatic protein-protein contacts, as modeled in Fig. 5d. H6-mediated interactions would be more favored than those driven by R9, because of the more extended arm of H6 (Fig. 5d). Although at pH 4, H6 also binds DNA (modeled in Fig. 5b), at this condition the nanoparticle itself is not stable as the protein aggregates (Fig. 4a and b). Then, the efficiency of the nanoparticles in mediating transgene delivery showed an optimal when assembled at pH 5.8

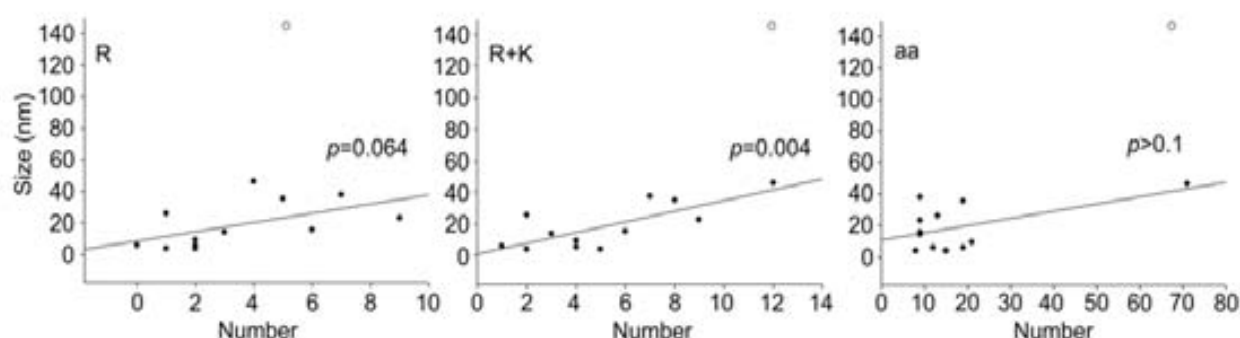


Fig. 3. Regression analyses between selected properties of all peptide tags used in this study (Tables 1 and 2) and the peak size of the chimerical constructs determined in low salt buffer. *R* stands for the number of arginine residues, *R + K* indicates the number of all cationic residues (arginines and lysines), and *aa* refers to the total number of residues of the peptide. The white symbol refers to data from CXCL12-empowered particles, and it has been excluded from the analyses.

(Fig. 4c), where R9 is free for non-architectonic functions. Again, this is irrespective of the conditions at which the particles are finally used in biological interfaces, that are expected to be around physiological pH.

Supplementary data related to this article can be found at doi: 10.1016/j.biomaterials.2012.08.033.

3.5. Generic tagging of building blocks with R9 and H6

As demonstrated above, the combination of a cationic peptide at the amino terminus of GFP with a poly-histidine enables this protein to self-assemble as regular sized nanoparticles through electrostatic interactions. In particular, R9 and T22 are excellent tags for this purpose, as they induce the formation of very stable regular sized entities poorly sensitive to high salt content. We wondered at which extent nanoparticle formation could be strictly linked to the particular structure of GFP (beta-barrel), and if a peptide pair such as R9 and H6 could functionalize proteins other than GFP to act as monomers of self-organizing protein nanoparticles. This was explored by using the structurally different,

tumor suppressor protein p53 (tetrameric, 43.7 kDa per monomer), that was functionalized with R9 and H6 following the same scheme than previously used for GFP. Interestingly, the addition of the end terminal tags to this protein resulted in a significant up-shift of their size (Fig. 6). This fact confirmed that the pair R9–H6 can confer self-organizing properties to proteins other than GFP, and that the architectonic tag concept could be considered as a principle with generic applicability in bionanotechnology.

4. Discussion

The construction of self-assembling protein-only nanoparticles from repetitive building blocks has been a rather neglected issue in nanomedicine, in contrast to the long run expertise accumulated in the fabrication of liposomes and polymeric particles with pre-defined nanoscale features [35–39]. Consequently, the current protein-based vehicles for drug delivery generated *de novo* include a catalog of rather amorphous entities [40] that are produced under no previous design. On the other hand, viruses [41–43], virus-like particles [44–47], parts of viral capsids [48], flagella-based devices

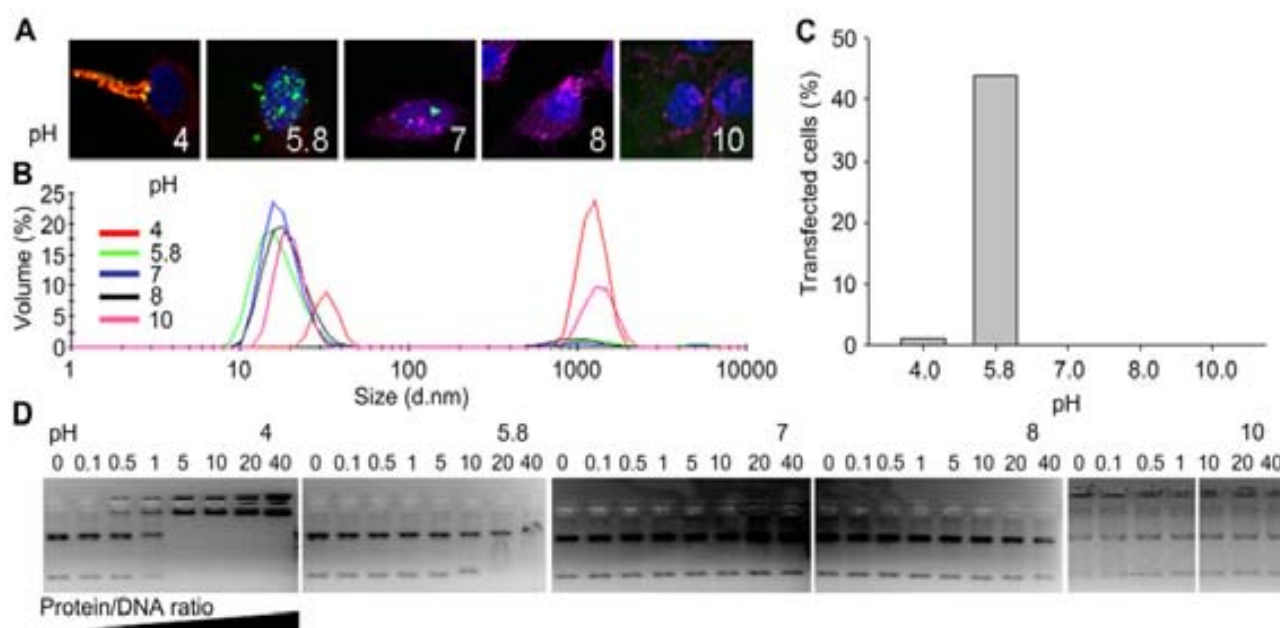


Fig. 4. Functional and structural characterization of R9–GFP–H6-based nanoparticles. (A) Confocal snap-shots of cultured HeLa cells exposed to protein-only R9–GFP–H6 nanoparticles for 24 h. Nanoparticles emitted green fluorescence, the cell membrane was stained with CellMask (rendering pink-reddish signal) and cell DNA with Hoechst 33342 (blue). (B) Size distribution of R9–GFP–H6 nanoparticles in absence of DNA. (C) Percentage of HeLa cells expressing a reported gene carrier by polyplexes formed at distinct pH values, at a protein/DNA ratio of 50. (D) DNA-binding abilities of R9–GFP–H6 nanoparticles at different pH values. (For interpretation of the references to color in this figure legend, the reader is referred to the web version of this article.)

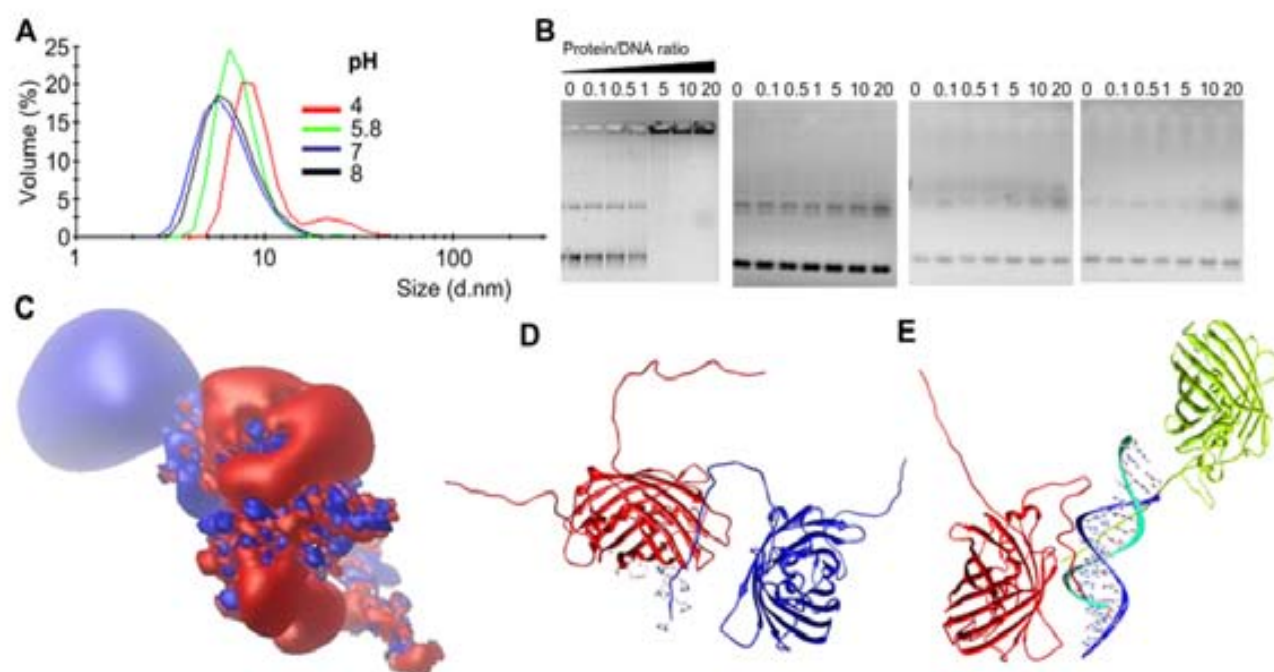


Fig. 5. Cross-interacting abilities of the protonated His-tag in R9-GFP-H6. (A) Size distribution measured by DLS of GFP-H6 constructs at different pH values. (B) DNA binding of GFP-H6 monitored by retardation assays at different pH values. (C) Polarization in the charge distribution of the R9-GFP-H6 monomer (blue cationic, red anionic) in which the electrostatic potential has been calculated in aqueous media by means of the Adaptive Poisson–Boltzmann Solver method [81]. (D) Interaction of the positively charged H6 peptide with the anionic pole of the R9-GFP-H6 monomer, modeled at pH 5.8. (E) Conformation of the positively charged H6 peptide of R9-GFP-H6 interacting with double stranded DNA, modeled at pH 5.8. (For interpretation of the references to color in this figure legend, the reader is referred to the web version of this article.)

[49–51], organelles [10] and other constructs formed by the natural oligomerization of natural proteins [52,53] maintain their natural self-organization pattern and are exploited for nanomedical purposes such as drug delivery, antigen presentation or as scaffolds for nano-fabrication [54,55], but with limited or null structural versatility. Conventional self-assembling peptides organize in aqueous solutions by the formation of cross-molecular beta sheet-based interactions, similar to those supporting amyloid deposition [56–60]. Such interactions result in fibril formation [56,57,61,62], that can finally derive in tailored materials such as membranes [14] of gels [13]. Unfortunately, when fused as tags to large proteins, self-assembling peptides prompt aggregation [15,16]. Therefore, the rational generation of man-made protein nanoparticles based on selected protein monomers, that is, polypeptides with appealing biological functions, has been so far poorly reached.

In this context, the few successful insights on the construction and modulation of protein-only nanoparticles have derived from unanticipated observations. As an illustrative example, the mixture of a fusogenic peptide from viral origin and a poly-lysine (K_{16}) renders the unexpected formation of spherical microparticles from 120 to 800 nm, whose size is regulated by salt concentration, pH and temperature [63]. Furthermore, the design of short peptides with appropriate charge distribution permits a semi-rational control of peptide self-assembling as 2D or 3D nanofiber-based complexes [64]. For larger proteins, the construction of elastin-mimetic protein polymers with self-assembling properties is among the most advanced examples of self-organizing, net-shaped materials [65].

In a previous study [17], we have observed that a poly-arginine peptide (R9) was able to promote the self-organization of a modular chimerical protein (His-tagged GFP) into regular 20 nm-sized nanoparticles suitable for drug delivery [18]. This finding revealed a novel potential of the well-known family of cell-penetrating Rn peptides [3–6,21,66–70], in promoting self-organization of holding proteins at the nanoscale level. The possibility of using specific peptide tags as directors of protein self-organization into nanoparticles with pre-defined properties is particularly appealing, as it should potentially allow the manipulation of their properties by conventional genetic engineering. To determine if this unsuspected architectonic ability could be shared by other cationic stretches we tested here nanoparticle formation of GFP-H6 as driven by R7, R6 and R3 (Table 1), and by nine additional peptides with unrelated amino acid sequences (Table 2). Interestingly, most of these tags induced the formation of fluorescent GFP oligomers of regular architecture (pseudo-spherical nanoparticles, Fig. 2), ranging from 20 to 100 nm (Tables 1 and 2). The fact that their formation and size was influenced in most cases by salt concentration (Figs. 1 and 2) indicates that monomer self-assembling was governed by electrostatic interactions between monomers. However, two particular constructs namely R9-GFP-

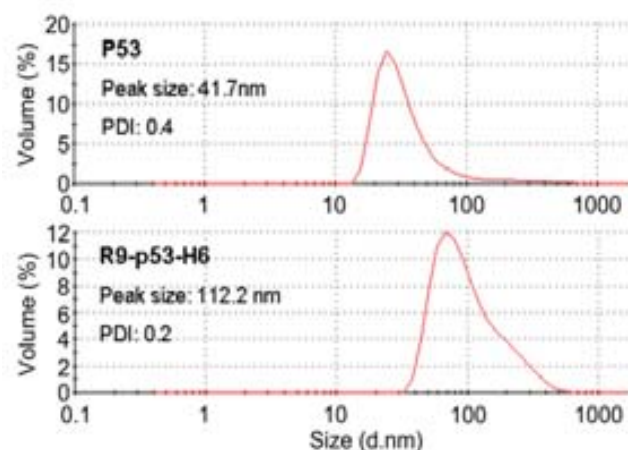


Fig. 6. Size distribution of p53 and R9-p53-H6 in elution buffer. PDI is polydispersion index.

H6 and at a minor extent T22–GFP–H6, empowered by highly cationic tags, were especially stable under variable salt content. The fact that diverse unrelated cationic peptides enabled monomers to self-organize into monodisperse nanoparticles confirms the self-organizing properties as a general property of cationic peptides (other than R9, Fig. 3), and also that the structure of the peptide tag itself is not critical for the assembling of the building blocks. Also, the beta-barrel core of GFP was nicely preserved in all the constructs as inferred from the fluorescence emission observed in all the particles (not shown, legends of Figs. 1–3).

On the other hand, data presented here reveal that the histidine tag (H6), commonly used for protein purification and as endosomal escaping agent promotes protein–protein and protein–DNA contacts, when the pH at which particles or polyplexes are formed decreases (Fig. 5 and Supplementary Video S1). Then, the structural dynamism offered by the partially protonated H6 tag and its competition with the cationic R9 tail for molecular interactions allows an unusual molecular flexibility that permits to adapt the protein particles as efficient carriers for DNA delivery by slightly decreasing the pH under neutral values. The H6 peptide, as an unusually versatile, pH-controlled architectonic tag complements the activities of R9 (or those of alternative cationic peptides), being the dual peptide set as a whole, a promising platform for the activation of defined protein monomers for regulatable cross-molecular interactions.

In summary, in this work we propose a novel concept of architectonic tagging for nanoscale construction by the use of a peptide pair. The fusion of a H6 tag at the carboxy terminus and a cationic peptide at the amino terminus of diverse proteins enable them to act as self-assembling monomers of protein-only nanoparticles. Both model proteins tested in this study namely GFP and p53, self-assembled when tagged with R9, T22 (and other cationic peptides) and H6 (Figs. 1, 2 and 6). At least in the case of GFP, in which biological activity of the monomer can be straightforwardly determined by fluorescence emission, it has been determined that assembly does not impair functionality. This fact makes the proposed peptidic platform very appealing to generate nanoparticles with potential for the delivery of either active proteins or associated nucleic acids. The administration of protein drugs as nanoparticles (by engineering them as building blocks) could largely increase stability, bioavailability and intracellular drug delivery [71], when comparing with the soluble, non-particulate counterpart. Interestingly, the size of the resulting construct, a critical parameter in nanomedicine [72], seems to be strongly influenced by the charge of the cationic tag (Fig. 3), which can be easily defined in anticipation by simple *in silico* protein design. Although further studies are obviously required to fully understand the mechanics of self-assembling and to adjust the methodological aspects of this principle, the observations reported here open intriguing possibilities for the pioneering rational design of tailored protein nanoparticles by conventional engineering of the primary amino acid sequence.

5. Conclusion

The combination of a cationic peptide and a hexa-histidine tail fused to the amino and carboxy termini, respectively, of different proteins enable them to act as building blocks of self-assembling nanoparticles whose properties are regulatable by pH during particle formation. These vehicles are also able to condense and deliver expressible DNA into mammalian cells. The architectonic properties of the tag pair at the nanoscale are supported by electrostatic contacts, primarily driven by the cationic tag and subsidiarily by H6. When protonated at slightly acidic pH, positively charged H6 replaces by competition the cationic tag and intervenes in the formation of stable contacts. The further implementation of

this bi-armed peptide platform should allow the biofabrication and formulation of desired drug proteins as protein-only nanoparticles, as an exciting alternative to the limited use of conventional, amyloidogenic self-assembling peptides in nanomedicine.

Acknowledgments

We appreciate the technical support of Fran Cortés from the Cell Culture Unit of Servei de Cultius Cel·lulars, Producció d'Anticossos i Citometria (SCAC), and from Servei de Microscòpia, both at the UAB, and the Protein Production Platform (PPP) of the CIBER de Bioingeniería, Biomateriales y Nanomedicina. We also acknowledge the financial support received for the design and production of artificial viruses for gene therapy to EV and AV from FISS (PS0900165), MINECO (ACI2009-0919), AGAUR (2009SGR-108) and CIBER de Bioingeniería, Biomateriales y Nanomedicina, an initiative funded by the VI National R&D&I Plan 2008–2011, Iniciativa Ingenio 2010, Consolider Program, CIBER Actions and financed by the Instituto de Salud Carlos III with assistance from the European Regional Development Fund. XZ is a recipient of a scholarship under the Post-graduate Study Abroad Program of The China Scholarship Council, China. UU and PS have received predoctoral fellowships from ISCIII, Spain, while JDE was supported through a FPU fellowship from MINECO, Spain. AV has been distinguished with an ICREA ACADEMIA award. EGF is supported by the Programa Personal de Técnico de Apoyo (Modalidad Infraestructuras Científico-Tecnológicas, MICINN).

Appendix A. Supplementary data

Supplementary data related to this article can be found at <http://dx.doi.org/10.1016/j.biomaterials.2012.08.033>

References

- [1] Uchida M, Klem MT, Allen M, Suci P, Flenniken M, Gillitzer E, et al. Biological containers: protein cages as multifunctional nanoplatfoms. *Adv Mater* 2007; 19:1025–42.
- [2] Kim HH, Choi HS, Yang JM, Shin S. Characterization of gene delivery in vitro and in vivo by the arginine peptide system. *Int J Pharm* 2007;335:70–8.
- [3] Futaki S, Suzuki T, Ohashi W, Yagami T, Tanaka S, Ueda K, et al. Arginine-rich peptides. An abundant source of membrane-permeable peptides having potential as carriers for intracellular protein delivery. *J Biol Chem* 2001;276:5836–40.
- [4] Vazquez E, Ferrer-Miralles N, Mangues R, Corchero JL, Schwartz Jr S, Villaverde A. Modular protein engineering in emerging cancer therapies. *Curr Pharm Des* 2009;15:893–916.
- [5] Vazquez E, Ferrer-Miralles N, Villaverde A. Peptide-assisted traffic engineering for nonviral gene therapy. *Drug Discov Today* 2008;13:1067–74.
- [6] Ferrer-Miralles N, Vazquez E, Villaverde A. Membrane-active peptides for non-viral gene therapy: making the safest easier. *Trends Biotechnol* 2008;26:267–75.
- [7] Toledo-Rubio V, Vazquez E, Platas G, Domingo-Espin J, Unzueta U, Steinkamp E, et al. Protein aggregation and soluble aggregate formation screened by a fast microdialysis assay. *J Biomol Screen* 2010;15:453–7.
- [8] Mastrobattista E, van der Aa MA, Hennink WE, Crommelin DJ. Artificial viruses: a nanotechnological approach to gene delivery. *Nat Rev Drug Discov* 2006;5:115–21.
- [9] Edelstein ML, Abedi MR, Wixon J. Gene therapy clinical trials worldwide to 2007 – an update. *J Gene Med* 2007;9:833–42.
- [10] Corchero JL, Cedano J. Self-assembling, protein-based intracellular bacterial organelles: emerging vehicles for encapsulating, targeting and delivering therapeutical cargoes. *Microb Cell Fact* 2011;10:92.
- [11] Aris A, Villaverde A. Modular protein engineering for non-viral gene therapy. *Trends Biotechnol* 2004;22:371–7.
- [12] Saccardo P, Villaverde A, Gonzalez-Montalban N. Peptide-mediated DNA condensation for non-viral gene therapy. *Biotechnol Adv* 2009;27:432–8.
- [13] Koutsopoulos S, Unsworth LD, Nagai Y, Zhang S. Controlled release of functional proteins through designer self-assembling peptide nanofiber hydrogel scaffold. *Proc Natl Acad Sci U S A* 2009;106:4623–8.
- [14] Zhang S, Holmes T, Lockshin C, Rich A. Spontaneous assembly of a self-complementary oligopeptide to form a stable macroscopic membrane. *Proc Natl Acad Sci U S A* 1993;90:3334–8.
- [15] Wu W, Xing L, Zhou B, Lin Z. Active protein aggregates induced by terminally attached self-assembling peptide ELK16 in *Escherichia coli*. *Microb Cell Fact* 2011;10:9.

104. Zhou H, King L, Wu W, Zhang X, Liu Z. Small α -helical-like peptides can drive soluble proteins into active aggregates. *Mol Cell Biol* 2012;32:11–19
105. Vazquez I, Rodríguez M, Pérez Gallo J, 1997–2023, Durango Espin J, Celisno J, et al. Protein-based self-assembly and intracellular trafficking powered by an arginine-rich 391-peptide. *Nanotechnology* 2022;33(25):2591–98
106. Vazquez I, Celisno J, Durango E, Rodríguez M, Durango Espin J, López Muñoz N, et al. Internalization and kinetics of nuclear migration of protein-only arginine-rich nanoparticles. *Biomaterials* 2019;112:1113–9
107. Vazquez I, Celisno J, Villaverde A. Post-production protein stability: how to survive beyond the cell factory. *Mol Cell Fact* 2011;13(4)
108. Martínez Alonso M, González Montaña M, Lario Frutos E, Villaverde A. Forming even 2-protein selectively from structural rich sup. bodies. *Mol Cell Fact* 2009;30(4)
109. Kinnaird Z, Wu H, McBride JJ, June KE, Kim MO, Davidson HL, et al. Transvascular delivery of small interfering RNA to the central nervous system. *Nature* 2007;448:49–53
110. Bradic M. A rapid and sensitive method for the quantitation of microgram quantities of protein utilizing a principle of protein-dye binding. *Anal Biochem* 1976;72:248–54
111. Dubrody J, Chardronnet P, Li H, McLean J, Jones J, Kyrke-Smith J, et al. PDB2PQS: expanding and upgrading automated preparation of macromolecular structures for molecular simulation. *Nucleic Acids Res* 2010;38:13722–5
112. Cavalli O, Skjorge I, Halvorsen H, POPS: The algorithm for solvent accessible surface areas of atoms and residues. *Nucleic Acids Res* 2003;31:4364–9
113. Lewis M, Fratton D, Weng H, Shen MY, Shi A. Protein structure modeling with MOPED. *Methods Mol Biol* 2008;426:145–59
114. Kelley TA, Mezulis M. Protein structure prediction on the Web: accuracy, usage and the Phylogeny Server. *Nat Protoc* 2009;4:463–51
115. Güer N, Perisch M, WABS-MODEL and the Swiss PDBViewer: An easy-to-use tool for comparative protein modeling. *Eukaryot Cell* 1995;18:2314–23
116. Wolf J, Kasper A, Zhang H, Menzies H, Boyko KJ, Brian D, et al. VADAR: a web server for quantitative evaluation of protein structure quality. *Nucleic Acids Res* 2011;39:416–9
117. Soriano C, Forde R, Benoit AM, HADDOCK: A protein-protein docking approach based on Bayesian statistical optimization. *J Am Chem Soc* 2011;133:1271–7
118. Phillips K, Brauer R, Wang W, Gurevitz I, Djikheerajid J, Voth O, et al. Scalable molecular dynamics with GROMACS. *Comput Chem* 2005;26:1781–809
119. Horn A, Artzner A, Yin Y, Stone JE, Schöten N, Jiang YMD. An introductory tutorial. *Curr Protoc Bioinform* 2018;Chapter 5:Unit 5.1
120. Ari A, Villaverde A. Molecular organization of protein-DNA complexes for cell targeted DNA delivery. *Bioherb Biophys Res Commun* 2006;338:471–61
121. Juez J, Caspales MV, Ferrer Miralles M, Larrea J, Galdano Z, Carrión JJ, et al. Intracellular CXCR4+ cell targeting with T22-engineered protein only nanoparticles. *Int J Nanomed* 2012;7:4511–44
122. Ferrer Miralles M, Corredo JJ, Kaur P, Ledro J, Gupta KJ, Villaverde A, et al. BioSignal: a method of heuristics rich peptides: merging bioinformatics and nanotechnology. *Mol Cell Fact* 2011;30:161
123. Zhang L, Prampattanarajakul D, He C, Huang M. Development of nanoparticles for intranasal drug delivery. *Curr Med Chem* 2010;17:543–58
124. Sarkar DK. Self-assembled lipidic nanoparticles for molecular medicine and applications. *Curr Drug Deliv Technol* 2009;9:137–8
125. Sarkar DK. Engineering of nanosystems for drug delivery. *Curr Drug Deliv Technol* 2009;9:491–501
126. Hayak M, Bassani C, Salmeri P, Basso JP. Lipid nanoparticles: a new platform for nanoparticles. *Int J Pharm* 2009;379:261–9
127. Patel D, Savant EK. Self-nanomedicine drug delivery systems: from latex development and synthesis to formulation and evaluation. *Thromb Res* 2010;184:19–26
128. Mahan A, Tang Z, Wu H, Wang J, Liu Y. Protein-based nanomedicine platform for drug delivery. *Nat Rev Drug Discov* 2010;9:1709–22
129. Mao C, Yuan CL, Cheng H, Gao S, Wu X, Qiu J, Gong G, et al. Viral-assembly of oriented quantum dot nanowires. *Proc Natl Acad Sci U S A* 2004;101:9946–51
130. Mao C, Shen GJ, Reiss HL, Kuznetsov N, Wang XY, Hutchins A, et al. Virus-based toolkit for directed synthesis of magnetic and semi-conducting nanowires. *Nature* 2004;433:213–7
131. Mao XJ, Kim DW, Yoo P, Chung Y, Lee Y. Protein-based nanomedicine platform for drug delivery. *Nat Rev Drug Discov* 2010;9:1709–22
132. Geoghegan J, Weyermann J, Zimmert A. Recombinant virus-like particles as drug delivery systems. *Curr Pharm Biotechnol* 2007;8(4):329–35
133. Xu YH, Zhang YQ, Xu XM, Song CL. Polyphosphazene virus-like particles as vehicles for the delivery of aptamer to genes. *Biochem Biophys Res Commun* 2009;381:414–48
134. Maloney EM, Sinden HA, Lee ST, Tankersley HA, Paschalis S, Lechner JG, et al. Human papillomavirus-like particles mediate functional delivery of plasmid DNA to antigen-presenting cells in vivo. *Vaccine* 2002;20:4270–5
135. Lee J, Schwartz C, Gu P. Construction of a herpesvirus phi29 DNA packaging motor and its application in nanotechnology and therapy. *Adv Biomed Eng* 2009;49:2084–81
136. Hirasaka Y, Miyaji M, Tada E, Jeechi Tg. A nano-motor powered by bacteria. *Proc Natl Acad Sci U S A* 2009;106:11638–43
137. Kurasa M, Muralidharan S, Topp BC. Generation and characterization of inorganic and organic nanofibers on non-oriented fibrous mats of nanoscale. *Nanopart J Mater Chem* 2007;17:2661–72
138. Doplarich K, Weiss RD, Mikheenko IP, Seckoff KL, Malachuk H. Manufacture of large palladium and gold nanoparticles on native and genetically engineered flagellin scaffolds. *Biomaterials* 2008;29:1874–86
139. Ari A, Felo JC, Knight A, Costello C, Villaverde A. Exploiting viral cell targeting ability in a single polypeptide: an easy-to-use, non-invasive vehicle for integrin-mediated DNA delivery and gene expression. *Biochem Biophys Res Commun* 2008;369:889–95
140. Hassan F, Ramoa GD, Bielecka-Bispyrak E, Anis K, Arizman A, Gal MJ, et al. A peptide-based dendrimer that enhances the phosphatidylcholine activity of PBA conjugates in cells. *Biomater Chem* 2009;2(1):27–36
141. Rodriguez Carmona E, Villaverde A. Nanotechnology: a central materials for innovative medicine. *Trends Microbiol* 2010;18:421–9
142. Villaverde A. Nanotechnology: nanotechnology and the next cell factories. *Mol Cell Fact* 2010;29:53
143. Strachan H, Humeau D. Purifying gene-silent chromatin formation in model oligomers. *Peptides* 2009;30:187–96
144. Reilly G, Sarda S, Jilka, Dharmalingam D. Dynamics of binding of peptides onto growing amyloid fibrils. *Proc Natl Acad Sci U S A* 2009;106:11946–51
145. Espigares A, Villar-Pique A, Sastre R, Ventura S. Yeast protein tag, a versatile amyloid induction factor in bacteria. *Mol Cell Fact* 2012;31:389
146. Villar-Pique A, Espigares A, Sastre R, de Lencastre M, Ventura S. Using bacterial inclusion bodies as a screen for amyloid aggregation inhibitors. *Mol Cell Fact* 2012;31:55
147. Lario Frutos E, Sastre R, de Lencastre M, Villaverde A, Ventura S. Biological role of inclusion bodies: a model for amyloid aggregation. *FEBS J* 2011;278:2879–92
148. Martínez Alonso M, González Montaña M, Lario Frutos E, Villaverde A. The functional quality of soluble recombinant polypeptides produced in Escherichia coli is defined by a wide conformational spectrum. *Appl Environ Microbiol* 2008;74:1373–8
149. Schaefer A de MA. Characterization of the aggregation induced during recombinant protein expression in systems. *ESM Biotechnol* 2007;19:13
150. Cellini L, Barberi M, Gobbiar JD, Rhee J, Ferguson MA, Segerson T, et al. Self-assembly of peptides into spherical nanoparticles for delivery of hydrophobic molecules to the cytosol. *ACS Nano* 2010;4:2870–84
151. Yang YL, Khoo C, Wang XM, Hsu A, Yuku H, Zhang G, Dossinger cell assembling peptide nanomaterials. *Nano Today* 2009;4:193–210
152. Wright ER, Lantzelli AP. Self-assembly of block copolymer derived from elastin nanoscale polypeptide sequences. *Adv Drug Deliv Rev* 2002;54:1173–84
153. Fukaya S, Makino T, Takahara A, Takahashi T, Sano M. Arginine-rich peptides and their internalization mechanisms. *Bioherb Res Trans* 2009;41:784–7
154. Mihaylova K, Chernouzeva IV. Arginine-rich cell-penetrating peptides: from endocytosis to nuclear delivery. *Adv Mol Biosci* 2010;2(2):239–49
155. Saito-Shikama H, Takahashi T, Murakami MK, Sawada H. The role of arginine-rich motif and beta-arches in the assembly and stability of hexameric capsid. *Virus Res* 2005;101:443–58
156. Lima D, Yonaka K, Aikawa T, Esuroto K. Arginine as an effective additive in gel permeation chromatography. *J Chromatogr A* 2001;924:29–36
157. De la Torre J, Cheloni M, Kurogi T, Fujita D, Phlo J, Aikawa T. Role of Arginine in protein folding, solubilization and purification. *Biochem J* 2004;381:101–8
158. Brian M. Enzymes in drug nanotechnology: dispatch mass transport through biological systems. *Trends Biotechnol* 2010;28:181–8
159. Jiang W, Kim SY, Rhee J, Chan WC. Nanoparticle-mediated cell-tissue response is size-dependent. *Mol Nanotechnol* 2008;3:147–50
160. Murakami T, Zhang Y, Koyama Y, Tanaka Y, Kuroki S, et al. Inhibitory mechanism of the CXCR4 antagonist T22 against human immunodeficiency virus type-1 infection. *Journal of Virology* 1999;73:2429–36
161. Anura A, Gál M, Schwartz O, Salmerón J, Montes M, Leiberich P, et al. HIV coreceptor downregulation as antiviral principle: HIV (alpha) dependent internalization of the chemokine receptor CXCR4 contributes to inhibition of HIV replication. *J Exp Med* 1999;189:139–49
162. Kistritz M, Rosenkötter MM, Jahn U, Salmerón J, Johnson MJ, Abolajo S, et al. A broad spectrum chemokine antagonist encoded by Simons' syndrome-associated herpesvirus. *Nature* 2007;447:104–9
163. Zhou M, Liu ZW, Liu JS, He JW, Huang ZW. A novel peptide antagonist of CXCR4 derived from the N-terminus of viral chemokine vMIP1b. *Biochem Biophys Res Commun* 2000;274:662–7
164. Deane JM, Regina A, Che C, Perrin J, Nguyen L, Gotsdiner K, et al. Identification and design of peptides as a new drug delivery system for the brain. *Int J Pharm* 2007;349:104–12
165. Miggel J, Huang F, Li, Song Ming C, Yi J, Li, Wang C. Peptide for drug migration across brain blood barrier and delivery systems comprising the gene. *Drug Deliv Rev* 2002;54(1):6703–11
166. Liu Y, Shen Y, Shen Y, Tang J, Shi H, Li J, Li J, Wang C, Shen Y, et al. Identification of an active site on the human alpha-5 chain glycoprotein domain that binds to CXCR4 and inhibits trafficking. *J Neurosci Res* 2004;76:4810–5
167. Jalkanen M, Jalkanen M. Synthesis of CXCR4 binds the CXCR4 terminal heparin-binding domain of integrin. *J Biol Chem* 1997;272:16117–25
168. Baker MW, Segrè D, Joseph S, Heston MJ, McCannan JA. Identification of nanosystems application for CXCR4 and the relevance. *Proc Natl Acad Sci U S A* 2001;98:10413–8

Paper 2

Internalization and kinetics of nuclear migration of protein-only, arginine-rich nanoparticles

Esther Vázquez, Rafael Cubarsi, Ugutz Unzueta, Mónica Roldán, Joan Domingo-Espín, Neus Ferrer-Miralles, Antonio Villaverde.

Biomaterials, 31, 9333-9339, 2010

The peptide architectonic tag pairs described above have allowed us to promote the self-assembly of functionalized proteins in size compatible protein-only nanoparticles. However, although it is intimately linked with their therapeutic applicability and potential toxicity, little is known about how do these nanoparticles interact, are internalized and migrate within target cells. Consequently, we wanted to analyze in this work the intracellular trafficking and stability of self-assembled protein nanoparticles when they are exposed to cultured cells.

In short, we have kinetically explored the uptake and intracellular migration of the R9-empowered reporter nanoparticles (R9-GFP-H6), which self-assemble in particulated entities of around 20nm in size, in different cultured cells. The results showed that protein nanoparticles were efficiently internalized and accumulated in both cell cytoplasm and nucleus, indicating that the nanoparticulated structure did not make an obstacle for their uptake in mammalian cells. Moreover, the observation of endosomal vesicles that contain proteins fully supported an endosomal internalization pattern. However, the fully fluorescent protein particles detected within the cells and their fast cytoplasmic migration strongly suggested early endosomal escape ability. Additionally, the fast nuclear accumulation pattern together with the intra-cytoplasmic convergent and not random nuclear trajectory clearly indicated an active nuclear localization of protein nanoparticles. In this regard, the kinetic analysis proved the cytoplasmic membrane to be the limiting step in the nanoparticle accumulation inside cell nucleus, and not the nuclear membrane.

Therefore, self-assembling protein-only nanoparticles have been proven to be promising tools for intracellular nucleic acid or drug delivery in mammalian cells, being the cytoplasmic uptake the major critical barrier in the intracellular trafficking process.



Internalization and kinetics of nuclear migration of protein-only, arginine-rich nanoparticles

Esther Vázquez^{a,b,c}, Rafael Cubarsi^{d,c}, Ugutz Unzueta^{a,b,c}, Mónica Roldán^e, Joan Domingo-Espín^{a,b,c}, Neus Ferrer-Miralles^{a,b,c}, Antonio Villaverde^{a,b,c,*}

^a *Institute for Biotechnology and Biomedicine, Universitat Autònoma de Barcelona, Bellaterra, 08193 Barcelona, Spain*

^b *Department of Genetics and Microbiology, Universitat Autònoma de Barcelona, Bellaterra, 08193 Barcelona, Spain*

^c *CIBER de Bioingeniería, Biomateriales y Nanomedicina (CIBER-BBN), Bellaterra, 08193 Barcelona, Spain*

^d *Departament de Matemàtica Aplicada IV, Universitat Politècnica de Catalunya, Jordi Girona 1-3, 08034 Barcelona, Spain*

^e *Servei de Microscòpia, Universitat Autònoma de Barcelona, Bellaterra, 08193 Barcelona, Spain*

ARTICLE INFO

Article history:

Received 30 July 2010

Accepted 24 August 2010

Available online 24 September 2010

Keywords:

Nanoparticle
Genetic engineering
Protein
Biocompatibility
Drug delivery

ABSTRACT

Understanding the intracellular trafficking of nanoparticles internalized by mammalian cells is a critical issue in nanomedicine, intimately linked to therapeutic applications but also to toxicity concerns. While the uptake mechanisms of carbon nanotubes and polymeric particles have been investigated fairly extensively, there are few studies on the migration and fate of protein-only nanoparticles other than natural viruses. Interestingly, protein nanoparticles are emerging as tools in personalized medicines because of their biocompatibility and functional tuneability, and are particularly promising for gene therapy and also conventional drug delivery. Here, we have investigated the uptake and kinetics of intracellular migration of protein nanoparticles built up by a chimerical multifunctional protein, and functionalized by a pleiotropic, membrane-active (R9) terminal peptide. Interestingly, protein nanoparticles are first localized in endosomes, but an early endosomal escape allows them to reach and accumulate in the nucleus (but not in the cytoplasm), with a migration speed of $0.0044 \pm 0.0003 \mu\text{m/s}$, ten-fold higher than that expected for passive diffusion. Interestingly, the plasmatic, instead of the nuclear membrane is the main cellular barrier in the nuclear way of R9-assisted protein-only nanoparticles.

© 2010 Elsevier Ltd. All rights reserved.

1. Introduction

Nanometric protein cages are promising vehicles in nanomedicine [1] as they are not only convenient containers for pharmaceuticals but can also perform specific intermolecular interactions. Natural viruses are the best examples of protein-only nanosized cages that have been traditionally studied and are currently in use in gene therapy [2]. Virus-like particles (VLPs) and artificial viruses are under continuous development mainly for biosafety concerns but also in the search of more tuneable systems [3]. The term 'artificial viruses' refers to manmade constructs designed to mimic viral organization and trafficking patterns, and which are more flexible than VLPs in terms of functional engineering [4–6]. In fact, the incorporation of selected proteins, protein domains or short functional motifs permits the resulting

particles to carry out particular steps in the cell delivery process, such as receptor binding, endosomal escape, intra-cytoplasmic migration or nuclear entrance [7,8]. The construction of multifunctional proteins by genetic engineering, combining selected functional peptides (that provide these desired functions individually) in a single chimerical protein is a convenient way of generating structural components for artificial viruses [5].

Many of the multifunctional proteins used as building blocks of artificial viruses contain Tat (the transactivator protein of the human immunodeficiency virus) [9] or Tat-inspired amino acid sequences, that is, arginine-rich motifs [8,10]. Interestingly, poly-arginines are highly pleiotropic peptides and their incorporation into artificial viruses permits several functions to be covered simultaneously. Arginine-based peptides of around ten residues exhibit blood–brain barrier (BBB) characteristics and cell membrane-crossing activities [11] but also promote DNA condensation and nuclear delivery [8]. Recently, we showed how a commonly used arginine-rich peptide (R9), displayed in combination with a polyhistidine (H6) motif, exhibits intriguing features that promote the self-assembling of the fusion protein into

* Corresponding author. Institute for Biotechnology and Biomedicine, Universitat Autònoma de Barcelona, Bellaterra, 08193 Barcelona, Spain.

E-mail address: prof.a.villaverde@gmail.com (A. Villaverde).

nanoarticulate entities, which are very useful for delivering expressible DNA and protein-based functional drugs [12].

However, very little is known about how R9 and related peptides drive the migration of the associated agents inside the cytoplasm, or the pattern of R9-empowered nuclear shuttling. In fact, apart from natural viruses, the trafficking of protein-based nanoparticles has so far remained a rather neglected area. Here we have kinetically explored the intracellular trafficking of an R9-empowered protein vehicle, and show that there is endosomal-based cell penetration of R9 nanoparticles (an issue still under strong debate for Tat-inspired membrane-active peptides [9]), early endosomal escape, active nuclear delivery, and concentration-dependent nuclear penetration of individual particles that permits their steady accumulation in the nucleus (but not in the cytoplasm). The implications of these findings are discussed in light of the rational design of tailored vehicles for both protein and nucleic acid delivery, and also within the context of the biological impact that protein nanoparticles, as common biomaterials in nanomedicine, might have on their target cells.

2. Material and methods

2.1. Protein production

Production of R9-GFP-H6 was triggered in *Escherichia coli* Rosetta BL21 (DE3) controlled by an isopropyl β -D-1-thiogalactopyranoside (IPTG) inducible-T7 promoter by 1 mM IPTG [12]. Cells from dense cultures were harvested by centrifugation (7650 g for 10 min at 4 °C), and resuspended in 20 mM Tris-HCl pH 7.5, 500 mM NaCl, 10 mM Imidazole, 5 mM β -mercaptoethanol and mechanically disrupted by sonication [13]. The soluble protein was separated by centrifugation at 14,841 g for 15 min at 4 °C, filtered through 0.22 μ m-filters, and purified by chromatography in Ni²⁺ columns in an AKTA FPLC. Fluorescence emission of chimerical GFP constructs similar to that used here has been shown to be representative of the conformational quality and stability of the whole fusion protein [14].

2.2. Cell culture

HeLa (ATCC-CCL-2) cell lines were cultured in MEM (GIBCO, Rockville, MD) supplemented with 10% Foetal Calf Serum (GIBCO) and incubated at 37 °C and 5% CO₂ in a humidified atmosphere. Human glioma U87-MG cells were cultured in RPMI supplemented with 10% Foetal Bovine Serum and 4 mM α -Glutamine. Mouse glioma GL261 cells, kindly provided by Carles Arus' group (UAB) after signing an MTA with the USA repository organization, were grown in RPMI 1640 supplemented with 10% FBS and 4 mM α -Glutamine. Chinese hamster ovary CHO-K1 cells (ATCC-CCL-61) were cultured in F-12 Kaighn's medium (GIBCO) supplemented with α -Glutamine and 10% FBS.

2.3. Confocal microscopy, time-lapse and tracking analysis

Cells (around 2×10^4 cells/cm²) were seeded on bottom-glass culture dishes (MatTek Corp., Ashland). The nuclei was stained with Hoechst 33342 (20 μ g/ml, Molecular Probes) and plasma membrane was labelled with CellMask™ Deep Red (2.5 μ g/ml, Molecular Probes) for 5 min in darkness, followed by further washing with PBS (Sigma–Aldrich Chemie GmbH). 1 μ M of R9-GFP-H6 nanodisks was added to the cell culture immediately after cell staining for time-lapse analysis. For regular confocal imaging in 3D, the protein was added to the cells 20–24 h before the staining and the confocal analysis. Cultured cells were examined using a TCS-SP5 (Leica Microsystems, Heidelberg, Germany) confocal laser scanning microscope with a CO₂ and temperature controlled atmosphere. Images were taken using a 63 \times (NA 1.4, oil) Plan-Apochromatic objective, a blue diode (405 nm) for nuclei, an argon laser (488 nm) for GFP proteins and He Ne laser (633 nm) for plasma membrane. Z-series were collected at 0.5 μ m intervals.

The particle tracking in the cell was evaluated using 4D time-lapse. Projections were obtained from 19 serial optical sections (z-step = 0.5 μ m). The stack of images was acquired every 15 min for 12 h. To determine the protein localization different projections were generated from the xyz-series versus time using Imaris X64 v. 6.2.0 software (Bitplane, Zürich, Switzerland). The overall average speed of protein (μ m/s) in 3D was computed by tracking position versus time with the same software, using the built-in spots function. This function was used to calculate centroids of fluorescent objects and to generate migratory tracks [15]. Protein tracks were generated with "autoregressive motion" algorithm and have been validated manually to eliminate all algorithm-generated errors. Average individual protein speeds were calculated from individual protein tracks.

Mean fluorescence intensity (MFI) of protein (xyz data sets) was measured using Leica LAS AF software, version 2.0.0. The software's region of interest (ROI)

function was used to determine the protein MFI of a nucleus and total cell from the scanned image. The mean and standard error were calculated for all the ROIs examined ($n = 11$). Integrated fluorescence intensity (IF) of protein was quantified using the Metamorph software package v. 5.0r1 (Universal Imaging, West Chest, PA, USA). Fluorescence measures were expressed in arbitrary units.

3. Results

3.1. Internalization and subcellular localization of R9-based protein nanoparticles in different cell lines

The chimerical protein R9-GFP-H6 self-organizes as nanoparticles of around 20 nm with a rather planar, pseudo-spherical morphology, that internalize cultured HeLa cells through the solvent-exposed R9 motif [12]. The mechanics of cellular internalization of Tat-derived motives is still unknown [3,8,9], but diverse experimental evidence suggests that Tat and other cationic peptides bind cells through the heparan sulphate present in the vast majority of mammalian cell types [16–20]. In our case, HeLa (human cervical) cells [12] and all the additionally tested cell lines, namely CHO-K1 (hamster ovarian), GL261 (murine glioma) and U87-MG (human glioma), internalized R9-GFP-H6 nanoparticles (Fig. 1A), and consistently showed both cytoplasmic and nuclear localization according to the fluorescence emission. This demonstrated that the nanoparticulate organization of R9-GFP-H6 does not represent a bottleneck for the internalization of the R9-containing protein and permitted to exclude any strong cell-dependence in the uptake process. In addition, the occurrence of fluorescent particles in the nucleus indicates that the cargo GFP is highly stable during intracellular migration and nuclear transport, and that a significant fraction of the particles (if not all) escape the lysosomal pathway in a functional, fluorescent form.

Interestingly, several authors have suggested both endosomal-dependent and endosomal-independent pathways for Tat and Tat-inspired cationic peptides [3,8,9], which indicates that these uptake styles could depend on the properties of the specific construct. In this context, nothing is known about the uptake of cationic peptides when they are organized as protein nanoparticles. When cultured cells were exposed to R9-GFP-H6 nanoparticles, the occurrence of punctual yellow fluorescence indicated an association between particles and the cell membrane in endosomes, resulting from the merging of red and green fluorescence signals (Fig. 1B). In addition, the 3D Imaris dissection of target cells (Fig. 1C) showed images compatible with the endosomal localization of internalized nanoparticles and fully sustained the hypothesis of an endosomal pattern of cell internalization for R9-GFP-H6.

3.2. Nuclear shuttling kinetics of R9-based protein nanoparticles

The presence of green fluorescence in the cell nuclei ([12] and Fig. 1A) was indicative of endosomal escape, which is expected for proteins containing polyarginine and polyhistidine (membrane-active) peptides [8]. However, we were interested in determining to what extent the nuclear membrane imposed a bottleneck for the mobility of R9-GFP-H6 nanoparticles and which fraction of the internalized material entered the nucleus. In addition, we expected to gain some insights into the mechanics of the protein nanoparticle migration within the cell.

Therefore, we kinetically analyzed the trajectories of nanoparticles from the extracellular media to both the cytoplasmic and nuclear compartments through their fluorescence emission. When the density of nanoparticles derived from confocal image analysis was plotted, a regular increase in the values for both the total cell and the cytoplasm were observed (Fig. 2A). This indicated that during the experimental time (more than 8 h), the protein particles

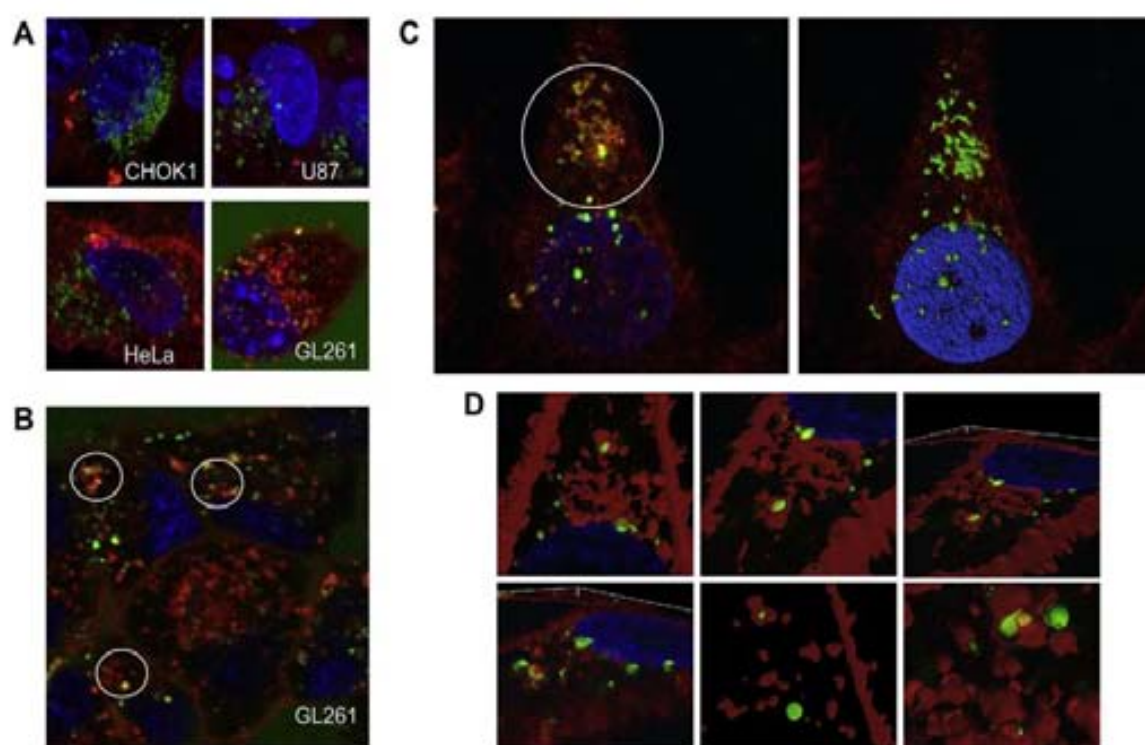


Fig. 1. Uptake of R9-functionalized protein nanoparticles. **A.** Fluorescent R9-GFP-H6 nanoparticles observed in different cell lines with confocal microscopy following exposure (between 20 and 24 h), showing both cytoplasmic and nuclear localizations. In **B.** GL261 cells were stained with Hoechst and CellMask previously to R9-GFP-H6 addition. Examples of intracellular yellow fluorescent structures are indicated by circles. **C.** At the top left, a conventional confocal image shows intense green and red fluorescence merging into a yellow signal in endosomes (white circle), in one representative HeLa cell exposed to R9-GFP-H6 nanoparticles. On the right, isosurface representation of the same cell within a three-dimensional volumetric $x-y-z$ data field. **D.** Projections of the cell at different angles and magnifications, showing the embedding of green fluorescent nanoparticles within membrane structures. Cell membranes were stained with CellMask™ Deep Red (red fluorescence) and the nucleus with Hoechst 33342 (blue fluorescence). R9-GFP-H6 nanoparticles naturally emit green fluorescence.

were continuously crossing both the cytoplasmic and nuclear membranes with undetectable proteolytic degradation and in a proper protein conformation that sustained fluorescence emission [14]. The accumulation in the nucleus was indirectly confirmed by the slope of the nuclear fluorescence, being higher than that of the whole cell signal (Fig. 2A). These slopes were compatible with similar (in the same order of magnitude) entry rates of R9-GFP-H6 in both the cytoplasm and the nucleus. In absolute terms, the

number of R9-GFP-H6 nanoparticles (monitored by integrated fluorescence instead average fluorescence in confocal sections) in the nucleus and the cytoplasm reached similar values at the end of the experimental time (Fig. 2B).

For a detailed kinetic analysis, data should be studied from a model of diffusion according to Fick's law. However, since individual protein molecules acted as assembled, higher order, particulate entities, the fluorescence $\phi(t)$ of the internalized particles as

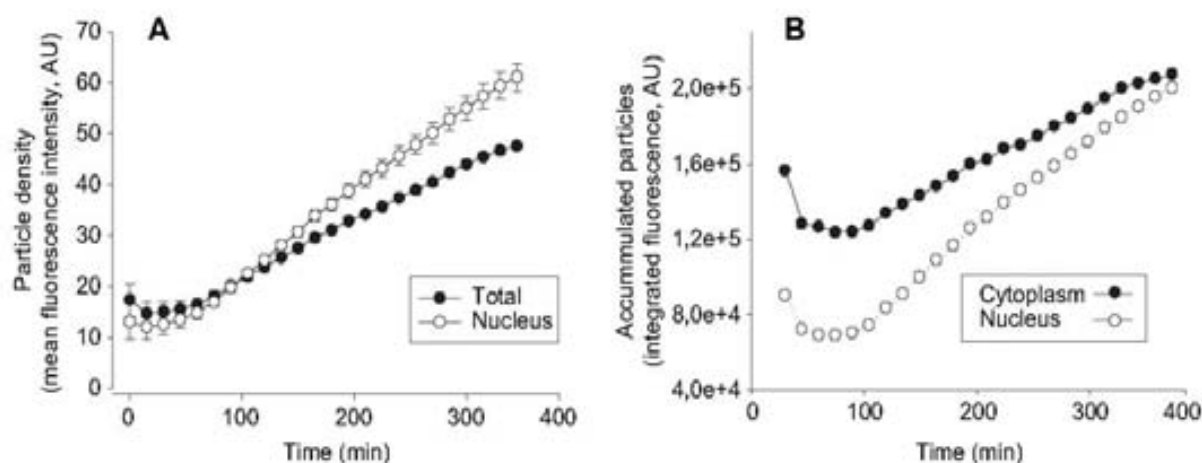


Fig. 2. Kinetics of accumulation of R9-GFP-H6 in cultured HeLa cells during steady exposure to the nanoparticles, monitored by time-lapse confocal analysis. In **A.** density of particles in the whole cell and in the nucleus, and in **B.** accumulation of nanoparticles in the nucleus and cytoplasm. AU are arbitrary units. Depicted data derive from a single representative cell in which multiple z sections have been independently analyzed.

a function of time empirically showed behaviour analogous to population dynamics with limited growth, according to the differential equation:

$$F'(t) = p\phi + q; \quad q > 0, \quad p < 0 \quad (1)$$

where p and q are constants, where $F(t) = \ln \phi(t)$, and the relative variation rate of fluorescence is given by $F'(t) = d \ln \phi(t) / dt$. At the beginning of the experiment, if $\phi = 0$ then F' takes the value q , which is the maximum increasing rate of fluorescence. Afterwards, F' decreases progressively to zero, when the fluorescence becomes stabilized. Maximum fluorescence is reached at $L = -q/p$. Unlike a population model, a value of $\phi > L$ would make no sense here. The parameters of the model were obtained by discretizing Eq. (1) with a three-point estimation of the time derivative $F'(t)$. The overdetermined linear system was solved by the least squares method, which led to the optimal estimates listed in Table 1 for the model cell depicted in Fig. 3A and B. The higher q value for the nucleus in comparison with that obtained for the cytoplasm revealed an immediate and extremely efficient nuclear entry of particles at initial experimental times, also indicating that nuclear entry is not triggered by a threshold particle concentration in the cytoplasm. The regression lines derived from Eq. (1) for the total cell and for both compartments can be seen in Fig. 3A, and showed a good adjustment of the data to the model, except in a short time interval (between vertical lines). When the total fluorescence predicted by the model in all compartments was plotted along the experimental time, we determined that such a discontinuity in the regularity of the model occurred at around 5 h post-exposure for a period of about 1 h (Fig. 3B), in which the uptake of nanoparticles by the cell was enhanced. Very interestingly, the transient stimulation of the internalization of R9-GFP-H6 resulted in an immediate increase of the nuclear entry of the particles (Fig. 3B). Both the higher uptake and the consequent stipulation of nuclear transfer were confirmed in all the studied individual cells, although at different levels of intensity (see additional examples in Fig. 3C). This indicated that the fluorescent particles do not accumulate in the cytoplasm but only in the nucleus and that the cellular uptake is a bottleneck for their nuclear penetration.

Irrespective of the causes of the discontinuity of R9-GFP-H6 uptake at 5 h after exposure, which deserves further investigation, the temporal coincidence in the increase of fluorescence transfer from both the extracellular media to the cytoplasm and from the cytoplasm to the nucleus demonstrates that the nuclear membrane is not a bottleneck for intracellular protein trafficking, and that the nuclear accumulation of R9-GFP-H6 depends strictly on the availability of the protein in the cytoplasm. Therefore, the plasmatic membrane instead of the nuclear membrane appears as the main physical barrier for the nuclear delivery of R9-empowered protein nanoparticles. This could be accounted for by the slow particle uptake compared to the more efficient nuclear entrance, which could be related to the endosome-linked internalization style. Irrespective of this fact, the number of nanoparticles occurring in the cytoplasm and the nucleus at 8 h post-exposure was similar (Fig. 3B), which again is in agreement with the higher density in the fluorescence signal found in the nucleus (Fig. 2B).

At this stage, individual fluorescent particles were tracked with serial confocal analysis of the target cells until they entered the nucleus (Supplementary video). The particles can be seen to have random trajectories in the external media; however, while once they have reached the cytoplasm they show convergent movements towards the nuclear compartment. This approach permitted us to make an accurate estimation of the actual speed of internalized particles, that moved at $0.0044 \pm 0.0003 \mu\text{m/s}$ ($n = 110$, monitored from 0 to 5 h) in the cytosol (93.2% of the particles were mobile), while in the nucleus, only 40% of the particles moved, most of them remaining at fixed positions. The average speed of those observed as mobile in the nucleus was $0.0042 \pm 0.0007 \mu\text{m/s}$ ($n = 29$, monitored from 5 to 12 h), a value similar to that observed for the cytoplasmic migration.

Supplementary video related to this article can be found at 10.1016/j.biomaterials.2010.08.065.

4. Discussion

The interaction between cells and nanoparticles is a matter of major interest in nanomedicine, especially regarding the biological effects that these particles have on biological systems [21], which seem to be strongly size-dependent [22]. In this context, the uptake of carbon nanotubes [23], peptide-activated metal particles [24], metal-polymer [25] and metal-lipid hybrid [26] particles, polymeric particles [27–29], lipidic vesicles [30] and polymer-lipid hybrids [31] or peptide-functionalized polymers [32] (among others) are currently under in depth study and semi-rational design. Most of these studies are focused on the ability of these entities to deliver associated drugs, especially nucleic acids for substitutive gene therapy (in the nucleus) or for gene silencing (in the cytoplasm). Full-length proteins such as antibodies or short peptides have often been used to functionalize these nanoparticles, especially to provide specific binding to target cell-surface receptors [33], as cationic agents for DNA condensation [10] or as nuclear localization signals for gene delivery [34]. Interestingly, apart from driving specific interactions for cell-targeted drug delivery [35], many natural proteins exhibit self-assembling activities (resulting in viral capsids or nanostructured cell organelles such as pili or flagella). As proteins are fully biocompatible macromolecular materials and because they are highly tuneable through conventional genetic engineering and biological synthesis, the potential of protein nanocages (natural and manmade) is nowadays fully recognized [1]. However, the intracellular trafficking of protein nanoparticles other than viruses or virus-like entities has so far not been studied in depth.

We recently designed a chimerical protein containing GFP as both scaffold and reporter protein and two membrane-active peptides (R9 and H6) at the amino and carboxy terminus respectively [12]. R9 is a pleiotropic motif that, in addition to its membrane-crossing, DNA binding and nuclear localization activities, is able to promote R9-GFP-H6 self-assembly as building blocks of 20 nm-sized nanodisks, with high cell penetrability and able to deliver expressible DNA into the nucleus. H6 is a membrane-

Table 1
Model parameters p , q , and L with their standard deviation for the model cell analyzed in Fig. 3A and B.

Cell compartment	p (AU ⁻¹ min ⁻¹)	q (min ⁻¹)	L (AU)
Whole cell	$-1.51 \times 10^{-8} \pm 1.23 \times 10^{-9}$	$0.82 \times 10^{-2} \pm 0.44 \times 10^{-3}$	$5.43 \times 10^3 \pm 5.31 \times 10^4$
Cytoplasm	$-2.11 \times 10^{-8} \pm 2.89 \times 10^{-9}$	$0.63 \times 10^{-2} \pm 0.53 \times 10^{-3}$	$2.97 \times 10^3 \pm 4.80 \times 10^4$
Nucleus	$-4.05 \times 10^{-8} \pm 2.69 \times 10^{-9}$	$1.02 \times 10^{-2} \pm 0.46 \times 10^{-3}$	$2.53 \times 10^3 \pm 2.03 \times 10^4$

AU: arbitrary fluorescence units; min: minutes.

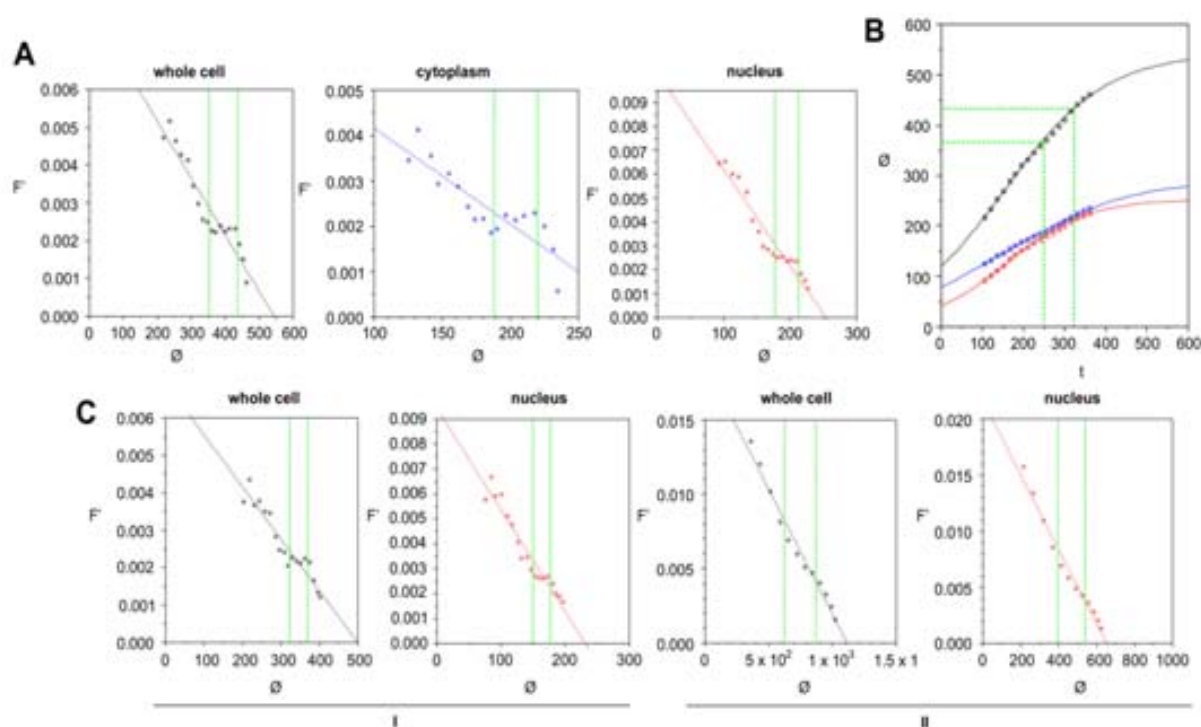


Fig. 3. R9-GFP-H6 particle concentration in different cell compartments monitored by the fluorescence flow according to Equation (1). In A, F versus θ for a whole representative cell, and for its cytoplasm and nucleus separately. In B, θ is plotted versus time (in min), to show the accumulation of nanoparticles in different compartments. Vertical green lines indicate the temporal period in which the uptake of particles increase and the experimental data is not accounted for by the kinetic model. C. The internalization of R9-GFP-H6 is modelled for two additional cells (I and II), showing different extents of the uptake stimulation, which are always coincident in time when the whole cell and the nuclear compartment alone are monitored.

active peptide [8] that allows fast protein purification from producing bacteria. Disk-shaped nanoparticles are of particular interest in nanomedicine as they appear as being specially suitable for delivery to specific organs, such as heart and lung [36]. In addition, their diameter below 30 nm permits the crossing of the nuclear pore in non-dividing cells without energy expenses, as shown in other types of nanoparticles [37,38], a fact that dramatically favours nuclear entry and enhances transgene expression levels. Furthermore, the multifunctional properties of the R9 motif grant the resulting constructs with activities that perform sequentially during both particle generation and cell penetration, in the line of the recently proposed Logic-Embedded Vector concept [39]. R9-GFP-H6 nanoparticles enter several cell types through endosomal pathways (Fig. 1A) and steadily accumulate into the nucleus (Fig. 2), and the cytoplasm is a mere intermediate in the nuclear transfer. Under our working conditions, all the individually analyzed HeLa cells exposed to R9-GFP-H6 nanoparticles showed a transient increase of the uptake rate at around 5 h after exposure (Fig. 3), which was coincident with the time in which important areas of the culture reached full confluence. Although the cellular mechanics of this event need to be investigated further, such stimulation of internalization caused an immediate enhancement of the nuclear import of the particles from the cytoplasm (Fig. 3). This suggests that the efficiency of the nuclear penetration is dependent on the cytoplasmic concentration of particles. Moreover, the nuclear membrane, generally considered as a main biobarrier in nanoparticulate drug delivery [36], is not a critical obstacle for R9-GFP-H6, while the plasmatic membrane seems to be a more important bottleneck in the whole transfer process. The average shuttling speed of R9-GFP-H6 in the cytoplasm is $0.0044 \mu\text{m/s}$, which is much higher than observed for passive diffusion [40]. Both the high speed and the more ordered trajectories of R9-GFP-H6 in the cytoplasm compared to the

random movement before it enters the cells (Supplementary video), strongly support active transport to the nucleus. In this compartment, particles were observed to move at the same speed but only for a short period of time, after which they remain fully immobile and tend to aggregate. In previous research on chemically different, non-protein nanoparticles as models, cytoplasmic speeds have been estimated to be $0.00032 \mu\text{m/s}$ for passive diffusion (polyethylenimine/DNA large particles [40]), $0.06 \mu\text{m/s}$ for actin-linked transport (poly[lactic-co-glycolic acid] and lipoplexes [41]) and $2 \mu\text{m/s}$ for microtubule-linked transport (lipoplexes [42]), with no references to intranuclear movement. The speed observed with R9-protein particles does not completely fit with these values from non-protein materials, but it would be roughly compatible with dinein- or actin-mediated migration, especially considering that the obtained speed data was an average of the endosomal and port-endosomal migration phases.

The protein transduction domain (PTD, $^{47}\text{YGRKKRRQRRR}^{57}$) of the HIV Tat protein (or the whole Tat protein) has been largely employed as a Trojan horse for the intracellular delivery of both therapeutic proteins and nucleic acids [9], but TAT-inspired poly-arginine motives seem to be optimal for cell penetration because directed molecular evolution to search for 12-mer alternatives has not yet rendered alternative transducing peptide sequences with improved efficacies [43]. In this regard, the endosomal uptake of R9-GFP-H6 nanoparticles supports their lack of toxicity in the exposed cultures, which, however, could be a matter of concern in translocation-based entrance due to the mechanical perturbations exerted on the plasma membrane [3]. Apart from the biosafety generally expected in protein nanoparticles, R9-empowered protein nanoparticles, as protein-only entities, are suitable of tailoring by conventional protein engineering to improve their performance. According to our data, the cellular internalization rather than the nuclear entry should be the target of any further genetic tuning.

5. Conclusions

Arginine-rich (R9), protein-only nanoparticles of 20 nm enter mammalian cells via endosomes from which they immediately escape, and continuously penetrate the nuclear compartment in converging, not random trajectories, at steady rates. The cytoplasmic speed of the particles is 0.0044 $\mu\text{m/s}$, ten times higher than that observed in passive diffusion, and this rate is shortly kept in the nuclear compartment until their final arrest. Protein nanoparticles accumulate in the nucleus but not in the cytoplasm, and the cellular uptake is a limiting factor for the nuclear entry, the nuclear membrane being not a critical barrier for such R9-empowered particles. The high migration rate and nuclear avidity, the intracellular stability and the previously shown abilities to self assemble and to condense DNA, make the R9-based protein-only nanoparticles promising tools for delivery of nucleic acids of functional proteins. Since proteins are highly tuneable materials, their properties, and those conferred by the pleiotropic R9 motif, can be further engineered to fulfil specific drug delivery requirements.

Acknowledgments

We are indebted to the Cell Culture Unit of the Servei de Cultius Cel·lulars, Producció d'Anticòssos i Citometria (SCAC), and to the Servei de Microscòpia, both at the UAB. We also appreciate the financial support received for the design and production of artificial viruses for gene therapy to AV and EV from MICINN (BIO2007-61194 and ACI2009-0919), FISS (PS0900165), AGAUR (2009SGR-108) and CIBER de Bioingeniería, Biomateriales y Nanomedicina (specially through the IMAFEN and PROGLIO intramural projects 2008–2011), an initiative funded by the VI National R&D&I Plan 2008–2011, Iniciativa Ingenio 2010, Consolider Program, CIBER Actions and financed by the Instituto de Salud Carlos III with assistance from the European Regional Development Fund. AV has been distinguished with an ICREA ACADEMIA award.

Appendix

Figures with essential color discrimination. Fig. 3 in this article is difficult to interpret in black and white. The full color image can be found in the on-line version, at doi:10.1016/j.biomaterials.2010.08.065.

References

- [1] Uchida M, Klem MT, Allen M, Suci P, Henniken M, Varpness Z, et al. Biological containers: protein cages as multifunctional nanoplatfoms. *Adv Mater* 2007;19:1025–42.
- [2] Edelstein ML, Abedi MR, Wixon J. Gene therapy clinical trials worldwide to 2007 – an update. *J Gene Med* 2007;9:833–42.
- [3] Ferrer-Miralles N, Vázquez E, Villaverde A. Membrane-active peptides for non-viral gene therapy: making the safest easier. *Trends Biotechnol* 2008;26:267–75.
- [4] Douglas KL. Toward development of artificial viruses for gene therapy: a comparative evaluation of viral and non-viral transfection. *Biotechnol Prog* 2008;24:871–83.
- [5] Aris A, Villaverde A. Modular protein engineering for non-viral gene therapy. *Trends Biotechnol* 2004;22:371–7.
- [6] Mastrobattista E, van der Aa MA, Hennink WE, Crommelin DJ. Artificial viruses: a nanotechnological approach to gene delivery. *Nat Rev Drug Discov* 2006;5:115–21.
- [7] Vázquez E, Ferrer-Miralles N, Mangués R, Corchero JL, Schwartz Jr S, Villaverde A. Modular protein engineering in emerging cancer therapies. *Curr Pharm Des* 2009;15:893–916.
- [8] Vázquez E, Ferrer-Miralles N, Villaverde A. Peptide-assisted traffic engineering for nonviral gene therapy. *Drug Discov Today* 2008;13:1067–74.
- [9] Chauban A, Tikoo A, Kapur AK, Singh M. The taming of the cell penetrating domain of the HIV Tat: myths and realities. *J Control Release* 2007;117:148–62.

- [10] Saccardo P, Villaverde A, Gonzalez-Montalban N. Peptide-mediated DNA condensation for non-viral gene therapy. *Biotechnol Adv* 2009;27:432–8.
- [11] Kumar P, Wu H, McBride JL, Jung KE, Kim MH, Davidson BL, et al. Transvascular delivery of small interfering RNA to the central nervous system. *Nature* 2007;448:39–43.
- [12] Vázquez E, Roldán M, Díez-Gil C, Unzueta U, Domingo-Espín J, Cedano J, et al. Protein nanodisk assembling and intracellular trafficking powered by an arginine-rich (R9) peptide. *Nanomedicine* 2010;5:259–68.
- [13] Feliú JX, Cubarsi R, Villaverde A. Optimized release of recombinant proteins by ultrasonication of *E. coli* cells. *Biotechnol Bioeng* 1998;58:536–40.
- [14] García-Fruitos E, Martínez-Alonso M, González-Montalban N, Valli M, Mattanovich D, Villaverde A. Divergent genetic control of protein solubility and conformational quality in *Escherichia coli*. *J Mol Biol* 2007;374:195–205.
- [15] Zaman MH, Trapani LM, Sieminski AL, Mackellar D, Gong H, Kamm RD, et al. Migration of tumor cells in 3D matrices is governed by matrix stiffness along with cell-matrix adhesion and proteolysis. *Proc Natl Acad Sci U S A* 2006;103:10889–94.
- [16] Ziegler A, Seelig J. Interaction of the protein transduction domain of HIV-1 Tat with heparan sulfate: binding mechanism and thermodynamic parameters. *Biophys J* 2004;86:254–63.
- [17] Hakansson S, Jacobs A, Caffrey M. Heparin binding by the HIV-1 tat protein transduction domain. *Protein Sci* 2001;10:2138–9.
- [18] Belting M. Heparan sulfate proteoglycan as a plasma membrane carrier. *Trends Biochem Sci* 2003;28:145–51.
- [19] Sandgren S, Cheng F, Belting M. Nuclear targeting of macromolecular poly-anions by an HIV-Tat derived peptide. Role for cell-surface proteoglycans. *J Biol Chem* 2002;277:38877–83.
- [20] Tyagi M, Rusnati M, Presta M, Giacca M. Internalization of HIV-1 tat requires cell surface heparan sulfate proteoglycans. *J Biol Chem* 2001;276:3254–61.
- [21] Riehemann K, Schneider SW, Luger TA, Godin B, Ferrari M, Fuchs H. Nanomedicine – challenge and perspectives. *Angew Chem Int Ed Engl* 2009;48:872–97.
- [22] Jiang W, Kim BY, Rutka JT, Chan WC. Nanoparticle-mediated cellular response is size-dependent. *Nat Nanotechnol* 2008;3:145–50.
- [23] Lamm MH, Ke PC. Cell trafficking of carbon nanotubes based on fluorescence detection. *Methods Mol Biol* 2010;625:135–51.
- [24] Aaron J, Travis K, Harrison N, Sokolov K. Dynamic imaging of molecular assemblies in live cells based on nanoparticle plasmon resonance coupling. *Nano Lett* 2009;9:3612–8.
- [25] Thomas M, Klibanov AM. Conjugation to gold nanoparticles enhances poly-ethylenimine's transfer of plasmid DNA into mammalian cells. *Proc Natl Acad Sci U S A* 2003;100:9138–43.
- [26] Li P, Li D, Zhang L, Li G, Wang E. Cationic lipid bilayer coated gold nanoparticles-mediated transfection of mammalian cells. *Biomaterials* 2008;29:3617–24.
- [27] Peng L, Liu M, Xue YN, Huang SW, Zhuo RX. Transfection and intracellular trafficking characteristics for poly(amidoamine)s with pendant primary amine in the delivery of plasmid DNA to bone marrow stromal cells. *Biomaterials* 2009;30:5825–33.
- [28] Perumal OP, Inapagolla R, Kannan S, Kannan RM. The effect of surface functionality on cellular trafficking of dendrimers. *Biomaterials* 2008;29:3469–76.
- [29] Barua S, Rege K. The influence of mediators of intracellular trafficking on transgene expression efficacy of polymer–plasmid DNA complexes. *Biomaterials* 2010;31:5894–902.
- [30] Karve S, Alaoui A, Zhou Y, Rotolo J, Sofou S. The use of pH-triggered leaky heterogeneities on rigid lipid bilayers to improve intracellular trafficking and therapeutic potential of targeted liposomal immunotherapy. *Biomaterials* 2009;30:6055–64.
- [31] Masuda T, Akita H, Niikura K, Nishio T, Ukawa M, Enoto K, et al. Envelope-type lipid nanoparticles incorporating a short PEG-lipid conjugate for improved control of intracellular trafficking and transgene transcription. *Biomaterials* 2009;30:4806–14.
- [32] Vasir JK, Labhasetwar V. Quantification of the force of nanoparticle–cell membrane interactions and its influence on intracellular trafficking of nanoparticles. *Biomaterials* 2008;29:4244–52.
- [33] Balestrieri ML, Napoli C. Novel challenges in exploring peptide ligands and corresponding tissue-specific endothelial receptors. *Eur J Cancer* 2007;43:1242–50.
- [34] Pouston CW, Wagstaff KM, Roth DM, Moseley GW, Jans DA. Targeted delivery to the nucleus. *Adv Drug Deliv Rev* 2007;59:698–717.
- [35] Brown KC. Peptidic tumor targeting agents: the road from phage display peptide selections to clinical applications. *Curr Pharm Des* 2010;16:1040–54.
- [36] Serda RE, Godin B, Blanco E, Chiappini C, Ferrari M. Multi-stage delivery nanoparticle systems for therapeutic applications. *Biochim Biophys Acta*; 2010 May 21 [Epub ahead of print] PMID: 20493927.
- [37] Tkachenko AG, Xie H, Coleman D, Glomm W, Ryan J, Anderson MF, et al. Multifunctional gold nanoparticle-peptide complexes for nuclear targeting. *J Am Chem Soc* 2003;125:4700–1.
- [38] Fink TL, Klepczyk PJ, Oette SM, Gedeon CR, Hyatt SL, Kowalczyk TH, et al. Plasmid size up to 20 kbp does not limit effective in vivo lung gene transfer using compacted DNA nanoparticles. *Gene Ther* 2006;13:1048–51.
- [39] Ferrari M. Frontiers in cancer nanomedicine: directing mass transport through biological barriers. *Trends Biotechnol* 2010;28:181–8.

40. Yin J, Wirth D, Harel J. Efficient in vivo transport of gene-transmitters to the cell nucleus. *Proc Natl Acad Sci USA* 2004;101:4828–32.
41. Ng CP, Goodman JL, Park IK, Fan MT. Polyamine surface engineering of plasmid DNA nanoparticles to enhance intra-cellular trafficking by a first-passal strategy. *Biomaterials* 2006;47:951–8.
42. Berson JL, Puri MI. Analysis of the intracellular carriers employed by nonviral gene carriers in a model of spatially controlled delivery to neurons. *J Gene Med* 2009;10:187–97.
43. Ma Z, Ma J, Liu X, Rao Cuo PL. Characterization of a class of cationic peptides able to facilitate efficient protein transduction in vivo and in vitro. *Mol Ther* 2000;2:119–27.

Paper 3

Intracellular CXCR4⁺ cell targeting with T22-empowered protein-only nanoparticles

Ugutuz Unzueta, María Virtudes Céspedes, Neus Ferrer-Miralles, Isolda Casanova, Juan Cedano, José Luis Corchero, Joan Domingo-Espín, Antonio Villaverde, Ramón Mangués, Esther Vazquez.

Int J Nanomedicine, 7, 4533-4544, 2012

Targeted delivery of drugs and nucleic acids, has turned out to be a very promising tool in nanomedicine and more especially in cancer medicine where targeted therapies for metastatic tumor cells are urgently demanded. In this context, the aim of this work was to construct self-assembling protein nanoparticles directed to CXCR4 expressing cells (a cell surface receptor marker associated with several severe human pathologies, including metastatic colorectal cancer) and assess their biodistribution in metastatic colorectal cancer models.

Four different CXCR4 specific ligands fused to His-tagged GFP-based reporter proteins, which self-assemble in monodisperse nanoparticles, were tested for their ability to specifically internalize in a CXCR4⁺ cultured cancer cells. Although all the generated self-assembled nanoparticles succeeded in their internalization ability, the T22-empowered particles proved to be by far the most efficient in penetrating target cells via a rapid, receptor-specific endosomal route, showing stable accumulation of the fluorescent nanoparticles in the perinuclear cell region. The excellent *in vitro* performance of T22-empowered protein nanoparticles observed, encouraged us to proceed with further *in vivo* biodistribution assays in an orthotopic metastatic colorectal cancer murine model. Intravenous injection of T22-empowered self-assembling nanoparticles resulted in a stable accumulation of the nanoparticles exclusively in the primary tumor and all the macro and micrometastatic foci for more than 24h, being internalized in CXCR4 positive cells as it was described *in vitro*. Peptide accumulation showed no toxicity in both *in vitro* and *in vivo* metastatic colorectal cancer models.

In this study, the peptide T22 has been shown to be an unusually powerful tag for intracellular targeting of CXCR4⁺ cells, offering a wide spectrum of possibilities not only for the specific drugs and nucleic acids delivery, but also as a diagnostic agent.

Intracellular CXCR4⁺ cell targeting with T22-empowered protein-only nanoparticles

This article was published in the following Dove Press journal:
International Journal of Nanomedicine
14 August 2012
Number of times this article has been viewed

Ugutx Unzueta¹⁻³
María Virtudes Céspedes^{2,4}
Neus Ferrer-Miralles¹⁻³
Isolda Casanova^{2,4}
Juan Cedano⁵
José Luis Corchero¹⁻³
Joan Domingo-Espín¹⁻³
Antonio Villaverde¹⁻³
Ramón Mangués^{2,4}
Esther Vázquez¹⁻³

¹Institut de Biotecnologia i de Biomedicina,
²Departament de Genètica i de Microbiologia, Universitat Autònoma de Barcelona, Bellaterra, Barcelona,
³CIBER en Bioingeniería, Biomateriales y Nanomedicina, Bellaterra, Barcelona,
⁴Oncogenesis and Antitumor Drug Group, Biomedical Research Institute Sant Pau, Hospital de la Santa Creu i Sant Pau, Barcelona, Spain; ⁵Laboratory of Immunology, Regional Norte, Universidad de la República, Salto, Uruguay



Correspondence: Antonio Villaverde
Institut de Biotecnologia i de Biomedicina,
Universitat Autònoma de Barcelona,
Bellaterra, 08193 Barcelona, Spain
Tel +349 3581 3086
Fax +349 3581 2011
Email antoni.villaverde@uab.cat

Background: Cell-targeting peptides or proteins are appealing tools in nanomedicine and innovative medicines because they increase the local drug concentration and reduce potential side effects. CXC chemokine receptor 4 (CXCR4) is a cell surface marker associated with several severe human pathologies, including colorectal cancer, for which intracellular targeting agents are currently missing.

Results: Four different peptides that bind CXCR4 were tested for their ability to internalize a green fluorescent protein-based reporter nanoparticle into CXCR4⁺ cells. Among them, only the 18 mer peptide T22, an engineered segment derivative of polyphemusin II from the horseshoe crab, efficiently penetrated target cells via a rapid, receptor-specific endosomal route. This resulted in accumulation of the reporter nanoparticle in a fully fluorescent and stable form in the perinuclear region of the target cells, without toxicity either in cell culture or in an in vivo model of metastatic colorectal cancer.

Conclusion: Given the urgent demand for targeting agents in the research, diagnosis, and treatment of CXCR4-linked diseases, including colorectal cancer and human immunodeficiency virus infection, T22 appears to be a promising tag for the intracellular delivery of protein drugs, nanoparticles, and imaging agents.

Keywords: peptide tag, CXCR4, intracellular targeting, self-assembling, nanoparticles, colorectal cancer

Introduction

Unlike conventional therapies, nanomedicine and innovative medicines in general pursue targeted intracellular delivery of chemotherapy and imaging agents, and are expected to result in significantly lower effective therapeutic doses, production costs, and toxicity.¹ Cell-penetrating peptides offer a broad potential for efficient internalization of attached cargo because of their affinity for and associated ability to cross cell membranes.^{2,3} However, because these activities are not dependent on specific cell surface receptors, appropriate cell targeting and biodistribution of therapeutic complexes cannot be achieved using cell-penetrating peptides. The discovery of disease-linked cell surface markers enables subsequent identification of specific ligands for receptor-mediated endocytosis. These entities should be capable of driving the uptake of large macromolecular complexes such as nanoparticles, which are useful in a therapeutic context as drug carriers and stabilizers. The CXC chemokine receptor 4 (CXCR4) plays a role in inflammation, autoimmunity, ischemia, and stem cell mobilization.⁴ In addition, CXCR4 is a coreceptor for the human immunodeficiency virus (HIV)⁵ and an important stem cell marker in several common human cancers,^{6,7} including metastatic colorectal cancer.^{8,9}

Therefore, developing new therapeutic agents targeted to CXCR4 is a recognized priority in emerging medicines,⁴ but because CXCR4 ligands remain poorly studied and peptides suitable for CXCR4-mediated endocytosis are not available, intracellular targeting to CXCR4⁺ cells is still not feasible. In the present study, we describe peptide T22, a known antagonist of CXCR4, that binds to and penetrates CXCR4⁺ cells efficiently via CXCR4-specific endocytosis. T22 is an engineered version polyphemusin II peptide from the horseshoe crab, in which three substitutions at residues Tyr5, Lys7, and Tyr12 dramatically increase the natural affinity of this peptide for CXCR4.^{10,11} When fused to a self-assembling green fluorescent protein (GFP)-based building block, T22 promotes fast perinuclear accumulation of stable and highly fluorescent nanoparticles without cytotoxicity, both in cell culture and in vivo. Thus, we propose T22 as a novel cell-targeting peptide suitable for functionalization of nanoparticles and appropriate for intracellular delivery in CXCR4-associated medicines.

Materials and methods

Protein design, production, purification, and characterization

Four chimeric genes were designed inhouse and provided by Genent (Regensburg, Germany). Using *NdeI/HindIII* restriction sites, these genes were introduced into pET22b (Novagen 69744-3). All the encoded proteins were produced in *Escherichia coli* Origami B (BL21, OmpT⁻, Lon⁻, TrxB⁻, Gor⁻, Novagen) overnight at 20°C upon addition of 0.1 mM isopropyl- β -D-thiogalactopyronaside. Bacterial cells were then centrifuged for 45 minutes (5000 g at 4°C) and resuspended in Tris buffer (Tris 20 mM, pH 8.0, NaCl 500 mM, imidazole 10 mM) in the presence of ethylenediamine tetra-acetic acid-free protease inhibitor (Complete EDTA-Free, Roche, Basel, Switzerland). The cells were disrupted at 1100 psi in a French press (Thermo FA-078A) and their proteins were purified by 6 \times His tag affinity chromatography using HiTrap Chelating HP 1 mL (GE Healthcare, Piscataway, NJ) columns with an AKTA purifier FPLC (GE Healthcare). Elution was achieved by a linear gradient of Tris 20 mM, pH 8.0, 500 mM NaCl, and 500 mM imidazole, and the proteins eluted were finally dialyzed against phosphate-buffered solution (140 mM NaCl, 7.5 mM Na₂HPO₄, 2.5 mM NaH₂PO₄) plus 10% glycerol, pH 7.4, against carbonate buffer (166 mM NaCO₃H + 333 mM NaCl, pH 7.4) or against Tris 20 mM + NaCl 500 mM, pH 7.5. The integrity of the resulting proteins was checked by both mass spectrometry and N-terminal sequencing using the Edman degradation method, and

their amounts were determined by Bradford's assay.¹² In addition, all products were analyzed by Coomassie-stained sodium dodecyl sulfate polyacrylamide gel electrophoresis and anti-His Western blot analysis. The fusion proteins were named according to N \rightarrow C modular organization by the name of the CXCR4 ligand, followed by GFP and H6 (hexahistidine tail).

TEM, fluorescence determination, and dynamic light scattering

Purified proteins were diluted to 0.2 mg/mL and contrasted by evaporation of 1 nm platinum layer in carbon-coated grids. Samples were visualized in a Hitachi H-7000 transmission electron microscope. Fluorescence of the nanoparticles was determined in a Cary Eclipse fluorescence spectrophotometer (Varian Inc, Palo Alto, CA) at 510 nm using an excitation wavelength of 450 nm. The volume and size distribution of the nanoparticles was determined by dynamic light scattering at 633 nm (Zetasizer Nano ZS, Malvern Instruments Limited, Malvern, Worcestershire, UK).

Protein stability analysis

Stability of the T22-GFP-H6 (amino terminus of a His-tagged enhanced GFP) was analyzed in triplicate in human serum (S2257-5ML, Sigma, St Louis, MO) at 37°C, with agitation and at a final concentration of 0.23 μ g/ μ L. Fluorescence was determined as described earlier, and the integrity of the T22-GFP-H6 was confirmed by sodium dodecyl sulfate polyacrylamide gel electrophoresis and further Western blotting. Nitrocellulose membranes were developed using an anti-GFP rabbit polyclonal serum.

Cell culture and confocal laser scanning microscopy

The cells were cultured in modified Eagle's medium (Gibco, Rockville, MD) supplemented with 10% fetal calf serum (Gibco), and incubated at 37°C and 5% CO₂ in a humidified atmosphere. Nanoparticles were added to the cell culture in the presence of Optipro medium (Gibco) 20 hours before confocal analysis, except for the time-course and internalization studies in the presence of serum (complete medium). For confocal analysis, the cells were grown on MatTek culture dishes (MatTek Corporation, Ashland, MA). The nuclei were labeled with 0.2 μ g/mL Hoechst 33342 (Molecular Probes, Eugene, OR) and the plasma membranes with 2.5 μ g/mL CellMask™ Deep Red (Molecular Probes) for 10 minutes in the dark. The cells were washed in phosphate-buffered saline (Sigma-Aldrich Chemie GmbH, Steinheim, Germany).

Live cells were recorded by TCS-SP5 confocal laser scanning microscopy (Leica Microsystems, Heidelberg, Germany) using a Plan Apo 63 × /1.4 (oil HC × PL APO lambda blue) objective as described elsewhere.¹³ To determine particle localization inside the cell, stacks of 10–20 sections for every 0.5 μm of cell thickness were collected and three-dimensional models were generated using Imaris version 6.1.0 software (Bitplane, Zürich, Switzerland) as reported previously.¹⁴ Cell samples were analyzed after treatment with 1 mg/mL trypsin (Gibco) for 15 minutes on a FACS-Canto system (Becton Dickinson, Franklin Lakes, NJ) using a 15 mW air-cooled argon ion laser at 488 nm excitation. Fluorescence emission was measured with a D detector (530/30 nm band pass filter). Cell viability was determined by 3-(4,5-dimethylthiazol-2-yl)-2,5-diphenyltetrazolium bromide (MTT) assay as described elsewhere.¹⁵ An HeLa cell line was obtained from the American Type Culture Collection (reference CCL-2, Manassas, VA) and SW1417 was a generous gift from Xavier Mayol (Institut Municipal D'Investigació Mèdica, Barcelona, Spain).¹⁶

Molecular modeling

Protein homology models were generated using Modeller, Pyre, and Swiss-PdbViewer as reported earlier.¹⁷ Also, different Haddock models were obtained, in which the binding residues were established using crystallographic data from multimeric forms of GFP (1GFL, 1JC0, 3GJ2, 2QLE, 1EMC) and the higher interaction energy solutions resulting from protein-protein docking calculation.

Biodistribution analysis

Five-week-old female Swiss nu/nu mice, weighing 18–20 g (Charles River, France) maintained in specific pathogen-free conditions, were used for the *in vivo* experiments. All procedures were approved by the Hospital de Sant Pau animal ethics committee. To generate a metastatic colorectal cancer model, the mice were injected with 2 million SW-1417 cells via the cecal wall, using an orthotopic cell microinjection technique.¹⁸ Two months after microinjection, when local tumor and metastases had appeared, each experimental animal received a single intravenous bolus of T22-GFP-H6 nanoparticles resuspended in a 20 mM Tris, 500 mM NaCl, pH 7.4 buffer, at a dose of 20 μg (n = 3 mice) or 500 μg (n = 3 mice). Control animals received a single bolus of empty buffer. After euthanizing the mice at 5, 24, or 48 hours post-administration, we measured *ex vivo* the amount of nanoparticles in normal and tumor-bearing organs from the experimental and control mice, quantifying the fluorescence

emitted by each organ. To this end, primary tumors, organs bearing metastatic foci, and several samples of normal tissue (kidney, liver, lung, heart) were obtained at necropsy, cut into slices, and placed in separate wells to detect the emitted signal using IVIS[®] Spectrum equipment (Xenogen Biosciences, Waltham, MA). The amount of nanoparticles distributed in each tissue was calculated as the increased fluorescent (FLI) ratio. The fluorescence signal was first digitalized, displayed as a pseudocolor overlay, and expressed as radiant efficiency. Thereafter, the FLI ratio was calculated for each organ, dose, and post-treatment time, dividing the FLI signal from the nanoparticle-treated mice by the FLI signal from the control mice. Finally, all organs were collected and fixed with 4% formaldehyde in phosphate-buffered solution for 24 hours, and then embedded in paraffin for histological and immunohistochemical evaluation.

Immunohistochemistry

Sections of normal and tumor tissues 4 μm thick were stained with hematoxylin and eosin. The sections were examined histopathologically to analyze the primary tumor and to search for metastatic foci in organs with no macroscopic metastases. Paraffin-embedded tissue sections were deparaffinized, rehydrated, and washed in phosphate-buffered solution with Tween-20. Antigen retrieval was performed using citrate buffer at 120°C. After quenching peroxidase activity by incubating the slides in 3% H₂O₂ for 10 minutes, the slides were washed in phosphate-buffered solution with Tween-20. The slides were incubated for 30 minutes with the primary antibody against CXCR4 (1:20, Biotrend, Destin, FL) to detect expression of this receptor in normal tissue and tumor tissue. A primary anti-His antibody (1:1000; Abcam, Cambridge, UK) was used to detect nanoparticle accumulation and localization in normal and tumor (primary or metastatic) tissue. After incubation, the samples were washed in phosphate-buffered solution with Tween-20 and incubated with the biotinylated secondary antibody for 30 minutes at room temperature. Finally, the sections were counterstained with hematoxylin and mounted using DPX mounting medium. Representative pictures were taken using Cell[^]B software (Olympus Soft Imaging) at 200× and 1000× magnifications.

Statistical analysis

The data were evaluated by one-way Anova analysis of variance with a confidence level of 99.9% (*P* < 0.001). Dose-response plots were analyzed by nonlinear regression analysis using SigmaPlot 10. The data for both the HeLa and

SW1417 cells fitted into a double rectangular hyperbolic function, with a significance level of 99.9% ($P < 0.001$). All data were expressed as the mean \pm standard error of the mean.

Results

Screening CXCR4 peptidic ligands for cell-targeted internalization

To identify peptides suitable for use as tags for CXCR4-mediated cell internalization of large macromolecular complexes, four known molecular ligands of CXCR4, namely peptide T22, the protein domains CXCL2 and vCCL2, and V1, an amino-terminal peptide of vCCL2 (Figure 1A), were tested for their ability to promote receptor-mediated delivery of attached macromolecular entities into CXCR4-expressing cells. All these protein segments were fused to GFP-H6. This fluorescent protein, when containing cationic peptides at its amino terminus, shows a tendency to self-assemble as regular-sized nanoparticles, presumably by electrostatic interaction between monomers.¹³ Because of their emission of fluorescence, these nanoparticles are very convenient reporters for use in internalization and trafficking studies.¹⁴ Four equivalent modular constructs differing only by the CXCR4 ligand (Figure 1B) were designed according to this strategy, produced in bacteria, and purified as full-length forms of the expected molecular mass and N-terminal amino acid sequence (Figure 2). Their reactivity in anti-His Western blot analysis indicated protein integrity also at the C-terminus. Only vCCL2 showed partial degradation at the N-terminus, but retained most of the expected molecular mass (Figure 2). This proteolytic instability was observed under all tested production conditions and in several *E. coli* strains tested as hosts (data not shown). In addition, the single major peak in mass spectroscopy and the unambiguous N-terminal

sequence, coincident with a few dominant bands in Western blot analysis, indicated the existence of conformational isoforms of vCCL2.

When these proteins were added to the culture medium, HeLa (CXCR4⁺) cells exposed to T22-GFP-H6 were ten-fold more fluorescent than those exposed to V1, CXCL12, and vCCL2 fusion (Figure 3). Interestingly, cell uptake of CXCL12 and V1 has been reported previously,^{19,20} but the excellent performance of T22 was completely unexpected because its ability to internalize cells has not been previously suggested or described, despite its well known properties as an CXCR4 antagonist.²¹ As expected, the untagged parental GFP-H6 building block did not label the cells.

CXCR4-dependent cell uptake of T22-empowered constructs

The high cell penetrability of T22-activated GFP was further confirmed by confocal microscopy of treated HeLa cell cultures (Figure 4A). In full agreement with data from Figure 3, no penetration of GFP-H6 was observed, while some uptake of CXCL12 and to a minor extent some vCCL2-GFP-H6 was seen. V1-GFP-H6 was observed inside cells as low in abundance and poorly fluorescent punctuate entities. Three-dimensional reconstructions of individual cells exposed to T22-GFP-H6 indicated perinuclear localization of fluorescence in the form of nanoparticles (Figure 4B). Discrete yellow merging signals (green particles incorporated into red membranous vesicles) were observed close to the plasma membrane (Figure 4C), indicative of uptake by endosomes. The finding of nanoparticles within the endosomes was fully confirmed by three-dimensional confocal reconstructions as yellow spots, some of them fully internalized in the cytoplasm and separate from the plasma membrane (Figure 4C, inset). However, the relative low proportion of yellow signals and

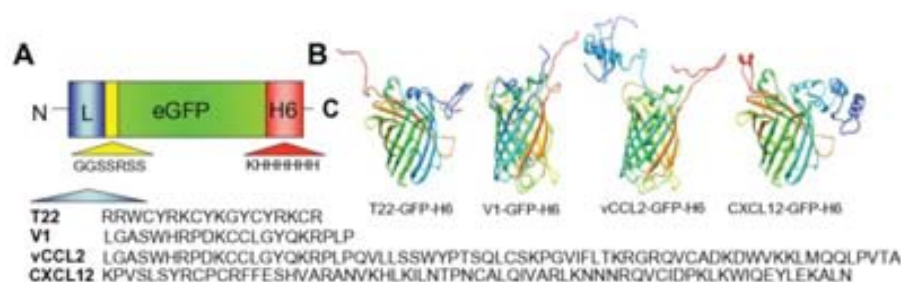


Figure 1 Features of protein constructs containing peptidic CXCR4 ligands. **(A)** Schematic representation of CXCR4-binding constructs indicating their modular composition. A linker (yellow box) commonly used in phage display was inserted between the protein ligand (L, blue) and eGFP (green). The amino acid sequences of the four ligands are shown. In all cases, an additional amino terminal methionine, derived from the cloning strategy adapted to *Escherichia coli* was expected. **(B)** Predicted structure of the different GFP-derived constructs. The color code of panel A is maintained here for both ligand- (blue) and H6- (red) overhanging ends.

Abbreviation: GFP, green fluorescent protein.

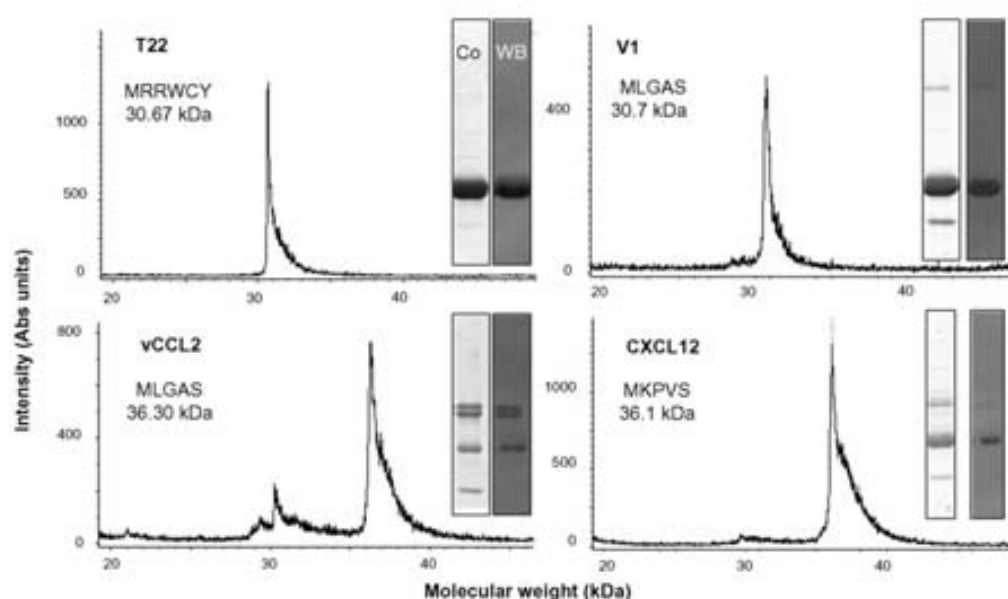


Figure 2 Biochemical characterization of protein constructs upon protein purification.

Notes: Mass spectrometry of the purified constructs indicating the experimental molecular weight. The obtained N-terminal sequence is also shown, always coincident with the predicted sequence (Figure 1A). Protein integrity is also shown through Coomassie blue-stained sodium dodecyl sulfate polyacrylamide gel electrophoresis gels (Co) and by H6 immunodetection in Western blot (WB).

rapid accumulation of nanoparticles close to the nuclear region through fast cytoplasmic trafficking (Figure 4D) were indicative of early endosomal escape. This was probably promoted by the accompanying hexahistidine tag, that has powerful endosomolytic properties,²² inducing early endosomal escape in related protein-only nanoparticles.¹⁴ Ten minutes after exposure to these T22 constructs, the uptake of nanoparticles was already evident, and the amount of intracellular fluorescence progressively increased for up to 24 hours at least (Figure 4E).

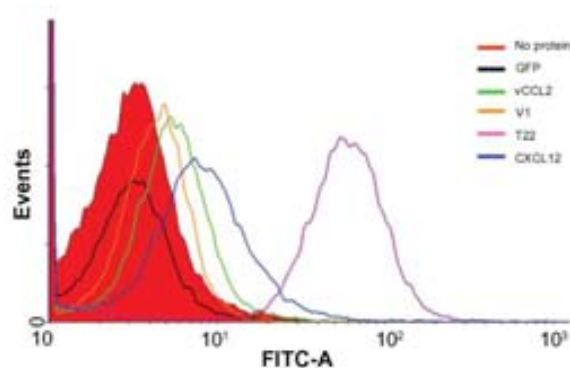


Figure 3 Differential internalization of CXCR4 ligands.

Notes: Internalization of T22-GFP-H6 and alternative constructs in HeLa cells, monitored by flow cytometry 24 hours after exposure.

Abbreviation: GFP, green fluorescent protein.

To exclude the possibility that T22-mediated penetration of GFP was limited to a particular cell type, we also evaluated the intracellular fluorescence in exposed CXCR4⁺ SW1417 cells, a human cell line used to generate a mice model of metastatic colorectal cancer for preclinical studies through orthotopic implantation.¹⁸ Again, strong penetration (Figure 5A) and perinuclear fluorescence labeling (Figure 5B) were seen in this model, indicative of efficient penetration of the nanoparticles. No changes in cell morphology (which would have been indicative of toxicity) were observed (Figures 4A and 5A), or when compared with cells exposed to parental GFP-H6 (Figures 4A and 5C). Furthermore, viability of T22-GFP-H6-exposed SW1417 cells remained unaffected up to 72 hours after exposure (Figure 5D), even when high protein concentrations were added. On the other hand, penetration of T22-GFP-H6 was observed to be dose-dependent (Figure 5E) in both human HeLa and SW1417 cells, and efficiently inhibited by increasing amounts of SDF1 α (Figure 5F), the natural ligand of CXCR4.²³ These data confirm the specificity of intracellular delivery driven by the T22 peptide.

Stability and architecture of T22-empowered GFP nanoparticles

The confocal microscopy analyses shown in Figures 4 and 5 indicate that T22-GFP-H6 has a nanostructure, as has been

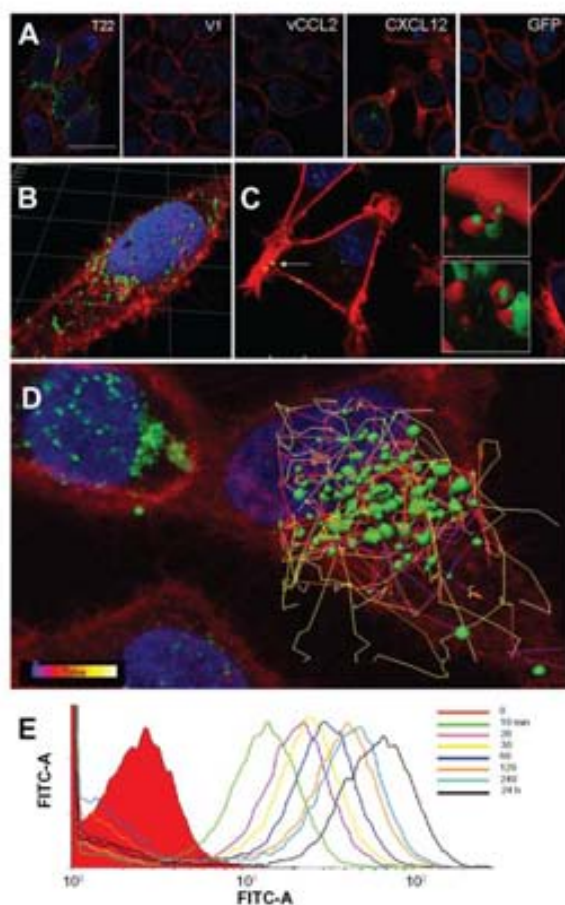


Figure 4 Differential internalization and intracellular trafficking of CXCR4 ligands. (A) Confocal images of HeLa cells exposed to differently tagged proteins for 24 hours. Nuclei are labeled in blue and cell membranes in red. Bar indicates 20 μm . (B) Detail of a HeLa cell exposed to T22-GFP-H6, showing the intracellular localization of nanostructured, fluorescent entities, in an isosurface representation within a three-dimensional volumetric x-y-z data field. (C) Yellow spots in the cell membrane, marked with an arrow, indicate early endosomal localization of green fluorescent particles (merging of red and green signals). In the insets, details of endosome-embedded fluorescent particles dissected by three-dimensional reconstruction. (D) Intracellular tracking of individual fluorescent particles monitored by confocal microscopy. (E) Time course monitoring of T22-GFP-H6 internalization in HeLa cells by flow cytometry.

Abbreviation: GFP, green fluorescent protein.

previously demonstrated for the related construct, R9-GFP-H6.¹³ Although precise characterization of these assemblies is beyond the scope of this study, we were interested in confirming that T22-GFP-H6 is organized in nanoparticle form and that T22 can achieve targeted internalization of large macromolecular complexes. If so, T22 would be of broad interest for the functionalization of other categories of nanoparticles (eg, nonproteins) in emerging medicine. First, we determined that the construct was highly stable in human serum (Figure 6A) and able to internalize target cells fully in the presence of fetal

bovine serum (Figure 6B). These features are suggestive of proteolytic stability, tight architecture, and regular organization of T22-GFP-H6 building blocks, in contrast with the random particle size and morphologies observed during amorphous protein aggregation, even in the form of soluble aggregates.²⁴⁻²⁷ Indeed, the mean size of T22-GFP-H6, measured by dynamic light scattering, was 13.45 nm (Figure 6C), a value fully compatible with images of these nanoparticles under transmission electron microscopy (Figure 6D) showing relatively monodispersed entities. To assess further the structural and functional stability of T22-empowered nanoparticles, we determined their size distribution after storage for one year at -80°C , and also at room temperature for an additional 24 hours, followed by one additional step of freezing and thawing. As observed (Figure 7A), no important variations in nanoparticle size were observed, in agreement with their high stability in human serum (Figure 6A). After 24 hours of incubation at room temperature, we observed a slight tendency for the nanoparticles to become more compact entities, although the reduction in size was very moderate (around 1 nm on average). These nanoparticles were indistinguishable from the original material in terms of their ability to internalize cultured cells (Figure 7B). All these data confirm that the presence of T22, as it occurs with the cationic peptide R9, imparts self-organizing properties to His-tagged GFP, that cannot form multimeric complexes on its own.¹³

Given that T22 is also highly cationic (note its primary sequence in Figure 1A), we wondered if this peptide could promote electrostatic interaction between monomers to achieve stable nanoparticulate entities. To explore this possibility, we generated a charge map of T22-GFP-H6 (Figure 8A). The highly dipolar charge distribution of the multifunctional protein did indeed enable tight electrostatic contact between the charged sides of the GFP beta barrel and the consequent generation of regular oligomers. Two stable multimeric assemblies of T22-GFP-H6 monomers into approximately 13 nm nanoparticles are shown in Figure 8B, but alternative arrangements of the building blocks were also thermodynamically feasible (data not shown). Further structural analyses are in progress to elucidate the nature of the architectonic properties of T22, beyond those associated with its cell-targeting ability.

T22-mediated intracellular targeting in a model of metastatic colorectal cancer

The excellent *in vitro* performance of T22 in receptor-specific intracellular targeting and the architectonic

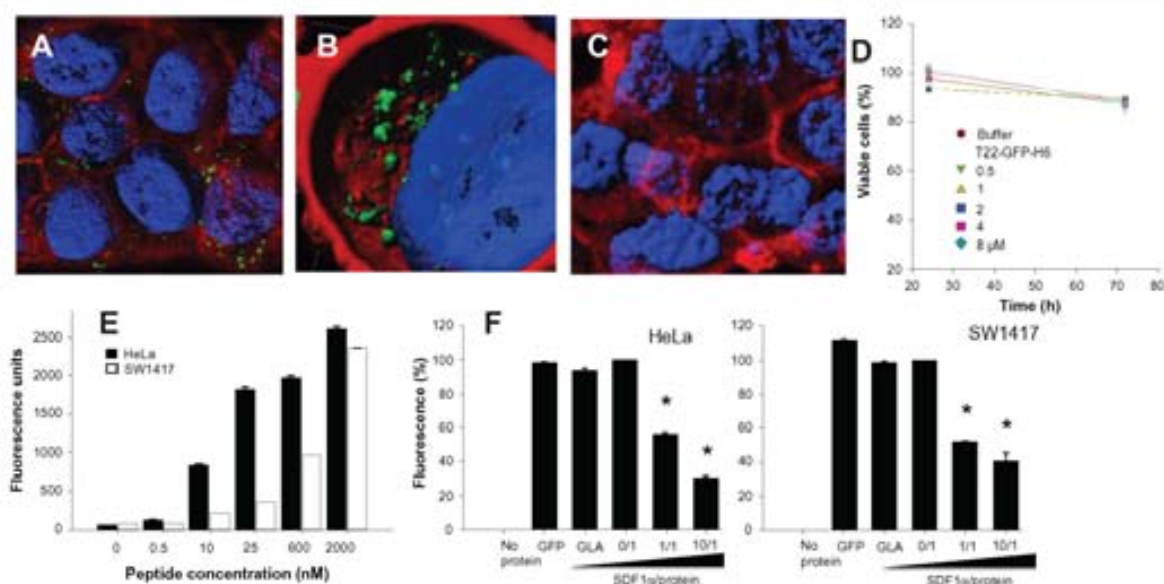


Figure 5 Internalization of T22-GFP-H6 in SW1417 cells. **(A)** Isosurface representation of T22-GFP-H6-exposed SW1417 cells within a three-dimensional volumetric x-y-z data field. **(B)** The particulate nature of the protein and the perinuclear accumulation are clearly observed. **(C)** Isosurface representation of GFP-H6-exposed SW1417 cells showing lack of fluorescence. **(D)** MTT analysis of SW1417 cells exposed to different concentrations of T22-GFP-H6. As a control, we used determined viability of cells exposed to the storing buffer alone. Values are referred to cell viability of cultures not exposed to the buffer. **(E)** Dose-response curve of T22-GFP-H6 internalization in HeLa and SW1417 cells. Data adjusted to hyperbolic equations with $r^2 = 0.9620$ for HeLa cells and $r^2 = 0.9978$ for SW1417 cells (both $P < 0.001$). **(F)** Inhibition of T22-GFP-H6 internalization in HeLa and SW1417 cells by increasing competitor/protein ratios of the natural CXCR4 ligand SDF1 α .

Notes: GFP-H6 and human GLA were included as negative controls. Asterisks indicate significant differences when comparing with any of the negative controls ($P < 0.001$). **Abbreviations:** GFP, green fluorescent protein; GLA, α -galactosidase.

robustness of T22-empowered nanoparticles encouraged us to proceed further with in vivo biodistribution analyses in a CXCR4⁺ mouse model of metastatic colorectal cancer¹⁸ (Figure 9A). Upon tail vein administration, the green fluorescence in local tumors (Figure 9B) and metastatic foci (Figure 9C) was much more intense than the background levels observed in buffer-treated mice (Figures 9A and 10A). The fluorescent signal was dose-dependent, peaked at 5 hours, and remained relatively stable for at least 24 hours (Figure 10A). This temporal profile is again indicative that the nanoparticles have high in vivo stability for at least one day following administration. When analyzing other tissues, we observed fluorescent metastatic foci in the peritoneum and lymph nodes but not in healthy organs (Figure 9B and C, Figure 10A and B), indicating tumor-specific targeting of the nanoparticles and accurate CXCR4-linked biodistribution. Finally, as in the cell cultures, we also observed cytosolic localization of T22-GFP-H6 by immunohistochemistry in both local tumor and metastatic foci (Figure 10C), demonstrating efficient cell internalization of the T22-functionalized constructs in vivo. No fever or other signs of toxicity were observed in any of the treated animals during the study (data not shown).

Discussion

Controlling cell targeting and penetrability of drugs and imaging agents is a major issue in emerging medicine. Successful identification of efficient intracellular targeting agents is expected to result in dramatic increases in drug stability and efficacy, as well as in significant reduction of toxicity and production costs. Given that the cell membrane is a major biological barrier for chemicals and particulate entities,²⁸ identification of "Trojan horses" for selective intracellular delivery, ie, peptides or antibodies which selectively bind cell surface receptors and promote selective uptake of attached cargos,²⁹ is a major demand in preclinical and clinical research, especially in cancer chemotherapy. However, very few of these peptides prove to be suitable for internalization of macromolecular complexes or nanoparticles, and lack of targeting remains a major obstacle in the design of effective drugs and full development of nanomedicine.³⁰ In cancer chemotherapy, incorporation of monoclonal antibodies as drug targeting agents has had limited benefit for patients because of poor tumor penetration³¹ and unexpectedly rapid development of chemoresistance.³² Also, generic use of antitumor antibodies for targeting is controversial because only 0.001%–0.01% of these localize to the target site upon administration.³³ Despite the steady identification of tumor-homing peptides,^{34,35} tags

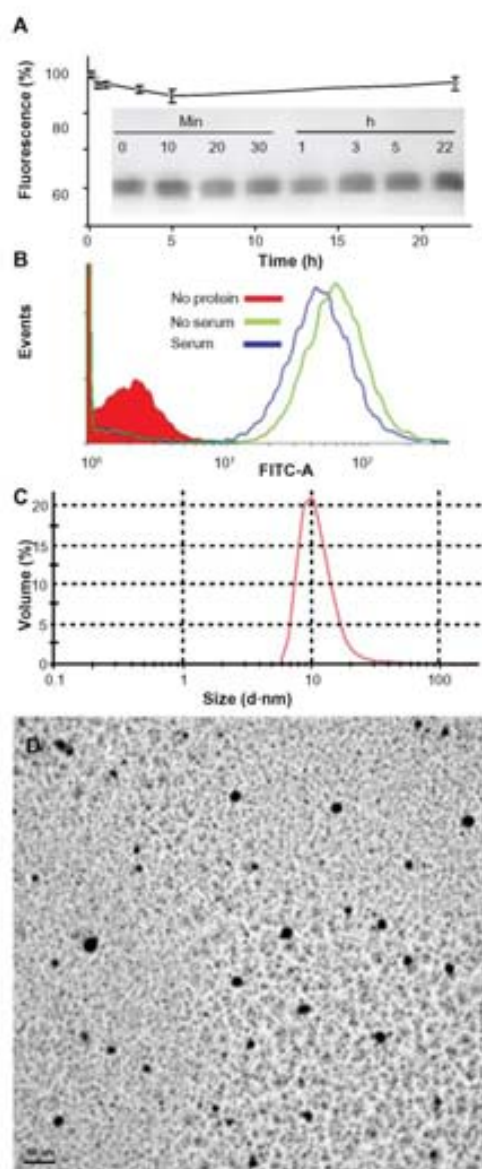


Figure 6 Characterization of T22-empowered nanoparticles. (A) Remaining fluorescence during incubation of T22-GFP-H6 in human serum. In the inset, integrity of T22-GFP-H6 monomers monitored by Western blot. (B) Internalization of T22-GFP-H6 in HeLa cells in the presence of 10% fetal calf serum, monitored by the number of fluorescent cells. (C) Dynamic light scattering size analysis of T22-GFP-H6 nanoparticles in NaCO_3H buffer. (D) Transmission electron microscopy of T22-GFP-H6 nanoparticles.

Abbreviation: GFP, green fluorescent protein.

for receptor-dependent internalization of macromolecular complexes and nanoparticles are still unavailable.³⁶ In this study, we identified that T22, a short amino acid segment (Figure 1A), is an unusually strong agent for intracellular targeting in CXCR4⁺ cells, the selectivity, stability and efficacy of penetration of which have been fully demonstrated in cell culture (Figures 3–5) and in vivo (Figures 9 and 10).

In addition, we produced T22 at high yields in a recombinant form as a domain of a highly stable modular protein (Figure 2), demonstrating lack of toxicity of this peptide in *E. coli* and pointing to the feasibility of production of further (improved or adapted) engineered versions.

Interestingly, T22 had been previously identified as a CXCR4 ligand and explored in the context of antiretroviral therapies,³⁷ because CXCR4 is a coreceptor for HIV and T22 inhibits viral attachment. However, the ability of T22 to penetrate cells was not suspected. Importantly, internalization of T22 does not depend on mere interaction with CXCR4, because other ligands tested in this study failed to promote efficient uptake (Figures 3 and 4), even showing that affinity for the receptor was higher than for T22.¹⁰ Dissociation between affinity for the receptor and endocytosis might account for the limited penetrability and poor uptake of antibody-empowered drugs.^{31,38} Other CXCR4 ligands previously investigated for targeted drug delivery showed very low or null penetration, even revealing themselves as agonists of CXCR4 and stimulating cell division.³⁹ In contrast, in our hands, T22-exposed cells never showed significant proliferation compared with controls (data not shown). The efficient endosomal escape of the constructs generated might be due to the proton-sponge activity of the accompanying polyhistidines that, while useful for one-step protein purification, act also as a proton sponge, permitting endosomal disruption and delivery of the functionalized materials into the cytoplasm.²²

On the other hand, when tested in an in vivo animal model of colorectal cancer, in which CXCR4⁺ cells were associated with aggressiveness, T22-empowered nanoparticles selectively localized not only in the primary tumor but also in metastatic foci (Figures 9C, 10B and C) confirming good stability of the protein-only nanoparticles generated in this study and suggesting that these nanoparticles might eventually be able to be attached to drugs to control tumor spread. This would be especially promising if used in the early stages of disease, because current treatment strategies for colorectal cancer are targeted to the primary tumor rather than to disseminated disease.⁴⁰ Moreover, achieving higher intracellular concentrations of anticancer agents is expected to lead to a better antitumor effect, given that most of the chemotherapeutic agents used have a steep dose-response relationship.⁴¹ In the same context, precise targeting of imaging agents to metastatic foci would create additional diagnostic strategies.

Finally, T22 was able to impart self-organizing properties to GFP-H6, as has been previously shown for another cationic

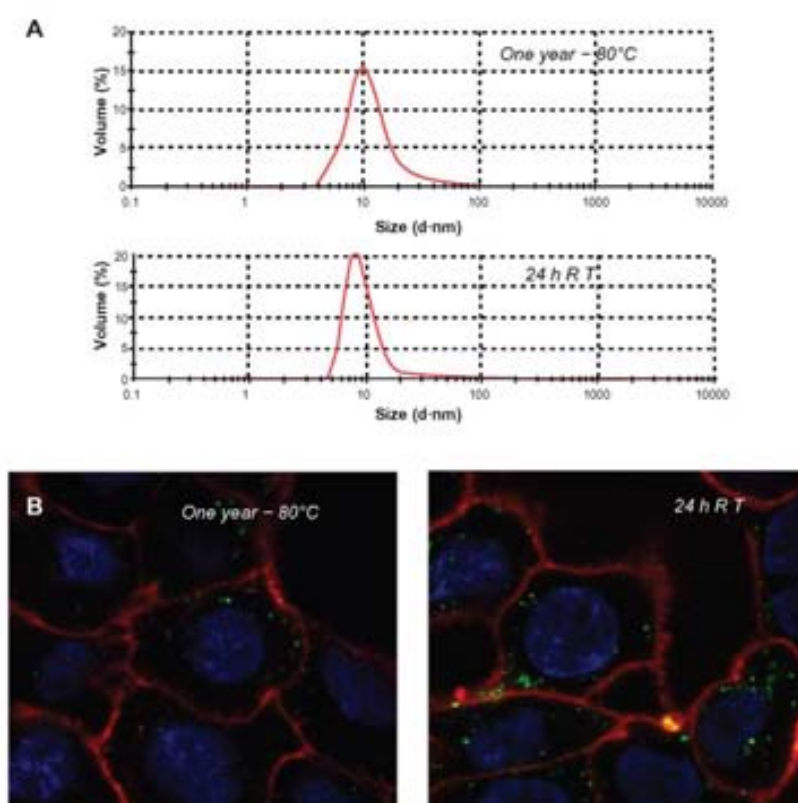


Figure 7 Stability of T22-GFP-H6 nanoparticles. **(A)** Size distribution of T22-GFP-H6 nanoparticles after one year of storage at -80°C . The same sample was further incubated at room temperature for 24 hours, submitted to one additional freezing and thawing step and analyzed. **(B)** These samples were tested for their ability to internalize SW1417, showing uptake images comparable with those shown in Figures 4 and 5. **Abbreviations:** GFP, green fluorescent protein; RT, room temperature.

stretch, namely the receptor-independent cell-penetrating peptide, R9.¹³ The resulting building blocks, probably establishing electrostatic contact due to their dipolar nature (Figure 8), form relatively monodispersed protein-only nanoparticles about 13 nm in size (Figure 6), with proteolytic stability in human serum (Figure 6A) on systemic administration (Figures 9 and 10) and remaining assembled and fully functional under different storage conditions (Figure 7). Interestingly, T22-

empowered building blocks are highly fluorescent (22.8 fluorescence units/ μg), indicative of a poor impact of the peptide on GFP. V1-GFP-H6 shows slightly lower fluorescent emission (12.4 fluorescence units/ μg), being sufficiently high to monitor cell penetration, indicative of the conformational constraints imposed by the peptide on the building block.

Although the nanoscale architectonic properties imparted by T22 to the holding building block are secondary in terms of their CXCR4-dependent intracellular targeting ability, they warrant further investigation as architectonic tags for construction of protein-only nanoparticles.^{42,43} Self-assembling peptides, presently under intense investigation in diverse nanomedical applications,⁴⁴⁻⁴⁷ base their organizing properties on amyloid-like cross-molecular interactions, and when produced in “cell factories” such as *E. coli*, tend to aggregate as amorphous protein deposits.⁴⁸ CXCR4 is an important cell surface marker in HIV infection,⁵ metastatic colorectal cancer,⁵⁰ and other neoplasms,⁶ so incorporation of T22 as a targeting agent offers many opportunities for functionalization of drugs and nanoparticles for intracellular delivery,



Figure 8 Molecular modeling of T22-GFP-H6 monomers and nanoparticles. **(A)** Electrostatic field of the T22-GFP-H6 building monomer (cationic in blue and anionic in red). **(B)** Potential organization of T22-GFP-H6 as pentamers of 11.1 nm (left) and as octamers of 13.3 nm (right), in which the intervention of T22 assists the electrostatic self-assembly of the multimeric protein complex. **Abbreviation:** GFP, green fluorescent protein.

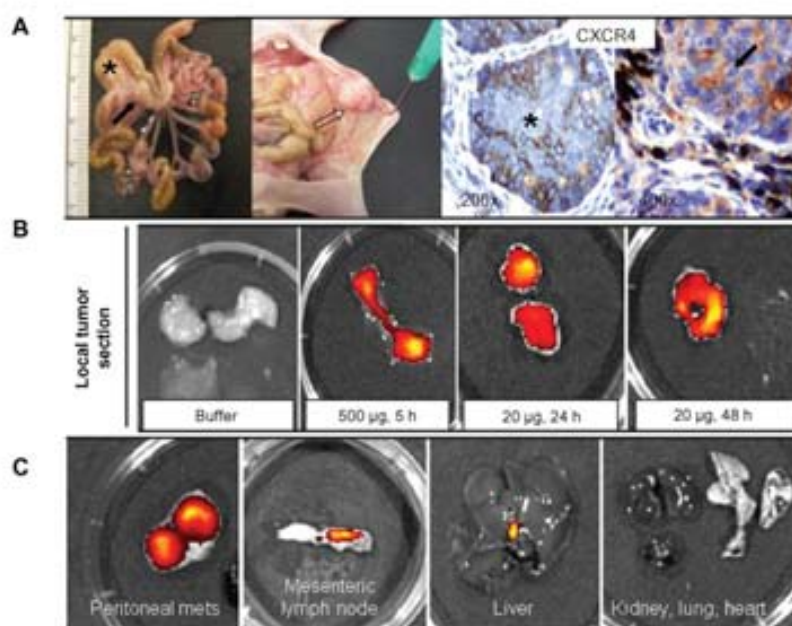


Figure 9 Biodistribution of T22-empowered nanoparticles in an animal model of colorectal cancer. (A) Nude mouse bearing a local tumor (black asterisk), mesenteric lymph node (black arrow), and peritoneal metastases (empty arrow) after microinjecting 2×10^6 SW1417 human colorectal cancer cells into the cecal wall. The local tumor and mesenteric lymph node metastases overexpress CXCR4 in this model, as assessed by immunohistochemistry. (B) Selective biodistribution of T22-GFP-H6 in local tumor tissues 5, 24, or 48 hours after intravenous administration of 500 µg or 20 µg of nanoparticles as measured ex vivo. Fluorescence was undetectable in tumors from buffer-treated animals. (C) Accumulation of nanoparticles in peritoneal and lymph node metastases. No fluorescence was observed in any normal (liver, kidney, lung, heart) tissue, except for the biliary vesicle which showed fluorescence both in control and experimental animals.

Abbreviations: GFP, green fluorescent protein.

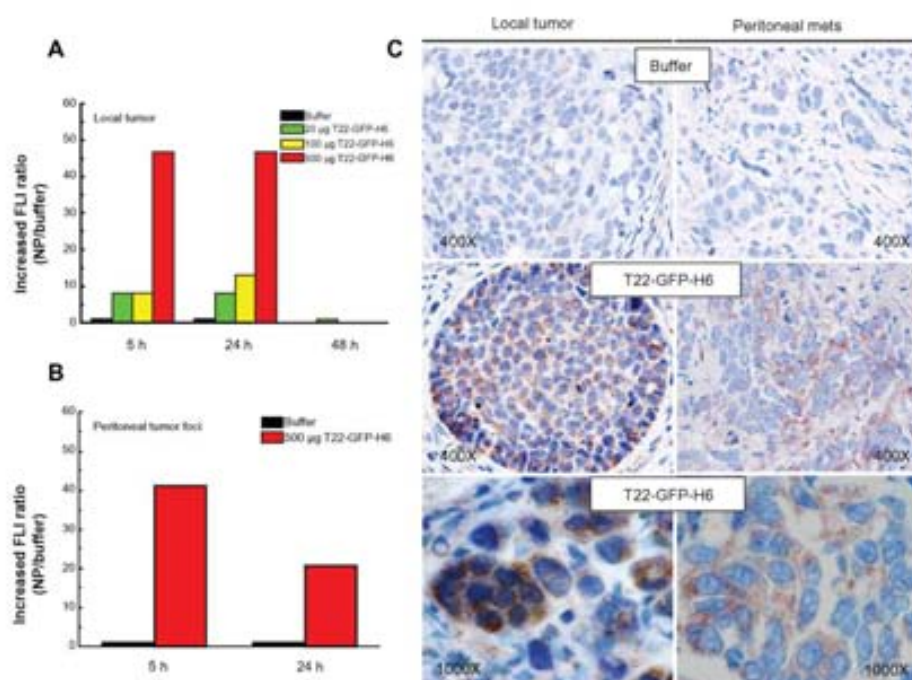


Figure 10 Accumulation of T22-empowered nanoparticles in colorectal cancer metastatic foci. Enhanced green fluorescence associated with nanoparticle accumulation in local tumors (A) and peritoneal metastases (B) in experimental mice, as compared with buffer-treated controls. (C) Anti-His tag immunostaining showing cytosolic localization of T22-GFP-H6 in local tumor tissue and peritoneal metastases in mice injected with T22-NP, which was absent in control animals injected with buffer.

Abbreviations: FI, increased fluorescence; GFP, green fluorescent protein.

especially for disorders in which CXCR4 expression plays a pathophysiological role, including cancer, inflammation, autoimmunity, and ischemic lesions.⁴

Conclusion

The peptide T22, a known ligand of CXCR4, has been shown to be an unusually powerful tag for intracellular targeting in CXCR4⁺ cells, both in cell culture and in vivo. T22 is able to mediate the internalization of self-assembling protein-only nanoparticles 13 nm in mean diameter, keeping the stability and fluorescence emission of GFP-based building blocks. Rapid endosomal uptake and perinuclear accumulation of T22-empowered nanoparticles without cytotoxicity offer a wide spectrum of diagnostic and therapeutic opportunities for use of T22 in emerging nanomedicine to treat CXCR4-linked diseases, for which intracellular targeting agents are currently missing.

Acknowledgments

We appreciate the technical support of Fran Cortés from the Cell Culture Unit of the Servei de Cultius Cellulars, Producció d'Anticossos i Citometria, of the Servei de Microscòpia, and of the Protein Production Platform (CIBER-BBN). We also acknowledge the financial support received for the design and production of artificial viruses for gene therapy to EV, RM, and AV from FIS (PS0900165, PS0900965), MICINN (ACI2009-0919), AGAUR (2009SGR-108), and CIBER de Bioingeniería, Biomateriales y Nanomedicina, an initiative funded by the VI National R&D&i Plan 2008–2011, Iniciativa Ingenio 2010, Consolider Program, CIBER Actions and financed by the Instituto de Salud Carlos III with assistance from the European Regional Development Fund. UU and JDE have received predoctoral fellowships from ISCIII and MICINN, respectively, and AV has received an Institució Catalana de Recerca i Estudis Avançats Academia award.

Disclosures

UU, EV, NFM, AV, RM, IC, and MVC are cited as inventors in a patent application (EP11382005.4) covering the therapeutic use of T22. All other authors report no conflicts of interest in this work.

References

1. Pautler M, Brenner S. Nanomedicine: promises and challenges for the future of public health. *Int J Nanomedicine*. 2010;5:803–809.
2. Ferrer-Miralles N, Vazquez E, Villaverde A. Membrane-active peptides for non-viral gene therapy: making the safest easier. *Trends Biotechnol*. 2008;26:267–275.
3. Milletti F. Cell-penetrating peptides: classes, origin, and current landscape. *Drug Discov Today*. March 23, 2012. [Epub ahead of print.]

4. Peled A, Wald O, Burger J. Development of novel CXCR4-based therapeutics. *Expert Opin Investig Drugs*. 2012;21:341–353.
5. Wilen CB, Tilton JC, Doms RW. Molecular mechanisms of HIV entry. *Adv Exp Med Biol*. 2012;726:223–242.
6. Klonisch T, Wiehce E, Hombach-Klonisch S, et al. Cancer stem cell markers in common cancers – therapeutic implications. *Trends Mol Med*. 2008;14:450–460.
7. Sun X, Cheng G, Hao M, et al. CXCL12/CXCR4/CXCR7 chemokine axis and cancer progression. *Cancer Metastasis Rev*. 2010;29:709–722.
8. Kim J, Mori T, Chen SL, et al. Chemokine receptor CXCR4 expression in patients with melanoma and colorectal cancer liver metastases and the association with disease outcome. *Ann Surg*. 2006;244:113–120.
9. Liang Z, Yoon Y, Votaw J, Goodman MM, Williams L, Shim H. Silencing of CXCR4 blocks breast cancer metastasis. *Cancer Res*. 2005;65:967–971.
10. Liang X. CXCR4, inhibitors and mechanisms of action. *Chem Biol Drug Des*. 2008;72:97–110.
11. Murakami T, Zhang TY, Koyanagi Y, et al. Inhibitory mechanism of the CXCR4 antagonist t22 against human immunodeficiency virus type 1 infection. *J Virol*. 1999;73:7489–7496.
12. Bradford MM. A rapid and sensitive method for the quantitation of microgram quantities of protein utilizing the principle of protein-dye binding. *Anal Biochem*. 1976;72:248–254.
13. Vazquez E, Roldan M, Diez-Gil C, et al. Protein nanodisk assembling and intracellular trafficking powered by an arginine-rich (R9) peptide. *Nanomedicine (Lond)*. 2010;5:259–268.
14. Vazquez E, Cubarsi R, Unzueta U, et al. Internalization and kinetics of nuclear migration of protein-only, arginine-rich nanoparticles. *Biomaterials*. 2010;31:9333–9339.
15. Seras-Franzoso J, Diez-Gil C, Vazquez E, et al. Bioadhesiveness and efficient mechanotransduction stimuli synergistically provided by bacterial inclusion bodies as scaffolds for tissue engineering. *Nanomedicine (Lond)*. 2012;7:79–93.
16. Barbera VM, Martin M, Marinoso L, et al. The 18q21 region in colorectal and pancreatic cancer: independent loss of DCC and DPC4 expression. *Biochim Biophys Acta*. 2000;1502:283–296.
17. Baig MS, Manickam N. Homology modeling and docking studies of Comamonas testosteroni B-356 biphenyl-2,3-dioxygenase involved in degradation of polychlorinated biphenyls. *Int J Biol Macromol*. 2010;46:47–53.
18. Cespedes MV, Espina C, Garcia-Cabezas MA, et al. Orthotopic microinjection of human colon cancer cells in nude mice induces tumor foci in all clinically relevant metastatic sites. *Am J Pathol*. 2007;170:1077–1085.
19. Amara A, Gall SL, Schwartz O, et al. HIV coreceptor downregulation as antiviral principle: SDF-1alpha-dependent internalization of the chemokine receptor CXCR4 contributes to inhibition of HIV replication. *J Exp Med*. 1997;186:139–146.
20. Zhou NM, Luo ZW, Luo JS, Hall JW, Huang ZW. A novel peptide antagonist of CXCR4 derived from the N-terminus of viral chemokine vMIP-II. *Biochemistry*. 2000;39:3782–3787.
21. Fujii N, Nakashima H, Tamamura H. The therapeutic potential of CXCR4 antagonists in the treatment of HIV. *Expert Opin Investig Drugs*. 2003;12:185–195.
22. Ferrer-Miralles N, Corchero JL, Kumar P, et al. Biological activities of histidine-rich peptides; merging biotechnology and nanomedicine. *Microb Cell Fact*. 2011;10:101.
23. Kucia M, Jankowski K, Reza R, et al. CXCR4-SDF-1 signalling, locomotion, chemotaxis and adhesion. *J Mol Histol*. 2004;35: 233–245.
24. Toledo-Rubio V, Vazquez E, Platas G, et al. Protein aggregation and soluble aggregate formation screened by a fast microdialysis assay. *J Biomol Screen*. 2010;15:453–457.
25. Domingo-Espin J, Vazquez E, Ganz J, et al. The nanoparticulate architecture of protein-based artificial viruses is supported by protein-DNA interactions. *Nanomedicine (Lond)*. 2011;6:1047–1061.
26. Vazquez E, Corchero JL, Villaverde A. Post-production protein stability: trouble beyond the cell factory. *Microb Cell Fact*. 2011;10:60.

27. Martinez-Alonso M, Gonzalez-Montalban N, Garcia-Fruitos E, Villaverde A. The functional quality of soluble recombinant polypeptides produced in *Escherichia coli* is defined by a wide conformational spectrum. *Appl Environ Microbiol*. 2008;101:1353–1358.
28. Riehemann K, Schneider SW, Luger TA, Godin B, Ferrari M, Fuchs H. Nanomedicine – challenge and perspectives. *Angew Chem Int Ed Engl*. 2009;48:872–897.
29. Dietz GP, Bahr M. Delivery of bioactive molecules into the cell: the Trojan horse approach. *Mol Cell Neurosci*. 2004;27:85–131.
30. Duncan R, Gaspar R. Nanomedicine(s) under the microscope. *Mol Pharm*. 2011;8:2101–2141.
31. Thurber GM, Schmidt MM, Wittrup KD. Factors determining antibody distribution in tumors. *Trends Pharmacol Sci*. 2008;29:57–61.
32. Ellis LM, Hicklin DJ. Resistance to targeted therapies: refining anticancer therapy in the era of molecular oncology. *Clin Cancer Res*. 2009;15:7471–7478.
33. Jain M, Venkatraman G, Batra SK. Optimization of radioimmunotherapy of solid tumors: biological impediments and their modulation. *Clin Cancer Res*. 2007;13:1374–1382.
34. Laakkonen P, Vuorinen K. Homing peptides as targeted delivery vehicles. *Integr Biol (Camb)*. 2010;2:326–337.
35. Enback J, Laakkonen P. Tumour-homing peptides: tools for targeting, imaging and destruction. *Biochem Soc Trans*. 2007;35:780–783.
36. Mocellin S, Lise M, Nitti D. Targeted therapy for colorectal cancer: mapping the way. *Trends Mol Med*. 2005;11:327–335.
37. Rusconi S, Scozzafava A, Mastrolorenzo A, Supuran CT. An update in the development of HIV entry inhibitors. *Curr Top Med Chem*. 2007;7:1273–1289.
38. Segal NH, Saltz LB. Evolving treatment of advanced colon cancer. *Annu Rev Med*. 2009;60:207–219.
39. Egorova A, Kiselev A, Hakli M, Ruponen M, Baranov V, Urtni A. Chemokine-derived peptides as carriers for gene delivery to CXCR4 expressing cells. *J Gene Med*. 2009;11:772–781.
40. Sleeman J, Steeg PS. Cancer metastasis as a therapeutic target. *Eur J Cancer*. 2010;46:1177–1180.
41. Skipper HE, Schabel FM Jr, Mellett LB, et al. Implications of biochemical, cytotoxic, pharmacologic, and toxicologic relationships in the design of optimal therapeutic schedules. *Cancer Chemother Rep*. 1970;54:431–450.
42. Villaverde A. Nanotechnology, bionanotechnology and microbial cell factories. *Microb Cell Fact*. 2010;9:53.
43. Vazquez E, Villaverde A. Engineering building blocks for self-assembling protein nanoparticles. *Microb Cell Fact*. 2010;9:101.
44. Sadatmousavi P, Soltani M, Nazarian R, Jafari M, Chen P. Self-assembling peptides: potential role in tumor targeting. *Curr Pharm Biotechnol*. 2011;12:1089–1100.
45. Zhao Y, Tanaka M, Kinoshita T, Higuchi M, Tan T. Self-assembling peptide nanofiber scaffolds for controlled release governed by gelator design and guest size. *J Control Release*. 2010;147:392–399.
46. Kyle S, Aggeli A, Ingham E, McPherson MJ. Recombinant self-assembling peptides as biomaterials for tissue engineering. *Biomaterials*. 2010;31:9395–9405.
47. Huang H, Sun XS. Rational design of responsive self-assembling peptides from native protein sequences (dagget). *Biomacromolecules*. 2010;11:3390–3394.
48. Wu W, Xing L, Zhou B, Lin Z. Active protein aggregates induced by terminally attached self-assembling peptide ELK16 in *Escherichia coli*. *Microb Cell Fact*. 2011;10:9.

International Journal of Nanomedicine

Publish your work in this journal

The International Journal of Nanomedicine is an international, peer-reviewed journal focusing on the application of nanotechnology in diagnostics, therapeutics, and drug delivery systems throughout the biomedical field. This journal is indexed on PubMed Central, MedLine, CAS, SciSearch®, Current Contents®/Clinical Medicine,

Submit your manuscript here: <http://www.dovepress.com/international-journal-of-nanomedicine-journal>

Dovepress

Journal Citation Reports/Science Edition, EMBASE, Scopus and the Elsevier Bibliographic databases. The manuscript management system is completely online and includes a very quick and fair peer-review system, which is all easy to use. Visit <http://www.dovepress.com/testimonials.php> to read real quotes from published authors.

Since the following studies continuing this work have not been accepted for publication yet, they will be presented as a Manuscripts sent for publication and placed in the annex of this PhD thesis.

- **Manuscript 1: (annex 1, page. 115)**
 - In vivo architectonic stability of fully *de novo* designed protein-only nanoparticles.

- **Manuscript 2: (annex 2, page. 137)**
 - Sheltering DNA in Self-organizing, protein-only nano-shells as artificial viruses for gene delivery.

- **Manuscript 3: (annex 3, page. 157)**
 - Improved performance of protein-based recombinant gene therapy vehicles by adjusting downstream procedures.

In the following pages you will find a short abstract of each of those Manuscripts. Please look up the corresponding annex to find the whole Manuscript.

Manuscript 1

In vivo architectonic stability of fully *de novo* designed protein-only nanoparticles.

María Virtudes Céspedes, Ugutz Unzueta, Witold Tatkiewicz, Patricia Alamo, Xu Zikung, Isolda Casanova, José Luis Corchero, Oscar Conchillo, Juan Cedano, Xavier Daura, Imma Ratera, Jaume Veciana, Neus Ferrer-Miralles, Esther Vazquez, Antonio Villaverde, Ramón Mangues.

Submitted to ACS Nano.

Intermolecular interactions involved in protein-only nanoparticle formation and promoted by peptidic architectonic tags have been extensively explored in previous studies. However, whether those interactions are strong enough to ensure the stability of the self-assembled protein nanoparticles *in vivo* or not, has not yet been fully explored. Being this issue critical for the design and development of self-assembling protein nanoparticles, the aim of this study was to determine the stability of generated supramolecular complexes *in vivo*.

For that purpose, we analyzed the rapid renal clearance of different functionalized self-assembled protein building blocks compared with other closely related protein variants that do not form nanoparticles, upon intravenous administration *in vivo*. We used the renal clearance as *in vivo* particle size indicator since renal filtration occurs over approximately 6 nm, a size slightly higher than the monomeric protein building blocks used in this study. We observed that the self-assembled protein nanoparticles stably accumulated in their respective target cells but not in kidney while non-assembled monomeric protein variants were quickly cleared from the circulating system and highly accumulated in kidney. These results were reproduced when comparing two formats of T22-iRFP-H6 proteins, as monomer or as self-assembled nanoparticles, depending on the salt content of the storage buffer, being the first format quickly cleared by the kidney while the second one localized at target cells *in vivo*. These results prove the strong architectonic stability of the nanoparticulated supramolecular entities *in vivo*, confirmed *in vitro* by the difficulty to disassemble already formed T22-iRFP-H6 nanoparticles, when we increase the content of salt in the storage buffer. These findings suggest that nanoparticle's structural stability *in vivo* may be supported not only by weak electrostatic interactions, but also by additional van der Waals forces and hydrogen bonds to maintain their structural integrity while travelling in the blood stream, as observed in performed *in silico* analysis.

Manuscript 2

Sheltering DNA in Self-organizing, protein-only nano-shells as artificial viruses for gene delivery.

Ugutz Unzueta, Paolo Saccardo, Joan Domingo-Espín, Juan Cedano, Oscar Conchillo, Elena García-Fruitós, Maria Virtudes Céspedes, José Luis Corchero, Xavier Daura, Ramón Mangues, Neus Ferrer-Miralles, Antonio Villaverde, Esther Vazquez.

Submitted to Nanomedicine: Nanotechnology, Biology and Medicine.

Once self-assembled protein-only nanoparticles have been proven to be an excellent and stable material for their use *in vivo*, by incorporating additional functional domains supporting nucleic acid condensation, the protein nanoparticles can be associated with a cargo DNA for their use in gene therapy. In this context, the aim of this study was to characterize the DNA condensation and protection capacity of nucleic acid binding domains in self-assembling protein nanoparticles for their use as artificial viruses.

In this regard, we incubated previously reported R9-empowered nanoparticles with an external cargo DNA at different conditions and subsequently analyzed the generated supramolecular structures by Dynamic Light Scattering, confocal microscopy and DNase protection assays. The incubation of self-assembling protein with DNA at optimal transfection conditions, resulted in virus-like spherical and rod shaped particles, both containing the cargo DNA completely shielded in the inner part of the structure. Generated rod-shaped shells resulted to be morphologically similar to capsid proteins observed in some plant viruses such as tobacco mosaic virus (TMV), strongly supporting a virus-like organization. Moreover, performed DNA hydrolysis assays where protein-DNA polyplexes were incubated in the presence of DNase I, proved the self-assembled nanostructures to be protective for their cargo DNA. Thus, in this study we have demonstrated functionalized self-assembled protein nanoparticles to have an unexpected architectonic potential when combined with an external DNA and also to be a new promising nanomaterial for their use as non-viral vectors for gene delivery.

Manuscript 3

Improved performance of protein-based recombinant gene therapy vehicles by adjusting downstream procedures.

Ugutuz Unzueta, Paolo Saccardo, Neus Ferrer-Miralles, Ramón Mangues, Esther Vázquez, Antonio Villaverde.

Submitted to Biotechnology Progress

Self-assembling protein-only nanoparticles have been proposed to be a very promising tool for their use as nucleic acids delivery vectors upon incorporating all the necessary functional domains supporting DNA condensation, cell binding, internalization, endosomal escape and nuclear transport. However, since their gene delivery capacity has been yet unexplored, the aim of this study is to determine the suitability of generated artificial viruses as targeted nucleic acid delivery vectors for gene therapy approaches.

In this context, different versions of CXCR4⁺ cell-targeted multifunctional protein nanoparticles (artificial viruses) were rationally created and tested for their ability to efficiently condensate a reporter gene containing external plasmid DNA and successfully deliver it in cultured CXCR4⁺ target cells. Surprisingly, none of them were able to efficiently bind the cargo DNA and consequently to express the reporter gene in target cells. Performed additional analyses showed that all these nanoparticles had already condensed nucleic acids from the bacterial expression system used for recombinant protein production and therefore, their nucleic acid binding domains were not functional to bind additionally added external DNA. We optimized a DNase / RNase treatment of pre-purified proteins to efficiently remove undesired bacterial nucleic acids and consequently, we obtained nucleic acid free nanoparticles, that proved to successfully bind added external DNA and to express a reporter gene in CXCR4⁺ cells more efficiently. Thus, these results show the effects of the bacterial host when producing a recombinant artificial virus with nucleic acid binding domains and suggest an additional purification step to obtain functional recombinant protein-only artificial viruses.



Discussion

1. Construction and intracellular trafficking of self-assembling protein nanoparticles.

Many different types of nanoparticles have been developed since nanomedicine began by using materials of diverse chemical origin such as lipids, polymers, proteins, metals or carbon nanotubes among others⁹⁸. Among them, protein nanoparticles appear to be specially promising for biomedical uses due to their high biocompatibility, biodegradability and functional diversity, in addition to high versatility of design. These features make protein nanoparticles a powerful and extremely plastic material that can be adapted to essentially any clinical requirement³³². Moreover, being proteins a material of biological origin, they can be produced in a wide spectrum of biological platforms and many different functions can be incorporated in the same polypeptide chain by conventional protein engineering³³².

Nanoparticle size, being one of the most important parameters not only for *in vivo* biodistribution, but also regarding toxicity and uptake into target cells, is a characteristic difficult to control⁸⁸⁻⁹⁰. In different non-peptidic nanoparticles including liposomes, polymers, silicon or gold nanoparticles among others, it has been extensively explored the generation of particles with predefined nanoscale features, generally by chemical or mechanical fine fabrication procedures^{136-140, 333-339}. However, the *de novo* development of self-assembling protein-only nanoparticles generated by the rational assembling of repetitive monomeric building blocks into regular size particles has not been fully explored in nanomedicine.

Currently described protein-based vectors, have been generally developed using already known natural proteins or protein segments with tendency to oligomerize as viruses, virus like particles, parts of viral capsids, flagella-based devices or subcellular organelles^{141, 254, 340-350}. Although these types of vehicles have been extensively used for different biomedical applications such as drug delivery or antigen presentation^{351, 352}, they usually show null or limited structural versatility. On the other hand, conventional self-assembling proteins are in general amyloidogenic protein segments that organize by cross-molecular beta sheet-based interactions³⁵³⁻³⁵⁷ and form fibers, membranes or hydrogels^{358, 359}. However, when fused as tag to proteins, they usually induce protein aggregation^{360, 361}.

Therefore, the rational generation of *de novo* designed self-assembling protein-only nanoparticles for biomedical purposes needs to be further explored. Only isolated cases of successful protein-only nanoparticles construction and structural modulation have been reported, being all of them derived from unanticipated observations^{362, 363}.

Apart from nanoparticle's size, the way nanoparticles interact with target cells represents a critical issue in nanomedicine, especially regarding important issues such as toxicity, internalization and cargo delivery ability. The cellular uptake of different

Discussion

types of nanoparticles has already been deeply studied, mainly regarding drug and nucleic acid delivery as in the case of carbon nanotubes, polymeric particles, lipid vesicles, polymer-lipid hybrid particles, metal-polymers, metal-lipid hybrid particles, peptide-active metal particles or peptide functionalized polymers among others^{132-135, 364-369}. As described before, many peptides have been incorporated to functionalize other types of nanoparticles, especially to confer them specific cell targeting. However, although different protein-only nanoparticles have already been generated showing drug or nucleic acid delivery potential¹⁷⁸, the intracellular trafficking of these protein nanoparticles other than viruses or virus like particles has so far not been studied in depth.

In a previous study, we observed how the pleiotropic poly-arginine (R9) peptide was able to induce the self-assembling of a His-tagged GFP protein into 20 nm regular size nanoparticles (**Annex 4**)³⁷⁰. Moreover, those particles showed very high cell penetrability and were able to condense and deliver an expressible DNA into mammalian cells³⁷⁰. Thus, this work reported for the first time how the R9 peptide, which had been previously described for its cell penetrating activity, blood brain barrier crossing ability and DNA condensing capacity^{172, 173, 253, 371}, also shows architectonic properties unsuspected before. The possibility of incorporating specific peptides to proteins as architectonic tags for their self-assembling induction into nanoparticles with predefined properties appears as a very convenient strategy, since it would make possible to rationally design and induce the self-assembling of proteins with appealing biological properties into regular size protein-only nanoparticles.

On this background, we wanted to deeply study which are the protein's features conferring self-assembling ability and thus, explore the possibility of effectively modulating their architectonic properties in order to produce nanoparticles of suitable size for their optimal biomedical application.

First of all, in order to determine if the architectonic properties previously described in R9-empowered particles were shared among different cationic stretches, three different poly-arginine (R7,R6 and R3) and other 9 unrelated cationic peptides were tested for their architectonic ability upon incorporated into the same His-tagged GFP protein (**see paper 1, table1 and 2**). Most of them showed the ability to induce the self-assembling of the chimerical proteins into regular pseudo-spherical (**paper 1, figure 2**) nanoparticles ranging in size between 20 and 100 nm (**paper 1, table1 and 2**) which assembling properties were clearly affected by salt concentration, strongly indicating thus, that protein's self-assembling process was driven by electrostatic interactions between protein monomers (**paper 1, Figure 1 and 2**). Moreover, the completely different origin of the self-assembling inducing peptides, proved their architectonic ability to be determined by their cationic nature but not by their structure.

Hexahistidine tag, commonly used for protein purification processes and also known for its endosomal escape ability, has been suggested in this study to be involved in protein-protein and protein-DNA interactions when the pH at which nanoparticles are generated gets slightly acidified and consequently the histidines gets partially protonated (**paper 1, figure 5 and supplementary video S1**). Apparently, positively charged histidines are able to compete with cationic R9 tags for the intermolecular interactions, partially releasing the R9 peptide from its architectonic role and consequently allowing it to recover its DNA condensing activity and cell penetrating ability. This allows the construct, all together, to act as efficient DNA delivery carrier (**paper 1, figure 4**). Therefore, hexahistidines have been proposed to act as pH-regulatable architectonic tags that when exposed together with the R9 or any other cationic architectonic tag in the same polypeptidic chain, can complement the activity of the cationic peptide. Thus, the dual peptides set as a whole can induce the regulatable self-assembling of the protein.

In order to prove the universality of the system, the R9 and H6 tag pair were exposed in the amino and carboxy termini respectively of the human p53 protein, a completely different protein both in sequence and structure, and the generated nanoparticles were subsequently tested and compared with the non-functionalized wild type protein. The obtained results proved that the architectonic properties showed by the peptide tags described before were extensible to other proteins and was not something exclusive of GFP based scaffolds (**paper 1, figure 6**). Moreover, generated fully fluorescent nanoparticles, strongly suggested that the assembling process does not imply any loss of protein activity, at least in the case of GFP in which activity can be easily tracked by fluorescence detection.

Interestingly, correlation analysis performed between different protein parameters and the resulting nanoparticle's properties, showed that the size of the generated constructs were significantly influenced by the charge of the cationic tag (**paper 1, figure 3**). Being nanoparticle size so critical parameter for their successful biomedical application, this strategy not only would potentially allow to predict the size of the resulting nanoparticles, but it also would consequently permit to rationally modulate the properties of architectonic tags in order to create a size compatible nanoparticle. Therefore, although further studies are required to fully understand the mechanisms involved in those self-assembling processes, the observations reported in this study open a wide spectrum of possibilities for the rational design of self-assembling protein-only nanoparticles which properties can be regulated by conventional engineering.

These particles appear to be of particular interest in nanomedicine not only as a promising alternative to the limited use of conventional self-assembling amyloidogenic proteins, but also for their potential utility in nucleic acid or drug delivery strategies. However, although it is intimately linked with their therapeutic applicability and

Discussion

potential toxicity, very little is known about how do these nanoparticles interact, are internalized or migrate within the cells. In this regard, we prompted to kinetically explore the uptake and intracellular trafficking of the R9 peptide-empowered nanoparticles in different cultured mammalian cell lines.

We have observed that R9-empowered GFP-H6 nanoparticles efficiently enter different cell lines via endosomal route and quickly accumulate into the cell nucleus (**paper 2, figure 1 and 2**), being the observed highest nuclear accumulation rate coincident in time with the highest cytoplasmic protein uptake rate (**paper 2, figure 3**). This has proven the nuclear localization of R9-empowered nanoparticles to be strongly dependent on cytoplasmic protein concentration, and the cell cytoplasm to be just a mere intermediary in the route of the nanoparticles towards the cellular nucleus. Therefore, the cytoplasmic protein uptake seems to be the most important bottleneck in the whole nuclear transfer process and not the nuclear membrane, which in general is considered to be the main biological barrier in nanoparticle's drug delivery³⁷². Moreover, the endosomal uptake of R9-GFP-H6 proteins did not show any detectable toxicity in exposed cells.

Performed kinetic studies, reported a converging cytoplasmic protein movement ten times faster than that estimated to be by passive diffusion³⁷³ (**Paper 2, supplementary video**). Being this fast and not random movement towards the cell nucleus more compatible with actin or dynein mediated transport than to other described mechanisms³⁷³⁻³⁷⁵, especially considering that reported speed data was an average of endosomal and post-endosomal migration phases, an active nuclear transport mechanism was strongly suggested (**table 6**).

Nanomaterial	Transport mechanism	Speed ($\mu\text{m}/\text{sg}$)	Reference
R9-GFP-H6	To be determined	0.0044	Paper 2
Polyethylenimine / DNA	Passive diffusion	0.00032	317
Poly[lactic-co-glycolic acid]	Actin-linked transport	0.06	318
Lipoplexes	Microtubule-linked transport	2	319

Table 6. Cytoplasmic transport mechanism and speed of different nanomaterial.

Taken all together: the lack of detectable toxicity, the high biocompatibility expected for proteins, the efficient R9-empowered particles uptake and nuclear avidity and their regulatable architectonic properties, make R9-GFP-H6 and in general self-assembling protein-only nanoparticles a very promising tool for the therapeutic delivery of drugs or nucleic acids in mammalian cells.

2. *In vivo* biodistribution and stability of cell-targeted, self-assembling protein nanoparticles.

Since nanomedicine and innovative medicine emerged, controlling cell targeting and drug penetrability has been one of the most pursued objectives. Conventional therapies are still far from being efficient owing to their lack of cell specificity and its associated systemic toxicity which strongly limit the administrable dose. However, achieving an efficient cell targeting, not only allows increasing local drug concentration and consequently its efficacy, but it also permit to decrease their toxicity and production costs.

Being the cell membrane generally considered as the main biological barrier for the uptake of drugs and particulate entities³⁷⁶, the identification of antibodies or peptide ligands recognizing specific cell surface receptors and inducing the attached cargo internalization³⁷⁷ is one of the most demanded issues in clinical research. In this context, cancer medicine is a clear example of this urgent need of specific targeting, since conventional therapies show really high systemic toxicity and are not effective enough. Especially in colorectal cancer, where metastatic foci appear usually at early stages of the pathology and where current therapies do not significantly improve patients' survival, the development of targeted therapies, especially when directed to metastatic cells, appear to be a really promising alternative to current therapeutic strategies.

In this regard, in previous experiments, targeted vectors were administrated in combination with conventional chemotherapy and it showed to be more effective than the chemotherapy alone^{15, 59}. However, although some heartening results have been described, only really few of hitherto tested nanoparticles have shown to be effective, especially since the lack of efficient targeting is still the major obstacle in the design of those therapies⁹⁸. Some recently described assays, where antibodies were used to target drugs to tumor cells, proved antibodies to be really inefficient, being only between 0.001% - 0.01% of administrated complexes localized in tumor cells and showing really low cell penetrability^{76, 98, 378}. Moreover, cases of rapid chemoresistance development were also reported³⁷⁹. Thus, even though different tumor-homing peptides are currently been identified, targeting tags for a correct and efficient receptor-specific internalization of functionalized nanoparticles are still not available³⁸⁰⁻³⁸².

Overcoming the different biological barriers existing within an *in vivo* system is an essential requisite for any construct aimed to achieve a successful targeting. In this context, many different parameters have been described to be critical for *in vivo* biodistribution of nanoparticles, including their size, shape, surface charge distribution and properties of the nanomaterial. Among them, nanoparticle size has been reported

Discussion

to be one of the most relevant features influencing their biodistribution⁷⁷. Therefore, it is very important to be able to construct size compatible nanoscale entities whose structural stability is not affected when administered in living organisms, since any alteration in nanoparticle's size could represent a dramatic change in their biodistribution pattern.

In this context, our aim was to identify different efficient receptor-specific peptide ligands specifically recognizing the CXCR4 receptor, which is overexpressed in different human pathologies including metastatic colorectal cancer³⁸³⁻³⁸⁷, in order to design and construct functionalized CXCR4⁺ cell-targeted self-assembling protein-only nanoparticles.

In this regard, four different GFP-H6 based chimerical constructs, each of them containing already described different CXCR4 specific ligands, were designed and successfully produced in *E. coli* (**paper 3, figure 1 and 2**). Although all of them internalized successfully, the T22 peptide, an engineered segment derivative of polyphemusin II from the horseshoe crab, proved to be by far the most efficient one in the selective intracellular targeting of CXCR4⁺ cultured cells (**paper 3, figure 3 and 4A**). The fully fluorescent T22-empowered protein constructs were efficiently internalized by a rapid receptor-specific endosomal route and stably accumulated in the perinuclear region of different CXCR4⁺ cell lines in absence of any significant toxicity (**paper3, figure 4 and 5**).

Interestingly, although the T22 peptide had already been extensively studied as CXCR4 receptor specific ligand in HIV virus uptake inhibition assays³⁸⁸, its appealing cell penetration ability had never been previously reported. From our results, we can conclude that protein internalization process is not exclusively dependent of their receptor binding capacity. Although the other three constructs generated in this work also showed CXCR4 binding ability, their internalization efficiency resulted to be significantly lower than the one occurring with T22-empowered proteins (**paper 3, figure 3**); even when their described receptor affinity was higher than the one reported for T22 peptide²⁶¹. Some other performed studies using antibodies and other CXCR4 specific ligands, showed also to have very low penetrability even in the cases where CXCR4 induced cell proliferation were stimulated. In our hands, T22-GFP-H6 constructs in spite of efficiently interacting with the receptor, never showed any significant cell proliferation stimulation. Therefore, this data clearly proved that the affinity for the receptor, the intracellular signaling activation and internalization are completely independent phenomena.

Protein intracellular tracking was performed to determine cytosolic migration speed. The single fluorescence entities found within the cells, non-overlapped with membrane staining, and determined high intracytosolic mobility speed, strongly suggested a rapid endosomal escape ability of T22-empowered protein constructs

(paper 3, figure 4D). As histidines endosmotic ability has already been extensively described in the literature, our protein's early endosomal escape ability could probably be mediated by its hexaHistidine tag³⁸⁹.

We further studied the architectonic ability of T22, a highly cationic peptide, as part of a His-tagged polypeptide. T22-empowered constructs showed the ability to self-assemble in regular size nanoparticles of around 13nm, probably driven by electrostatic interactions between the highly dipolar protein monomers **(paper 3, figure 6 and 8)**. Their functional preservation, determined by fluorescence detection, proved the self-assembling process to have poor impact on the protein structure. Moreover, the generated nanoparticles not only showed high proteolytic stability in serum, but also proved to be structurally very stable, being still fully functional after different storage conditions **(paper 3, figure 6 and 7)**.

The excellent *in vitro* performance of T22-empowered self-assembling protein nanoparticles strongly encouraged us to further proceed with *in vivo* biodistribution assays using an orthotopic metastatic colorectal cancer murine model. Intravenous administration of the particulated entities resulted in a stable accumulation of nanoparticles in the primary tumor and all the metastatic foci (but not in any normal tissue) for more than 24 hours in absence of any sign of toxicity **(paper 3, figure 9 and 10)**. Furthermore, immunohistochemical assays showed that the nanoparticles not only accumulated in tumor tissue, but they also were efficiently internalized in CXCR4⁺ cells, as described *in vitro* **(paper3, figure 10)**. No protein was found in liver, kidneys, or lungs, which are the typical organs where nanoparticles are prompted to accumulate depending on their size^{77, 78, 81, 86} **(paper3, figure 9)**. These results strongly suggested that *in vitro* generated T22-empowered nanoparticles remained stably assembled as particulated entities after *in vivo* administration, since the nanoparticle size (around 13nm) is big enough to efficiently avoid renal clearance but also small enough to avoid accumulation in other organs such as lungs, liver or spleen. However, whether the *in vitro* generated intermolecular interactions induced by previously described architectonic tag pairs were strong enough to ensure nanoparticles' stability *in vivo* or not, was still not explored.

The electrostatic intermolecular interactions proposed for our self-assembling nanoparticles are presumably weaker than those occurring in other natural supramolecular protein complexes such as viruses or other self-assembling proteins. Then, the possibility that the self-assembled nanoparticles get immediately disassembled after being administrated in the circulatory system cannot be dismissed. Therefore, being this issue critical not only for the design and development of architectonic tags based protein nanoparticles, but also for their successful biodistribution *in vivo*, we determined in this study the structural stability of our protein nanoparticles by analyzing their renal clearance. Since all the protein

Discussion

nanoparticles used in this study show higher or lower nanoparticle size than 6 nm, cutoff size at which renal filtration occurs, depending on whether they are in their monomeric or assembled form, the renal clearance appears an excellent indicator of circulating particles' stability.

The obtained results showed how the injected non-assembling protein constructs were very quickly cleared by the renal system upon systemic administration while the inoculated self-assembled protein nanoparticles were not (**Manuscript 1, figure 1**). Plasma stability and biodistribution assays proved the efficient nanoparticle accumulation in their respective target tissues the reason why they were not detected in kidney (**Manuscript 1, figure 2**). Interestingly, T22-empowered iRFP protein constructs were found to self-assemble in nanoparticles of around 15 nm in size when stored in low salts concentration buffer, while they remained in their monomeric form when stored in a high salt concentration buffer (**Manuscript 1, figure 3A**). When testing the renal clearance of both formats of the same protein administered *in vivo*, we observed once again a fast renal clearance in the case of the non-assembled construct while the assembled one was efficiently accumulated in their target cells and not in kidney (**Manuscript 1, figure 3B**). These results fully supported the nanoparticle size-dependent biodistribution observed in previous models.

In this study, we have fully demonstrated that *in vitro* self-assembled protein nanoparticles are structurally stable *in vivo*. However, being simple electrostatic interactions described in previous works (**paper 1**) presumably too weak forces to maintain nanoparticles' structural stability *in vivo*, obtained results strongly suggest that other additional forces might be participating in their structural stabilization. In this regard, performed *in silico* studies fully supported additional van der Waals and hydrogen bonds to be generated after the initial electrostatic interactions, conferring enough structural stabilization to maintain nanoparticles' structural integrity *in vivo* (**Manuscript 1, figure 4 and table 1**).

All together, the peptide T22 appears to be an unusually powerful tag for intracellular targeting in CXCR4⁺ cells, whose use opens a wide spectrum of possibilities not only for targeted therapies, but also for diagnosis. Moreover, T22-empowered self-assembling nanoparticles appear as a very promising tool for targeted drug or nucleic acid delivery in CXCR4 linked pathologies, for which intracellular targeting agents are still missing, and especially in metastatic colorectal cancer, where current treatment strategies are targeted to the primary tumor rather than to the disseminated disease³⁹⁰. All this, prompted us to apply for an European patent based on the use of the T22 peptide for targeted intracellular delivery of therapeutic molecules in CXCR4⁺ cells (EP2012/050513) published on 2012/09/03 (WO2012/095527) (**Annex 5**).

3. Self-assembling protein nanoparticles towards the gene therapy in colorectal cancer.

One of the major aims of non-viral gene therapy has been the construction of size compatible and tunable nanoparticles that efficiently mimic different viral functions, such as nucleic acids binding and condensation, specific cell recognition, internalization and genetic cargo delivery in the appropriate subcellular compartment, for the successful targeted delivery of nucleic acids. In this context, the term “artificial viruses” has been proposed to describe virus-like constructs that show those specific viral functions^{128, 130, 391}.

Among the different materials used to create artificial viruses including polymers and lipids among others, protein-only artificial viruses appear to be the most appealing ones, since despite not being yet as efficient as viral vectors, their biosecurity and biocompatibility make them the most promising alternative to those efficient but not safe viral vectors³³².

Virus like particles (VLPs) are one of the currently most studied versions of protein-only artificial viruses, which taking advantage of their natural self-assembling ability, have already been successfully used in some gene therapy studies. However, their lack of flexibility has strongly limited their general applicability²⁴⁷. In this context, the generation of artificial viruses using fully de novo designed multifunctional proteins appears as a very promising strategy since their extremely high plasticity of design, make them possible to be easily adapted to any clinical need by simple protein engineering procedures (Figure 13).

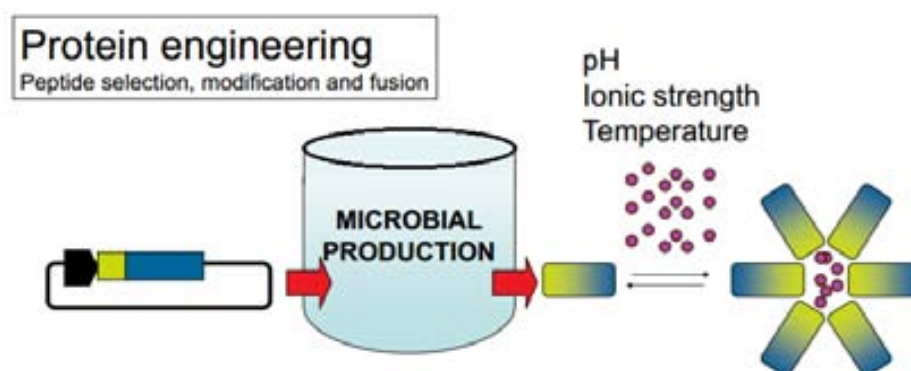


Figure 13: De novo construction of multifunctional protein artificial viruses. Self-assembling peptide sequences (green box) can be fused to a multifunctional protein (blue) to produce self-organizing artificial viruses. The assembling of protein building blocks into supramolecular entities can be controlled *in vitro* to allow the incorporation of cargo nucleic acids or drugs. (Modified from Vazquez E. *et al* 2010).

Discussion

Different multifunctional protein-based artificial viruses have already been successfully generated and used in gene therapy approaches^{129, 172, 192-194}. However, unlike other types of protein-based artificial viruses that take advantage of their natural self-assembling capacity, de novo designed multifunctional proteins have generally failed to promote predefined nanoscale organization. Only few cases where engineered self-assembling proteins have successfully assembled into nanoparticles of defined structure have been reported³⁹².

Apart from protein's intermolecular interactions, protein-DNA interactions can also strongly affect proteins supramolecular structure and size, consequently affecting their functionality. In this context, only few studies have been performed to analyze the interactions between multifunctional proteins and DNA molecules. These studies, which have generally been performed using non-assembling multifunctional proteins, have shown that the interactions between cationic peptides and DNA usually result in the generation of polydisperse soluble aggregates; probably driven by unordered inter-protein interactions^{255, 256}. Some studies where the DNA molecules drove the stabilization of aggregation prompt multifunctional proteins into monodisperse nanoparticulated entities have also been reported (**Annex 6**)¹⁷⁷. However, the supramolecular organization of the polyplexes generated by the interaction between multifunctional self-assembling protein nanoparticles and DNA molecules remains so far unexplored.

In this context, we wanted to study how functionalized self-assembling nanoparticles interact with DNA and how the generated supramolecular organization affects their functionality, especially regarding their suitability as artificial viruses for targeted gene therapy.

In this regard, we incubated previously reported R9-empowered self-assembling protein nanoparticles with an external cargo DNA at different conditions and subsequently analyzed the generated supramolecular structures. When using nanoparticles generated at pH 7 and 8, the resulting complex size did not change from that reported for the protein itself³⁷⁰ (**Manuscript 2, figure 1A**). At pH 4 and 10, again in agreement with previously reported data (**paper 1**), the protein-DNA complexes showed strong aggregation tendency probably driven by the denaturing conditions (**Manuscript 2, figure 1A**). However, at pH 5.8, in which R9-empowered nanoparticles have been reported to show their optimal transfection efficiency (**paper 1**), protein-DNA complexes interestingly divided in two different regular size populations of 38 nm and 700-800 nm respectively with no signs of protein aggregation (**Manuscript 2, figure 1A**). When these polyplexes were analyzed by confocal microscopy during exposure to cultured cells, small spherical shape (**Manuscript 2, figure 1B and 1C**) and larger rod-shaped (**Manuscript 2, figure 1D and 1E**) virus-like protein particles, which perfectly fitted respectively with those

populations detected by dynamic light scattering (**Manuscript 2, figure 1A**), were found within the cells; both of them containing cargo DNA completely shielded in the inner part of the structure (**Manuscript 2, figure 1G**). However, many of the observed spherical shape protein particles were found to be empty, strongly suggesting that spherical virus like structure, although being more abundant within the cells, are less efficient embedding DNA than rod-shaped structures (**Manuscript 2 figure 1B y 1C**).

Generated rod-shaped shells, resulted to be morphologically similar to capsid proteins observed in some plants viruses such as tobacco mosaic virus (TMV), strongly supporting a virus-like organization. In this context, *in silico* represented superimposition of RNA-containing rod-shaped TMV structure and an energetically stable disk-shaped molecular representation of the R9-GFP-H6 nanoparticles generated at pH 5.8, showed to have strong coincidences in diameter, monomer organization and spatial distribution of arginine residues in the inner part of the central cavity of the structure (**Manuscript 2, figure 1F**).

This virus-like organization was further supported by DNase I hydrolysis assays were R9-GFP-H6 polyplexes resulted to be highly protective for their cargo DNA (**Manuscript 2, figure 2**). Similarly, self-assembling T22-GFP-H6 nanoparticles also resulted to be protective for their cargo DNA, although in agreement with a lower DNA binding capacity observed, the measured protection effect resulted to be also smaller (**Manuscript 2, figure 2**). However, when exposing HNRK-DNA polyplexes to DNase I, this protein, which does not exhibit architectonic properties, failed in protecting its cargo DNA (**Manuscript 2, figure 2**). These results are fully in agreement with the data reported in a previous study where HNRK-DNA supramolecular structures showed to have the cargo DNA clearly overhanging from the structure instead of being trapped in the inner part of a shell-like structure (**Annex 6**)¹⁷⁷.

It is not clear why the R9-GFP-H6 proteins organize in spherical-shaped and rod-shaped structures when incubating with a cargo DNA at slightly acidic pH. It is possible that at pH 5.8 where histidines are in an in-equilibrium protonation stage (Imidazole group $pK_a=6$)³⁸⁹, histidines can actively participate in the nanoparticles' supramolecular organization, conferring to the whole construct enough structural dynamism and flexibility to organize in both, spherical or disc-shaped cylindrical structures. The high dipolar charge distribution of protein monomers strongly suggest the possibility of proteins being oriented with their positively charged surfaces towards the inner part of the structure in contact with the DNA, for which spherical and rod-shaped structures could be the most appropriate morphologies for the generation of stable protein-protein interactions. In agreement whit that, performed Z-potential analysis of protein-DNA polyplexes proved to be more negatively charged on their surface that the protein nanoparticles alone (**Manuscript 2, figure 2B**).

Discussion

Some protein intermolecular interaction models supporting spherical-shaped or rod-shaped organizations were generated *in silico* (**Manuscript 2, figure 3**). In these models, as previously described (**Manuscript 1**), additional intermolecular interactions apart from electrostatic ones, such as van der Waals forces or hydrogen bonds, were suggested to be significantly contributing to the structural stabilization.

All together, in this study we have demonstrated that functionalized self-assembling protein nanoparticles show an unexpected architectonic potential when combined with an external cargo DNA, what make them a very appropriate material for their use as non-viral vectors in gene therapy. At that end, we wanted to determine the suitability of this type of artificial viruses as targeted gene delivery vectors in CXCR4 expressing cells, a receptor overexpressed in metastatic colorectal cancer cells.

In this regard, five different T22-empowered multifunctional protein nanoparticles were designed and generated to be tested for their ability to efficiently condensate a reporter gene and deliver it into CXCR4⁺ cells (**Manuscript 3, figure 1A**). Once the constructs were successfully produced and purified, we tested their DNA condensation ability by electrophoretic mobility shift assays (EMSA). Surprisingly, obtained results showed that none of them were able to efficiently bind the added DNA (**Manuscript 3, figure 2**). Moreover, the intense fluorescence signal detected in all the negative controls, strongly suggested that purified protein samples already contain nucleic acids (**Manuscript 3, figure 2, inset**). This was fully in agreement with the data obtained by spectrophotometry analysis, where all the protein samples showed to strongly absorb at 260 nm, wave length at which nucleic acids show their maximum absorbance³⁹³ (**Manuscript 3, table 1**). Our results suggested that purified multifunctional self-assembling proteins had already condensed nucleic acids from the bacterial expression system used for their recombinant production and therefore, they were not able to bind additionally added external DNA. Performed additional assays showed that this phenomenon completely depends on the presence of highly positively charged regions in the protein, usually utilized as nucleic acid binding domains. The previously described R9-GFP-H6 protein, whose cationic tag contains a smaller number of positively charged aminoacids, showed also bacterial nucleic acids attached (**Manuscript 3, table 2**), but unlike T22-empowered constructs, it still maintained additional external DNA binding capacity (**paper 1**), probably since its cationic region was not fully saturated by bacterial nucleic acids. When a series of alternative mutant versions of the R9-empowered protein, in which positively charged arginine residues were progressively substituted by neutral aminoacids, were analyzed, proteins showed to progressively lose their bacterial nucleic acid binding capacity, as the cationic tag was becoming more neutral (**Manuscript 3, table 2**).

As a consequence of this previously completely unexpected event, when generated artificial viruses were tested for their ability to deliver a cargo DNA in CXCR4⁺ cells, they completely failed in the expression of the reporter gene, even though all protein constructs showed efficient cell penetrability (**Manuscript 3, figure 1B and 1C**).

Different DNase and RNase hydrolysis assays were performed in order to optimize a protocol to efficiently remove bacterial nucleic acids from protein constructs. Obtained results showed that multifunctional proteins contained both, bacterial DNA and RNA attached, and that only with combined DNase / RNase treatments was possible to obtain nucleic acid-free samples (**Manuscript 3, figure 3A**). In this context, an optimized protocol of combined DNase and RNase hydrolysis of pre-purified proteins, allowed to efficiently purify nucleic acid-free protein particles that had fully recovered their external DNA condensation capacity (**Manuscript 3, table 1 and figure 3B**).

When one of these purified nucleic acid-free multifunctional proteins named T22-NGFPK-H6, which apart of a nucleic acid binding domain contains a nuclear localization signal, was complexed with an external cargo DNA and compared with the non-treated protein version for its ability to deliver and express a reporter gene in CXCR4⁺ cells, the obtained results showed that although both versions were able to efficiently penetrate inside target cells, only the pre-treated version succeeded in the condensation and delivery of a expressible DNA into target cells. (**Manuscript 3, figure 4**).

Thus, to our knowledge, these results have reported for the first time a previously unsuspected fact occurring when producing recombinant artificial viruses with nucleic acids binding domains that results strongly detrimental for their functionality and suggest an additional purification step to obtain fully functional recombinant protein-only artificial viruses.



Conclusions

1. Self-assembly of monomeric proteins into regular size nanoparticles is induced by the incorporation of cationic architectonic tag pairs (one of them being a poly-histidine), thus allowing the *de novo* design of protein nanoparticles with predefined structural properties.
2. The architectonic ability of peptide tags is determined by their cationic nature, being the nanoparticle size influenced by the net positive charge of the tag.
3. Hexahistidine peptide acts as a pH-regulatable architectonic tag complementing the activity of a second cationic tag, provided both tags are protonated.
4. Protein self-assembly process is initially driven by electrostatic interactions between protein monomers. In addition, putative van der Waals interactions and hydrogen bonds might be also involved in *in vivo* intermolecular stability.
5. The cytoplasmic but not the nuclear membrane is the most important biological barrier in the uptake of self-assembled R9-GFP-H6 protein during the nuclear transfer process.
6. R9-empowered protein nanoparticle uptake follows endocytic pathway leading to nuclear accumulation, and resulting non-toxic process for mammalian cells.
7. CXCR4 Receptor-specific affinity of peptide ligands and their internalization ability have been proven to be independent events.
8. T22 peptide is an unusually powerful tag for selective intracellular targeting in CXCR4⁺ cells.
9. Targeted self-assembling protein only nanoparticles tested along this study have been proven not to be toxic for *in vivo* administration in mice.
10. T22-empowered protein nanoparticles of optimal size selectively biodistribute in CXCR4⁺ cells *in vivo*, being a very promising tool for targeted drug or nucleic acid intracellular delivery in CXCR4-linked pathologies.
11. *In vitro* generated intermolecular interactions during protein nanoparticle assembling process are strong enough to ensure nanoparticle's structural stability *in vivo*.

Conclusions

- 12.** Functionalized self-assembled protein nanoparticles that contain nucleic acid binding domains, show appealing capacity to generate virus-like structures when combined with an external DNA for gene therapy approaches.
- 13.** Generated supramolecular structures contain the cargo DNA completely shielded in the inner part of the virus-like structure protected against DNase I mediated hydrolysis. This property makes these complexes an excellent tool for their use as non-viral artificial viruses in gene therapy.
- 14.** Recombinant expression in bacterial hosts of self-assembling proteins that contain nucleic acid binding domains, usually results in bacterial nucleic acid binding, being strongly detrimental for their functionality as artificial viruses.
- 15.** Additional DNase / RNase hydrolysis treatment is required during recombinant multifunctional protein purification in order to obtain fully functional nucleic acid-free artificial viruses.
- 16.** The high biocompatibility expected for proteins, their regulatable architectonic properties and the strong nuclear avidity, make R9-GFP-H6 nanoparticles and in general self-assembling protein-only nanoparticles, a very promising material for the therapeutic delivery of drugs and nucleic acids in mammalian cells.



Annex

Annex 1

Manuscript 1:

In vivo architectonic stability of fully *de novo* designed protein-only nanoparticles.

María Virtudes Céspedes, Ugutz Unzueta, Witold Tatkiewicz, Patricia Alamo, Xu Zikung, Isolda Casanova, José Luis Corchero, Oscar Conchillo, Juan Cedano, Xavier Daura, Imma Ratera, Jaume Veciana, Neus Ferrer-Miralles, Esther Vazquez, Antonio Villaverde, Ramón Mangues.

Submitted to ACS Nano.

In vivo architectonic stability of fully *de novo* designed protein-only nanoparticles.

María Virtudes Céspedes^{1, 2}, *Ugutx Unzueta*^{2, 3, 4}, *Witold Tatkiewicz*^{2, 5}, *Patricia Álamo*^{1, 2}, *Xu Zikung*^{2, 3, 4}, *Isolda Casanova*^{1, 2}, *José Luis Corchero*^{2, 3, 4}, *Oscar Conchillo*³, *Juan Cedano*⁶, *Xavier Daura*^{3, 7}, *Imma Ratera*^{2, 5}, *Jaume Veciana*^{2, 5}, *Neus Ferrer-Miralles*^{2, 3, 4}, *Esther Vazquez*^{2, 3, 4}, *Antonio Villaverde*^{2, 3, 4*}, and *Ramón Mangués*^{1, 2}

1 Oncogenesis and Antitumor Drug Group, Biomedical Research Institute Sant Pau (IIB-SantPau), Hospital de la Santa Creu i Sant Pau, C/ Sant Antoni Maria Claret, 167, 08025 Barcelona, Spain

2 CIBER de Bioingeniería, Biomateriales y Nanomedicina (CIBER-BBN), Bellaterra, 08193 Barcelona, Spain

3 Institut de Biotecnologia i de Biomedicina, Universitat Autònoma de Barcelona, Bellaterra, 08193 Barcelona, Spain

4 Department de Genètica i de Microbiologia, Universitat Autònoma de Barcelona, Bellaterra, 08193 Barcelona, Spain

5 Department of Molecular Nanoscience and Organic Materials, Institut de Ciència de Materials de Barcelona (CSIC), Bellaterra, 08193 Barcelona, Spain

6 Laboratory of Immunology, Regional Norte, Universidad de la República, Gral. Rivera 1350; Salto, 50.000, Uruguay

7 Institució Catalana de Recerca i Estudis Avançats (ICREA), Barcelona, Spain

* Corresponding author: A. Villaverde; antoni.villaverde@uab.cat

Keywords: Protein nanoparticles; Building blocks; Genetic engineering, Biodistribution; Targeting; Drug delivery

Abstract

The *de novo* design of protein building blocks to self-assemble as functional nanoparticles is a challenging task in innovative medicines, which urgently demand novel, versatile and biologically safe vehicles for imaging, drug delivery and gene therapy. While viruses and virus-like particles show severe limitations in use, protein-only nanocarriers are increasingly reachable by engineering of protein-protein interactions between self-assembling building blocks. We have explored if such cross-molecular contacts, as promoted by end-terminal cationic peptides and oligohistidines, are stable enough for the resulting nanoparticles to overcome biological barriers in such assembled form. The analyses of renal clearance and biodistribution in mice of several model proteins reveal long-term architectonic stability, allowing systemic circulation and tissue targeting as nanoparticulate material. This observation fully supports the value of genetically designed protein building blocks and of peptidic tags with architectonic roles, for the biofabrication of smart, robust and multifunctional nanoparticles with medical applicability that mimic structure and functional abilities of viral capsids.

A wide spectrum of materials is under examination for the construction of nanoparticles as molecular carriers in diagnosis and therapy (1). While several candidates are technically promising and economically feasible, biocompatibility issues severely compromise their applicability (2). Proteins are ideal materials for therapeutic purposes, because of their functionalities, easy production, tuneability and full biocompatibility. Regarding drug delivery, natural examples point out proteins as ideal nano- or micro-cages for molecular carriage. Infectious viruses (3, 4), virus-like particles (VLPs) (5) and more recently bacterial microcompartments (BMC) (6) and eukaryotic vaults (7) are being explored to transport and deliver nucleic acids, peptides or proteins, chemicals, metals and quantum dots, among others. However, biosafety concerns in the case of viruses, and limited flexibility in re-adapting the tropism and geometry in the case of VLPs, vaults and BMCs stress the need of functionally versatile, highly tuneable protein nanocages. The highly organized protein shells of viruses are formed by self-assembling building blocks that interact through a complex combination of electrostatic, hydrophobic, van der Waals and hydrogen bond contacts (8). So far, the de novo design of self-assembling protein monomers for tailored construction has been rather reluctant to rational design. Self-assembling amyloidogenic peptides, although showing a wide spectrum of applications in nanomedicine (9), are unable to generate regular sized shells for controlled drug encapsulation, and their biological fabrication poses important challenges. Concerning full proteins, a limited number of engineering approaches have rendered self-organizing cages, mainly by adapting oligomerization domains of natural oligomeric proteins (10, 11). Recently (12), we have described a new protein engineering principle, based on the combined use of two different cationic peptides (one of them being a polyhistidine). These agents, fused at either the end termini of recombinant proteins confer tagged monomers (different protein species including GFP and p53) with a strong dipolar charge distribution that support spontaneous self-organization as monodisperse nanoparticulate materials. The size of resulting nanoparticles can be regulated by the composition of cationic residues of the N-terminal tag and by the ionic strength (12), and they have been proved useful, upon convenient modular functionalization of the monomers, for the intracellular and intranuclear delivery of proteins (13) and expressible DNA (14). In particular, T22-GFP-H6 shows an excellent biodistribution in metastatic colorectal cancer animal models (15) in which CXCR4⁺ cells have a prevalent role (T22 is a ligand of CXCR4 (16)), proving their medical applicability. However, whether the intermolecular interactions promoted by

Annex

the cationic peptides plus histidine tails are strong enough to ensure the stability of nanoparticles *in vivo* remains fully unexplored. Being these interactions presumably weaker and less complex than those supporting assembling of infectious viruses, VLPs, vaults and BMC shells, it could be not ruled out that the nanoparticles formed *in vitro* would be immediately disassembled once administered, as the blood stream and intracellular media are rich in charged molecules. Being this issue critical for the further development of peptide-based architectonic tags and for the de novo design of improved protein nanocages, we have determined here their architectonic stability upon *in vivo* administration. Since the *in situ* detection of nanoparticulate material in target tissues might be technically unaffordable, we have determined the renal clearance and biodistribution of two types of nanoparticles, formed by the self-assembling building block proteins R9-GFP-H6 and T22-GPP-H6 respectively. Their parental, monomeric species GFP-H6 as well as other two closely related variants that do not form nanoparticles have been used as controls. As renal filtration occurs for compounds with a size lower or around 6 nm (17), a size slightly higher than the monomer GFP-H6 (and related species) and lower than any assembled versions of the modular proteins (~13 nm or larger) (12), renal clearance should be an excellent reporter of the *in vivo* stability of circulating nanoparticles.

Results and discussion

When H6-tagged GFP is empowered by additional N-terminal cationic peptides, the resulting constructs act as self-organizing monomers that form protein-only nanoparticles of sizes ranging from 10 to 50 nm approximately (12). These particles are immediately observed upon protein purification from recombinant bacteria by His-affinity chromatography, and we presume that they are assembled in the storage buffer against which the protein sample is dialyzed after elution. Being cationic, peptides R9 and T22 fused at the N-terminus of GFP-H6 support the self-assembling of the whole construct as particles of ~20 nm and ~13 nm respectively. In contrast, the non-cationic peptides Ang-and Seq fail in promoting any supramolecular organization, and the size of the chimerical proteins matched in both cases that of GFP-H6 (between 4 and 5 nm, Figure 1A). Upon single intravenous (i.v.) administration in mice at equal doses, Ang-GFP-H6, Seq-GFP-H6 and the parental GFP-H6 accumulated in kidney, indicative of renal clearance and in agreement with their monomeric status also *in vivo* (Figure 1 B, C). Contrarily, R9-GFP-H6 and T22-GFP-H6 were not observed in kidney (Figure 1 B,

C), suggesting that the nanoparticulate architecture reached by these proteins *in vitro* (Figure 1 D) is maintained *in vivo* during circulation in blood. However, it could be not discarded that the absence of protein in kidney would be due to a high proteolytic instability in plasma and fast degradation. However, T22-GFP-H6 was highly stable in plasma *in vitro*, and when administered to colorectal cancer mice models, it accumulated in primary tumors and metastatic foci as measured by its fluorescence emission. The combination of all these data was indicative that the protein reached its target in a full-length form. In this particular construct, note that the N-terminal cationic peptide T22 was at the same time an architectonic tag and a cell-specific ligand, as it specifically binds and internalize CXCR4+ cells (15, 16).

Regarding R9-GFP-H6, we determined here that this construct was also fully stable in plasma and serum (Figure 2 A). On the other hand, when screening main organs for the presence of the protein we observed R9-GFP-H6 in brain (Figure 2B). This was not completely unexpected as previous findings from other researchers suggested a BBB-crossing potential of R9 and related arginine rich peptides (18, 19). Since neither R9- nor T22-empowered proteins were detected in lung (not shown), the possibility of unspecific protein aggregation could be also excluded and the absence of these proteins in kidney, as presented in Figure 1B, must be exclusively attributed to their nanoparticulate organization that prevented size-dependent clearance. Renal filtration of parental GFP-H6 and related non-assembling proteins also indicated that these constructs, with a size very close to the threshold for filtration, do not tend to aggregate or assemble *in vivo* and that they keep their monomeric form during circulation in blood.

While being a highly exciting finding and offering an enormous potential in the design of artificial viruses and protein nanoparticles for medical purposes, the high architectonic stability *in vivo* of R9-GFP-H6 and T22-GFP-H6 was not anticipated. Being the architectonic tags R9 and T22 highly cationic and the whole chimerical constructs showing a dipolar charge distribution (12), we expected electrostatic charges being the main drivers of protein assembly. Then, nanoparticle stability in media with a high load of charged components, such as bloodstream (negatively charged proteins and a wide catalogue of ions) was at least initially surprising, as we could presume molecular competition between charged agents and particle dissociation. To test the apparent 'structural memory' of protein nanoparticles supporting the observed stability,

Annex

we evaluated renal clearance of a new modular protein (T22-IRFP-H6) upon administration. This construct is equivalent to T22-GFP-H6 but in this case, the core of the monomer is IRFP, a fluorescent protein with sequence and structure unrelated to those of GFP. Purified in low salt buffer, the construct self-organizes as nanoparticles of 15 nm but in high salt buffer the protein remains monomeric and nanoparticles are not formed (Figure 3A). When administering the two versions of the same protein to mice (oligomeric and monomeric), renal clearance was observed for the protein in high salt buffer but not for the protein version that assembled *in vitro* in low salt buffer (Figure 3 B, C), indicating again the prevalence in the bloodstream of the same architecture adopted *in vitro*. Furthermore, adding salt to the protein purified in low salt buffer (to reach the salt concentration of high salt buffer) does not alter particle size *in vitro* (Figure 3 D), indicative of a tight organization of the oligomer and of robust cross-molecular interactions that are not responsive to further media changes after assembling. These results clearly indicate that once nanoparticles are formed, their architecture remains stable both *in vitro* and *in vivo*, and that while salt content modulates the initial pattern of protein-protein interactions it does not disturb the structure of the supramolecular complexes. The cross-molecular contacts between monomers could be then more complex than mere electrostatic interactions and probably similar to those occurring in natural oligomers, viruses and related entities.

To evaluate this possibility, we modeled protein-protein interactions in R9-GFP-H6, enlarging the spectrum of potential contacts over simpler models obtained before (12, 14). Different probable star-shaped oligomers (pentamers) resulted from the docking process depending on the conformation adopted by the overhanging end terminal peptides, all of them in the range of 15-30 nm and compatible with the nanoparticle size (Figure 4). When resolving the energetics organizing the monomers, complex combinations of electrostatic interactions, van der Waals forces and hydrogen bonds were found in all cases (Table 1), as in those occurring in natural protein complexes (20). The strong weight of van der Waals forces and hydrogen bonds revealed that electrostatic contacts, although important, were not the unique drivers of self-assembling of the modular monomers. In fact, capsid proteins interact mainly through a combination of electrostatic repulsion, hydrophobic attraction and specific contacts between given pairs of amino acids. These interactions impose a certain restriction in the orientation of the interaction during complex formation, and once this is formed the

weaker van der Waals forces complete the assembly (21). Varying the acidity and salinity conditions (or the concentration of Ca^{2+} ions) adjusts the relative balance between these competing interactions, thereby favouring assembly or disassembly.

Being protein-only nanoparticles are extremely promising in nanomedicine because of biocompatibility issues and the extreme functional versatility offered by protein engineering tools, protein self-assembling is far from full rational control. This is due to our so far negligence in linking molecular architecture with the forces that regulate protein-protein interactions (20). In fact, the complexity that allows the correct assembling of a virus capsid shell is not reflected by the apparent simplicity of the capsid components and it cannot be predicted in advance from the analysis of the monomers. Here we prove that the assembly promoted by a short cationic peptide (such as R9 or T22) combined with a hexahistidine, fused to the end termini of different proteins acting as monomers, mimic the organization of natural protein complexes such as viral shells, what confer a high stability of the nanoparticle once administered in the bloodstream. Although ionic strength appears as important during the nanoparticle organization this parameter does not affect the stability of already formed particles, what allows these entities overcoming biological barriers and reaching their target in a nanoparticulate form. The principle based on the addition of architectonic tags other than oligomerization domains offer a wide and unexpected plasticity in the design of multifunctional modular monomers (a diversity of protein species being suitable as cores), and opens a plethora of opportunities for the fully de novo design of robust protein-based carriers (artificial viruses) for emerging nanomedical applications.

Methods

Proteins and protein purification

R9-GFP-H6 and T22-GFP-H6 are modular proteins in which the cationic peptides R9 (nine arginines, (19)) and T22 (derived from polyhemusin, (21)) are fused respectively to the amino terminus of a hexahistidine C-tagged GFP (GFP-H6). These peptides, apart from providing positive charges that create a dipolar building block (15), confer targeting properties to the resulting nanoparticle. In the case of T22, a ligand of CXCR4 (21), has been experimentally confirmed already as the protein, after injection, accumulates in primary and metastatic foci in a colorectal cancer model of metastasis,

Annex

as immunodetected in histological sections (15). Ang-GFP-H6 and Seq-GFP-H6 are closely related proteins that do not form nanoparticles, as the amino-terminal tags are not cationic (15). T22-IRFP-H6 was designed in house, and synthetic genes were provided and subcloned into pET22b plasmid vector (using NdeI and HindIII restriction sites) by Genscript (Piscataway, USA). T22-IRFP-H6 has the same modular scheme than T22-GFP-H6 but the monomer core was the near-infrared fluorescent protein IRFP (22) instead GFP. All proteins were produced from pET22b in *Escherichia coli* strain Origami B (BL21, OmpT-, Lon-, TrxB-, Gor- (Novagen)) overnight at 20 °C upon 1 mM IPTG addition, and purified by Histidine-tag affinity chromatography as described (12). Briefly, we used HiTrap Chelating HP 1 ml columns (GE Healthcare) in an ÄKTA purifier FPLC (GE Healthcare). Cell extracts were disrupted at 1100 psi in a French Press (Thermo FA-078A) and soluble and insoluble fractions separated by centrifugation at 20,000g for 45 min at 4°C. The soluble fraction was charged onto HiTrap column and subsequently washed with Tris 20 mM, NaCl 500 mM, Imidazole 10 mM, pH=8 buffer. Protein were eluted by linear gradient of high imidazole concentration buffer (20 mM Tris, 500 mM NaCl, 500 mM Imidazole, pH=8). Once in elution buffer, proteins were dialyzed against the most appropriate buffer regarding stability, which was carbonate buffer (166 mM NaHCO₃, pH 7.4) for Ang-GFP-H6, Seq-GFP-H6, T22-GFP-H6 and T22-IRFP-H6, and Tris dextrose (20 mM Tris, 5% dextrose pH 7.4) for GFP-H6 and R9-GFP-H6. The high salt buffer was always obtained by adding NaCl to the buffer to get a final concentration of 500 mM for GFP-H6, R9-GFP-H6 and T22-IRFP-H6. Once dialyzed, proteins were stored at -80 °C until use.

Analysis of protein stability

R9-GFP-H6 stability was analyzed by following its fluorescence emission upon diluting in triplicate, in either human serum (Sigma, ref: S2257-5ML, at a final concentration of 0.23 µg/µl), or in human and mouse plasmas (at a final concentration of 0.11 µg/µl). Human blood was obtained from a healthy donor in the Hospital de Sant Pau. Murine blood, approximately 250 µl per mouse was obtained from the submandibular facial vein of five control mice (25 g) in heparanized tubes. A plasma pull sample was obtained by centrifugation the total blood at 600 g for 10 min at 4°C. Right after dilution, samples were harvested (Time “0”) as reference values (taken as 100 %) of

initial fluorescence. Protein dilutions were further incubated (at 37°C, in agitation) and samples were taken, at different time points, up to 22 hours.

Dynamic light scattering

Volume size distribution of nanoparticles and monomeric GFP fusions were measured using a dynamic light scattering (DLS) analyzer at the wavelength of 633 nm, combined with non-invasive backscatter technology (NIBS) (Zetasizer Nano ZS, Malvern Instruments Limited, Malvern, U.K.). Samples were measured at 20°C. DLS measurements of solvents were used as controls. The measurements were performed in triplicate.

Atomic force microscopy

Atomic force microscopy (AFM) analyses were performed in liquid with a commercial atomic force microscope (PicoSPM 5100 from Molecular Imaging Agilent Technologies, Inc., Santa Clara, CA, USA) operating in acoustic mode. 9R-GFP-His proteins in 20 mM Tris pH 7.5 buffer + 5 % dextrosa 4 µg/ul (20 µl) were dropped onto a freshly cleaved mica surface and imaged in liquid. T22-GFP-His proteins in sodium bicarbonate 1.4 %, pH 7.4 buffer, 4.3 µg/ul (50 µl) pH 7.5 buffer + 5 % dextrosa 4 µg/ul (20 µl) were dropped onto a freshly cleaved mica surface and imaged in liquid. For the acoustic mode measurements, a silicon (Applied NanoStructures, Inc.) tip, with a radius of 10 nm, a nominal spring constant of 0.6–3.7 N/m and a resonance frequency of 43-81 kHz was used.

Animals and administration regime

Five-week-old female Swiss nu/nu mice weighing between 18 and 20 g (Charles River, L-Abreslle, France), maintained in SPF conditions, were used for *in vivo* studies. All the *in vivo* procedures were approved by the Hospital de Sant Pau Animal Ethics Committee. We assessed 2h post-administration, the *in vivo*, stability, biodistribution and renal clearance of the protein GFP-H6, R9-GFP-H6 and T22-GFP-H6 nanoparticles and Seq1- and Ang-empowered constructs after the i.v. administration of 500 µg/mouse (n=3 mice). The control mice (n=3) were administered i.v. in the appropriate buffer (20 mM Tris, 5 % Dextrose pH 7.5 for R9-GFP-H6, 20 mM Tris, 500 mM NaCl pH 7.4 for T22-GFP-H6 and 166 mM NaC03H pH 7.5 for Seq1- and Ang-empowered constructs).

Annex

We also assessed the stability and renal clearance of T22-IRFP-H6 dissolved in high salt carbonate buffer (+) or low salt carbonate buffer (-) by i.v. administration of 50 µg/mouse (n=3 mice), 24 h post-administration. Control mice were administered i.v. with the same buffer.

Biodistribution of nanoparticles in mice

At 2 hours post administration, mice were anesthetised with isoflurane and whole-body fluorescence was monitored using the IVIS® Spectrum equipment (Xenogen, France). Subsequently, necropsy was performed and all organs were removed and placed individually into wells to determine the emitted fluorescence of GFP-H6 derived nanoparticles or the near infrared fluorescence signal of IRFP-H6 derived nanoparticles using the IVIS® Spectrum. Once this was done, all these organs were collected, fixed in 4% formaldehyde in phosphate buffer for 24 hours and finally embedded in paraffin for the histological and immunohistochemical evaluation. The fluorescence signal was digitalized, and after subtracting the autofluorescence it was displayed as a pseudocolor overlay and expressed in terms of Radiant efficiency by each protein, group (control or experimental), dose and time .

Histopathology and immunohistochemistry for GFP-His-tag proteins

Four-micrometer-thick sections were stained with H&E for histopathological analyses. Paraffin-embedded tissue sections (4 µm) were de-paraffinized, re-hydrated and washed in PBS-T. Antigen retrieval was performed by citrate buffer at 120°C. After quenching peroxidase activity by incubating in 3 % H₂O₂ for 10min, the slides were washed in PBS-T. Then they were incubated 30 minutes with the primary antibody against GFP-tag (1:100; St Cruz) or His-tag (1:1000; Abcam), washed in PBS-T and incubated with the biotinylated secondary antibody for 30 min at room temperature. Finally, sections were counterstained with Haematoxylin and mounted using DPX mounting medium. Representative pictures were taken using Cell[^]B software (Olympus Soft Imaging) at 400x magnification.

Molecular modeling

Models of R9-GFP-H6 monomers were built using modeller 9v2 (24) and docked using HADDOCK v 2.0 (23), enforcing C5 symmetry and using N-terminal arginine residues

as the active residues (Figure 4). The models were generated using the same protocols previously described (24). The energetics of the models were analysed with FoldX using the function AnalyseComplex (25).

Figure 1

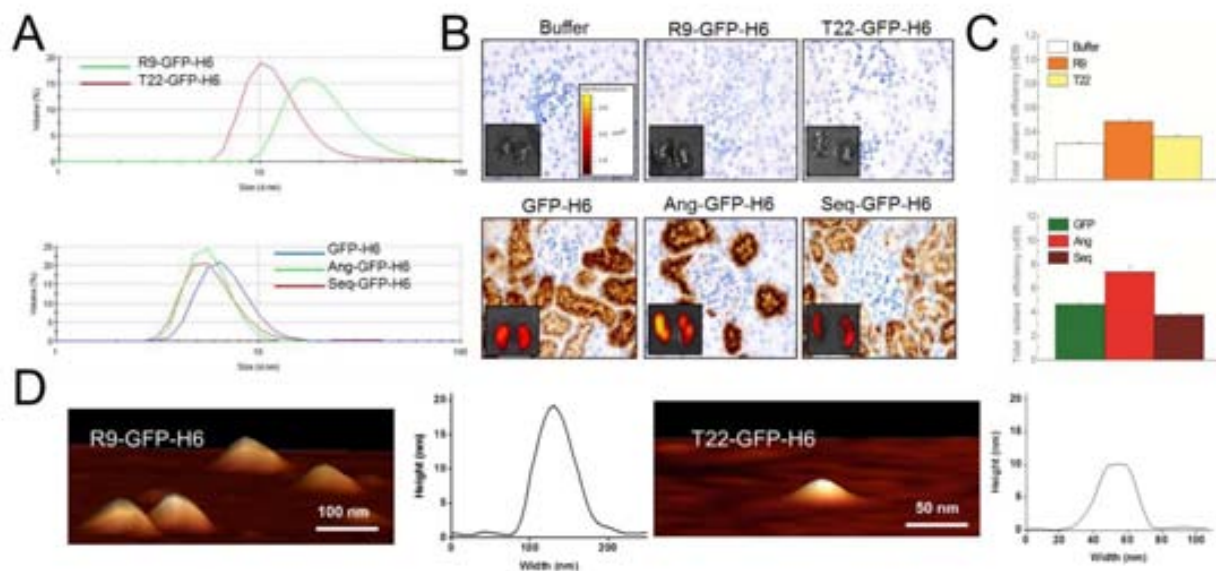


Figure 1. *In vitro* assembling of protein-only nanoparticles and renal clearance *in vivo*. A) Size of protein complexes formed by distinct GFP variants, measured by DLS. Representative experiments are shown. B) Immunohistochemical detection of the different nanoparticles, using anti-GFP antibodies, in the renal tissue glomeruli (400x magnification) 2 hours after the i.v. administration of 500 μg of each protein. The green fluorescence signal in kidneys registered *ex vivo* of a representative mouse for each group is shown in the insets. C) Quantitative determination of fluorescence in analysed kidneys expressed as the total radiant efficiency ($\text{ph}/\text{sec}/\text{cm}^2/\text{sr}/\mu\text{W}/\text{cm}^2$) of right and left kidneys for each mouse. D) AFM images of randomly selected nanoparticles formed by R9 and T22-empowered nanoparticles and topography cross-sections of isolated particles. Measurements have been done in liquid with a tip radius of 10 nm and thus the width (but not the high) of the particles is inherently overestimated.

Figure 2

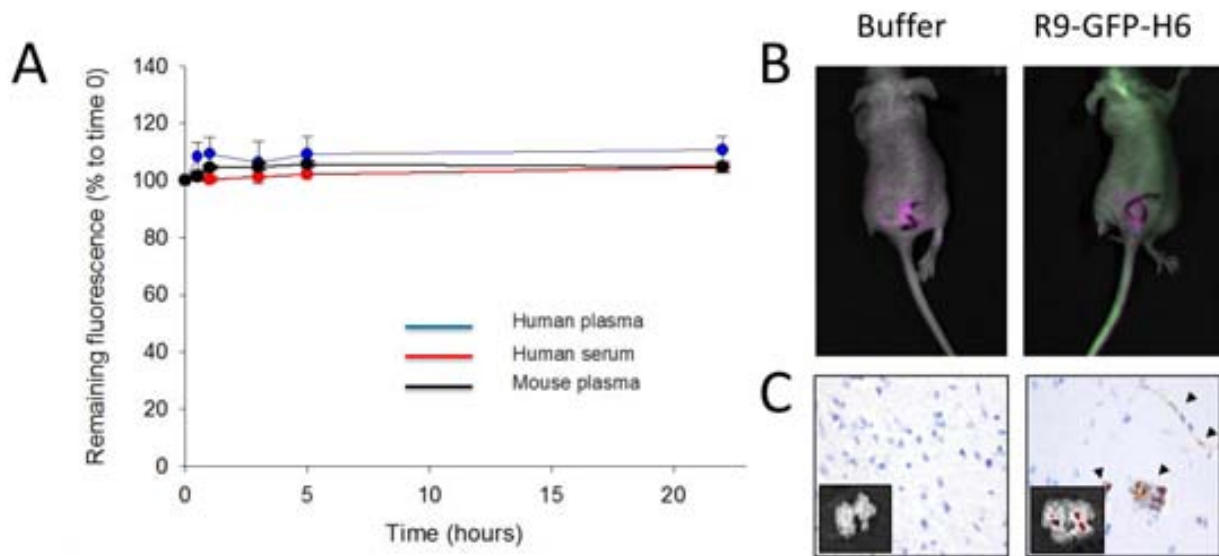


Figure 2. Stability and biodistribution of R9-GFP-H6. A) *In vitro* stability of R9-GFP-H6 in different media, monitored by fluorescent emission. B) *In vivo* whole-body recording of a representative mouse after 2 hours i.v. administered with buffer alone or 500 μg of R9-GFP-H6. The mouse administered with the nanoparticle shows fluorescence signal in the brain C) Immunohistochemical detection of the nanoparticle, using and anti-GFP antibody, in mouse brain sections 2 hours after iv administration of 500 μg of R9-GFP-H6 or buffer alone (400x magnification). Insets show green fluorescence signal recording in *ex vivo* brain sagittal sections of a representative mouse. Arrows show nanoparticle accumulation in the brain parenchyma.

Figure 3

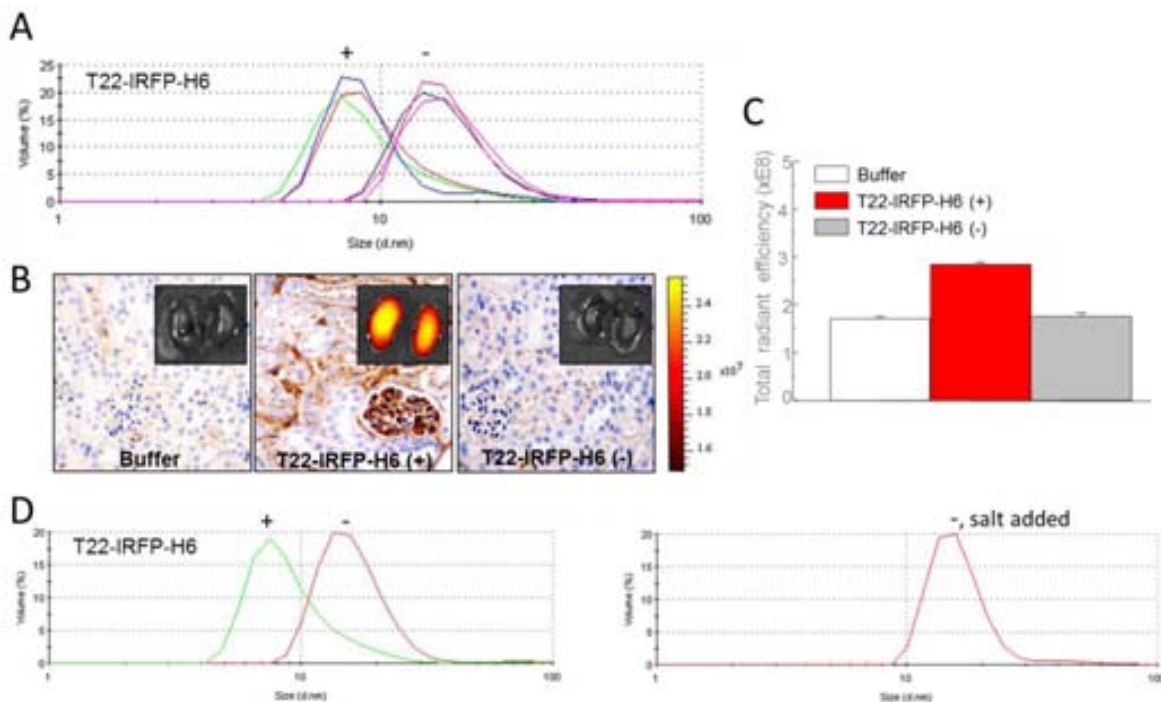


Figure 3. Structural memory of protein-only nanoparticles. A) DLS size analysis of T22-IRFP-H6 purified in low salt (-, carbonate buffer) and high salt (+, carbonate buffer + 334 mM NaCl). Different measures are plotted to evidence robustness of data. B) Immunohistochemical analysis, using an antibody that detects the Histidine tag, of the glomeruli in mouse kidney sections 24 hours after 50 μg i.v. administration of high (+) or low (-) salt T22-IRFP-H6 nanoparticles (400x magnification). Insets show IRFP fluorescence signal detected *ex vivo* in kidneys of a representative mouse for each group, after subtracting the autofluorescence. C) The total radiant efficiency (ph/sec/cm²/sr/ μW /cm²) determined for each group. D) DLS size analysis of T22-IRFP-H6 purified in either low (carbonate buffer, -) and high (carbonate buffer + 334 mM NaCl, +) salt buffers, and of T22-IRFP-H6 purified in low salt buffer and in which salt was added latter.

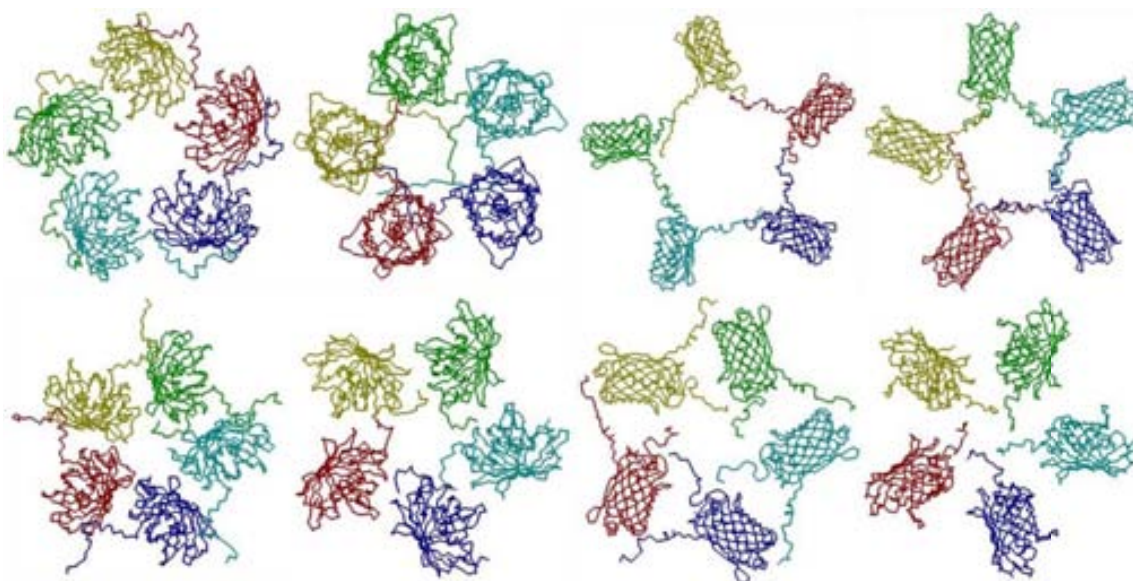
Figure 4

Figure 4. Different conformations of R9-GFP-H6 oligomers obtained in the docking process by using different configurations of overhanging R9 and H6 peptides. Models in the top row, were generated with HADDOCK (23) using R9 residues as active and H6 residues as passive. Models in the bottom row, were generated declaring only R9 residues as active. The energetics governing protein-protein interactions are given in Table 1 for each model.

Table 1. Summary of energetics governing monomer-monomer interactions in models depicted in Figure 4.

Model ^a	Hydrogen bond ^b	Van der Waals ^b	Electrostatics ^b
UP 1	-47,34	-65	-21,56
UP 2	-44,97	-57,16	-6,61
UP 3	-29,13	-42,38	-7,33
UP 4	-31,6	-38,18	-10,85
DOWN 1	-26,45	-30,56	2,86
DOWN 2	-23,13	-25,79	-4,6
DOWN 3	-12,64	-20,78	1,02
DOWN 4	-7,57	-11,83	12,21

^a Models refer to those depicted in Figure 4, in top and bottom rows, numbered from left to right.

^b Values were calculated with Foldix and are given in kcal/mol.

AUTHOR INFORMATION

Corresponding Author

* Corresponding author: A. Villaverde; Institut de Biotecnologia i de Biomedicina, Universitat Autònoma de Barcelona, Bellaterra, 08193 Barcelona, Spain.
antoni.villaverde@uab.cat

Author Contributions

The manuscript was written through contributions of all authors. All authors have given approval to the final version of the manuscript.

Funding Sources

The authors also acknowledge the financial support granted to E.V. (PI12/00327) and R.M. (PI12/01861) from FIS, to A.V. and J. V. from Agència de Gestió d'Ajuts Universitaris i de Recerca (grants 2009SGR-108 to A.V., SGR2009-516 to J.V. and 2009-SGR-1437 to R.M.), to J.V. from DGI (grant CTQ2010-19501) and from the Centro de Investigación Biomédica en Red (CIBER) de Bioingeniería, Biomateriales y Nanomedicina (NANOPROVIR and NANOCOMETs projects), financed by the Instituto de Salud Carlos III with assistance from the European Regional Development Fund. U.U. received a fellowship grant from MINECO. W.T. is grateful to the Consejo Superior de Investigaciones Científicas (CSIC) for a “JAE-pre” fellowship. A.V. has been distinguished with an ICREA ACADEMIA Award.

ACKNOWLEDGMENT

We appreciate the technical support of Fran Cortés from the Cell Culture Unit of Servei de Cultius Cel.lulars Producció d'Anticossos i Citometria (SCAC, UAB), and of Amable Bernabé from Soft Materials Service (ICMAB-CSIC/CIBER-BBN). We are also indebted to Nanotoxicology Platform and Protein Production Platforms (<http://www.bbn.ciber-bbn.es/programas/plataformas/equipamiento>). W.T. is grateful to the Consejo Superior de Investigaciones Científicas (CSIC) for a “JAE-pre” fellowship. A.V. has been distinguished with an ICREA ACADEMIA Award.

ABBREVIATIONS

BMC, bacterial microcompartment; GFP, green fluorescent protein; i.v. intravenous; VLP, virus-like particle.

REFERENCES

- (1) Villaverde A *Nanoparticles in Translational Science and Medicine*; Academic Press (Elsevier): London, 2011.
- (2) Sharifi, S.; Behzadi, S.; Laurent, S.; Forrest, M. L.; Stroeve, P.; Mahmoudi, M. Toxicity of Nanomaterials. *Chem. Soc. Rev.* **2012**, *41*, 2323-2343.
- (3) Giacca, M.; Zacchigna, S. Virus-Mediated Gene Delivery for Human Gene Therapy. *J. Control Release* **2012**, *161*, 377-388.
- (4) Edelstein, M. L.; Abedi, M. R.; Wixon, J. Gene Therapy Clinical Trials Worldwide to 2007--an Update. *J. Gene Med.* **2007**, *9*, 833-842.
- (5) Ma, Y.; Nolte, R. J.; Cornelissen, J. J. Virus-Based Nanocarriers for Drug Delivery. *Adv. Drug Deliv. Rev.* **2012**, *64*, 811-825.
- (6) Corchero, J. L.; Cedano, J. Self-Assembling, Protein-Based Intracellular Bacterial Organelles: Emerging Vehicles for Encapsulating, Targeting and Delivering Therapeutical Cargoes. *Microb Cell Fact.* **2011**, *10*, 92.
- (7) Rome, L. H.; Kickhoefer, V. A. Development of the Vault Particle As a Platform Technology. *ACS Nano.* **2012**.
- (8) Zlotnick, A. Are Weak Protein-Protein Interactions the General Rule in Capsid Assembly? *Virology* **2003**, *315*, 269-274.
- (9) Lakshmanan, A.; Zhang, S.; Hauser, C. A. Short Self-Assembling Peptides As Building Blocks for Modern Nanodevices. *Trends Biotechnol* **2012**, *30*, 155-165.
- (10) Doll, T. A.; Raman, S.; Dey, R.; Burkhard, P. Nanoscale Assemblies and Their Biomedical Applications. *J. R. Soc. Interface* **2013**, *10*, 20120740.
- (11) Yang, Y.; Burkhard, P. Encapsulation of Gold Nanoparticles into Self-Assembling Protein Nanoparticles. *J. Nanobiotechnology.* **2012**, *10*, 42.
- (12) Unzueta, U.; Ferrer-Miralles, N.; Cedano, J.; Zikung, X.; Pesarrodona, M.; Saccardo, P.; Garcia-Fruitos, E.; Domingo-Espin, J.; Kumar, P.; Gupta, K. C.; Mangués, R.; Villaverde, A.; Vazquez, E. Non-Amyloidogenic Peptide Tags for the Regulatable Self-Assembling of Protein-Only Nanoparticles. *Biomaterials* **2012**, *33*, 8714-8722.
- (13) Vazquez, E.; Cubarsi, R.; Unzueta, U.; Roldan, M.; Domingo-Espin, J.; Ferrer-Miralles, N.; Villaverde, A. Internalization and Kinetics of Nuclear Migration of Protein-Only, Arginine-Rich Nanoparticles. *Biomaterials* **2010**, *31*, 9333-9339.

- (14) Vazquez, E.; Roldan, M.; ez-Gil, C.; Unzueta, U.; Domingo-Espin, J.; Cedano, J.; Conchillo, O.; Ratera, I.; Veciana, J.; Daura, X.; Ferrer-Miralles, N.; Villaverde, A. Protein Nanodisk Assembling and Intracellular Trafficking Powered by an Arginine-Rich (R9) Peptide. *Nanomedicine (Lond)* **2010**, *5*, 259-268.
- (15) Unzueta, U.; Cespedes, M. V.; Ferrer-Miralles, N.; Casanova, I.; Cedano JA; Corchero JL; Domingo-Espin, J.; Villaverde A; Mangues, R.; Vazquez E Intracellular CXCR4⁺ Cell Targeting With T22-Empowered Protein-Only Nanoparticles. *Int. J. Nanomedicine* **2012**, *7*, 4533-4544.
- (16) Murakami, T.; Zhang, T. Y.; Koyanagi, Y.; Tanaka, Y.; Kim, J.; Suzuki, Y.; Minoguchi, S.; Tamamura, H.; Waki, M.; Matsumoto, A.; Fujii, N.; Shida, H.; Hoxie, J. A.; Peiper, S. C.; Yamamoto, N. Inhibitory Mechanism of the CXCR4 Antagonist T22 Against Human Immunodeficiency Virus Type 1 Infection. *J. Virol.* **1999**, *73*, 7489-7496.
- (17) Feng, B.; LaPerle, J. L.; Chang, G.; Varma, M. V. Renal Clearance in Drug Discovery and Development: Molecular Descriptors, Drug Transporters and Disease State. *Expert. Opin. Drug Metab Toxicol.* **2010**, *6*, 939-952.
- (18) Kumar, P.; Wu, H.; McBride, J. L.; Jung, K. E.; Kim, M. H.; Davidson, B. L.; Lee, S. K.; Shankar, P.; Manjunath, N. Transvascular Delivery of Small Interfering RNA to the Central Nervous System. *Nature* **2007**, *448*, 39-43.
- (19) Saccardo, P.; Villaverde, A.; Gonzalez-Montalban, N. Peptide-Mediated DNA Condensation for Non-Viral Gene Therapy. *Biotechnol. Adv.* **2009**, *27*, 432-438.
- (20) Leckband, D. Measuring the Forces That Control Protein Interactions. *Annu. Rev. Biophys. Biomol. Struct.* **2000**, *29*, 1-26.
- (21) Murakami, T.; Zhang, T. Y.; Koyanagi, Y.; Tanaka, Y.; Kim, J.; Suzuki, Y.; Minoguchi, S.; Tamamura, H.; Waki, M.; Matsumoto, A.; Fujii, N.; Shida, H.; Hoxie, J. A.; Peiper, S. C.; Yamamoto, N. Inhibitory Mechanism of the CXCR4 Antagonist T22 Against Human Immunodeficiency Virus Type 1 Infection. *Journal of Virology* **1999**, *73*, 7489-7496.
- (22) Filonov, G. S.; Piatkevich, K. D.; Ting, L. M.; Zhang, J.; Kim, K.; Verkhusha, V. V. Bright and Stable Near-Infrared Fluorescent Protein for in Vivo Imaging. *Nat. Biotechnol.* **2011**, *29*, 757-761.
- (23) Dominguez, C.; Boelens, R.; Bonvin, A. M. HADDOCK: a Protein-Protein Docking Approach Based on Biochemical or Biophysical Information. *J. Am. Chem. Soc.* **2003**, *125*, 1731-1737.

- (24) Vazquez, E.; Roldan, M.; ez-Gil, C.; Unzueta, U.; Domingo-Espin, J.; Cedano, J.; Conchillo, O.; Ratera, I.; Veciana, J.; Daura, X.; Ferrer-Miralles, N.; Villaverde, A. Protein Nanodisk Assembling and Intracellular Trafficking Powered by an Arginine-Rich (R9) Peptide. *Nanomedicine. (Lond)* **2010**, *5*, 259-268.
- (25) Guerois, R.; Nielsen, J. E.; Serrano, L. Predicting Changes in the Stability of Proteins and Protein Complexes: a Study of More Than 1000 Mutations. *J. Mol. Biol.* **2002**, *320*, 369-387.

Annex 2

Manuscript 2:

Sheltering DNA in Self-organizing, protein-only nano-shells as artificial viruses for gene delivery.

Ugutx Unzueta, Paolo Saccardo, Joan Domingo-Espín, Juan Cedano, Oscar Conchillo, Elena García-Fruitós, Maria Virtudes Céspedes, José Luis Corchero, Xavier Daura, Ramón Mangués, Neus Ferrer-Miralles, Antonio Villaverde, Esther Vazquez.

Submitted to Nanomedicine: Nanotechnology, Biology and Medicine.

Original article

Nanomedicine: Nanotechnology, Biology and Medicine

Sheltering DNA in self-organizing, protein-only nano-shells as artificial viruses for gene delivery.

Ugutx Unzueta ^{1, 2, 3 §}, Paolo Saccardo ^{1, 2, 3 §}, Joan Domingo-Espín ^{1, 2, 3}, Juan Cedano ⁴, Oscar Conchillo ¹, Elena García-Fruitós ^{3, 1, 2}, María Virtudes Céspedes ^{3, 5}, José Luis Corchero ^{3, 1, 2}, Xavier Daura ^{1, 6}, Ramón Mangues ^{5, 3}, Neus Ferrer-Miralles ^{1, 2, 3}, Antonio Villaverde ^{1, 2, 3*}, and Esther Vázquez ^{1, 2, 3*}

¹ Institut de Biotecnologia i de Biomedicina, Universitat Autònoma de Barcelona, Bellaterra, 08193 Barcelona, Spain

² Departament de Genètica i de Microbiologia, Universitat Autònoma de Barcelona, Bellaterra, 08193 Barcelona, Spain

³ CIBER de Bioingeniería, Biomateriales y Nanomedicina (CIBER-BBN), Bellaterra, 08193 Barcelona, Spain

⁴ Laboratory of Immunology, Regional Norte, Universidad de la República, Gral. Rivera 1350; Salto, 50.000, Uruguay

⁵ Grup d'Oncogènesi i Antitumorals, Institut de Recerca, Hospital de la Santa Creu i Sant Pau, Barcelona, Spain

⁶ Institució Catalana de Recerca i Estudis Avançats (ICREA), Barcelona, Spain

§ Equally contributed

* Corresponding authors: A. Villaverde; antoni.villaverde@uab.cat

E. Vazquez; esther.vazquez@uab.cat

Keywords: Nanoparticles; protein building blocks; self-assembling; artificial viruses; gene therapy

Abstract

By recruiting functional domains supporting DNA condensation, cell binding, internalization, endosomal escape and nuclear transport, modular single-chain polypeptides can be tailored to associate with cargo DNA for cell-targeted gene therapy. Recently, an emerging architectonic principle at the nanoscale has permitted tagging protein monomers for self-organization as protein-only nanoparticles. We have studied here the accommodation of plasmid DNA into protein nanoparticles assembled with the synergistic assistance of end terminal poly-arginines (R9) and poly-histidines (H6). Data indicate a virus-like organization of the complexes, in which a DNA core is surrounded by a solvent-exposed protein layer. This finding validates end-terminal cationic peptides as pleiotropic tags for the mimicry of viral architecture in artificial viruses, representing a promising alternative to the conventional use of viruses and virus-like particles.

Background

Non-viral gene therapy and in general emerging nanomedicines aim to the mimicry of viral activities in tuneable nanoparticles, for the cell-targeted delivery of cargo nucleic acids (and other drugs)^{276, 277}. Among a diversity of tested materials (including lipids, natural polymers, quantum dots, carbon nanotubes and dendrimers), proteins offer full biocompatibility, biodegradability, and a wide spectrum of functionalities that can be further adjusted by genetic engineering. Such a functional versatility is in contrast with the null control so far exercised over the supramolecular organization of de novo designed building blocks for protein-based complexes²⁷⁸. While protein nanoparticles based on natural cages, mainly infectious viruses²⁷⁹, virus-like particles (VLPs)²⁸⁰, eukaryotic vaults²⁸¹ and bacterial microcompartments (BMCs)²⁸² take advantage of the evolutionarily optimized self-assembling activities of their building blocks, fully the novo multifunctional protein monomers fail to reach predefined nanoscale organization. Only a very limited number of approaches, based on the engineering of oligomerization domains present in nature have resulted in the successful construction of efficient building blocks for protein shell generation²⁸³. Complexes of DNA and cationic proteins often result in polydisperse soluble aggregates probably derived from intrinsically disordered protein-protein interactions^{284, 285}, or in which the DNA itself plays a leading architectonic role, stabilizing aggregation-prone protein monomers in form of monodisperse nanoparticles²⁸⁶. Self-assembling peptides, that organize as different types of nanostructured materials²⁸⁷, promote unspecific aggregation when fused to larger proteins^{288, 289}, making them useless as fine architectonic tags. In summary, the rational de novo design of protein monomers with self-assembling activities has remained so far unreachable. Very recently²⁹⁰, we have described that pairs of 'architectonic' peptides consisting of an N-terminal cationic stretch plus a C-terminal polyhistidine, when combined in structurally diverse scaffold proteins (GFP, p53 and others), generate strongly dipolar charged monomers that spontaneously self-assemble. The resulting constructs, ranging from 10 to 50 nm, show fast nuclear penetrability²⁹¹, high stability and proper biodistribution upon systemic administration²⁹². Yet these particles efficiently bind plasmid DNA for transgene expression and are very promising tools in nanomedicine²⁹³, their supramolecular organization remains so far unexplored.

Methods

Protein production and DNA binding

The modular organization of R9-GFP-H6²⁹³, T22-GFP-H6²⁹² and HNRK²⁸⁶ has been described elsewhere. GFP-H6 is a parental version of R9-GFP-H6 and T22-GFP-H6 that does not self-assemble under physiological conditions^{290, 293}. All these proteins were produced in bacteria following conventional procedures and purified in a single step by His-based affinity chromatography²⁹⁰, through activities assisted by the Protein Production Platform (CIBER-BBN) (<http://www.bbn.ciber-bbn.es/programas/plataformas/equipamiento>). Protein-DNA complexes were generated by incubation at appropriate ratios in HBS buffer (pH 5.8) for 60 min at room temperature. Volume size distributions of self-assembled protein nanoparticles and protein-DNA complexes were determined using a dynamic light scattering (DLS) analyzer at the wavelength of 633 nm, combined with non-invasive backscatter technology (NIBS) (Zetasizer Nano ZS, Malvern Instruments Limited, Malvern, U.K.).

Cell culture and confocal microscopy

HeLa (ATCC-CCL-2) cell line was cultured as previously described²⁹¹ and always monitored in absence of fixation to prevent internalization artefacts. Nuclei were labelled with 200 ng/ml Hoechst 33342 (Molecular Probes, Eugene, Oregon, USA) and plasma membranes with 2.5 µg/ml CellMask™ Deep Red (Molecular Probes, Invitrogen, Carlsbad, CA, USA) for 5 min. Cells exposed to nanoparticles were recorded with a TCS-SP5 confocal laser scanning microscope (Leica Microsystems, Heidelberg, Germany) with a Plan Apo 63x / 1.4 (oil HC x PL APO lambda blue) objective. Three-dimensional cell models were generated with the Imaris v. 6.1.0 software (Bitplane; Zürich, Switzerland).

DNA protection assay

In the buffers optimal for their respective stability^{286, 290}, R9-GFP-H6 and GFP-H6 (HBS pH 5.8), T22-GFP-H6 (carbonate buffer, pH 5.8) and HNRK (HBS + dextrosa pH 5.8) were mixed with 1 µg of plasmid DNA (pTurboFP635,²⁹³) at 1 and 2 retardation units. Mixtures were incubated at room temperature for 1 h and then treated with 0.5 µg/ml DNase I (Roche) at 37° C, in presence of 2.5 mM MgCl₂ and 0.5 mM CaCl₂. Samples were collected just before DNase I addition and at 5, 20 and 60 min of the digestion reaction. DNase I was inactivated by adding EDTA 2.3 µM final concentration and by heating the samples for 20 min at 70° C. The remaining DNA was released from protein complexes by adding 10 U of Heparin followed by 2 hours incubation at 25° C. Subsequently, samples were analyzed in 1% agarose gels. DNA

signals in agarose gel were interpreted and analyzed with Quatity One software (Bio-Rad).

Determination of Z potential

Z Potencial of protein nanoparticles or artificial viruses was determined in a dynamic light scattering (DLS) device (Malvern Nanosizer Z), in HBS buffer (pH 5.8, 10 µg/mL final protein concentration). Measurements were carried out at 25 °C using a disposable plastic cuvette. Each sample was analysed by triplicate.

Molecular modelling

To build R9-GFP-H6-based particles, a model of the monomer was first generated using Modeller 9v2²⁹⁴ and the pdb structure "1qyo" as described²⁹³. The structural models of the assembled monomers at pH 7 and pH 5.8 were then created using HADDOCK 2.0²⁹⁵, with the protonation states chosen according to pH and residue pKas. Defining R9 at the N-terminus as active and H6 at the C-terminus as passive and enforcing C5 symmetry led to star-shaped conformations. Alternative conformations were obtained when using the R9 tail as active residues and no passive ones. All these models were analysed with FoldX using the function "AnalyseComplex"²⁹⁶. The structural comparison of disks made of TMV coat protein and R9-GFP-H6 was generated using SwissPdbViewer*²⁹⁷ to superimpose the 2om3 PDB structure and the modelled building block²⁹⁸. To facilitate the visualization of the resulting models, images were generated using Chimera²⁹⁹ as rendering tool.

Results

Hexahistidine tails, when combined in single chain polypeptides with N-terminal cationic peptides, such as R9 or T22, promote assembling of these building blocks as regular particles at neutral or slightly acidic pH values²⁹⁰, at which the imidazol group gets protonated and the tag moderately cationic³⁰⁰. When nanoparticles formed by R9-GFP-H6 at pH 7 and 8 were incubated with DNA, particle size remained close to 20 nm (Figure 1 a), the size previously observed in absence of DNA²⁹⁰. At pH 4 and 10, protein-DNA complexes peaked at 0.8 and 2 μm respectively (Figure 1 a), which is in agreement with the tendency of the protein alone to form amorphous aggregates under denaturing conditions²⁹⁰. Interestingly, at slightly acidic pH (5.8), where the transfection mediated by R9-GFP-H6 had resulted more efficient^{290, 293}, the population of polyplexes split in two fractions, peaking at 38 and 700-800 nm respectively, with no symptoms of protein instability or aggregation (protein-only nanoparticles peaked between 20 and 30 nm). These polyplexes were examined by confocal microscopy during exposure to cultured cells, taking advantage of the natural green fluorescence of the protein partner and upon staining the DNA with the blue fluorescent dye Hoechst 33342. Small spherical particles (Figure 1 b,c) and larger rood-shaped versions (Figure 1 d, e) were observed, whose size fitted respectively to the two main peaks determined by DLS (Figure 1 a). The blue DNA signal appeared coincident with the green label, but its slightly smaller size suggested that DNA occurred in inner cavities of protein entities. Qualitatively, rood-shaped nanoparticles seemed more efficient in embedding DNA than the regular versions, as an important fraction of spheres, but not roods, appeared to be empty (Figure 1 b,c).

The rood-shaped forms strongly evoked the morphologies of capsid proteins observed in plant viruses. In this regard, a superimposition of the RNA-containing, rood-shaped tobacco mosaic virus (TMV) disk (a structural intermediate in the construction of helical capsids) and an energetically stable, planar, star-shaped molecular model of the self-assembled R9-GFP-H6 at pH 5.8 are presented (Figure 1 f), showing coincidence in diameter and in monomer organization. Interestingly, a similar spatial distribution of arginines around the central cavities was found in both viral and non-viral complexes (Figure 1 f, inset). Fine confocal sections and 3D isosurface reconstructions permitted to unequivocally confirm that a core DNA was shielded by a solvent-exposed protein layer (Figure 1 g), in a virus-like architectonic scheme. In this regard, DNA embedded in R9-GFP-H6 shells resulted highly protected from DNase I attack (Figure 2 a). This effect was similar to that promoted by the closely related, self-assembling construct T22-GFP-H6. Contrarily, the short modular peptide HNRK³⁰¹, that although being

positively charged does not exhibit architectonic properties, failed in protecting DNA from digestion (Figure 2 a). In the HNRK-DNA polyplexes, from which DNA overhangs, the nucleic acid is the main architectonic regulator of the resulting particles (of around 80 nm), the protein fraction being clustered by DNA instead of entrapping it in shell-like structures²⁸⁶.

Why at slightly acidic pH and in presence of DNA, R9-GFP-H6 ~20 nm-nanoparticles rearrange as alternative spherical or cylindrical shells remains to be solved, but it might be speculated that the dipolar nature of the building blocks would permit a reorganization of protein building blocks, to orient the positive protein patches at the inner surface of the shell, in contact with DNA. For that, spheres and cylinders would permit appropriate protein-protein interactions. In agreement with this hypothesis, the superficial charge of protein-only particles was -16.2 ± 1.8 mV, while in presence of plasmid DNA (2 RU) it shifted to a more negative value (-24.5 ± 2.0 mV) (Figure 2 b). Interestingly, by applying the same amount of protein, the number of nanoparticles was reduced by more than 50 % in the presence of DNA, consistent with a higher protein demand to form nanoparticles up to 800 nm than to form protein-only nanoparticles of ~20 nm. On the other hand, the organization of protein shells as spheres or alternatively as rods would require a certain degree of flexibility in monomer-monomer contacts, allowing alternative arrangements of the oligomers. The in-equilibrium protonation and charge profile of the histidine tail population ($pK \sim 6$)³⁰⁰, would confer enough structural versatility of these interactions supportive of spherical and disk-based cylindrical organization. In agreement, alternative stable versions of R9-GFP-H6 oligomers (pentamers) resulted from the docking process, sustained by slightly divergent styles of inter-molecular interactions (Figure 3). Such pentamers, similarly distributed oligomers (eg hexamers) of their combination, could support both spherical and rod-shaped architectures as in the case of virus shells. After careful analysis of these models, we have identified, apart from electrostatic interactions (-7.33 Kcal/mol), van der Waals forces as the main components keeping the monomers together (-42.38 Kcal/mol), in some cases with hydrogen bonds (-29.13 Kcal/mol) contributing significantly to the stability of the oligomers (data taken from the model disk represented in Figure 1 f and in Figure 3, left).

Discussion

The severe biological risks and negative media perception associated to the administration of natural viruses³⁰² have dramatically compromised the development of viral gene therapy^{303, 304} and prompted researchers to explore manmade alternatives as vehicles for the delivery of therapeutic genes. The artificial virus concept²⁷⁷ claims the use of nanoparticles, that upon convenient design, fabrication and engineering can successfully mimic properties of the viral infectious cycle that are relevant to transgene delivery and expression³⁰⁵. Nanotechnologies and material sciences offer interesting approaches to generate functional nanostructured carriers, and a spectrum of materials are being explored in this regard³⁰⁶, even under suspicion of potential toxicity³⁰⁷. Among them, proteins are the most versatile regarding structure and function, being fully biocompatible, suitable of biological fabrication and not posing safety of toxicity concerns. In fact, vaults and BMCs, or the recombinant version of viruses, namely VLPs, can be conveniently adapted to embed cargo molecules for targeted delivery³⁰⁸. In a more versatile approach, modular proteins containing cationic stretches for nucleic acid binding and condensation, as well as other functional segments such as cell penetrating peptides, ligands or nuclear localization signals, have been under continuous design to recruit virus-like functions in single chain molecules³⁰⁹⁻³¹¹. However, despite the functional versatility of these constructs they fail to reach ordered nanoscale structures, in most cases being the DNA the main driving force of the polyplex architecture²⁸⁶. In fact, the assembly of viral capsids results from a complex combination of intermolecular interactions including hydrophobic, electrostatic, van der Waals, and hydrogen bonds³¹² that are excluded from a rational design in the *novo* designed recombinant proteins. Recently, we have determined that a combination of a cationic peptide plus a hexahistidine, placed at the amino and carboxy termini respectively of modular proteins confer them the ability to self-organize as regular protein-only nanoparticles, able to penetrate target cells and to reach the nucleus in a very efficient way²⁹⁰⁻²⁹². We have here shown how at a slightly acidic pH and in presence of DNA, the contacts promoted by the hexahistidine tail are able to accommodate structural rearrangements, among others those promoting a re-orientation of cationic segments in the inner surface, that convert plain oligomers into more complex supramolecular structures, namely closed protein shells, in a virus-like fashion. Both conventional isometric and rod-shaped architectonic models occurring in natural viruses are spontaneously reached by the self-assembling of R9-GFP-GH6, efficiently embedding the foreign DNA in the inner cavity of a protein-only shell.

In summary, we have demonstrated for the first time how protein-based artificial viruses, namely functional nanoparticles formed by self-assembling protein shells shielding a core DNA, can be generated by the fully de novo design of building blocks. This fact not only validates R9 and H6 as pleiotropic peptides in vehicles for non-viral gene therapy, but it also reveals an unexpected architectonic potential of these tags in the generation of tuneable protein shells, whose properties can be further polished by conventional protein engineering. These versatile agents are promising alternatives to natural protein constructs, including viruses, VLPs, vaults and BMCs, which because of several limitations including rigid architecture but also biosafety concerns, are less suitable for engineering and adaptation to nanomedical purposes.

Acknowledgments

We appreciate the technical support of Fran Cortés from the Cell Culture Unit of Servei de Cultius Cel.lulars Producció d'Anticossos i Citometria (SCAC, UAB), and of Amable Bernabé from Soft Materials Service (ICMAB-CSIC/CIBER-BBN). The authors also acknowledge the financial support granted to E.V. from FIS (P112/00327) and to A.V. from Agència de Gestió d'Ajuts Universitaris i de Recerca (2009SGR-108), and from the Centro de Investigación Biomédica en Red (CIBER) de Bioingeniería, Biomateriales y Nanomedicina (NANOPROVIR project), financed by the Instituto de Salud Carlos III with assistance from the European Regional Development Fund. U.U. and P.S. received PhD fellowships from ISCIII and J.D.E. from MICINN. A.V. has been distinguished with an ICREA ACADEMIA Award.

Figure 1

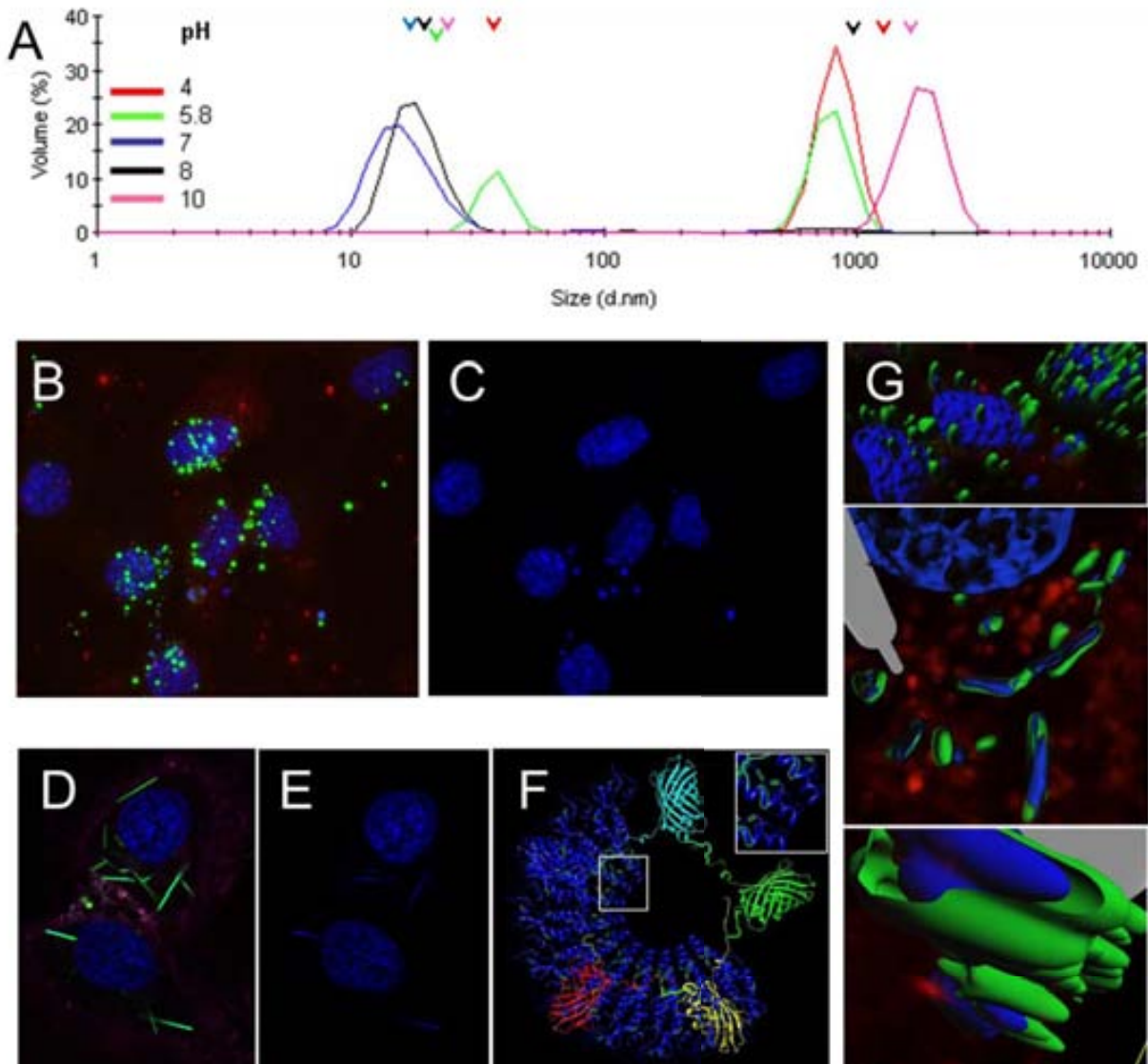


Figure 1. Molecular architecture of R9-GFP-H6-DNA polyplexes. A) Size distribution, measured of R9-GFP-H6-DNA polyplexes formed at different pH values. Main size peaks of protein-only nanoparticles previously determined in absence of DNA²⁹⁰, are shown by colored arrow heads as a reference. B) Spherical-shaped green fluorescent signal in HeLa cells exposed for 24 hours to R9-GFP-H6-DNA polyplexes. C) Spherical-shaped blue labels for the same field than in B, corresponding to the embedded DNA. D) Rod-shaped green fluorescent signal in HeLa cells exposed for 24 hours to R9-GFP-H6-DNA polyplexes. E) The same field than in D, showing blue fluorescence corresponding to the embedded DNA. F) Superimposition of TMV nanodisks and a R9-GFP-H6 molecular model of a stable, planar oligomer²⁹³. Arginines in the TMV coat protein are located in a radial distribution surrounding the

inner hole (shadowed in yellow, inset), in parallel to those of the R9 tail in R9-GFP-H6 monomers. G) Isosurface representation of polyplexes within a 3D volumetric x-y-z data field, showing the inner localization of the cargo DNA. Magnification progressively increases from top to bottom.

Figure 2

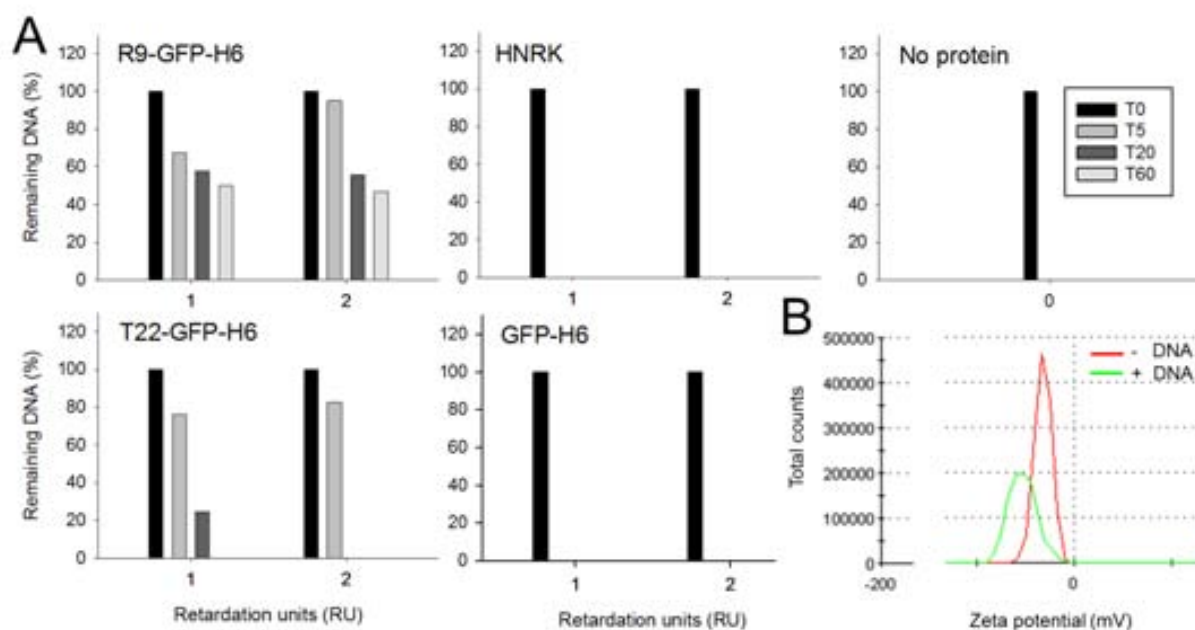


Figure 2. Functional and structural profiling of DNA-loaded nanoparticles. A) Remaining plasmid DNA after treatment with DNase I, resulting from protection mediated by protein shells at alternative retardation units. Different modular proteins were tested as indicated. At the right, the digestion of protein-free DNA is shown under the same conditions. T indicates time of digestion in min. B) Determination of the z-potential of R9-GFP-H6 nanoparticles, with and without DNA.

Figure 3

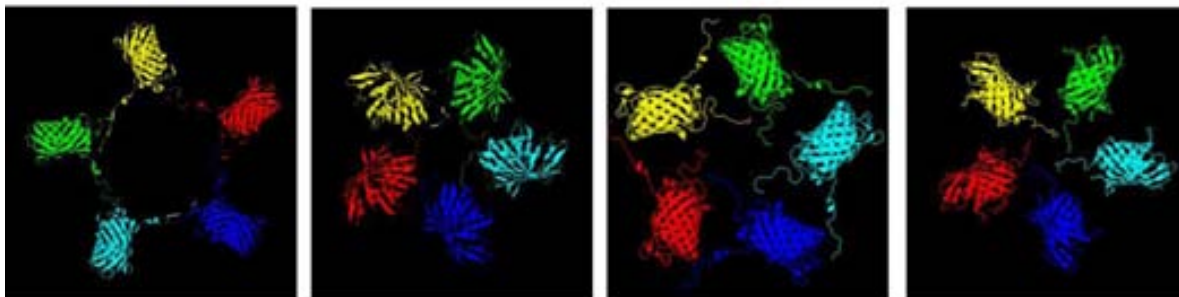
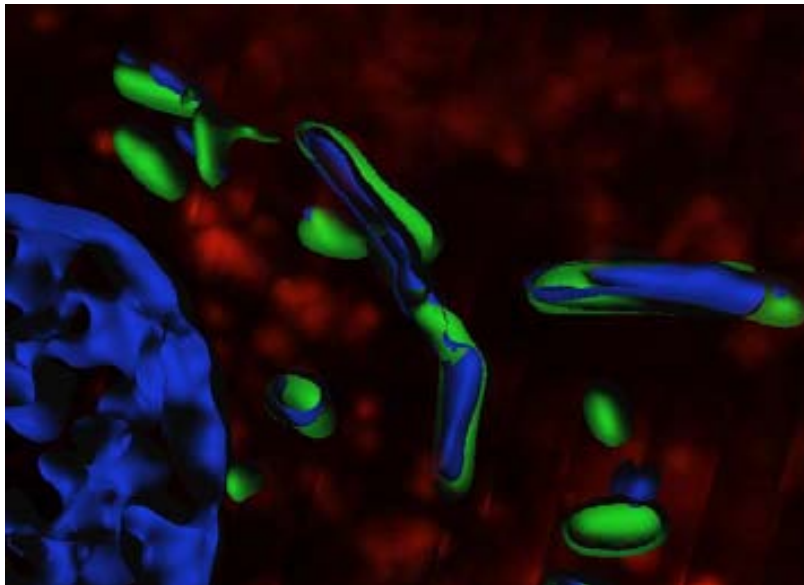


Figure 3. Potential monomer-monomer contacts in R9-GFP-H6 protein oligomers. Model configurations were obtained by docking simulations using HADDOCK at neutral pH, assuming a pentameric composition that is in agreement with experimental size of protein-only particles. The first model (left) was obtained using R9 residues as active and H6 residues as passive²⁹³ and it was used for the superimposition depicted in Figure 1 f. The remaining three models derived from using R9 residues as active and no passive ones. No significant differences in packing were obtained when performing the docking runs at pH 5.8, i.e. with doubly-protonated His (not shown).

GRAPHICAL ABSTRACT

3D Isosurface representation of internalized protein-DNA nanoparticles that are formed by green fluorescent building blocks and blue-labeled DNA. These artificial viruses, organized by means of synergistically acting end-terminal peptide tags, occur as rod-shaped entities in which the DNA core is shielded by a self-assembling, solvent-exposed protein shell. The red background corresponds to the cell membrane.



References

- 1 Wagner E: Strategies to improve DNA polyplexes for in vivo gene transfer: will "artificial viruses" be the answer? *Pharm Res* 2004;**21**:8-14.
- 2 Mastrobattista E, van der Aa MA, Hennink WE, Crommelin DJ: Artificial viruses: a nanotechnological approach to gene delivery. *Nat Rev Drug Discov* 2006;**5**:115-121.
- 3 Tu RS, Tirrell M: Bottom-up design of biomimetic assemblies. *Adv Drug Deliv Rev* 2004;**56**:1537-1563.
- 4 Giacca M, Zacchigna S: Virus-mediated gene delivery for human gene therapy. *J Control Release* 2012;**161**:377-388.
- 5 Ma Y, Nolte RJ, Cornelissen JJ: Virus-based nanocarriers for drug delivery. *Adv Drug Deliv Rev* 2012;**64**:811-825.
- 6 Han M, Kickhoefer VA, Nemerow GR, Rome LH: Targeted vault nanoparticles engineered with an endosomolytic peptide deliver biomolecules to the cytoplasm. *ACS Nano* 2011;**5**:6128-6137.
- 7 Corchero JL, Cedano J: Self-assembling, protein-based intracellular bacterial organelles: emerging vehicles for encapsulating, targeting and delivering therapeutical cargoes. *Microb Cell Fact* 2011;**10**:92.
- 8 Doll TA, Raman S, Dey R, Burkhard P: Nanoscale assemblies and their biomedical applications. *J R Soc Interface* 2013;**10**:20120740.
- 9 Aris A, Villaverde A: Engineering nuclear localization signals in modular protein vehicles for gene therapy. *Biochem Biophys Res Commun* 2003;**304**:625-631.
- 10 Aris A, Villaverde A: Molecular organization of protein-DNA complexes for cell-targeted DNA delivery. *Biochem Biophys Res Commun* 2000;**278**:455-461.
- 11 Domingo-Espin J, Vazquez E, Ganz J, Conchillo O, Garcia-Fruitos E, Cedano J, Unzueta U, Petegnief V, Gonzalez-Montalban N, Planas AM, Daura X, Peluffo H, Ferrer-Miralles N, Villaverde A: Nanoparticulate architecture of protein-based artificial viruses is supported by protein-DNA interactions. *Nanomedicine (Lond)* 2011;**6**:1047-1061.

- 12 Lakshmanan A, Zhang S, Hauser CA: Short self-assembling peptides as building blocks for modern nanodevices. *Trends Biotechnol* 2012;**30**:155-165.
- 13 Zhou B, Xing L, Wu W, Zhang XE, Lin Z: Small surfactant-like peptides can drive soluble proteins into active aggregates. *Microb Cell Fact* 2012;**11**:10.
- 14 Wu W, Xing L, Zhou B, Lin Z: Active protein aggregates induced by terminally attached self-assembling peptide ELK16 in *Escherichia coli*. *Microb Cell Fact* 2011;**10**:9.
- 15 Unzueta U, Ferrer-Miralles N, Cedano J, Zikung X, Pesarrodonna M, Saccardo P, Garcia-Fruitos E, Domingo-Espin J, Kumar P, Gupta KC, Manges R, Villaverde A, Vazquez E: Non-amyloidogenic peptide tags for the regulatable self-assembling of protein-only nanoparticles. *Biomaterials* 2012;**33**:8714-8722.
- 16 Vazquez E, Cubarsi R, Unzueta U, Roldan M, Domingo-Espin J, Ferrer-Miralles N, Villaverde A: Internalization and kinetics of nuclear migration of protein-only, arginine-rich nanoparticles. *Biomaterials* 2010;**31**:9333-9339.
- 17 Unzueta U, Cespedes MV, Ferrer-Miralles N, Casanova I, Cedano JA, Corchero JL, Domingo-Espin J, Villaverde A, Manges R, Vazquez E: Intracellular CXCR4⁺ cell targeting with T22-empowered protein-only nanoparticles. *Int J Nanomedicine* 2012;**7**:4533-4544.
- 18 Vazquez E, Roldan M, ez-Gil C, Unzueta U, Domingo-Espin J, Cedano J, Conchillo O, Ratera I, Veciana J, Daura X, Ferrer-Miralles N, Villaverde A: Protein nanodisk assembling and intracellular trafficking powered by an arginine-rich (R9) peptide. *Nanomedicine (Lond)* 2010;**5**:259-268.
- 19 N.Eswar, M.A.Marti-Renom, B.Webb, M.S.Madhusudhan, D.Eramian, M.Shen, U.Pieper, A.Sali: Comparative Protein Structure Modeling With MODELLER; 2009, pp 5.6.1-5.6.30, 200.
- 20 de Vries SJ, van Dijk AD, Krzeminski M, van DM, Thureau A, Hsu V, Wassenaar T, Bonvin AM: HADDOCK versus HADDOCK: new features and performance of HADDOCK2.0 on the CAPRI targets. *Proteins* 2007;**69**:726-733.
- 21 Guerois R, Nielsen JE, Serrano L: Predicting changes in the stability of proteins and protein complexes: a study of more than 1000 mutations. *J Mol Biol* 2002;**320**:369-387.

Annex

- 22 Guex N, Peitsch MC: SWISS-MODEL and the Swiss-PdbViewer: an environment for comparative protein modeling. *Electrophoresis* 1997;**18**:2714-2723.
- 23 Guex N, Diemand A, Peitsch MC: Protein modelling for all. *Trends Biochem Sci* 1999;**24**:364-367.
- 24 Pettersen EF, Goddard TD, Huang CC, Couch GS, Greenblatt DM, Meng EC, Ferrin TE: UCSF Chimera--a visualization system for exploratory research and analysis. *J Comput Chem* 2004;**25**:1605-1612.
- 25 Ferrer-Miralles N, Corchero JL, Kumar P, Cedano JA, Gupta KC, Villaverde A, Vazquez E: Biological activities of histidine-rich peptides; merging Biotechnology and Nanomedicine. *Microb Cell Fact* 2011;**10**:101.
- 26 Domingo-Espin J, Petegnief V, de VN, Conchillo-Sole O, Saccardo P, Unzueta U, Vazquez E, Cedano J, Negro L, Daura X, Peluffo H, Planas AM, Villaverde A, Ferrer-Miralles N: RGD-based cell ligands for cell-targeted drug delivery act as potent trophic factors. *Nanomedicine* 2012;**8**:1263-1266.
- 27 Edelstein ML, Abedi MR, Wixon J: Gene therapy clinical trials worldwide to 2007--an update. *J Gene Med* 2007;**9**:833-842.
- 28 Abbott A: Questions linger about unexplained gene-therapy trial death. *Nat Med* 2006;**12**:597.
- 29 Williams DA, Baum C: Medicine. Gene therapy--new challenges ahead. *Science* 2003;**302**:400-401.
- 30 Aris A, Villaverde A: Modular protein engineering for non-viral gene therapy. *Trends Biotechnol* 2004;**22**:371-377.
- 31 Villaverde A: Nanoparticles in translational science and medicine. London, Academic Press (Elsevier), 2011.
- 32 Sanvicens N, Marco MP: Multifunctional nanoparticles--properties and prospects for their use in human medicine. *Trends Biotechnol* 2008;**26**:425-433.
- 33 Rodriguez-Carmona E, Villaverde A: Nanostructured bacterial materials for innovative medicines. *Trends Microbiol* 2010;**18**:423-430.
- 34 Vazquez E, Ferrer-Miralles N, Mangues R, Corchero JL, Schwartz S Jr, Villaverde A: Modular protein engineering in emerging cancer therapies. *Curr Pharm Des* 2009;**15**:893-916.

- 35 Vazquez E, Ferrer-Miralles N, Villaverde A: Peptide-assisted traffic engineering for nonviral gene therapy. *Drug Discov Today* 2008;**13**:1067-1074.
- 36 Ferrer-Miralles N, Vazquez E, Villaverde A: Membrane-active peptides for non-viral gene therapy: making the safest easier. *Trends Biotechnol* 2008;**26**:267-275.
- 37 Zlotnick A: Are weak protein-protein interactions the general rule in capsid assembly? *Virology* 2003;**315**:269-274.

Annex 3

Manuscript 3:

Improved performance of protein-based recombinant gene therapy vehicles by adjusting downstream procedures.

Ugutzu Unzueta, Paolo Saccardo, Neus Ferrer-Miralles, Ramón Mangués,
Esther Vázquez, Antonio Villaverde.

Submitted to Biotechnology Progress

Improved performance of protein-based recombinant gene therapy vehicles by adjusting downstream procedures.

Ugutz Unzueta^{1,2,3}, Paolo Saccardo^{1,2,3}, Neus Ferrer-Miralles^{1, 2, 3,}, Ramón Mangués^{2,4}, Esther Vazquez^{1,2,3}, Antonio Villaverde^{1, 2, 3}

¹ Institut de Biotecnologia i de Biomedicina, Universitat Autònoma de Barcelona, Bellaterra, 08193 Barcelona, Spain

² CIBER de Bioingeniería, Biomateriales y Nanomedicina (CIBER-BBN), Bellaterra, 08193 Barcelona, Spain

³ Department de Genètica i de Microbiologia, Universitat Autònoma de Barcelona, Bellaterra, 08193 Barcelona, Spain

⁴ Oncogenesis and Antitumor Drug Group, Biomedical Research Institute Sant Pau (IIB-SantPau), Hospital de la Santa Creu i Sant Pau, C/ Sant Antoni Maria Claret, 167, 08025 Barcelona, Spain

* Corresponding author: A. Villaverde; antoni.villaverde@uab.cat

Keywords: Nanoparticles; Nucleic acids; Recombinant proteins; Cationic domains; Gene therapy; Downstream

Running head: Downstream of protein-based recombinant gene therapy vehicles

Abstract

Protein engineering offers a robust platform for the design and production in cell factories of a plethora of protein-based drugs, including non-viral gene therapy vehicles. We have determined here that a protein nanoparticle, formed by highly cationic protein monomers, fail to bind exogenous DNA and to promote detectable gene expression in target cells despite recruiting all the needed functions. Removal of DNA and RNA with nucleases previous to complexion with exogenous DNA dramatically enhances the ability of the protein to bind and transfer DNA to target cell nuclei. These data points out contaminant nucleic acids deriving from the cell factory as a major factor impairing the performance of protein-based artificial viruses and stress the need of a nuclease step in the downstream of proteins whose function is based on cationic domains.

Introduction

Non-viral gene therapy emerges as a safer alternative to virus-based nucleic acid delivery, which despite the recent approval of a few products by different medicament agencies (Oncorine, Gendicine and Glybera) still poses severe biosafety issues^{302, 313}. The main limitations for non-viral gene therapy are the low transfection efficacy when compared to viral delivery and the transient nature of gene expression. While treating specific conditions might require pulses of gene expression, compatible with the functional profile of non-viral approaches, a consensus exists in that gene transfer and expression levels offered by manmade constructs must be improved in order to raise non-viral gene therapy up to clinical standards³¹⁴⁻³¹⁶. Nanotechnologies and material sciences offer principles and tools for the fabrication of tailored vehicles addressed to increase efficacy and to confer specific functions. In this regard, a spectrum of materials is under exploration for the construction of nano-sized vehicles loadable with nucleic acids. Among them, those based on proteins as building blocks are specially promising, since polypeptides are fully biocompatible and highly versatile³¹⁷. In fact, protein functions can be adjusted by conventional genetic engineering, what offers the possibility to tailor specific activities such as cell-receptor binding and therefore, define biodistribution and establish cell-targeted delivery. Natural protein cages such as virus like particles (VLPs)^{318, 319}, bacterial microcompartments (BMCs)^{320, 321} and eukaryotic vaults^{281, 322} can be produced by recombinant DNA technologies and they have been explored as nanocages to deliver different kind of drugs, including nucleic acids. In addition, multifunctional proteins with modular architecture are especially appealing as diverse functions can be recruited in single polypeptide chains by means of gene fusion³⁰⁹⁻³¹¹, allowing the construct to mimic the set of biological activities displayed by natural viruses and relevant to gene transfer³⁰⁵. Different versions of modular proteins have been proved to be highly promising in the *in vitro* and *in vivo* delivery of therapeutic DNA³²³⁻³²⁵. Also, the fusion of oligomerization domains or shorter architectonic tags permits the self-organization of these hybrid building blocks as nanoparticles of sizes within the viral range^{290, 326}, altogether permitting the generation of 'artificial viruses' that reproduce the organization and function of these infectious agents²⁷⁷. On the other hand, the cost-effective production of recombinant proteins and the huge spectrum of cell factories available for this purpose offer, in addition, a high versatility regarding biofabrication and downstream^{327, 328}.

Most of the protein constructs intended as components of artificial viruses incorporate cationic stretches as DNA/RNA binding agents³²⁹. In this study, and by using a family of *de novo* designed, closely related modular building blocks produced in bacteria that self-assemble as nanosized cages, we have determined an unsuspected presence of bacterial nucleic acids as undesired contaminants that impair the gene delivery activities of the resulting artificial viruses. By removing these materials through appropriate nuclease treatments we show dramatic increases in the exogenous DNA binding capacity and in the gene expression levels achieved by the nanoparticles upon transfection. Nuclease treatment in downstream appears then as a crucial step in the preparation of cationic protein nanoparticles for gene therapy.

Materials and methods

Protein design, production and purification

Five chimeric genes encoding for different T22-empowered multifunctional constructs were designed in-house and provided by genscript (Piscataway, USA) already subcloned in a pET22b plasmid (Novagen 6744-3) using NdeI/HindIII restriction sites. R9-GFP-H6 protein derivatives (encoded in a pET21b plasmid) containing decreasing number of arginine residues were also design and constructed in-house by site directed mutagenesis of parental clone by replacing arginine residues for glycines or alanines to keep the length of the construct constant. All the T22-empowered proteins were produced in Escherichia coli Origami B (BL21, OmpT-, Lon-, TrxB-, Gor- (Novagen)) overnight at 20°C upon addition of 1 mM IPTG. R9-GFP-H6, R7-GFP-H6, R6-GFP-H6 and R3-GFP-H6 protein constructs were produced in Escherichia coli Rosetta BL21 (DE3) overnight at 25°C upon addition of 1mM IPTG. All the proteins were purified by Histidine tag affinity chromatography using HiTrap Chelating HP 1ml columns (Ge Healthcare) in an ÄKTA purifier FPLC (GE Healthcare). Cell extracts were disrupted at 1100psi by a French press (Thermo FA-078A) and soluble and insoluble fractions separated by centrifugation at 20,000 g for 45 min at 4°C. Only in protein samples treated for nucleic acids removal, additional step of DNase I and RNase hydrolysis (0.01 µg/µl DNase I, 0.01 µg/µl RNase, 2.5 mM MgCl₂, 0.5 mM CaCl₂) of soluble extract at 37°C for 1h was performed. Filtered cell soluble extract were loaded onto the HiTrap column and then washed with 20 mM Tris, 500 mM NaCl, 10 mM Imidazole, pH=8 buffer. Proteins were eluted with a lineal gradient of a high Imidazole concentration elution buffer (20 mM Tris, 500 mM NaCl, 500mM Imidazole, pH=8) and selected fractions then dialyzed against the buffer at which the proteins are more stable for 2h at room temperature: “20 mM Tris + 5%Dextrose” for T22-KGFP-H6, T22-GFPK-H6, T22-KGFPN-H6, T22-KGFPCmyc-H6, R9-GFP-H6, R3-GFP-H6 and GFP-H6), “20 mM Tris + 500 mM NaCl” for T22-GFP-H6, R7-GFP-H6, R6-GFP-H6 and “166 mM NaCO₃H + 334 mM NaCl” for T22-GFPK-H6 (DNase/RNase), T22-NGFPK-H6 (DNase/RNase). Proteins were then immediately stored at -80°C after 0.22 µm pore membrane filtration. Proteins were characterized by N-terminal sequencing and mass spectrometry (MALDI-TOF) and the amount determined by Bradford assays.

Dynamic light scattering (DLS)

Volume size distribution of protein nanoparticles were determined by dynamic light scattering at 633nm (Zetasizer Nano ZS, Malvern Instruments Limited, Malvern, UK).

Cell culture

Sw1417 cells were cultured in DMEM medium (Gibco, Rockville, MD) and HeLa cells in MEM medium (Gibco, Rockville, MD), both supplemented with 10% fetal calf serum (Gibco) and incubated at 37°C in a 5% CO₂ humidified atmosphere. Protein nanoparticles were added to cultured cells in presence of Optipro medium (Gibco) 24 h before protein internalization analysis in Sw1417 cells and 48 h before gene expression analysis in HeLa cells. HeLa cell line was obtained from American Type Culture Collection (ATCC, reference CCL-2, Manassas, VA) and Sw1417 cells were a generous gift from Xavier Mayol (Institut Municipal D'Investigacio Médica, Barcelona, Spain).

Protein internalization analysis

Nanoparticles uptake was analyzed by confocal laser scanning microscopy and flow cytometry 24 hours after nanoparticles exposure to Sw1417 cells. For confocal analysis cells were grown in MatTek culture dishes (MatTek Corporation, Ashland, MA). The nuclei were labeled with 0.2 µg/ml Hoechst 33342 (Molecular Probes, Eugene, OR) and the plasma membrane with 2.5 µg/ml CellMask™ Deep Red (Molecular Probes) for 10 minutes at Room Temperature and then washed in PBS buffer (Sigma-Aldrich Chemie GmbH, Steinheim, Germany). Live cells were recorded by TCS-SP5 confocal laser microscopy (Leica Microsystems, Heidelberg, Germany) using a Plan Apo 63x/1.4 (oil HC x PL APO lambda blue) objective. Hoechst 33342 DNA labels was excited with a blue diode (405 nm) and detected in the 415-460 nm range. GFP-proteins were excited with a Ar laser (488 nm) and detected in the 525-545 nm range. CellMask was excited with a HeNe laser (633 nm) and detected in the 650-775 nm range. For flow cytometry analysis, cell samples were treated with 1mg/ml Trypsin (Gibco) for 15min and then analysed on a FACS- Canto system (Becton Dickinson, Franklin Lakes, NJ). Protein fluorescence was excited using a 15 mW air-cooled argon ion laser at 488nm and detected by a 530/30 nm band pass filter D detector.

Determination of nucleic acids content

Nucleic acid contents within protein samples were determined by Ethidium Bromide staining in agarose gels and by a 200-350nm absorbance scanning in a UV/visible light spectrophotometer (Genequant 1300, GE Healthcare).

DNA retardation assays

DNA-protein incubation and DNA retardation assays were performed according to previously reported protocols (29).

Cell transfection

For expression experiments, 20 µg of T22-NGFPK-H6 protein (1 retardation unit) and 1 µg of Td Tomato gene containing pCDNA 3.1 plasmid were mixed into a final volume of 60 µl of buffer, and complexes were formed after 1 hour at room temperature, after which Optipro was added. The complex was gently added to HeLa cells, followed by incubation for 48 h at 37°C in 5% CO₂ atmosphere. TdTomato expression was monitored by flow cytometry and by fluorescence microscopy. Cells without treatment, or just incubated with the expression vector or the protein alone, were used as controls. TdTomato and GFP protein fluorescence was detected in no stained cells by fluorescence microscopy (Nikon eclipse TE2000-E) using 465-495 nm laser and 515-555 nm detector for GFP and 528-553 nm laser and 590-650 nm detector for Tdtomato. Red fluorescence in cells was quantified by flow cytometry using a FACS-Canto system (Becton Dickinson, Franklin Lakes, NJ) after detachment with 1mg/ml Trypsin (Gibco) for 15min. Td tomato protein fluorescence was excited using a 15 mW air-cooled argon ion laser at 488nm and detected by a 585/42 nm band pass filter.

Data analysis

Mean data, standard deviations and errors were calculated using Microsoft Office Excel 2003 (Microsoft) and all the graphical representations were done using Sigmaplot 10.0.

Results and discussion

T22-GFP-H6 is a modular protein monomer that self-assembles spontaneously as nanoparticles of around 13 nm upon purification from producing bacteria²⁹⁰. This protein is stable *in vivo* and targets primary tumor and metastatic foci in colorectal cancer, as the tag T22 promotes internalization into CXCR4+ cells²⁹². To adapt this construct to the delivery of therapeutic DNA for cancer therapies we added two additional modules to the polypeptide chain, namely a DNA-binding domain (a decalysine tail, K10) and a nuclear localization signal (NLS, either from SV40 T antigen or from the human C-myc nuclear protein). Different versions of the monomer were constructed containing one or both additional modules, as summarized in Figure 1A, and produced and purified from *E. coli*. All the proteins remained fluorescent and self-assembled in nanoparticles of between 30 and 45 nm (not shown). Internalization analysis of these constructs revealed a generic slight reduction in the uptake abilities when comparing with the parental construct T22-GFP-H6, which at high doses were not relevant for T22-KGFP-H6, T22-KGFPN-H6 and T22-GFPC-H6 (Figure 1B). All nanoparticles were observed to internalize upon exposure to CXCR4+ cells, and those containing NLS tags, namely T22-KGFPN-H6, T22-KGFPCmyc-H6 and T22-NGFPC-H6, showed a marked nuclear localization (Figure 1C). When determining the ability of these proteins to bind DNA through gel mobility assays, we surprisingly observed a lack of binding at the tested amounts (Figure 2), which would be not expected for K10-containing polypeptides. However, the high 260/280 ratio and the staining of protein-only samples in agarose gels (Figure 2, Table 1) were indicative of contaminant nucleic acids, probably derived from bacteria, that might interfere in the binding between cationic segments and exogenous DNA. Indeed, treatment with DNase and RNase of a model protein indicated the presence of a mixed population of nucleic acids as contaminants of protein samples, among which DNA seemed to be the most prevalent (Figure 3 A). A simple combined treatment with both nucleases effectively removed nucleic acids (Table 1) and conferred proteins with the ability to retard exogenous DNA as expected (Figure 3 B).

How the nucleic acid removal could enhance the performance of the nanoparticle in transgene delivery was investigated by combining T22-NGFPC-H6 with expressible DNA. When nuclease-treated and non-treated protein versions were compared, no expression of the reporter gene was observed by microscopy neither by flow cytometry, in complexes formed with non-treated protein samples (Figure 4 A, B). However, the nuclease treated vehicle promoted transgene expression in a significant percentage of cells (Figure 4 A), and gene expression levels were clearly over the background provided by non-treated samples (Figure 4 B).

Biofabrication of proteins as convenient carrier materials for non-viral gene therapy benefits from the advances of recombinant DNA technologies accumulated in the last 30 years. Many protein products are then used as pharmaceuticals with great success³²⁷ and an important sector of Pharma industries orbits around recombinant protein design and production. Cationic peptides or protein domains are commonly used as functional components of artificial viruses³²⁹, and in protein only vehicles they are usually incorporated as part of multifunctional proteins³⁰⁹. DNA condensation by short multifunctional proteins might have a structural role in the formation of protein/DNA nanoparticles³²⁵, while the incorporation of cationic end terminal peptides to more

complex building blocks drives their self-assembling as stable nanoparticles²⁹⁰ into which exogenous DNA is smoothly accommodated³²⁴. We have here constructed a series of modular building blocks in which several cationic peptides are combined to offer both architectonic abilities at the nanoscale and DNA condensing properties (Figure 1). T22-NGFPK-H6, for instance, contains the highly cationic T22, K10 and the protonated form of H6 (at slightly acidic pH). We observed that such a high concentration of cationic elements in the building block eclipsed its expected ability to bind and transfer DNA (Figure 2 and 4), a fact that was unapparent (and possibly milder) in other K10 containing multifunctional proteins^{284-286, 330}, probably less cationic in global. In agreement, Rn-GFP-H6 protein versions in which the number of N-terminal cationic residues (arginines) was engineered showed correlative amounts of attached nucleic acids (Table 2). The expected functions of the nanoparticles were however restored by a simple nuclease digestion step previous to the purification from bacteria (Figure 3). These data strongly suggest the need of including such a downstream step in the bioproduction of proteins as building blocks of artificial viruses, when their function is at least partially based on cationic, DNA-binding domains. Although regarding biosafety, contamination with nucleic acids is a particular issue in protein drugs produced in mammalian cells³³¹, the particular use of cationic proteins as DNA condensing agents stresses the need of surveillance and efficient removal treatment, for functional reasons, in any type of cell factory.

Acknowledgments

We appreciate the technical support of Fran Cortés from the Cell Culture Unit of Servei de Cultius Cel·lulars Producció d'Anticossos i Citometria (SCAC, UAB). We are also indebted to Protein Production Platform (<http://www.bbn.ciber-bbn.es/programas/plataformas/equipamiento>). We are also grateful to Maria Carme Fàbrega from IRB for her helpful comments. The authors also acknowledge the financial support granted to E.V. from FIS (PI12/00327) and to A.V. from Agència de Gestió d'Ajuts Universitaris i de Recerca (2009SGR-108), and from the Centro de Investigación Biomédica en Red (CIBER) de Bioingeniería, Biomateriales y Nanomedicina (NANOPROVIR project), financed by the Instituto de Salud Carlos III with assistance from the European Regional Development Fund. U.U. and P.S. received a PhD fellowship from ISCIII. A.V. has been distinguished with an ICREA ACADEMIA Award.

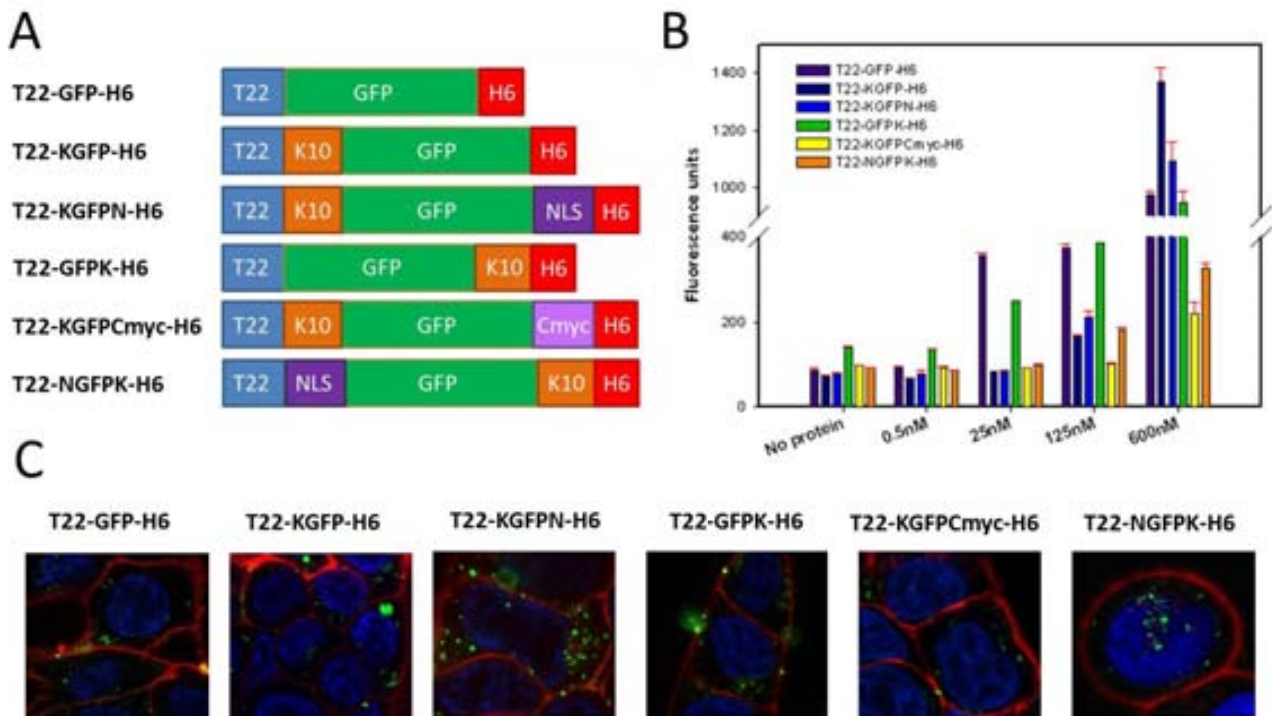


Figure 1: Description of T22-empowered multifunctional modular proteins and their internalization ability in CXCR4⁺ cells. **A)** Schematic representation of T22-empowered constructs. In blue, T22 peptide; in green, GFP; in orange: nucleic acid binding domain; in purple, nuclear localization signal; in red, poly-Histidine tag. NLS indicates the SV40 T antigen nuclear localization peptide. **B)** Dose-response curve of T22-empowered protein constructs internalization in Sw1417 cells. The parental T22-GFP-H6 construct is indicated as a reference. **C)** Confocal images of Sw1417 cells exposed to different T22-empowered multifunctional protein constructs for 24 hours. Cell membranes are labeled in red and cell nuclei in blue. Green spots correspond to the fluorescence of internalized nanoparticles.

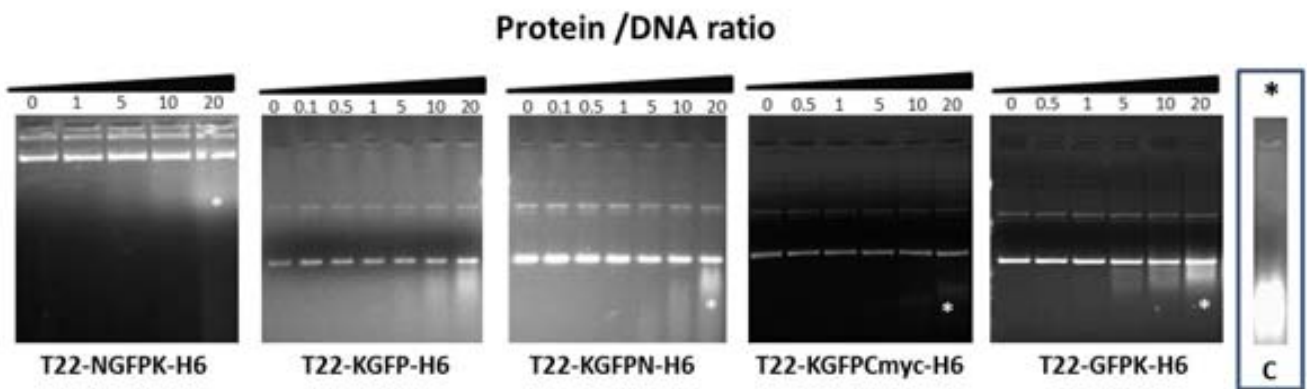


Figure 2: DNA-binding capacity of different protein constructs monitored by electrophoretic mobility shift of plasmid DNA (pTurbo FP365) in agarose gels. * nucleic acid signal detected in protein-only controls (C).

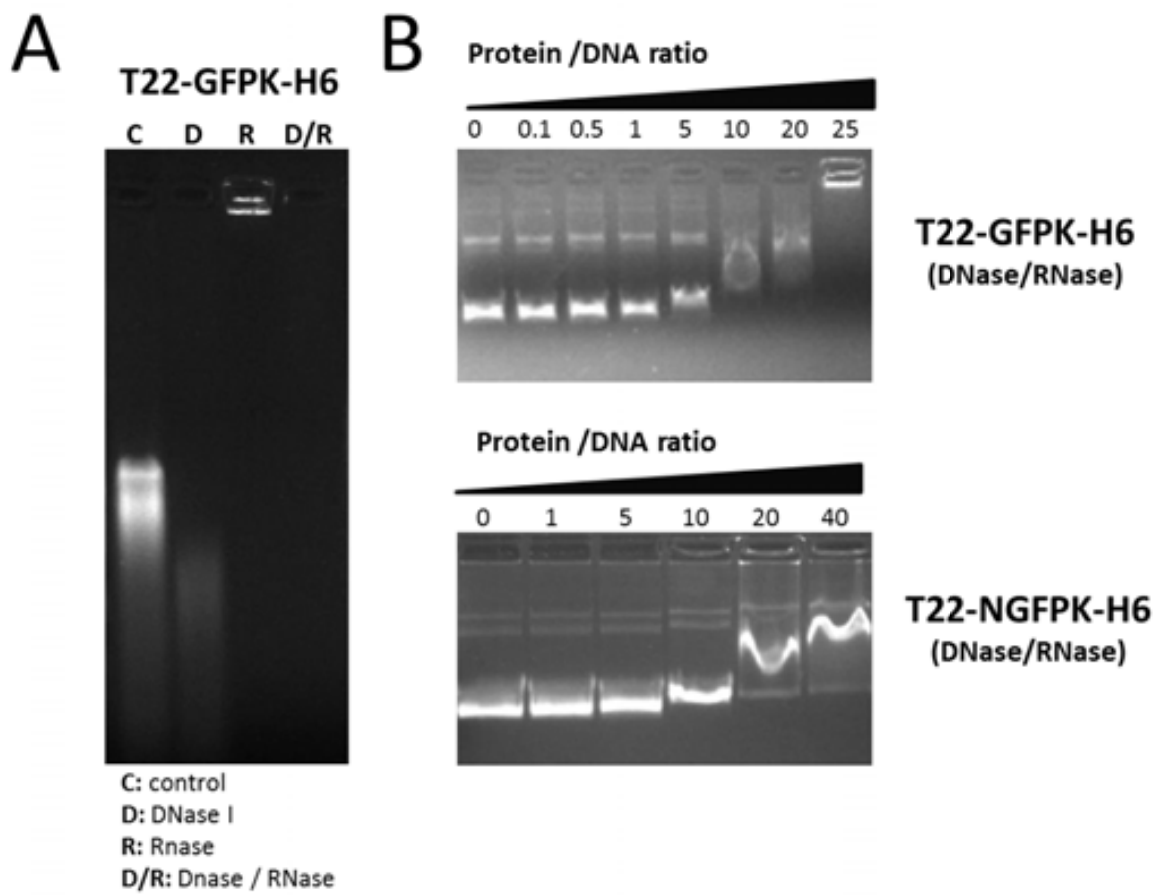


Figure 3: Nucleic acid removal from modular proteins. **A)** Nucleic acid removal in T22-GFPK-H6 after DNase and RNase digestion treatments. **B)** Evaluation of DNA-binding capacity of nucleic acid free T22-GFPK-H6 and T22-NGFPK-H6 protein constructs monitored by electrophoretic mobility shift assays.

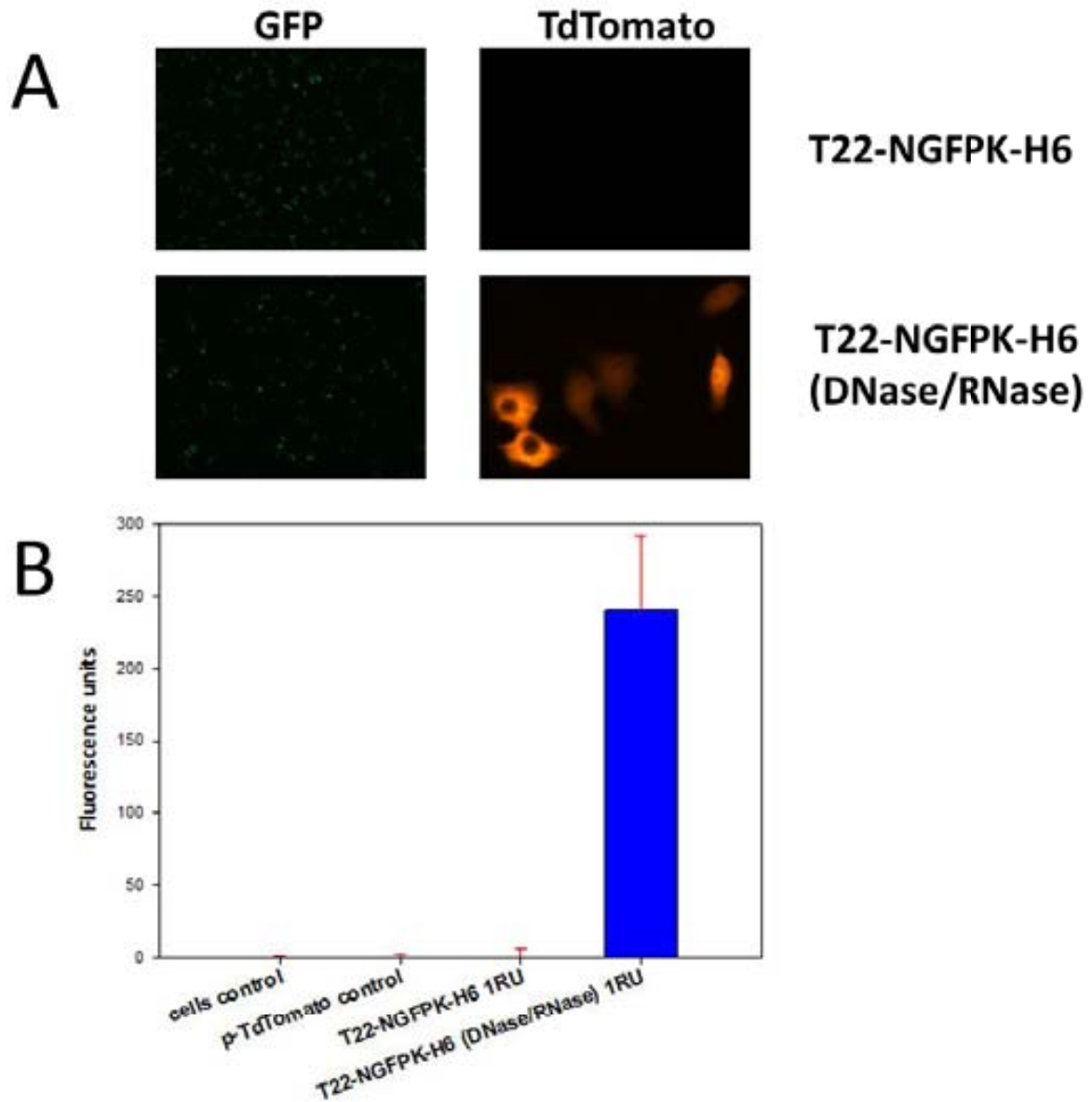


Figure 4: Evaluation of gene transfer properties of nucleic acid free T22-NGFPK-H6 in CXCR4⁺ cells compared with untreated protein constructs. **A)** Fluorescence microscopy images of HeLa cells exposed to T22-NGFPK-H6 / DNA polyplexes for 48 hours. Green fluorescence corresponds to GFP and orange fluorescence corresponds to TdTomato protein expressed from the transferred DNA. Fields were selected randomly but images are representative of the whole culture. **B)** TdTomato fluorescence of HeLa cells exposed to T22-NGFPK-H6 / DNA polyplexes for 48 hours.

Table 1. Ratio between absorbance at 260 and 280 nm in protein samples, untreated and treated with nucleases before purification.

Protein	T22-GFP-H6	T22-KGFP-H6	T22-KGFPN-H6	T22-KGFPCmyc-H6	T22-GFPK-H6	T22-GFPK-H6
260/280						
No nuclease treatment	0.89	1.54	2.04	1.51	1.38	2.05
Nuclease treatment	nd	nd	nd	nd	0.87	0.67

Nd: not determined

Table 2. Ratio between absorbance at 260 and 280 nm in samples of different versions of R9-GFP-H6, in which the number of N-terminal arginines varies.

Protein	R9-GFP-H6	R7-GFP-H6	R6-GFP-H6	R3-GFP-H6	GFP-H6
260/280	1.60	1.38	0.65	0.71	0.67

Reference List

- [1] J. Guo and H. Xin, Chinese gene therapy. Splicing out the West?, *Science*, 314 (2006) 1232-1235.
- [2] M. L. Edelstein, M. R. Abedi, and J. Wixon, Gene therapy clinical trials worldwide to 2007--an update, *J. Gene Med.*, 9 (2007) 833-842.
- [3] S. Li and L. Huang, Nonviral gene therapy: promises and challenges, *Gene Ther.*, 7 (2000) 31-34.
- [4] C. M. Wiethoff and C. R. Middaugh, Barriers to nonviral gene delivery, *J. Pharm. Sci.*, 92 (2003) 203-217.
- [5] M. Jafari, M. Soltani, S. Naahidi, D. N. Karunaratne, and P. Chen, Nonviral approach for targeted nucleic acid delivery, *Curr. Med. Chem.*, 19 (2012) 197-208.
- [6] E. Vazquez and A. Villaverde, Engineering building blocks for self-assembling protein nanoparticles, *Microb. Cell Fact.*, 9 (2010) 101.
- [7] H. Petry, C. Goldmann, O. Ast, and W. Luke, The use of virus-like particles for gene transfer, *Curr. Opin. Mol. Ther.*, 5 (2003) 524-528.
- [8] C. Georgens, J. Weyermann, and A. Zimmer, Recombinant virus like particles as drug delivery system, *Curr. Pharm. Biotechnol.*, 6 (2005) 49-55.
- [9] S. Cheng, Y. Liu, C. S. Crowley, T. O. Yeates, and T. A. Bobik, Bacterial microcompartments: their properties and paradoxes, *Bioessays*, 30 (2008) 1084-1095.
- [10] C. Fan, S. Cheng, Y. Liu, C. M. Escobar, C. S. Crowley, R. E. Jefferson, T. O. Yeates, and T. A. Bobik, Short N-terminal sequences package proteins into bacterial microcompartments¹, *Proc. Natl. Acad. Sci. U. S. A*, 107 (2010) 7509-7514.
- [11] M. Han, V. A. Kickhoefer, G. R. Nemerow, and L. H. Rome, Targeted vault nanoparticles engineered with an endosomolytic peptide deliver biomolecules to the cytoplasm, *ACS Nano.*, 5 (2011) 6128-6137.
- [12] L. H. Rome and V. A. Kickhoefer, Development of the Vault Particle as a Platform Technology, *ACS Nano.*, (2012).

- [13] E. Vazquez, N. Ferrer-Miralles, and A. Villaverde, Peptide-assisted traffic engineering for nonviral gene therapy, *Drug Discov. Today*, 13 (2008) 1067-1074.
- [14] N. Ferrer-Miralles, E. Vazquez, and A. Villaverde, Membrane-active peptides for non-viral gene therapy: making the safest easier, *Trends Biotechnol.*, 26 (2008) 267-275.
- [15] E. Vazquez, N. Ferrer-Miralles, R. Mangués, J. L. Corchero, Schwartz S Jr, and A. Villaverde, Modular protein engineering in emerging cancer therapies, *Curr. Pharm. Des.*, 15 (2009) 893-916.
- [16] A. Aris and A. Villaverde, Modular protein engineering for non-viral gene therapy, *Trends Biotechnol.*, 22 (2004) 371-377.
- [17] H. Peluffo, L. Acarin, A. Aris, P. Gonzalez, A. Villaverde, B. Castellano, and B. Gonzalez, Neuroprotection from NMDA excitotoxic lesion by Cu/Zn superoxide dismutase gene delivery to the postnatal rat brain by a modular protein vector, *BMC. Neurosci.*, 7 (2006) 35.
- [18] E. Vazquez, M. Roldan, C. ez-Gil, U. Unzueta, J. Domingo-Espin, J. Cedano, O. Conchillo, I. Ratera, J. Veciana, X. Daura, N. Ferrer-Miralles, and A. Villaverde, Protein nanodisk assembling and intracellular trafficking powered by an arginine-rich (R9) peptide, *Nanomedicine. (Lond)*, 5 (2010) 259-268.
- [19] J. Domingo-Espin, E. Vazquez, J. Ganz, O. Conchillo, E. Garcia-Fruitos, J. Cedano, U. Unzueta, V. Petegnief, N. Gonzalez-Montalban, A. M. Planas, X. Daura, H. Peluffo, N. Ferrer-Miralles, and A. Villaverde, Nanoparticulate architecture of protein-based artificial viruses is supported by protein-DNA interactions, *Nanomedicine (Lond)*, 6 (2011) 1047-1061.
- [20] U. Unzueta, N. Ferrer-Miralles, J. Cedano, X. Zikung, M. Pesarrodona, P. Saccardo, E. Garcia-Fruitos, J. Domingo-Espin, P. Kumar, K. C. Gupta, R. Mangués, A. Villaverde, and E. Vazquez, Non-amyloidogenic peptide tags for the regulatable self-assembling of protein-only nanoparticles, *Biomaterials*, 33 (2012) 8714-8722.
- [21] Y. Yang and P. Burkhard, Encapsulation of gold nanoparticles into self-assembling protein nanoparticles, *J. Nanobiotechnology.*, 10 (2012) 42.
- [22] E. Mastrobattista, M. A. van der Aa, W. E. Hennink, and D. J. Crommelin, Artificial viruses: a nanotechnological approach to gene delivery, *Nat. Rev. Drug Discov.*, 5 (2006) 115-121.

- [23] N. Ferrer-Miralles, J. Domingo-Espin, J. L. Corchero, E. Vazquez, and A. Villaverde, Microbial factories for recombinant pharmaceuticals, *Microb. Cell Fact.*, 8 (2009) 17.
- [24] J. L. Corchero, B. Gasser, D. Resina, W. Smith, E. Parrilli, F. Vazquez, I. Abasolo, M. Giuliani, J. Jantti, P. Ferrer, M. Saloheimo, D. Mattanovich, Schwartz S Jr, L. Tutino, and A. Villaverde, Unconventional microbial systems for the cost-efficient production of high-quality protein therapeutics, *Biotechnol. Adv.*, (2012).
- [25] P. Saccardo, A. Villaverde, and N. Gonzalez-Montalban, Peptide-mediated DNA condensation for non-viral gene therapy, *Biotechnol. Adv.*, 27 (2009) 432-438.
- [26] U. Unzueta, M. V. Cespedes, N. Ferrer-Miralles, I. Casanova, Cedano JA, Corchero JL, J. Domingo-Espin, Villaverde A, R. Mangues, and Vazquez E, Intracellular CXCR4⁺ cell targeting with T22-empowered protein-only nanoparticles, *Int. J. Nanomedicine*, 7 (2012) 4533-4544.
- [27] A. Aris, J. X. Feliu, A. Knight, C. Coutelle, and A. Villaverde, Exploiting viral cell-targeting abilities in a single polypeptide, non-infectious, recombinant vehicle for integrin-mediated DNA delivery and gene expression, *Biotechnol Bioeng*, 68 (2000) 689-696.
- [28] J. Domingo-Espin, E. Vazquez, J. Ganz, O. Conchillo, E. Garcia-Fruitos, J. Cedano, U. Unzueta, V. Petegnief, N. Gonzalez-Montalban, A. M. Planas, X. Daura, H. Peluffo, N. Ferrer-Miralles, and A. Villaverde, Nanoparticulate architecture of protein-based artificial viruses is supported by protein-DNA interactions, *Nanomedicine (Lond)*, 6 (2011) 1047-1061.
- [29] A. Aris and A. Villaverde, Molecular organization of protein-DNA complexes for cell-targeted DNA delivery, *Biochem. Biophys. Res. Commun.*, 278 (2000) 455-461.
- [30] A. Aris and A. Villaverde, Engineering nuclear localization signals in modular protein vehicles for gene therapy, *Biochem. Biophys. Res. Commun.*, 304 (2003) 625-631.
- [31] A. L. Demain and P. Vaishnav, Production of recombinant proteins by microbes and higher organisms, *Biotechnol. Adv.*, 27 (2009) 297-306.

Annex 4

Protein nanodisk assembling and intracellular trafficking powered by an arginine-rich (R9) peptide.

Esther Vázquez, Mónica Roldán, César Diez-Gil, Ugutz Unzueta, Joan Domingo-Espín, Juan Cedano, Oscar Conchillo, Imma Ratera, Jaume Veciana, Xavier Daura, Neus Ferrer-Miralles, Antonio Villaverde.

Nanomedicine (London), 5 (2), 259-268, 2010.



For reprint orders, please contact: reprints@futuremedicine.com

Protein nanodisk assembling and intracellular trafficking powered by an arginine-rich (R9) peptide

Aims: Arginine(R)-rich cationic peptides are powerful tools in drug delivery since, alone or when associated with polyplexes, proteins or chemicals, they confer DNA condensation, membrane translocation and blood–brain barrier crossing abilities. The unusual stability and high *in vivo* performance of their associated drugs suggest a particulate organization or R(n) complexes, which this study aimed to explore. **Materials & methods:** We have analyzed the particulate organization and biological performance in DNA delivery of a model, R9-containing green fluorescent protein by dynamic light scattering, transmission electron microscopy, atomic force microscopy, single cell confocal microscopy and flow cytometry. **Results:** A deep nanoscale examination of R9-powered constructs reveals a novel and promising feature of R9, that when fused to a scaffold green fluorescent protein, promote its efficient self-assembling as highly stable, regular disk-shaped nanoparticles of 20 × 3 nm. These constructs are efficiently internalized in mammalian cells and rapidly migrate through the cytoplasm towards the nucleus in a fully bioactive form. Besides, such particulate platforms accommodate, condense and deliver plasmid DNA to the nucleus and promote plasmid-driven transgene expression. **Conclusion:** The architectonic properties of arginine-rich peptides at the nanoscale reveal a new category of protein nanoparticles, namely nanodisks, and provide novel strategic concepts and architectonic tools for the tailored construction of new-generation artificial viruses for gene therapy and drug delivery.

KEYWORDS: artificial viruses · cationic peptides · gene therapy · nanoparticles · self-assembling · trafficking

Esther Vazquez, Mónica Roldán, César Díez-Gil, Ugutz Unzueta, Joan Domingo-Espín, Juan Cedano, Oscar Conchillo, Imma Ratera, Jaume Veciana, Xavier Daura, Neus Ferrer-Miralles & Antonio Villaverde*

Author for correspondence:
Institute for Biotechnology and Biomedicine, Universitat Autònoma de Barcelona, Bellaterra, 08193 Barcelona, Spain

avillaverde@servet.uab.es

*For a full list of affiliations please see back page

In drug-based therapies, most bioactive molecules need to overcome physical and biological barriers (generally cellular and nuclear membranes) to reach their molecular targets. Viruses have naturally evolved to acquire membrane-crossing activities that have been largely exploited as DNA (or RNA) nanocarriers for gene therapy (or gene silencing). However, the spectrum of undesired side effects observed during the controlled administration of such pathogenic agents [1], even upon genetic attenuation, prevents them from being considered as generic therapeutic agents and has severely compromised the further development of viral gene therapy [2,3]. Alternatively, 'artificial viruses' [4,5] are bio-safer nanosized constructs with orderly assembled components that mimic viral properties of relevance in drug delivery [6]. These molecular containers are formed by either synthetic (lipids or polysaccharides) or biologically produced (proteins) building blocks, or by a combination of both. Among them, protein-only nanoparticles are fully biocompatible and suitable for rational protein design through the fine tuning of their biophysical and biological properties, including those regulating the architectural features

(e.g., self-assembly and drug permeability) [7] or their biological interaction with the environment, namely receptor recognition, membrane crossing and nuclear targeting, among others [6].

For artificial viruses to achieve their targets they are usually functionalized with peptides or protein domains showing different biological activities, including, receptor binding, cell internalization, DNA condensation, endosomal escape, intracellular trafficking and nuclear transport [6]. Extended catalogues of peptides and small protein domains have so far been explored as functionalizing agents to fully cover the requirements of nanoparticle-driven delivery of nucleic acids, or eventually other drugs [8–14]. Among them, highly cationic proteins such as the HIV Tat, its 48–60 amino acid segment or other arginine-rich peptides have been shown to be highly bioactive and extremely promising as DNA and protein deliverers [14]. Polyarginine peptides of between 4 and 16 amino acids efficiently translocate the cell membrane, promoting the cellular uptake of associated molecules [15]. Irrespective of the membrane-crossing mechanisms that seem to be diverse under different experimental

future
medicine part of fsg

settings (endocytic versus nonendocytic translocation pathways) [13,16–18], DNA associated with synthetic R(n) peptides enters the nuclear compartment and promotes detectable levels of transgene expression [19,20]. Since the optimal length for cell internalization seems to be approximately eight residues [15,20], related species of the polyarginine peptide family (mainly R9, and to a lesser extent R6, R7 and R10) have been explored for the *in vitro* and *in vivo* delivery of p53 [21], p53-derived retro-inverso peptides [22], cyclosporine A [23] and peptidic nucleic acids [24]. Interestingly, R9-activated proteins cross the blood–brain barrier (BBB) [25], a highly promising ability for biomedical applications. Furthermore, in natural viruses, arginine-rich motifs also play essential roles in the encapsidation of viral genomes into protein shells [26].

Materials & methods

■ Protein production & purification

Green fluorescent protein (GFP) fusion proteins were produced in Rosetta BL21 (DE3) *Escherichia coli* as driven by an isopropyl β -D-1-thiogalactopyranoside (IPTG) inducible-T7 promoter in an pET21B⁺-derived plasmid. Bacteria were grown in luria bertani medium (750 ml) at 37 °C in shaker flasks until an optical density of 0.5, and gene expression was induced by 1 mM IPTG. After 3 h, cells were harvested by centrifugation (7650 g for 10 min at 4°C), washed in phosphate buffered saline (PBS) and stored at -80°C until use. The pellet was resuspended in buffer A (20 mM Tris-HCl pH 7.5, 500 mM NaCl, 10 mM imidazole, 5 mM β -mercaptoethanol) and cells disrupted by sonication in the presence of a tablet of EDTA-free protease inhibitor cocktail (Complete, 11873580001 from Roche). The soluble cell fraction was separated by centrifugation at 14,841 g for 15 min at 4°C. Upon filtration through 0.22 μ m filters, GFP fusions were purified by chromatography in Ni²⁺ columns in an ÄKTA™ Purifier (GE healthcare) fast protein liquid chromatography. Positive fractions in elution buffer (Tris-HCl 20 mM pH 7.5, 150 mM NaCl, 500 mM Imidazole, 5 mM β -mercaptoethanol) were collected, dialyzed against the desired buffer and quantified by Bradford's procedure. A standard HBS buffer at pH 5.8 [27] was used for most of the experiments (buffer 5 in FIGURE 1E). When indicated in some experiments, proteins were dissolved in 10 mM Tris HCl buffer pH 7.5 + 0.01% Tween 20 (buffer 2 in FIGURE 1E). The other buffers used for the experiment summarized in FIGURE 1E were as follows:

- * 20 mM Tris HCl pH 7.5 + 5% dextrose;
- * PBS 7.4 + 10% glycerol;
- * 20 mM Tris HCl pH 7.5 + 5% dextrose, 200 mM NaCl;
- * 10 mM Tris HCl pH 7.5 200 mM NaCl + 0.01% Tween 20.

Wild-type GFP was supplied by Nucliber (ref 632373).

■ Dynamic light scattering, transmission-electron microscopy & DNA retardation assays

Volume-size distributions of engineered GFP proteins and resulting complexes were measured using a dynamic light scattering analyzer at the wavelength of 633 nm, combined with noninvasive backscatter technology (Zetasizer Nano ZS, Malvern Instruments Limited, Malvern, UK). DNA–protein incubation, transmission-electron microscopy (TEM) of protein and DNA–protein complexes and DNA mobility assays were performed according to previously published protocols [27].

■ Atomic force microscopy

Atomic force microscopy (AFM) analyses were performed in air with a commercial atomic force microscope (PicoScan/PicoSPM 5500SL from Molecular Imaging Agilent Technologies, Inc., Santa Clara, CA, USA) operating in acoustic mode. 9R-GFP-H6 proteins in 10 mM Tris HCl pH 7.5 buffer were dropcasted onto a freshly cleaved mica surface and air dried before measuring. For the acoustic mode measurements, a monolithic supersharp silicon SSS-NCH-50 (Nanosensors, Inc.) tip, with a radius of 2 nm, a nominal spring constant of 10–130 N/m and a resonance frequency of 204–497 kHz was used.

■ Cell culture & confocal laser scanning microscopy

The HeLa (ATCC-CCL-2) cell line was used in all the experiments and monitored *in vivo* in absence of fixation, to prevent previously described internalization artifacts [28]. Cells were maintained in MEM (GIBCO, Rockville, MD, USA) supplemented with 10% fetal calf serum (GIBCO) and incubated at 37°C and 5% CO₂ in a humidified atmosphere. For confocal analysis, cells were grown on Mat-Teck culture dishes (Mat Teck Corp., Ashland, MA, USA). Nuclei were labelled with 20 μ g/ml Hoechst 33342 (Molecular Probes, Eugene, OR, USA) and the plasma membrane was labelled with

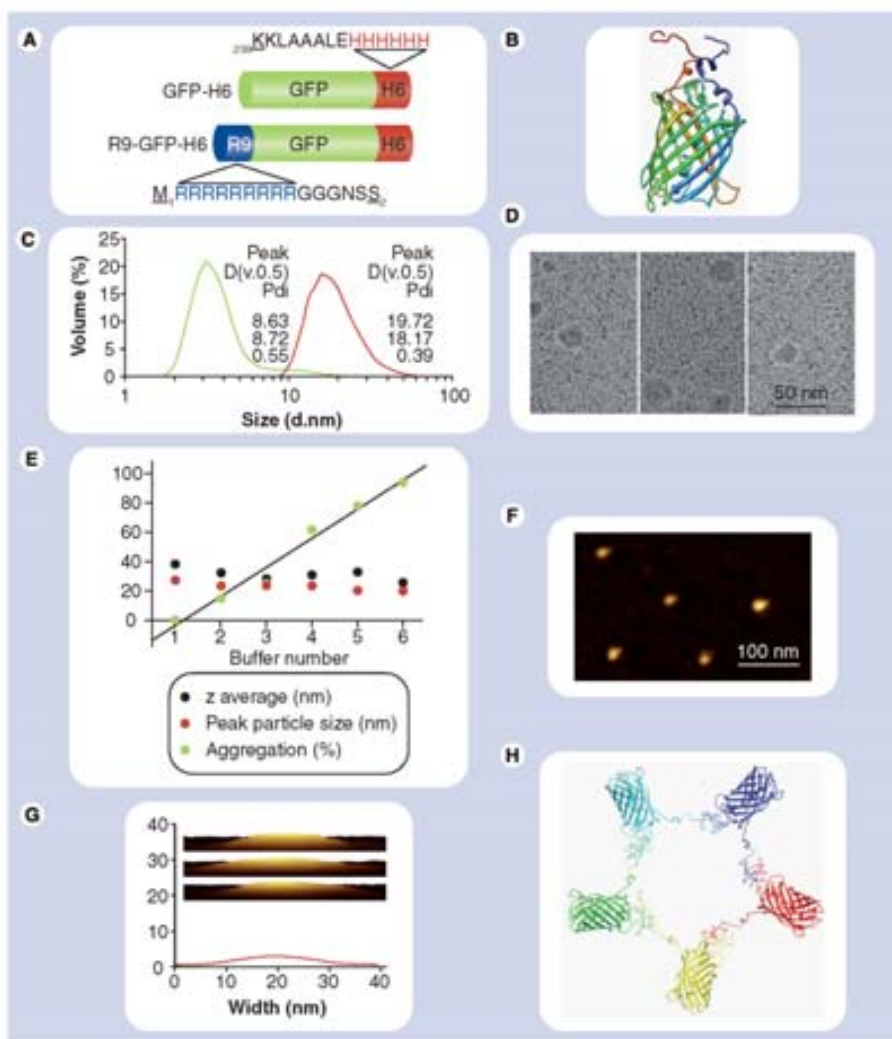


Figure 1. Description of R9-GFP-H6 modular protein and nanoscale characterization of R9-powered R9-GFP-H6 nanodisks. The amino acid sequences of polyarginine and polyhistidine tails are indicated in blue and red, respectively. R9 is accommodated between amino terminal residues M1 and S2 of GFP (underlined), while H6 is fused to the carboxy terminal residue of GFP (K238 underlined). Amino acids typed in bold face are those resulting from the cloning process. **(B)** Molecular modeling of R9-GFP-H6 showing one among the most probable spatial orientations of R9 (blue) and H6 (red) peptides. **(C)** Size distribution of soluble GFP-H6 (green plot) and R9-GFP-H6 (red plot) in 20 mM Tris buffer pH 7.5 + 5% dextrose determined by dynamic light scattering, the inset figures indicating (in nm) the peak size, the particle diameter under which there are 50% of the total volume of the population $D[v,0.5]$ and the pdi. **(D)** TEM images of randomly R9-GFP-H6 nanoparticles in the same Tris buffer. **(E)** Percentage of R9-GFP-H6 aggregation, particle size peak and z-average values of soluble R9-GFP-H6 nanoparticles in different buffers with the following composition: (1) 20 mM Tris HCl pH 7.5 + 5% dextrose; (2) 10 mM Tris HCl pH 7.5 + 0.01% Tween 20; (3) phosphate buffered saline 7.4 + 10% glycerol; (4) 20 mM Tris HCl pH 7.5 200 mM NaCl + 5% dextrose; (5) HBS pH 5.8; (6) 10 mM Tris HCl pH 7.5 200 mM NaCl + 0.01% Tween 20. **(F)** AFM analysis of randomly selected R9-GFP-H6 nanoparticles deposited on a mica surface. **(G)** Topography cross-section of an isolated particle. In the inset, 3D views of three randomly selected nanoparticles. **(H)** Molecular modeling of R9-GFP-H6 assemblies of sizes compatible with dynamic light scattering, TEM and AFM determinations. This star-shaped distribution pattern could admit up to ten individual R9-GFP-H6 molecules with minor alterations of particle size. AFM: Atomic force microscopy; GFP: Green fluorescent protein; pdi: Polydispersion index.

2.5 µg/ml CellMask™ Deep Red (Molecular Probes, Invitrogen, Carlsbad, CA, USA) for 5 min in the dark. Cells were washed in PBS (Sigma-Aldrich Chemie GmbH, Steinheim, Germany). Live cells were recorded with a TCS-SP5 confocal laser scanning microscope (Leica Microsystems, Heidelberg, Germany) using a Plan Apo 63×/1.4 (oil HC × PL APO λ blue) objective. Hoechst 33342 DNA labels was excited with a blue diode (405 nm) and detected in the 415–460 nm range. GFP proteins were excited with a Ar laser (488 nm) and detected in the 525–545 nm range. CellMask was excited with a HeNe laser (633 nm) and detected in the 650–775 nm range. To determine the protein localization inside the nucleus, stacks of 20–30 sections every 0.5 µm along the cell thickness were collected at intervals of 15 min over approximately 12 h. The projections of the series obtained were generated with Leica LAS AF software, and 3D models were generated using Imaris v. 6.1.0 software (Bitplane, Zürich, Switzerland). Profile analysis of fluorescence intensity was measured using Leica LAS AF software to determine the fluorescence intensity along the line segment in relation to the wavelength. The fluorescence intensity profiles were measured at the same laser excitation and photomultiplier gain settings from the cells.

■ Protein-mediated plasmid transfection

For gene expression experiments, 50 µg of 9R-GFP-H6 and 1 µg of TdTomato expression vector were mixed into 50 µl of HBSS pH 5.8 and incubated for 1 h at room temperature. Then, a convenient amount of Optimem was added and the full mixture was gently added to cultured HeLa cells that were further incubated for 4 h at 37°C in 5% CO₂ atmosphere. The cultures were then transferred to complete media for growth. After 48 h, TdTomato gene expression was monitored by flow cytometry. Nontreated cells or cells just exposed to the plasmid expression vector or the protein alone were used as controls.

■ Flow cytometry

Cell samples were analyzed after treatment with 0.5 mg/ml trypsin, 4Na in HBSS for 10 min on a FACSCanto system (Becton Dickinson), using a 15 W air-cooled argon-ion laser at 488 nm excitation. Fluorescence emission was measured with detector D (530/30 nm band pass filter) for EGFP and detector C (585/42 nm band pass filter) for TdTomato fluorescent protein.

■ Molecular protein modeling

To build the R9-GFP-H6 nanodisk model, a model of the monomer was first generated using Modeller 9v2 [29] and the protein data bank structure '1qyo' as a template. The arginine and histidine tails were modelled using the loop-model function of this package. The structural model of the complex was then created with HADDOCK 2.0 [30], defining the nine arginines from the N-terminal tail as active residues and the six histidines from the C-terminal tail as passive residues and enforcing C5 symmetry.

Results

Although never explored, the unusually high performance of arginine-rich peptides in functionalizing drugs and proteins under different conditions and experimental models, combined with the high stability of R9-based drugs in local and systemic delivery, made us wonder whether R9 itself might promote some form of spontaneous supramolecular organization to its associated molecules, causing the whole conjugate to act as a particulate material. To evaluate this possibility, we explored the potential self-assembly of a His-tagged (GFP-H6) GFP upon functionalization with an R9 peptide fused to its amino terminus (FIGURE 1A). In the final R9-GFP-H6 construct, both end terminal peptides resulted exposed to the solvent in the same pole of the GFP barrel (FIGURE 1B). The parental GFP-H6 and the engineered R9-GFP-H6 constructs were efficiently purified in a single-step affinity chromatography from the extracts of producing *E. coli* bacterial cells. Interestingly, GFP-H6 appeared in solution as particles of around 7 nm in diameter (FIGURE 1C), which is compatible with the molecular size of individual GFP molecules (3 × 5 nm), plus the hanging H6 tail. Surprisingly, the addition of the R9 tail promoted the spontaneous self-assembling of R9-GFP-H6 as a population of particulate species of around 20 nm, as determined by dynamic light scattering (FIGURE 1C). Interestingly, TEM examination of R9-GFP-H6 showed the protein as a particulate material of defined dimensions and regular round morphologies compatible with a spherical architecture, of sizes coincident with dynamic light scattering data (FIGURE 1D). The regularity in size and morphology indicated that these nanoparticles possessed an important level of inner organization. In agreement, such assemblies regularly occur as soluble entities in different buffers that differentially affect protein solubility (FIGURE 1E). This fact demonstrates that R9-driven particle formation results from

an ordered molecular assembling process rather than from an unspecific aggregation rendering insoluble protein clusters. AFM studies were performed over a mica substrate using a supersharp silicon 2-nm radius tip (Nanosensors, Inc.), in order to improve the image resolution. AFM analysis revealed that R9-GFP-H6 nanoparticles were not spherical but that they were instead organized as flattered spheres or nanodisks with dimensions of around 20×3 nm (FIGURE 1F & G). A molecular-structure model of the R9-GFP-H6 nanodisks was generated using the size and shape observed in the AFM images as constraints. The obtained solution for the structure of the complex predicted a star-shaped arrangement of five (or more) individual R9-GFP-H6 molecules (FIGURE 1H), in which the H6 and R9 terminal tails interact in the central region through histidine–arginine pairings [31]. This model is sufficiently flexible to explain the slight nanodisk-size variation shown in FIGURE 1C, and it could admit up to approximately ten individual R9-GFP-H6 molecules as building blocks of a single nanoparticle, that could still be compatible with the observed dimensions. In addition, this is an arrangement that explains the absence of larger aggregates.

It is noteworthy that the addition of R9 to GFP-H6 increased the hydrophilic nature of the protein (grand average of hydropathicity [GRAVY] of GFP is -0.557, and those of GFP-H6 and R9-GFP-H6 -0.617 and -0.725, respectively) and therefore its amphiphilicity (due to the polar situation of R9 in the GFP barrel, FIGURE 1B). However, the self-assembling of R9-GFP-H6 seemed to be determined by R9-driven cross-interactions (involving H6 residues) rather than by a conventional solvent exposure of the highly hydrophilic (R9 and H6) regions of the building blocks [32]. In this regard, R9 could architectonically act as multifunctional-adhesive-disordered tail. Interestingly, arginine is enriched in the proximity of protein–protein interfaces [33], due to its tendency to cross-associate in stacking-like arrangements [34] or in hydrogen-bonded ‘hubs’ [35].

At this stage, we wondered if these disk-shaped entities could penetrate mammalian cells keeping both the particulate organization and GFP fluorescence. Noteworthy, GFP fluorescent emission acts as a convenient reporter of the molecular integrity of individual building blocks, as it depends on the proper barrel formation and fluorophore maturation that occurs at late folding steps [35]. As expected, wild type GFP remained fully dispersed in the extracellular media upon exposure to cultured HeLa cells, the cell membrane acted as an efficient

barrier for the protein (FIGURE 2A), and no green signal was observed either in the cell cytoplasm or nucleus after 90 min of exposure (FIGURE 2B). Similarly, GFP-H6 remained fully excluded from cultured cells (FIGURE 2C & D), and the fluorescence of both GFP and GFP-H6 was fully dispersed in the extracellular media. However, R9-GFP-H6 nanoparticles were efficiently internalized and discrete fluorescent dots were observed in the cell cytoplasm, which progressively accumulates into the nucleus (FIGURE 2E & F). The nuclear targeting of R9-GFP-H6 was confirmed by single-cell image analysis (FIGURE 2G). Furthermore, the cytoplasmic trafficking and nuclear avidity of R9-GFP-H6 nanodisks was illustrated by the temporal tracking of these particles entering individual cells in volumetric reconstructions (FIGURE 2H), and confirmed in the absence of Hoechst 33342 and CellMask staining to avoid any enhancement of cell permeability eventually induced by these dyes (not shown). Interestingly, R9-GFP-H6 remained highly fluorescent during migration and inside both cell compartments (FIGURE 2H), being indicative of both protein and particle stability. The 3D imaging of the nanoparticles crossing the nuclear membrane (FIGURE 2G) could be compatible with the passage through the nuclear pores. Although 50 kDa seems to be a general limit for the free molecular passage across those pores (pentameric R9-GFP-H6 disks are approximately 150 kDa), the facilitated diffusion mechanism appears not having size restriction [36]. The inner diameter of nuclear pores ranges around 50–60 nm [37], and they can accommodate and translocate viral particles of 39 nm in diameter [38], larger than R9-driven nanodisks. In any case, the precise mechanism of nuclear entry as nanoparticles required further investigation, as it has been previously observed that synthetic R(n) peptides accumulate in the nucleus, the translocation mechanism remains unexplored [38].

The nuclear targeting of R9-GFP-H6 prompted to further explore the ability of the nanodisks to release expressible DNA in the nuclear compartment. Although isolated R(9–15) peptides are known to deliver expressible DNA [20], protein based, R9-powered molecular assemblies had never been explored in this regard. The parental GFP-H6 protein, despite the cationic nature provided by the H6 tail, was unable to bind DNA, as revealed by the failing of this construct in altering plasmid DNA mobility in gel electrophoresis (FIGURE 3A). By contrast, R9-GFP-H6 fully impeded DNA mobility at a mass protein–DNA ratio of 20 (this ratio consequently defined as one retardation unit [39]), this fact expectedly resulting from the

interaction between R9 and DNA [9]. Dynamic light scattering and TEM analysis of R9-GFP-H6 upon incubation with different plasmid amounts indicated that the size of nanoparticles was not visibly affected by DNA binding (Figure 3B & C), suggesting that the plasmid was efficiently condensed without dramatic rearrangements of the protein shell. In this regard, supercoiled plasmid DNA organize as minitoroids and spheroids [40], with sizes within the size range order than those of nanodisks. Furthermore, upon exposure to DNA-R9-GFP-H6 complexes, an important fraction of HeLa cell population showed red fluorescence (resulting from the production of the reporter fluorescent protein Td Tomato), as monitored by flow cytometry (Figure 3D). Such cell fraction was simultaneously emitting green fluorescence, derived from the biologically active R9-GFP-H6 that carried the DNA. The observed transgene expression confirms that R9-based nanodisks, despite being highly stable in the

extracellular media and during cytosolic trafficking, are able to release expressible DNA once the DNA-protein complexes have reached the nucleus. No appreciable differences in cell internalization of R9-GFP-H6 were observed when administered alone or as associated to plasmid DNA (not shown).

Discussion

Apart from the well described properties of polyarginine peptides as membrane translocators and cross-BBB carriers, the data presented here demonstrate their architectonic potential at the nanoscale through the fusion of an R9 tail to a scaffold GFP. This peptide triggers the spontaneous self-assembling of the chimerical protein as regular, highly ordered disk-shaped structures of 20×3 nm, probably formed by five or more building blocks, with a relatively low polydispersion index (Figure 1). These nanodisks are highly soluble and stable in a diversity of

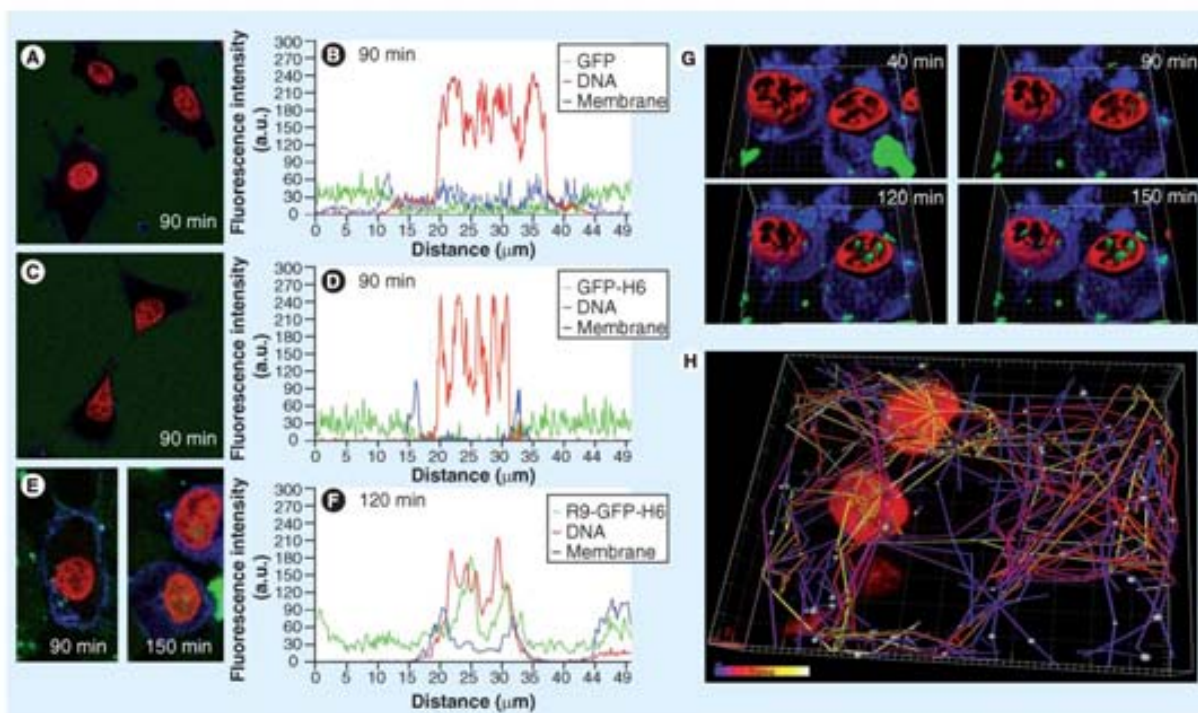


Figure 2. Confocal analysis of wild-type GFP, GFP-H6 and R9-GFP-H6 protein location in HeLa cells. Colour allocation: the cell membrane was labelled with CellMask (blue signal), cell DNA was labelled with Hoechst 33342 (red signal) and wild-type GFP, GFP-H6 and R9-GFP-H6 proteins produced a green signal. **(A)** Cultured cells exposed to wild-type GFP. **(B)** Fluorescence intensity profiles along a line segment of a randomly selected cell exposed to wild-type GFP, showing GFP, membrane cell and DNA signals. **(C)** Cultured cells exposed to GFP-H6. **(D)** Fluorescence intensity profiles along a line segment of a randomly selected cell exposed to GFP-H6. **(E)** Cultured cells exposed to R9-GFP-H6. **(F)** Fluorescence intensity profiles along a line segment of a randomly selected cell exposed to R9-GFP-H6. **(G)** Isosurface representation of HeLa cells within a 3D volumetric x-y-z data field after incubation with R9-GFP-H6. Note the time-dependent increase in the R9-GFP-H6 protein inside the nucleus. **(H)** Intracellular tracking of individual R9-GFP-H6 particles internalized by HeLa cells. Time spans from 20 to 300 min after exposure (from blue to white, in the individual tracks). a.u.: Arbitrary units; GFP: Green fluorescent protein.

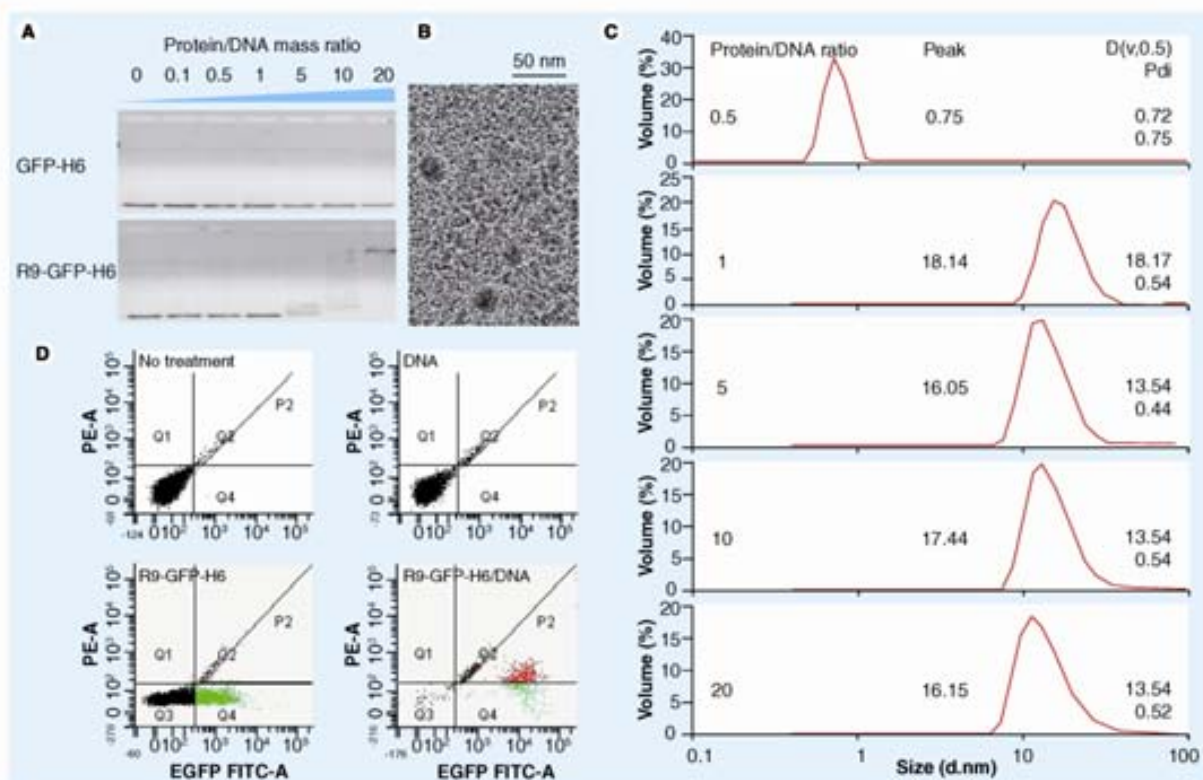


Figure 3. Evaluation of DNA-binding and gene transfer properties of R9-GFP-H6 nanodisks. (A) Retardation of plasmid DNA (pCDNA 3.1) migration in agarose gel electrophoresis promoted by increasing amounts of either GFP-H6 (top) or R9-GFP-H6. (B) TEM images of R9-GFP-H6-DNA complexes at a protein/DNA ratio of 20. (C) Particle size in R9-GFP-H6 and plasmid DNA mixtures as determined by dynamic light scattering, indicating (in nm) the peak size, the particle diameter under which there are 50% of the total volume of the population $D(v,0.5)$ and the pdi. Inset numbers at the left indicate protein/DNA ratios. (D) Fluorescence emission determined by flow cytometry of untreated HeLa cells and 48 h after exposed to plasmid DNA (pCDNA 3.1 encoding the *td tomato* gene), R9-GFP-H6 and R9-GFP-H6-DNA complexes at a protein/DNA ratio of 50 (2.5 retardation units). A prolonged trypsin treatment (see experimental section) was performed to prevent fluorescence eventually emitted by cell surface attached R9-GFP-H6. Q4 section corresponds to green fluorescence mediated by R9-GFP-H6, while P2 corresponds to red emission of *td Tomato*, the fluorescent reported protein encoded by the transferred plasmid vector and green fluorescence in the same cell. GFP: Green fluorescent protein; pdi: Polydispersity index.

buffers, even in those favoring protein aggregation. In addition, they are purified in a single step from crude extracts of producing bacteria and are efficiently internalized by cells in the particulate, fully functional organization. Their abilities to condense and deliver plasmid DNA to the nucleus make them intriguing platforms for their further functional tuning as artificial viruses for delivery of therapeutic transgenes or proteins. Interestingly, it has been reported that the spatial engineering of R9 peptide as tetramers significantly improves the internalization of this peptide and its associated molecules [41] and enhances the BBB crossing properties of arginine-rich peptides such as Tar [42]. Such an oligomer dependence of R9 potential as delivery agent easily accounts for the fast and efficient nuclear targeting of self-assembled R9-GFP-H6

particles. Therefore, among the current catalogue of forms that protein-based nanoplateforms for intracellular drug delivery may adopt, including cages, microspheres, virus-like particles, films, hydrogels and different types of rather amorphous nanostructures (recently reviewed in [7]), protein nanodisks should be considered as a novel class of protein planar assembles for DNA accommodation and transfer. Finally, the robustness of GFP fluorescent emission when functionalized with R9 indicates that the self-assembling properties conferred by the cationic peptide are compatible with proper protein conformation.

Under the urgent need of biologically produced improved protein drugs with tailored delivery properties [43], particularly in drug-reluctant, complex diseases such as cancer [44], the architectonic properties of R9 at the nanoscale reported here

might make this peptide a valuable module for the construction of improved, protein-based nanoconjugates for drug delivery in innovative biomedical approaches. The 'sticky' properties of R9 at a molecular level should permit an important extent of control in the generation of nanocomplexes, such that GFP-based nanodisks could represent powerful instruments in emerging nanomedical approaches to drug delivery and gene therapy.

Conclusion

By using multidisciplinary approaches, we demonstrate here that the R9 peptide, when fused to a reporter GFP protein, confers self-assembling properties to the whole construct, which spontaneously forms a novel type of disk-shaped, highly stable protein-based platform of approximately 20 nm in diameter. R9-powered nanodisks bind and condense plasmid DNA, efficiently penetrate cultured cells and rapidly reach the nucleus, where reporter transgenes are expressed. The intracellular trafficking or internalized nanodisks towards the nucleus does not compromise the particulate organization of the protein-DNA complexes or the proper folding of the individual building protein blocks. The stickiness of R9 at a molecular level and the consequent architectonic properties at the nanoscale might account for the unusual efficiency of these peptides as membrane active agents and as vehicles for systemic drug and DNA delivery. The multifunctional nature of R9 (and probably of closely related, highly cationic peptides) and in particular the so far ignored architectonic properties, make it an extremely useful tool for the design and fine tuning, through rational protein engineering, of tailored nanocarriers for DNA and drug delivery under the artificial virus concept.

Acknowledgements

The authors are indebted to Mary Cano, Marta Nadal and Carme Arnan for technical assistance in dynamic light scattering analysis, to Manuela Costa for technical assistance in flow cytometry, to Fran Cortés for technical assistance in cell culture, and Veronica Toledo and Rosa Mendoza from the CIBER de Bioingeniería Biomateriales y Nanomedicina (intramural IMAFEN project), Spain, for general laboratory assistance.

Financial & competing interests disclosure

The authors appreciate the financial support granted to Neus Ferrer-Miralles (EME2007-08, UAB), to Antonio Villaverde (BIO2007-61194 and EUI2008-03610 MICINN; 2009SGR108, AGAUR), to Jaume Veciana (CTQ2006-06333 MICINN; 2009SGRS16, AGAUR) and to Antonio Villaverde and Jaume Veciana from the CIBER de Bioingeniería, Biomateriales y Nanomedicina (CIBER-BBN), Spain. Ugutz Unzueta and Joan Domingo-Espín are recipients of predoctoral fellowships from MICINN, Spain, and Antonio Villaverde has been distinguished with an ICREA ACADEMIA award from AGAUR, Catalonia, Spain. The authors have no other relevant affiliations or financial involvement with any organization or entity with a financial interest in or financial conflict with the subject matter or materials discussed in the manuscript apart from those disclosed. No writing assistance was utilized in the production of this manuscript.

Ethical conduct of research

The authors state that they have obtained appropriate institutional review board approval or have followed the principles outlined in the Declaration of Helsinki for all human or animal experimental investigations. In addition, for investigations involving human subjects, informed consent has been obtained from the participants involved.

Executive summary

- The R9 peptide promotes the ordered self-assembling of a model green fluorescent protein (GFP) as disk-shaped, stable nanoparticles of approximately 20 × 3 nm.
- The GFP nanodisks (but not R9-free GFP) efficiently penetrate culture mammalian cells and accumulate in their nuclei a few hours after exposure.
- Since R9 also confers affinity for DNA, protein nanodisk-plasmid DNA complexes act as efficient artificial viruses for transgene delivery and expression.

Bibliography

- 1 Edelstein ML, Abedi MR, Wixon J: Gene therapy clinical trials worldwide to 2007 – an update. *J. Gene Med.* 9(10), 833–842 (2007).
- 2 Abbott A: Questions linger about unexplained gene-therapy trial death. *Nat. Med.* 12(6), 597 (2006).
- 3 Marshall E: Gene therapy. What to do when clear success comes with an unclear risk? *Science* 298(5593), 510–511 (2002).
- 4 Mastrobattista E, van der Aa MA, Hennink WE, Crommelin DJ: Artificial viruses: a nanotechnological approach to gene delivery. *Nat. Rev. Drug Discov.* 5(2), 115–121 (2006).
- 5 Douglas KL: Toward development of artificial viruses for gene therapy: a comparative evaluation of viral and non-viral transfection. *Biotechnol. Prog.* 24(4), 871–883 (2008).
- 6 Aris A, Villaverde A: Modular protein engineering for non-viral gene therapy. *Trends Biotechnol.* 22(7), 371–377 (2004).
- 7 MaHam A, Tang Z, Wu H, Wang J, Lin Y: Protein-based nanomedicine platforms for drug delivery. *Small* 5(15), 1706–1721 (2009).
- 8 Dietz GP, Baht M: Delivery of bioactive molecules into the cell: the Trojan horse approach. *Mol. Cell. Neurosci.* 27(2), 85–131 (2004).



- 9 Saccardo P, Villaverde A, Gonzalez-Montalban N: Peptide-mediated DNA condensation for non-viral gene therapy. *Biotechnol. Adv.* 27(4), 432–438 (2009).
- 10 Aina OH, Liu R, Sutcliffe JL, Marik J, Pan CX, Lam KS: From combinatorial chemistry to cancer-targeting peptides. *Mol. Pharm.* 4(5), 631–651 (2007).
- 11 Martin ME, Rice KG: Peptide-guided gene delivery. *AAFS J.* 9(1), E18–E29 (2007).
- 12 Low W, Mortlock A, Petrovska L, Dottorini T, Dougan G, Crisanti A: Functional cell permeable motifs within medically relevant proteins. *J. Biotechnol.* 129(3), 555–564 (2007).
- 13 Ferrer-Miralles N, Vazquez E, Villaverde A: Membrane-active peptides for non-viral gene therapy: making the safest easier. *Trends Biotechnol.* 26(5), 267–275 (2008).
- 14 Vazquez E, Ferrer-Miralles N, Villaverde A: Peptide-assisted traffic engineering for nonviral gene therapy. *Drug Discov. Today* 13(23–24), 1067–1074 (2008).
- 15 Futaki S, Suzuki T, Ohashi W *et al.*: Arginine-rich peptides. An abundant source of membrane-permeable peptides having potential as carriers for intracellular protein delivery. *J. Biol. Chem.* 276(8), 5836–5840 (2001).
- 16 Melikov K, Chernomordik IV: Arginine-rich cell penetrating peptides: from endosomal uptake to nuclear delivery. *Cell. Mol. Life Sci.* 62(23), 2739–2749 (2005).
- 17 Abes R, Arzumanov AA, Moulton HM *et al.*: Cell-penetrating-peptide-based delivery of oligonucleotides: an overview. *Biochem. Soc. Trans.* 35(Pt 4), 775–779 (2007).
- 18 Futaki S, Nakase I, Tadokoro A, Takeuchi T, Jones AT: Arginine-rich peptides and their internalization mechanisms. *Biochem. Soc. Trans.* 35(Pt 4), 784–787 (2007).
- 19 Kim HH, Choi HS, Yang JM, Shin S: Characterization of gene delivery *in vitro* and *in vivo* by the arginine peptide system. *Int. J. Pharm.* 335(1–2), 70–78 (2007).
- 20 Kim HH, Lee WS, Yang JM, Shin S: Basic peptide system for efficient delivery of foreign genes. *Biochim. Biophys. Acta* 1640(2–3), 129–136 (2003).
- 21 Takenobu T, Tomizawa K, Matsushita M *et al.*: Development of p53 protein transduction therapy using membrane-permeable peptides and the application to oral cancer cells. *Mol. Cancer Ther.* 1(12), 1043–1049 (2002).
- 22 Takayama K, Nakase I, Michiue H *et al.*: Enhanced intracellular delivery using arginine-rich peptides by the addition of penetration accelerating sequences (Pas). *J. Control Release* 138(2), 128–133 (2009).
- 23 Rothbard JB, Garlington S, Lin Q *et al.*: Conjugation of arginine oligomers to cyclosporin A facilitates topical delivery and inhibition of inflammation. *Nat. Med.* 6(11), 1253–1257 (2000).
- 24 Koppelhus U, Awasthi SK, Zachar V, Holst HU, Ebbesen P, Nielsen PE: Cell-dependent differential cellular uptake of PNA, peptides, and PNA-peptide conjugates. *Antisense Nucleic Acid Drug Dev.* 12(2), 51–63 (2002).
- 25 Kumar P, Wu H, McBride JL *et al.*: Transvascular delivery of small interfering RNA to the central nervous system. *Nature* 448(7149), 39–43 (2007).
- 26 Satheskumar PS, Lokesh GL, Murthy MR, Savithri HS: The role of arginine-rich motif and β -annulus in the assembly and stability of *Sebania mosaic virus* capsids. *J. Mol. Biol.* 353(2), 447–458 (2005).
- 27 Aris A, Villaverde A: Molecular organization of protein–DNA complexes for cell-targeted DNA delivery. *Biochem. Biophys. Res. Commun.* 278(2), 455–461 (2000).
- 28 Lundberg M, Wikstrom S, Johansson M: Cell surface adherence and endocytosis of protein transduction domains. *Mol. Ther.* 8(1), 143–150 (2003).
- 29 Eswar N, Marti-Renom MA, Webb B *et al.*: Comparative protein structure modeling with Modeller. In: *Current Protocols in Bioinformatics*. John Wiley & Sons, Inc. (Suppl. 15) 5.6.1–5.6.30 (2006).
- 30 de Vries SJ, van Dijk AD, Krzeminski M *et al.*: HADDOCK versus HADDOCK: new features and performance of HADDOCK2.0 on the CAPRI targets. *Protein* 69(4), 726–733 (2007).
- 31 Singh J, Thornton JM: *Atlas of Protein Side-Chain Interactions*. IRL press, Oxford, UK (1992).
- 32 Wang Y, Xu J, Zhang X: Tuning the amphiphilicity of building blocks: controlled self-assembly and disassembly for functional supramolecular materials. *Adv. Mat.* 21(28), 2849–2864 (2009).
- 33 Pednekar D, Tendalkar A, Durani S: Electrostatics-defying interaction between arginine termini as a thermodynamic driving force in protein–protein interaction. *Protein* 74(1), 155–163 (2009).
- 34 Vondrasek J, Mason PE, Heyda J, Collins KD, Jungwirth P: The molecular origin of like-charge arginine-arginine pairing in water. *J. Phys. Chem. B* 113(27), 9041–9045 (2009).
- 35 Zhang L, Patel HN, Lappe JW, Wachter RM: Reaction progress of chromophore biogenesis in green fluorescent protein. *J. Am. Chem. Soc.* 128(14), 4766–4772 (2006).
- 36 Talcott B, Moore MS: Getting across the nuclear pore complex. *Trends Cell Biol.* 9(8), 312–318 (1999).
- 37 Elad N, Maimon T, Frenkiel-Krispin D, Lim RY, Medalia O: Structural analysis of the nuclear pore complex by integrated approaches. *Curr. Opin. Struct. Biol.* 19(2), 226–232 (2009).
- 38 Greber UF, Fassati A: Nuclear import of viral DNA genomes. *Traffic* 4(3), 136–143 (2003).
- 39 Aris A, Feliu JX, Knight A, Coutelle C, Villaverde A: Exploiting viral cell-targeting abilities in a single polypeptide, non-infectious, recombinant vehicle for integrin-mediated DNA delivery and gene expression. *Biotechnol. Bioeng.* 68(6), 689–696 (2000).
- 40 Limanskaya OY, Limanskii AP: Imaging compaction of single supercoiled DNA molecules by atomic force microscopy. *Gen. Physiol. Biophys.* 27(4), 322–337 (2008).
- 41 Hassane FS, Ivanova GD, Bolewska-Pedyczak E *et al.*: A peptide-based dendrimer that enhances the splice-redirecting activity of PNA conjugates in cells. *Bioconjug. Chem.* 20(8), 1523–1530 (2009).
- 42 Schwarze SR, Ho A, Vocero-Akbani A, Dowdy SF: *In vivo* protein transduction: delivery of a biologically active protein into the mouse. *Science* 285(5433), 1569–1572 (1999).
- 43 Ferrer-Miralles N, Domingo-Espin J, Corchero JL, Vazquez E, Villaverde A: Microbial factories for recombinant pharmaceuticals. *Microb. Cell Fact.* 8, 17 (2009).
- 44 Vazquez E, Ferrer-Miralles N, Mangues R, Corchero JL, Schwartz S Jr, Villaverde A: Modular protein engineering in emerging cancer therapies. *Curr. Pharm. Des.* 15(8), 893–916 (2009).

Affiliations

- Esther Vazquez
Institute for Biotechnology and Biomedicine, Universitat Autònoma de Barcelona, Bellaterra, 08193 Barcelona, Spain
and
Department of Genetics and Microbiology, Universitat Autònoma de Barcelona, Bellaterra, 08193 Barcelona, Spain
and
CIBER de Bioingeniería, Biomateriales y Nanomedicina (CIBER-BBN), Bellaterra, 08193 Barcelona, Spain
- Mónica Roldán
Servei de Microscòpia, Universitat Autònoma de Barcelona, Bellaterra, 08193 Barcelona, Spain

- César Díez-Gil
Department of Molecular Nanoscience and Organic Materials, Institut de Ciència de Materials de Barcelona (CSIC), Bellaterra, 08193 Barcelona, Spain
and
CIBER de Bioingeniería, Biomateriales y Nanomedicina (CIBER-BBN), Bellaterra, 08193 Barcelona, Spain
- Ugutz Unzueta
Institute for Biotechnology and Biomedicine, Universitat Autònoma de Barcelona, Bellaterra, 08193 Barcelona, Spain
and
Department of Genetics and Microbiology, Universitat Autònoma de Barcelona, Bellaterra, 08193 Barcelona, Spain
and
CIBER de Bioingeniería, Biomateriales y Nanomedicina (CIBER-BBN), Bellaterra, 08193 Barcelona, Spain
- Joan Domingo-Espín
Institute for Biotechnology and Biomedicine, Universitat Autònoma de Barcelona, Bellaterra, 08193 Barcelona, Spain
and
Department of Genetics and Microbiology, Universitat Autònoma de Barcelona, Bellaterra, 08193 Barcelona, Spain
and
CIBER de Bioingeniería, Biomateriales y Nanomedicina (CIBER-BBN), Bellaterra, 08193 Barcelona, Spain
- Juan Codano
Institute for Biotechnology and Biomedicine, Universitat Autònoma de Barcelona, Bellaterra, 08193 Barcelona, Spain
and
Departament de Bioquímica i Biologia Molecular, Universitat Autònoma de Barcelona, Bellaterra, 08193 Barcelona, Spain
- Oscar Conchillo
Institute for Biotechnology and Biomedicine, Universitat Autònoma de Barcelona, Bellaterra, 08193 Barcelona, Spain
- Imma Ratera
Department of Molecular Nanoscience and Organic Materials, Institut de Ciència de Materials de Barcelona (CSIC), Bellaterra, 08193 Barcelona, Spain
and
CIBER de Bioingeniería, Biomateriales y Nanomedicina (CIBER-BBN), Bellaterra, 08193 Barcelona, Spain
- Jaume Veciana
Department of Molecular Nanoscience and Organic Materials, Institut de Ciència de Materials de Barcelona (CSIC), Bellaterra, 08193 Barcelona, Spain
and
CIBER de Bioingeniería, Biomateriales y Nanomedicina (CIBER-BBN), Bellaterra, 08193 Barcelona, Spain
- Xavier Daura
Institute for Biotechnology and Biomedicine, Universitat Autònoma de Barcelona, Bellaterra, 08193 Barcelona, Spain
and
Catalan Institution for Research and Advanced Studies (ICREA), 08010 Barcelona, Spain
- Neus Ferrer-Miralles
Institute for Biotechnology and Biomedicine, Universitat Autònoma de Barcelona, Bellaterra, 08193 Barcelona, Spain
and
Department of Genetics and Microbiology, Universitat Autònoma de Barcelona, Bellaterra, 08193 Barcelona, Spain
and
CIBER de Bioingeniería, Biomateriales y Nanomedicina (CIBER-BBN), Bellaterra, 08193 Barcelona, Spain
neus.ferrer@uab.cat
- Antonio Villaverde
Institute for Biotechnology and Biomedicine, Universitat Autònoma de Barcelona, Bellaterra, 08193 Barcelona, Spain
and
Department of Genetics and Microbiology, Universitat Autònoma de Barcelona, Bellaterra, 08193 Barcelona, Spain
and
CIBER de Bioingeniería, Biomateriales y Nanomedicina (CIBER-BBN), Bellaterra, 08193 Barcelona, Spain
avillaverde@servet.uab.es

Annex 5

Methods and reagents for efficient and targeted delivery of therapeutic molecules to CXCR4 cells.

(European patent)

Ugutx Unzueta, Esther Vázquez, Antonio Villaverde, Neus Ferrer, Maria Virtudes Céspedes, Ramón Mangues.

Títol	Pèptid per a l'entrega dirigida de proteïnes funcionals i àcids nucleïcs expressables a cèl·lules CXCR4+
Referència	T-2010/027
Investigador principal	Ugutx Unzueta, Esther Vazquez Gomez, Antonio Pedro Villaverde Corrales
Estat	Execució
Patents	
Títol	METHODS AND REAGENTS FOR EFFICIENT AND TARGETED DELIVERY OF THERAPEUTIC MOLECULES TO CXCR4 CELLS
Data sol·licitud	13-01-2011
Número de sol·licitud	EP11382005.4
País	Europe (EP)
Inventors	
Entitat titular	Universitat Autònoma de Barcelona, Institut de Recerca de l'Hospital de la Santa Creu i de Sant Pau, CIBER-BBN
Estat	Applied
Títol	METHODS AND REAGENTS FOR EFFICIENT AND TARGETED DELIVERY OF THERAPEUTIC MOLECULES TO CXCR4 CELLS
Data sol·licitud	13-01-2012
Número de sol·licitud	PCT/EP2012/050513
País	PCT
Inventors	Marta Virtudes Céspedes, Ramon Mangues Bafalluy, Neus Ferrer Miralles, Ugutz Unzueta, Esther Vazquez Gomez, Antonio Pedro Villaverde Corrales
Entitat titular	Universitat Autònoma de Barcelona, Institut de Recerca de l'Hospital de la Santa Creu i de Sant Pau, CIBER-BBN
Estat	Applied



MINISTERIO
DE INDUSTRIA, TURISMO
Y COMERCIO



Oficina Española
de Patentes y Marcas

Acknowledgement of receipt

We hereby acknowledge receipt of your request for grant of a European patent as follows

Submission number	300022897	
Application number	EP 1382005 4	
File No. to be used for priority declarations	EP 1382005	
Date of receipt	13 January 2011	
Your reference	P6461EP00	
Applicant	UNIVERSITAT AUTÓNOMA DE BARCELONA	
Country	ES	
Title	METHODS AND REAGENTS FOR EFFICIENT AND TARGETED DELIVERY OF THERAPEUTIC MOLECULES TO CXCR4 CELLS	
Documents submitted	package-data.xml	ep-request.xml
	application-body.xml	ep-request.pdf (5 p.)
	SPECEPO-1.pdf/P6461EP00 - Text for filing.pdf (59 p.)	SEQ1.PDF.pdf/P6461EP00 Sequence - string.pdf (13 p.)
	SEQ1.TXT.txt:Sequence 1.string_ST25.txt	f1002-1.pdf (1 p.)
	f1002-2.pdf (1 p.)	f1002-3.pdf (1 p.)
	f1002-4.pdf (1 p.)	f1002-5.pdf (1 p.)
	f1002-6.pdf (1 p.)	f1002-7.pdf (1 p.)
Submitted by	CN=A, Alconada Rodríguez 19383,O=ABG Patentes S.L.,C=DE	
Method of submission	Online	
Date and time receipt generated	13 January 2011, 17:49:14 (CET)	

PATENT COOPERATION TREATY

WO 2012/05527
PCT/EP2012/050513

ADVANCE E-MAIL

FROM THE INTERNATIONAL BUREAU

PCT

NOTIFICATION CONCERNING
AVAILABILITY OF THE PUBLICATION
OF THE INTERNATIONAL APPLICATION

TO
UNIVERSITAT AUTONOMA DE BARCELONA Edifici 4 Campus de Montbau E-08193 Bellaterra (Barcelona) del Valles ESPAINA

Mailing date (in accordance with Article 19 of the Treaty) 19 July 2012 (19.07.2012)		
Mailing date (in accordance with Article 19 of the Treaty) 12/10/2011		
IMPORTANT NOTICE		
International Application No. PCT/EP2012/050513	International filing date (in accordance with Article 11 of the Treaty) 13 January 2012 (13.01.2012)	Priority date (in accordance with Article 17 of the Treaty) 13 January 2011 (13.01.2011)
Applicant UNIVERSITAT AUTONOMA DE BARCELONA et al		

The applicant is hereby notified that the International Bureau

has published the above-mentioned international application in accordance with Article 19(2) of the Treaty, under No. WO/2012/05527.

has not published the above-mentioned international application in accordance with Article 19(2) of the Treaty, for the reasons stated in the report annexed to the international application, reference is made to Article 19(2)(b) of the Treaty for the reasons stated in the front page of the published international application.

A copy of the international application is available for viewing and downloading on WIPO's website at the following address: www.patentwipo.org in the appropriate field of the structured search engine (STN) "WebPubInt".

The applicant may also obtain a copy of the published international application from the International Bureau by sending an e-mail to pcp@ipc.wipo.int or by submitting a written request if the e-mail data is proved to be incorrect.

The International Patent Office 35, rue des Saussaies CHATEAUAUX, FRANCE	Mailing office Yveline Cussac
www.wipo.int/pct/en	e-mail: pcp@ipc.wipo.int

Annex 6

Nanoparticulate architecture of protein-based artificial viruses is supported by protein-DNA interactions.

Joan Domingo-Espín, Esther Vázquez, Javier Ganz, Oscar Conchillo, Elena García-Fruitós, Juan Cedano, Ugutz Unzueta, Valérie Petegnief, Nuria Gonzalez-Montalbán, Anna M Planas, Xavier Daura, Hugo Peluffo, Neus Ferrer-Miralles, Antonio Villaverde.

Nanomedicine (London), 6 (6), 1047-1061, 2011.



Nanoparticulate architecture of protein-based artificial viruses is supported by protein–DNA interactions

Aim & Methods: We have produced two chimerical peptides of 10.2 kDa, each contain four biologically active domains, which act as building blocks of protein-based nonviral vehicles for gene therapy. In solution, these peptides tend to aggregate as amorphous clusters of more than 1000 nm, while the presence of DNA promotes their architectonic reorganization as mechanically stable nanometric spherical entities of approximately 80 nm that penetrate mammalian cells through arginine–glycine–aspartic acid cell-binding domains and promote significant transgene expression levels. **Results & Conclusion:** The structural analysis of the protein in these hybrid nanoparticles indicates a molecular conformation with predominance of α -helix and the absence of cross-molecular, β -sheet-supported protein interactions. The nanoscale organizing forces generated by DNA–protein interactions can then be observed as a potentially tunable, critical factor in the design of protein-only based artificial viruses for gene therapy.

KEYWORDS: DNA–protein interaction · gene therapy · innovative medicine · nanomedicine · protein engineering · protein nanoparticle

Strategies for nonviral gene therapy are under continuous exploration, pressured by the undesired side effects observed in viral-based gene therapy trials [1–5]. In this context, the ‘artificial virus’ approach implies the use of noninfectious and biologically safe entities that mimic relevant features of the viral life cycle, as DNA carriers for the cell-targeted delivery of therapeutic nucleic acids [6–8]. Liposomes, carbohydrates and proteins are the most commonly used scaffolds for the construction of bio-inspired artificial viruses, although the functionalization necessary for specific receptor binding, endosomal escape and nuclear trafficking, among others, is mostly provided by proteins (namely peptides, full-length proteins or antibodies). In fact, proteins organized as cages in diverse forms, are considered excellent and fully biocompatible carriers for drug delivery [9]. In this regard, virus-like particles (VLPs) mainly formed by self-assembling capsid proteins from *Papillomaviridae* and *Polyomaviridae* viral families have been explored as gene therapy vehicles (once filled *in vitro* with nucleic acids) [10], either by keeping the original tropism of natural viruses or upon functionalization by the appropriate display of foreign functional peptides. These studies have also been extended to bacterial viruses, which might be more convenient regarding scaled-up production. For instance, phage MS2 VLPs loaded with antisense oligodeoxynucleotides and decorated with transferrin have been proven active on leukemia cancer cells [11]. However, despite

the convenient regularity of size exhibited by VLPs, their architectonic constraints limit their extensive engineering and the possibility of functional tuning.

A more versatile scheme of protein-based carriers for therapeutic nucleic acids are multifunctional proteins, constructed by the combination of appropriate functional domains fused in a single polypeptide chain [12]. The integrated domains enable the whole construct to mimic the activities of the infective viral cycle that are relevant to the targeted delivery of nucleic acids (namely binding of DNA or RNA, cell attachment and internalization, endosomal escape, proper cytoplasmic trafficking, eventual nuclear transport and nucleic acid release). The modular nature of such constructs permits the selection of functions using relevant peptides identified from nature or combinatorial libraries, and a functional redesign in iterative improvement processes [13,14]. Diverse protein vehicles within this category have been successful in promoting significant transgene expression levels *in vitro* [15–17] and therapeutic effects *in vivo* [18,19], proving the potential of this approach in the clinical context.

Interestingly, nonviral vehicles based on multifunctional proteins have been scantily characterized from the morphologic point of view. Therefore, information regarding how these proteins might organize as building blocks of higher order structures, and how protein–DNA complexes are formed and shaped is, in general, not available. Therefore, particle size

Joan Domingo-Espín^{1,2}, Esther Vazquez^{1,2}, Javier Ganz^{1,4}, Oscar Conchillo¹, Elena García-Fruitós^{1,2}, Juan Cedano¹, Ugutz Unzueta^{1,2}, Valérie Petegnief³, Nuria Gonzalez-Montalbán^{1,2}, Anna M Planas¹, Xavier Daura^{1,4}, Hugo Peluffo^{1,4}, Neus Ferrer-Miralles^{1,2} & Antonio Villaverde^{1,2}

¹Institute for Biotechnology & Biomedicine, Universitat Autònoma de Barcelona, Bellaterra, 08193 Barcelona, Spain

²CIBER de Biotecnología, Biomateriales y Nanomedicina (CIBER-BBN), Bellaterra, 08193 Barcelona, Spain

³Neurodegeneration Laboratory, Institut Pasteur de Montevideo, CP 11400, Montevideo, Uruguay

⁴Department of Histology & Embryology, Faculty of Medicine, UDELAR, CP 11800, Montevideo, Uruguay

⁵Departament d'Infermeria Clínica i Neurodegeneració, Institut d'Investigacions Biomèdiques de Barcelona (IIBB), Consejo Superior de Investigaciones Científicas (CSIC) Institut d'Investigacions Biomèdiques August Pi i Sunyer (IDIBAPS), Barcelona, Spain

⁶Catalan Institution for Research & Advanced Studies (ICREA), 08030 Barcelona, Spain

Author for correspondence: Tel.: +34 935 811 088

antonio.villaverde@uab.cat

future medicine part of fsg

and molecular organization, nanoscale properties potentially critical for cell attachment, internalization and endosomal escape remain excluded from potential tailoring. To approach this issue, in *Escherichia coli* we produced two different versions of very short structural proteins as subunits for artificial viruses based on alternative combinations of four functional domains (an integrin-binding motif, an endosomal escape domain, a nuclear localization signal and a DNA-binding, cationic peptide) joined in short peptide stretches. Significant levels of transgene expression driven by the complexes have been observed, proving the appropriate selection of the functional domains. On the other hand, in the absence of DNA, protein blocks self-organize as amorphous, polydisperse particulate entities ranging from a few nanometers up to approximately 1 μm . However, in presence of DNA, protein–DNA complexes appear as tight and rather monodisperse spherical-like nanoparticles of approximately 80 nm in diameter that resemble bacterial inclusion bodies (IBs), in which proteins remain attached by β -sheet-based cross-molecular interactions. However, both protein modeling and structural analysis of these complexes reveal an unexpected molecular organization that does not rely on protein–protein cross-molecular interactions but that is instead supported by protein–DNA interactions. Such DNA-mediated organization seems to generate an optimal architectural pattern of artificial viruses based on short multifunctional proteins as building blocks.

Materials & methods

■ Plasmid construction & protein sequence

Plasmid pET28aTEV, derived from pET28a (Invitrogen) in which the DNA sequence encoding the thrombin cleavage site was substituted by a DNA fragment encoding a tobacco etch virus (TEV) protease cleavage site, was used to generate constructs pET28aTEV-HKRN and pET28aTEV-HNRK. HKRN and HNRK correspond to DNA sequences coding for selected modules in the specified order (Figure 1A). Plasmids were constructed by introducing synthetic oligonucleotides, encoding the corresponding modules, into selected restriction enzyme sites of the multiple cloning site of pET28aTEV. The arginine–glycine–aspartic motif used here derives from the foot-and-mouth disease virus (serotype C₁) cell-binding protein [20], and it is known to bind mammalian cells through $\alpha_5\beta_1$ and $\alpha_3\beta_1$ integrins [21,22]. The

nuclear localization signal of the Simian virus 40 (SV40) large T-antigen [23] has been universally used for the nuclear transport of delivered drugs and DNA [24]. The polylysine (Lys) tail (K10) is a cationic peptide extensively used as a DNA-condensation agent in artificial viruses [25], while the polyhistidine tail (H6) is both an efficient endosomal-escape peptide [24] and a convenient tag for one-step protein purification from bacterial cell extracts [26]. Finally, the biologically irrelevant central amino acid stretch in both HKRN and HNRK was added to enlarge the mass of the resulting modular peptides and to make them more stable in bacterial cells, according to our previous experience [Domingo-Espín, Unpublished Data].

■ Protein production & purification

The production of both chimerical proteins was triggered by the addition of 1 mM IPTG to plasmid-containing BL21(DE3) *E. coli* cell cultures (at OD = 0.4–0.6) growing in Luria–Bertani medium at 37°C. After 4 h, cells were harvested by centrifugation, washed with phosphate-buffered saline and stored at -80°C until use. The pellet was resuspended in lysis buffer (20 mM Tris-HCl pH 8, 500 mM NaCl and 6 M GuHCl) and cells were disrupted by sonication in the presence of EDTA-free protease inhibitor cocktail tablets. The soluble fraction was separated by centrifugation at 15,000 g for 45 min at 4°C and filtered through 0.22- μm filters. Proteins were purified in a single step by Ni²⁺ affinity chromatography in an ÄKTA™ FPLC (GE Healthcare) using a 20 CV linear gradient to 100% of elution buffer (20 mM Tris-HCl pH 8.0, 500 mM NaCl, 6 M ClHGu and 1 M imidazole). Positive fractions were collected and passed through a PD-10 desalting column (GE Healthcare) with 4-(2-hydroxyethyl)-1-piperazineethanesulfonic acid-buffered saline and quantified by Bradford's method. Finally, proteins were stored at -80°C until use. IBs used for scanning electron microscopy were purified as described elsewhere [27].

■ Mass spectrometry

Mass spectrometry was performed on 0.5 μl of protein sample mixed with 0.5 μl 2,4-dihydroxyacetophenone (10 mg/ml in 20 mM ammonium citrate, 30% acetonitrile) spotted onto a ground steel plate (Bruker) and allowed to air-dry at room temperature. MALDI-mass spectra were recorded in the positive ion mode on an Ultraflex time-of-flight instrument (Bruker). Ion acceleration was set to 20 kV. All mass spectra were externally calibrated using a standard protein mixture.

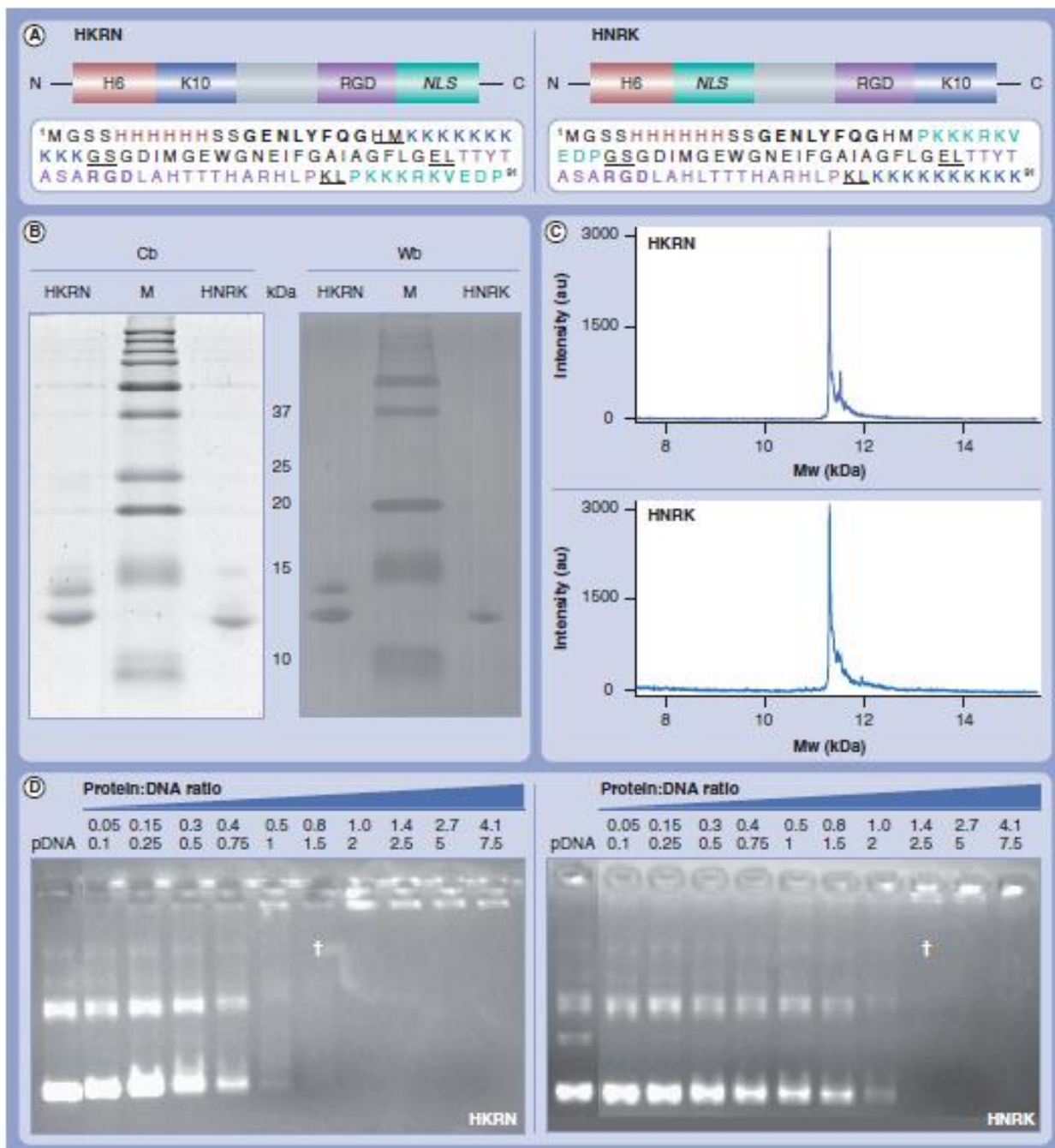


Figure 1. HKRN and HNRK organization and main features. (A) Distribution of functional modules in HKRN, HNRK and the amino acid sequence of the whole protein constructs. In both cartoons and sequence, the histidine (H) tail is labeled in red, the lysine (K) tail in dark blue, the FMDV cell binding (arginine–glycine–aspartic [RGD]) in purple and the SV40 nuclear localization signal (NLS) in green. The irrelevant central region is depicted in grey. In the amino acid sequences, residues resulting from the cloning process are underlined, a tobacco etch virus protease target site introduced between H and the immediate carboxy module is indicated in boldface and the RGD motif within the FMDV peptide is shown in italics. Sizes of the modules in the cartoons are not intended to be representative of the actual length in the protein segments. (B) Cb staining and Wb analysis (using an anti-His antibody) of SDS-PAGE of HKRN and HNRK upon purification. Molecular masses of the markers (M) are indicated in the central column. (C) Mass spectrometry of both pure proteins. (D) Up-shift of pcDNA3.1 (harboring the tdTomato gene) mobility in agarose gel electrophoresis as induced by increasing amounts of HKRN and HNRK. †The protein–DNA charge and mass ratios at which migration of DNA is fully impeded (one retardation unit).

■ Retardation assay

Different protein amounts were incubated with 300 ng of pcDNA3-tdTOMATO plasmid DNA resulting in 0.05, 0.1, 0.25, 0.5, 0.75, 1, 1.5, 2.5, 5 and 7.5 protein/DNA w/w ratios, which corresponded to 0.05, 0.15, 0.30, 0.40, 0.50, 0.80, 1.00, 1.40, 2.70 and 4.10 protein/DNA charge ratios, respectively. Mixtures were incubated in microcentrifuge tubes at room temperature for 1 h in 4-(2-hydroxyethyl)-1-piperazineethanesulfonic acid-buffered saline, and complex formation was detected in 0.8% agarose gels. One retardation unit (RU) is defined as the minimum protein/DNA ratio that does not allow DNA migration on agarose gels.

■ Electron microscopy

Complexes of protein and DNA were observed using transmission electron microscopy (TEM) with the aid of negative staining. One drop of the mixture was applied to glow-discharged carbon-coated copper grids (SPI Supplies®) for 5 min and then drained off with filter paper. Subsequently, one drop of 2% uranyl acetate was placed on the grid for 2–3 min before being drained off. The grid was then placed in a transmission electron microscope (Jeol JEM 1400) operating at an accelerating voltage of 120 kV. Images were acquired using a CCD camera (Gatan) and saved as 8-bit images. A series of micrograph images were obtained tilting the sample from -60° to $+60^\circ$ with a 914 High Tilt Holder.

Inclusion bodies were analyzed by scanning electron microscopy by standard procedures using Quanta FEI 200 field-emission gun environmental scanning electron microscope.

■ Structural analysis

For circular dichroism (CD), samples were prepared at a protein concentration of 200 μ M. Two samples were incubated with DNA at different ratios corresponding to 0.5 and 2 RU. Cuvettes with path lengths of 0.1 cm were used, and eight scans recorded at 50 nm min (response of 2 s) in a JASCO 715 spectropolarimeter were averaged for each variant. For Fourier-transformed infrared spectroscopy (FTIR), samples were analyzed in a Bruker Tensor 27 FTIR spectrometer (Bruker Optics Inc.) For each spectrum, 16 scans were acquired at a spectral resolution of 4 cm^{-1} in the 4000–600 cm^{-1} range in the transmission mode. All processing procedures were carried out to optimize the quality of the spectrum in the amide I region

ranging from 1750 to 1550 cm^{-1} . Second derivatives of the amide I band spectra were used to determine the frequencies at which the different spectral components were located.

■ Protein structure modeling

The 3D structures of the chimeric peptides were modeled with modeller 9v7 [28] using the coordinates of the original protein segments (when available) as templates. Thus, the structures of the nuclear localization signal and arginine–glycine–aspartic modules were based on chain B of IQIS [29] and chain 5 of IQGC [30], respectively. The poly-Lys module was modeled, on the sole basis of the force field, as an unstructured segment, in line with the structural diversity reported for poly-Lys peptides [31] and the disorder of the poly-Lys tail in the structure with PDB code 1KVN [32]. The central region was modeled using chain A of 1HA0 [33] as a template (61.9% similarity). Hexa-histidine peptides have become one of the most popular tags for protein purification, but the abundance of His-tagged protein models contrast with the lack of structure in which this tag has been successfully solved. This fact clearly indicates that this region tends to be intrinsically unstructured and it was not suitable for modeling under our approach, being then absent in the models.

■ Dynamic light scattering

Volume-size distribution of DNA–protein complexes at different weight ratios was determined in a dynamic light scattering device (Zetasizer Nano ZS, Malvern Instruments Limited) using DTS (Nano) version 5.10 software for data evaluation.

■ Transfection, flow cytometry analysis & fluorescent microscopy

The HeLa (ATCC-CCL-2) cell line was maintained in minimal essential medium (GIBCO) supplemented with 10% fetal calf serum (GIBCO) and incubated at 37°C and 5% CO_2 in a humidified atmosphere in 24-well plates at a cell confluence of 70–80%. The vectors pcDNA3-tdTOMATO and pEGFP-C1 (Clontech), carrying the gene of the fluorescent proteins tdTOMATO and EGFP, respectively, were used to monitor DNA transfection. DNA–HKRN or DNA–HNRK complexes were prepared incubating different amounts of protein in 50 μ l OptiPRO (GIBCO) medium and different amounts of DNA in 50 μ l OptiPRO (GIBCO) medium. After 5 min, DNA–protein complexes were generated by mixing DNA and protein at specified protein–DNA ratios at room

temperature for 1 h. A total of 100 μ l OptiPRO (GIBCO) was then added to the mixture and then to the cells. Transfection and gene expression was monitored by flow cytometry in a FACSCalibur system (Becton Dickinson) at 24 h and confirmed at 48 h post-transfection in a fluorescence microscope (Nikon ECLIPSE TE2000-E). As controls, we used nontreated cells, cells exposed only to the protein and cells exposed only to plasmid DNA.

Primary cell cultures

Cortical neuron cultures were prepared from 18-day-old Sprague–Dawley rat embryos (Charles River Laboratories), as described previously [34]. Animals were anaesthetized and killed by cervical dislocation. All procedures were approved by the Ethical Committee for Animal Use (CEEA) at the University of Barcelona, Spain. Cells were seeded on 24-well plates at a density of 1580 cells/ mm^2 in neurobasal medium supplemented with 2% B27 supplement, 0.5 mM glutamine and 0.1 mg/ml gentamycin. Partial medium changes were performed *in vitro* on days 4 and 7. Transfection was performed *in vitro* on day 10 as for HeLa cells, except that the transfection medium was neurobasal:conditioned medium (2:1). Gene expression was confirmed at 24 h postinfection in a fluorescence microscope (Olympus IX71).

Luciferase gene expression

HKRN or HNRK were incubated at room temperature for 1 h with pGL3-BOS-luciferase reporter plasmid (kindly provided by Marta Barrachina) at the indicated ratios of protein/DNA in 20–30 μ l of Opti-MEM[®] medium. Subconfluent HEK293 cells were washed once with Opti-MEM and then incubated with the protein/DNA complexes for 4 h. The medium was then removed and cells maintained in DMEM+10% fetal bovine serum for another 48 h. The measurement of luciferase activity was performed according to the manufacturer's instructions (Luciferase Reporter Gene Detection Kit, SIGMA Cat. LUC1-1KT). As a control reference, cells were transfected with lipofectamine 2000 (Invitrogen, 2 μ g lipofectamine + 1 μ g DNA/well on 24-well plate) and data were expressed as percentage relative light units per μ g of protein in the samples compared with lipofectamine 2000.

Results

The chimerical genes encoding the multifunctional proteins HKRN and HNRK were constructed by ligation of partially overlapping

and complementary oligonucleotides, encoding four selected protein domains, in which the codon usage had been optimized for *E. coli*. Both polypeptides, containing the same functional motifs displayed in alternative positions (FIGURE 1A), were successfully produced in *E. coli* BL21 (DE3) pLysS, in full-length forms and at reasonably high yield (~4 μ g of protein per ml of culture). Western blot analyses of purified proteins revealed the absence of truncated protein versions and the minor occurrence of high molecular mass immunoreactive species, especially in HKRN, which might indicate a tendency to form supramolecular structures (FIGURE 1B). The occurrence of such cross-interactions was supported by the high purity observed in samples of both proteins (FIGURE 1C), and the absence of major isoforms derived from partial proteolysis. When HKRN and HNRK were challenged in DNA retardation assays, HKRN showed a higher capability (1 RU corresponding to a protein/DNA mass ratio of 1.5 and to a DNA/protein charge ratio of 0.8) than HNRK (1 RU corresponding to a protein/DNA mass ratio of 2.5 and to a DNA/protein charge ratio of 1.3) to impede the mobility of plasmid DNA (FIGURE 1D). This divergence could be accounted by either a different oligomerization potential or by a different performance of the DNA binding domain (K10) as alternatively positioned in HKRN and HNRK. In the first case, K10 was placed in an internal position within the amino terminal protein moiety and in HNRK, this peptide overhanged as a C-terminal end.

The resulting protein–DNA complexes (non-viral vehicles) were tested in HeLa cell cultures for their ability to promote expression of a plasmid-harbored reporter transgene. Although the design of nonviral vehicles for gene therapy is a rather trial-and-error process, we expected that the combination of the FMDV integrin-binding motif, the SV40 nuclear localization signal, the His-based endosomal escape peptide and the Lys-based DNA binding stretch could summarize the main viral functions required for cell uptake and trafficking of the cargo DNA and result in significant levels of nuclear gene delivery and expression. In agreement with this presumption, flow cytometry analysis of cultured cells 48 h after exposure to HKRN–DNA and HNRK–DNA complexes revealed the occurrence of significantly prevalent cell subpopulations expressing the reporter tdTomato gene. In this context, more than 10% of HeLa cells transfected with HNRK-based vehicles emitted red fluorescence, indicating the proper nuclear delivery and release

of the carried DNA. However, being still significant, DNA delivery mediated by HKRN resulted in rather moderate transgene expression that was detected in only 0.5% of the cell population (FIGURE 2A). In order to eliminate the chance that this value could be due to experimental noise, we examined the cultures treated with HKRN-based complexes by fluorescence microscopy *in situ*. Clear fluorescence emission in individual cultured HeLa cells was detected when using two different reporter genes, namely *EGFP* and *tdTomato* (involving >10% of cells at 24 h; FIGURE 2B, top, middle panel). Furthermore, in primary cultures of neurons and glia, several cells strongly expressing *tdTomato* were observed 24 h after transfection with the DNA–HKRN complex. A cell with neuronal morphology strongly expressing the *tdTomato* gene in the cell body and neurites is shown in the inset of FIGURE 2B, bottom, demonstrating that neurons can be effectively transfected and the transgene transcribed and translated into protein. An additional transfection experiment on Hek293 cells with a third reporter luciferase (*luc*) gene confirmed the consistent transgene expression mediated by HKRN (FIGURE 2C). These data demonstrate the stability, robustness and good performance of both HKRN and HNRK as nonviral gene vectors and the appropriateness of the selected protein modules to mediate DNA delivery, being the modular distribution in HNRK more convenient for the proper mimicking of viral functions.

Intriguingly, the morphology and structure of protein–DNA complexes in nonviral gene therapy has been historically neglected, and for protein-based vehicles other than VLPs, the concept of an artificial virus refers exclusively to functional (instead of nanoscale physical) properties. Therefore, at this stage, we were especially interested in evaluating the architectonic properties of both constructs as building blocks of artificial viruses, and how these multifunctional protein subunits should be organized to bind plasmid DNA. To explore the molecular organization of the artificial viruses we approached their structural analysis from different angles. Interestingly, the TEM images of both peptides alone indicated the occurrence of amorphous, highly dispersed protein clusters of approximately 1 μm without any apparent morphological pattern and internal organization (FIGURE 3A). However, the protein–DNA complexes formed by HKRN and HNRK organized as regular, pseudo-spherical nanoparticles of approximately 80 nm in diameter (FIGURES 3A), morphologically resembling bacterial IBs [35–37] (although these

last particles can be slightly larger, up to 450 nm in diameter [35]). The molecular reorganization of the protein building blocks induced by the addition of DNA occurred at 0.5 but not 2 RU (FIGURE 3B), and it did not prevent the emergence of larger protein clusters (FIGURE 3B, see arrow). These micron-sized particles, as seen by dynamic light scattering, are probably transient and reversible clusters of the 80-nm particles promoted by overhanging DNA molecules, since complexes of this size were uniquely, consistently and abundantly observed by TEM (FIGURE 3A). Despite the absence of nanosized particles at 2 RU, the size variability of DNA–protein complexes was strongly reduced when comparing with proteins alone (FIGURE 3B), indicating that the presence of DNA promoted conformational alterations on the holding proteins with impact in their oligomeric organization. The regularity of size in the protein–DNA complexes compared with the protein alone also indicates protein-condensing abilities of plasmid DNA that reduce the molecular stickiness (their aggregation tendency) of HKRN and HNRK proteins. This fact strongly suggests that the cationic poly-Lys stretches, responsible for DNA binding in multifunctional proteins [25] and whose charge is expected to be neutralized in the complexes, effectively drive the unspecific formation of higher order, protein-alone clusters shown in FIGURE 3A. Taken together, these data indicate that HKRN and HNRK, apart from exhibiting the functions associated to their forming protein domains, act as efficient building blocks for the construction of artificial viruses under the architectonic scope of this term.

A $\pm 60^\circ$ TEM scan of HNRK revealed a slightly flattened ellipsoid form of the protein–DNA complexes (FIGURE 4A), again very similar to the images of IBs formed by other proteins seen by atomic force microscopy [35]. In fact, HKRN and HNRK themselves are both partially found as IBs in the cytoplasm of the producing bacteria (FIGURE 4C). In this context, we were interested in determining the eventual architectonic coincidences between protein–DNA complexes and IBs formed by the protein counterparts. As determined by conformational analysis through FTIR [38–40], IBs gain their mechanical structure and shape by cross-molecular protein–protein interactions supported by a β -sheet-based, amyloid-like architecture [41,42], and we wondered if the architecture of the 80-nm artificial viruses formed by HKRN–DNA and HNRK–DNA complexes could also be supported by protein–protein interactions.

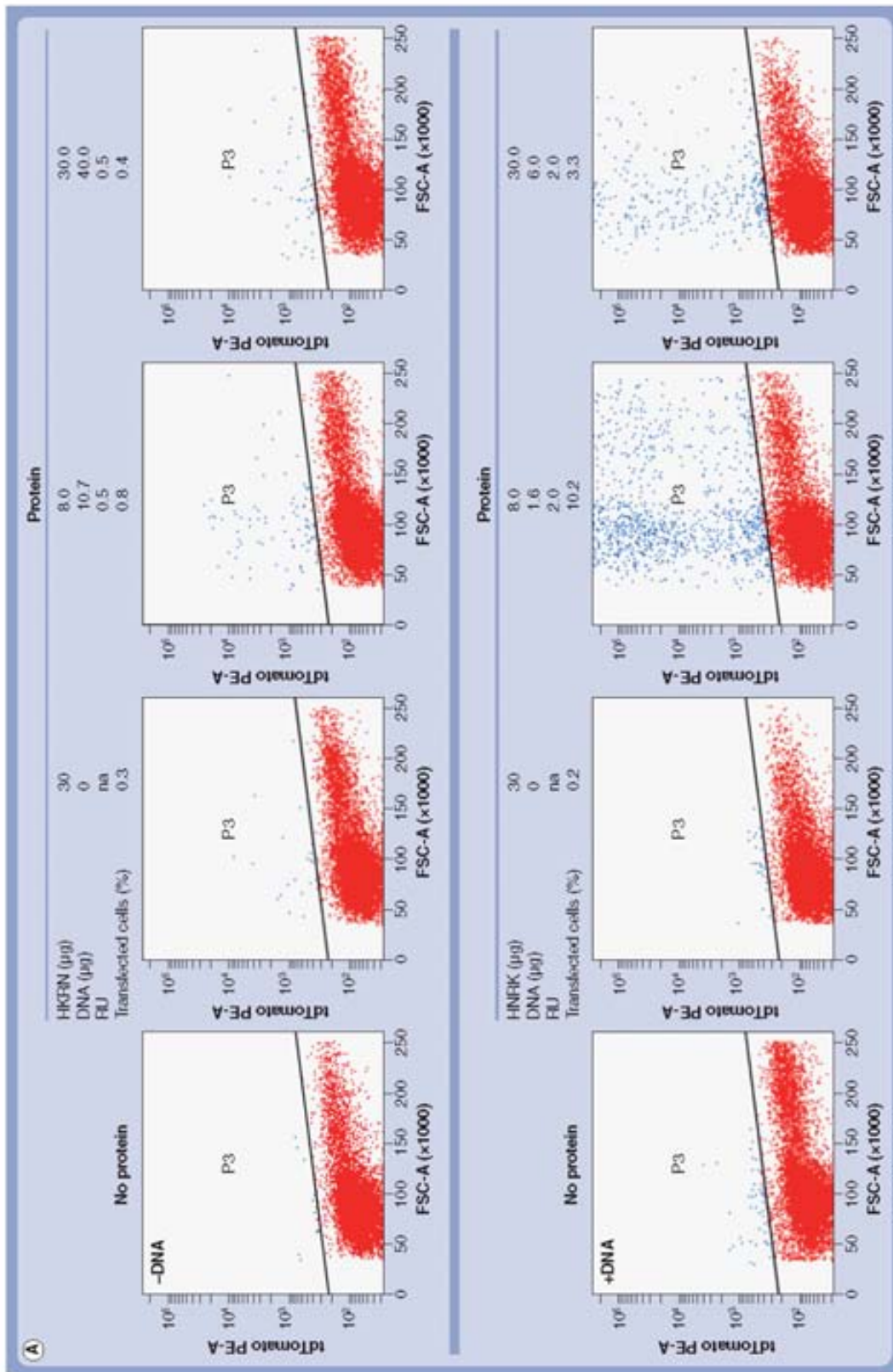


Figure 2. Transgene expression mediated by HKRN- and HNRK-based artificial viruses. (A) Fluorescence emission determined by flow cytometry of cultured HeLa cells 48 h after exposure to 24 μ g of pCDNA3.1 or in the absence of foreign DNA (no protein). Cells were also exposed to HKRN-DNA and HNRK-DNA complexes and to these proteins alone (protein), and the P2 section in the plots corresponds to the red fluorescence emitted by the IdTomato protein. The percentages of fluorescent cells are indicated above each plot. na: Not available

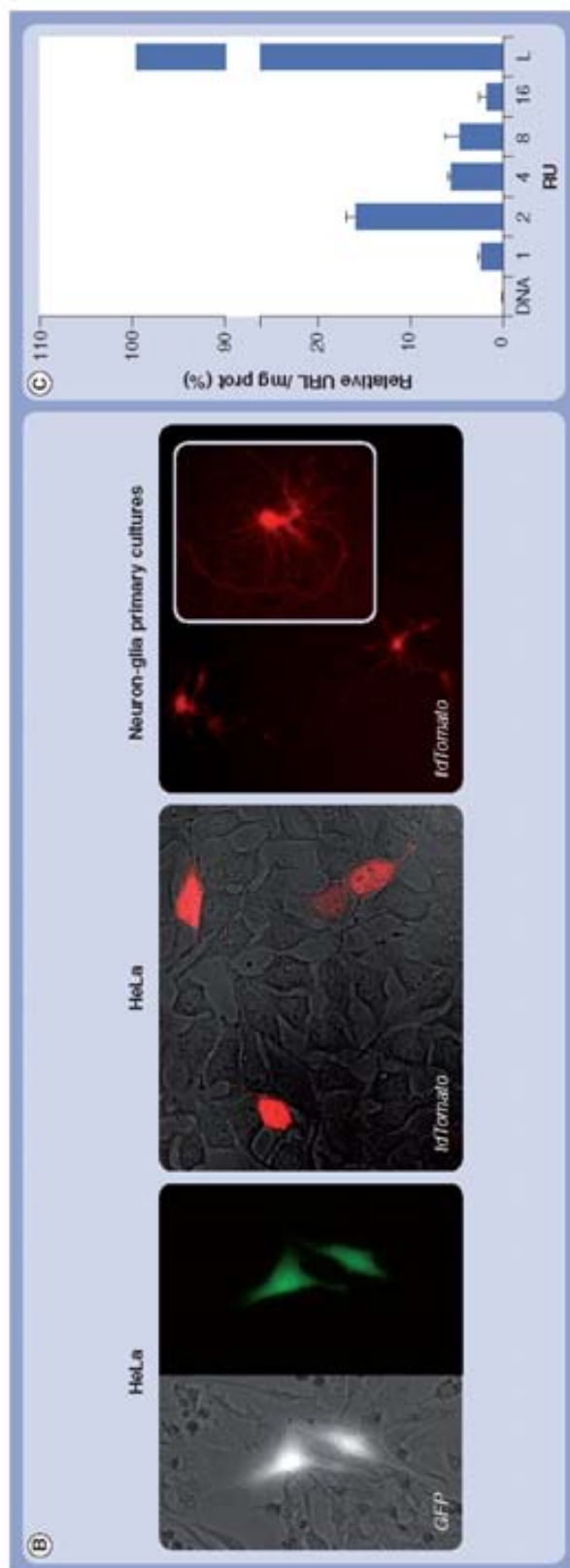


Figure 2 (cont.). Transgene expression mediated by HKRN- and HNRK-based artificial viruses. (B) Fluorescence microscopy of cultured cells 48 h after exposure to HKRN-pBOS complexes formed at 1, 2, 4, 8 and 16 RU (each experiment was performed at 28.8 µg of HKRN-pBOS alone at a concentration equivalent to 2 RU (5.75 µg/well) as used as negative control. Lipofectamine 2000 (2 µg/well + 1 µg pBOS) was used as a positive control (L).

Therefore, we approached the FTIR analysis of artificial viruses and their protein building blocks taking HNRK as a model. HNRK conformational features were analyzed under different biophysical states, such as naturally occurring IBs in bacteria, in soluble form, lyophilized and in complexes with DNA. The conformational status of HNRK in IBs was found to be similar to those described previously as formed by other recombinant proteins, and characterized by the presence of extended, cross-molecular β -pleated sheet elements peaking at 1621 cm^{-1} (FIGURE 4B, top) [39,42,43]. On the other hand, in the HNRK-DNA complexes other secondary elements not present in HNRK IBs, such as native α -helices and unordered structures, were also detected (corresponding to the overlapped region between 1640 and 1660 cm^{-1}). In agreement with that observed by *in silico* modeling (FIGURE 4D) and as expected for short peptides, both HNRK and HNRK are, in general, unstructured. However, some locally structured regions inherited from their templates were noted in the models, namely a three to ten helix spanning residues 44–47 in HNRK and 45–48 in HNRK, apart from some additional turns and bends (FIGURE 4D). Accordingly, soluble HNRK was seen to have α -helix elements peaking at 1654 cm^{-1} (FIGURE 4B, center, green line). Interestingly, upon lyophilizing, HNRK seemed to evolve in a more lightly loose and unordered structure, as it can be seen by the broad peak between 1640 and 1660 cm^{-1} (FIGURE 4B, center, black line).

In agreement with the structural impact of DNA on the complexes suggested by dynamic light scattering data (FIGURE 3), the presence of the plasmid DNA had a critical effect on the peptide structure (FIGURE 4B, bottom), preventing the smooth deconstruction of α -helices observed during the lyophilization of HNRK alone. In addition, HNRK α -helices gained looseness along with the increase of DNA-HNRK ratio, as can be seen by the slight shift from lower wavenumber, from 1653 cm^{-1} in the lyophilized sample without DNA (FIGURE 4B, bottom, black line) to 1651 and 1650 cm^{-1} in the HNRK 2 RU and 0.5 RU (FIGURE 4B, bottom, red line and blue line, respectively). This minor but significant shift might suggest that the binding of DNA to the protein shells is not a random, but an organized event possibly involving the central α -helix region of the peptide. Such interaction could account for the architectonic organization emerging in the artificial viruses and absent in the protein building blocks alone. The gain of peptide organization promoted by DNA was further confirmed

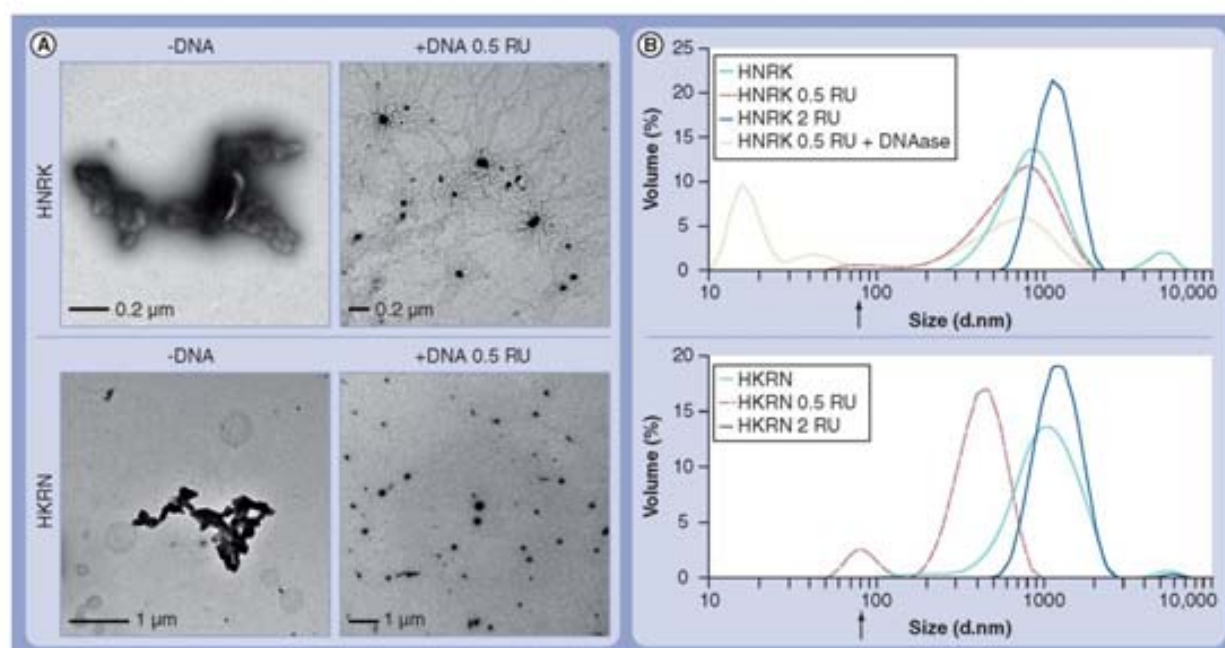


Figure 3. Size and morphology of HNRK and HKRN and their derived artificial viruses. (A) Representative transmission electron microscopy images of both HNRK and HKRN alone and as complexes with plasmid pcDNA3.1. **(B)** Effective size of protein particles alone or protein–DNA complexes (HNRK at the top and HKRN at the bottom) determined by dynamic light scattering (80 nm is marked with an arrow). The size of HNRK-based artificial viruses treated with DNase (7 $\mu\text{g}/\text{ml}$) for 30 min at 37°C is also shown (top, spotted line).

by CD analysis of HNRK alone and combined with DNA (FIGURE 4E), as evidenced by the reduction of the deep valley at 200 nm in the spectrum of the peptide in solution, which corresponds to disordered structure. In addition, the CD spectra of HNRK–DNA complexes at different ratios are compatible with the presence of secondary structures, such as α -helix or antiparallel β -sheet [44], which is particularly supported by the rising of peaks between 210 and 220 nm (FIGURE 4E). These results are in agreement with the FTIR spectra and with the compact nanoparticulated protein–DNA structures observed by TEM.

In summary, the FTIR analysis discarded any IB-like organization of artificial viruses and both FTIR and CD spectra demonstrated that the architecture of these particles is not based on cross-molecular protein–protein contacts but that it is instead supported by charge-dependent, but potentially stereospecific DNA–protein interactions. These contacts generate artificial viruses able to transfect expressible DNA, with morphologies and sizes within the nanoscale and compatible with those found optimal for efficient cell interaction and further uptake (in the range of those exhibited by natural virus particles) [45–47]. A further evidence of the architectonic role of DNA in the organization of artificial viruses is that, upon treatment with DNase,

the HNRK-based artificial viruses disassemble in smaller entities whose lower range sizes (up to ~ 10 and ~ 40 nm), are compatible with those of peptide oligomers (FIGURE 3B).

Discussion

Artificial viruses are manmade constructs designed to mimic viral activities important for the cell-targeted delivery of therapeutic nucleic acids [7], and represent safer alternatives to viral gene therapy [2,6]. Lipids and polysaccharides with different molecular organizations are commonly used to protect nucleic acids that remain embedded in the core of the particle. However, because of the ability of proteins to interact with specific ligands, these vehicles are often functionalized with antibodies, peptides or whole proteins in an attempt to target a given cell type or tissue. Although tissue targeting in drug delivery can also be effectively achieved by distally applying magnetic force on paramagnetic drug carriers [48], the versatility of protein engineering offers unique opportunities for the fine tailoring of the biological properties of artificial viruses to attain, for instance, complex biodistribution maps.

In the context of the tunable nature of proteins, artificial viruses can be efficiently constructed by uniquely using these macromolecules,

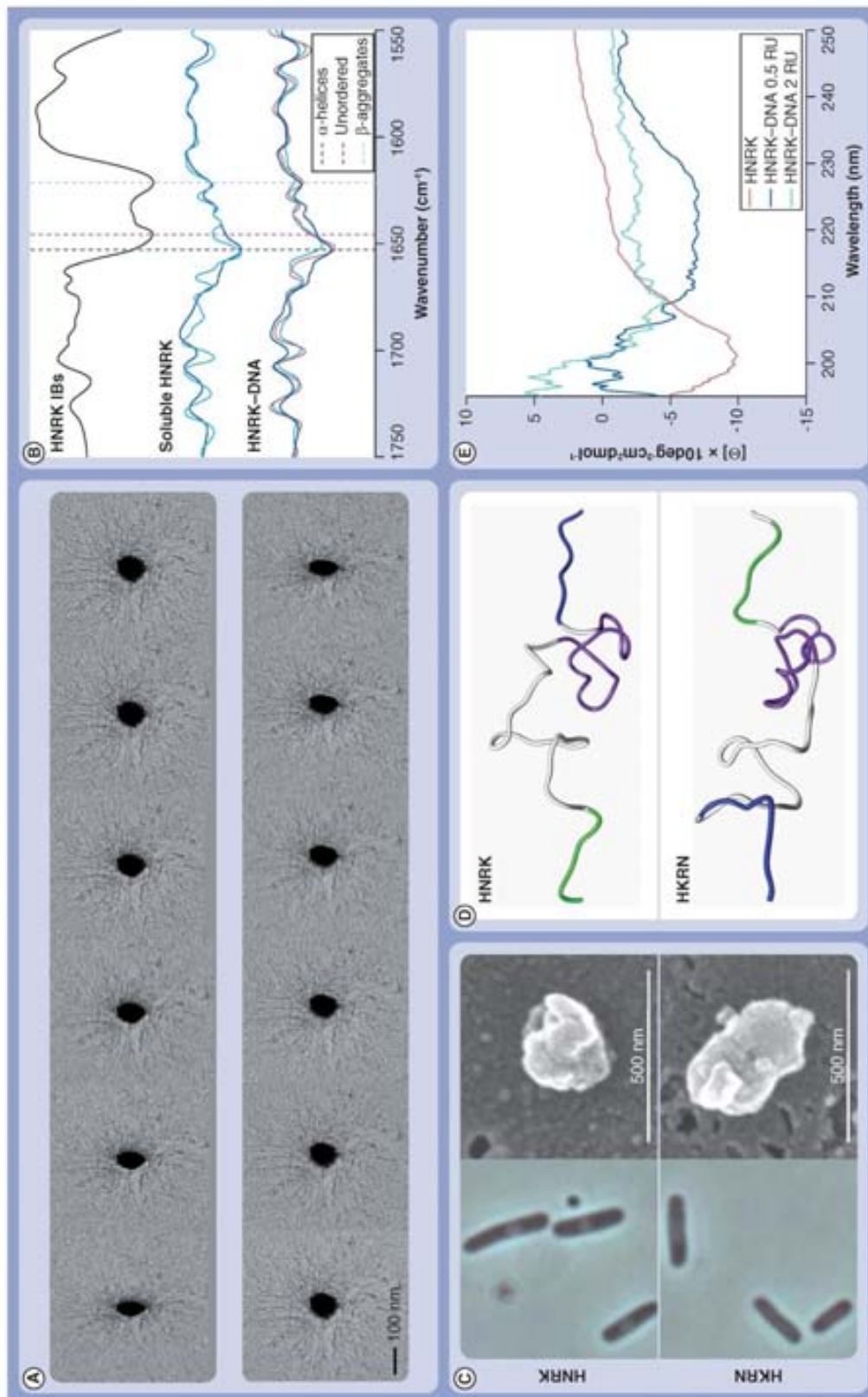


Figure 4. Molecular organization and conformation of HNRN and HNRK building blocks. (A) Selection of TEM micrograph images from a series of images acquired at inclinations from -60° to $+60^\circ$. (B) Second derivative attenuated total reflectance-Fourier transformed infrared spectroscopy spectra in the Amide I region ranging from 1750 to 1550 cm^{-1} . Vertical lines correspond to aggregated β -strands, unordered structures and α -helices peaking at 1621, 1648 and 1653 cm^{-1} , respectively. Top: second derivative spectrum of HNRK inclusion bodies; middle: second derivative of lyophilized (solid dark blue line) and soluble HNRK (solid light blue line); bottom: second derivative spectra of lyophilized HNRK (solid dark blue line), HNRK 2 RU (solid red line) and HNRK 0.5 RU (solid blue line). (C) HNRK- and HNRN-producing *Escherichia coli* cells showing cytoplasmic inclusion bodies (left), and those inclusion bodies as observed by SEM upon purification (right). (D) HNRK and HNRN models in which the different modules are colored according to the color pattern of [Figure 1A](#). Note that the His segments are not shown. (E) Circular dichroism spectra of HNRK in solution and combined with DNA at two different RU. Spectra of the peptide-DNA complexes were obtained after subtracting the spectra of DNA alone recorded at the corresponding concentrations.

provided all the functions required by nucleic acid condensation and intracellular delivery are embraced. In this regard, an intriguing approach to protein-based artificial viruses is the design of multifunctional recombinant proteins [12], which contain, in a single polypeptide chain, functional peptides from different origins. By appropriate peptide selection and combination as functional modules, these units confer cellular specificity and intracellular traffic to the DNA–protein complexes [13,14]. Those functional peptides can either be inserted in permissive sites of a scaffold protein, or sequentially fused as a new, non-natural peptide or short protein [49] and produced in recombinant microorganisms. Examples of constructs generated in bacteria by these alternative strategies can be found elsewhere [12]. Importantly, bacterially produced macromolecules are biocompatible, as proved by the high number of protein drugs approved for human therapy obtained in *E. coli* [50] (even being not a ‘generally recognized as safe’ [GRAS] organism), and also by the wide spectrum of bacterial materials used in classic and emerging medicines [51]. Therefore, the exploration of protein particles derived from bacterially produced components is perfectly reasonable regarding their potential clinical applicability.

From the material science point of view, the organization of protein-based cages has been classified according to rather general schemes [9,52], but the precise architecture of proteinaceous artificial viruses other than those based on VLPs remains poorly explored. In fact, multifunctional proteins based on large scaffold proteins such as *E. coli* β -galactosidase for instance [53,54], organize as amorphous polydisperse protein clusters whose properties seem to be defined by protein features (the enzyme is a tetramer of approximately 460 kDa [55]), rather than by the presence of DNA [56]. Upon addition, plasmid DNA does not modify the morphology of the complexes. In the same context, arginine-rich peptides, when displayed on the surface of a chimerical green fluorescent protein, provide self-assembling properties to the fusion protein (rendering planar 20-nm particles) also irrespectively of the presence of DNA [15].

Here we have explored the nanoscale organization of two short multifunctional proteins, namely HKRN and HNRK (FIGURE 1), which are shown to be competent in gene delivery by using both cultured cell lines and primary cell culture models (FIGURES 2A & 2B). The transgene expression levels and stability that were reached in this study were comparable or higher than those observed

with previous prototypes of artificial viruses based on multifunctional proteins [15,53,54,56,57]. The less active modular protein version, namely the construct HKRN, achieved approximately 18% of the expression level observed when using lipofectamine (FIGURE 2C). The slight differences in the ability to retain and deliver expressible DNA are obviously due to the alternative disposition of functional motifs, and the end terminal location of the cationic K10 peptide seems to be especially convenient for the performance of the whole vehicle. However, apart from such a punctual observation, no dramatic differences in the performance of HKRN and HNRK have been observed. This is indicative of an important extent of functional independence of the diverse modules composing the building block, which seems to be hardly affected by their particular position in the fusion peptide and also by the surrounding partner motifs. The mere sequential fusion of functional domains without any scaffolding protein seemed a favorable strategy regarding productivity in bacteria, when comparing with the moderate yield in which high molecular mass-engineered β -galactosidases had been obtained previously [53,56].

The building blocks alone tend to passively aggregate as amorphous clusters with average sizes of approximately 1 μ m (FIGURE 3). However, the presence of DNA dramatically modifies the organization of the protein, and at 0.5 RU it induces the formation of protein–DNA nanoparticles of approximately 80 nm from which DNA molecules eventually overhang (FIGURES 3A & 4A). These artificial viruses, having optimal size regarding their potential interaction with mammalian cells and further uptake [45], are able to promote the transgene expression in targeted cultured cells, as observed by several models (FIGURE 2), again more efficiently than amorphous vehicles based on larger scaffold proteins [53,56].

Interestingly, the organization of HKRN–DNA and HNRK–DNA complexes is not dependent on protein–protein interactions but on the sticky, glue-like potential of DNA (FIGURES 3B & 4B), that seems to show avidity for the internal α -helix exhibited by both proteins (FIGURE 4D). The architectonic properties of DNA in creating regular nanoparticles, based on charge-dependent interactions [25], strongly depend on the protein–DNA ratio (FIGURE 3B) and are probably more apparent when interacting with short peptides than with large proteins, as no DNA-induced architectonic changes in larger protein building shells have been previously reported [15,56]. In this context,

the particle size (80 nm) observed here by using two short chimerical proteins has resulted very similar to that observed when associating other short peptides with plasmid DNA, namely in adenoviral core peptide μ -DNA complexes (80–120 nm [58,59]) and in intermediates in toroid formation by histidylated poly-Lys-DNA complexes (80–100 nm [60]). Poly-Lys-DNA and polyornithine-DNA polyplexes have rendered, however, slightly larger particles (150–200 nm [61]). These organizing forces are probably dependent on the ability of DNA to alter the conformation of the shell proteins ($\Phi_{125\text{K}2\text{E}4}$). In this context, it has been previously proved, by elegant analysis that short peptides affect the local, distal secondary and tertiary structure of bound DNA [62], but according to the data presented here the conformational changes in protein-DNA artificial viruses are mutually induced.

In the context of multifunctional large proteins, we have previously shown that multifunctional recombinant vehicles for DNA delivery efficiently induce the *in vivo* expression of a reporter [19] and a therapeutic gene [18], followed by reduced infarct volume and functional recovery of treated animals [18], in a model of acute brain injury. Interestingly, the functional modules present in the protein shell can contribute, in synergy with the therapeutic gene, to the clinical recovery of the treated animals [57]. Being clearly efficient in local administration, further *in vivo* experiments are needed to evaluate the potential of the proposed strategy for artificial virus construction in systemic gene therapy protocols, and how the protein-DNA complexes could be adapted to escape from the reticuloendothelial system.

Irrespective of that, the nanometric organizing abilities of DNA-multifunctional protein complexes, reported for the first time in this study, opens intriguing possibilities for the design and development of improved artificial viruses. The small size of the protein counterpart facilitates the DNA-mediated particle self organization, through interactions with the cationic protein motif. The functional plasticity of the multifunctional protein approach, combined with the particle size adjustment should permit the generation of chemically hybrid and improved bionanoparticles for gene therapy but also conventional drug delivery.

Conclusion

We have biologically produced short, mainly unordered multifunctional peptides as building blocks of protein-based artificial viruses, which have shown an excellent performance

in transgene delivery under different biological models. Interestingly, the artificial viruses resulting from protein-DNA associations are pseudo-spherical entities with regular particle sizes of approximately 80 nm, at specific protein-DNA ratios in the range of those promoting high transgene expression levels. A structural characterization of the protein components in these artificial viruses has revealed that the global architecture of the particles is not driven by protein-protein interactions but on the contrary, unexpectedly supported by the embedded DNA. The nucleic acids act as a compacting, molecular glue that affects the conformation of the protein building blocks, altering the α -helix structure of the central region, minimizing their aggregation tendency and promoting an ordered, self organization of the complexes in sizes compatible with an efficient receptor-mediated cell uptake and proper intracellular trafficking to the cell nucleus. This first description of the architectonic properties of DNA at the nanoscale opens intriguing opportunities for a better rational design of artificial viruses for gene therapy regarding their molecular and physical organization.

Future perspective

A better comprehension of the DNA-protein and protein-protein interactions in the context of nanoparticles for drug and DNA delivery (at this moment a rather neglected area) should offer new engineering tools for the semi-rational or rational tuning of the nanoscale properties of artificial viruses, which is expected to fully expand in the next decade. The incorporation of protein-only vehicles (other than VLPs) in the nanomedical scenario will offer intriguing possibilities for the flexible development of smart drugs, especially when applying modular/multifunctional protein engineering principles. However, the biocompatibility and safety of protein-based nanoparticles should be combined with enhanced stability and improved targeting, the major challenges in the immediate generation of powerful drugs at the clinical level.

Acknowledgements

The authors are indebted to the Cell Culture and Cytometry Unit of the Servei de Cultius Cel·lulars, Producció d'Anticòs i Citometria (SCAC), and to the Servei de Microscòpia, both at the Universitat Autònoma de Barcelona, and to Agustín Correa (UPR) and Gonzalo Obal (UBP) from the Institut Pasteur de Montevideo for their excellent technical help. Antonio Villaverde has been distinguished with an ICREA ACADEMIA award.

Financial & competing interests disclosure

The authors appreciate the financial support received for the design and production of artificial viruses for gene therapy from MRCINN (BIO2007-61194 and AGL2009-0919), AGAUR (2009SGR-108) and CIBER de Bioingeniería, Biomateriales y Nanomedicina (CIBER-BBN, Spain), an initiative funded by the VI National R+D+i Plan 2008–2011, Iniciativa Ingenio 2010, Consolider Program, CIBER Actions and financed by the Instituto de Salud Carlos III with assistance from the European Regional Development Fund. We also thank ANIL, Ministerio de Educación y Cultura, Uruguay, for financial support. The authors have no other relevant affiliations or financial involvement with any

organization or entity with a financial interest in or financial conflict with the subject matter or materials discussed in the manuscript apart from those disclosed.

No writing assistance was utilized in the production of this manuscript.

Ethical conduct of research

The authors state that they have obtained appropriate institutional review board approval or have followed the principles outlined in the Declaration of Helsinki for all human or animal experimental investigations. In addition, for investigations involving human subjects, informed consent has been obtained from the participants involved.

Executive summary

- Short chimerical proteins produced in bacteria, that contain four functional domains relevant to intracellular trafficking, promote high transgene expression levels when used as artificial viruses.
- The presence of DNA promotes conformational changes in the protein moiety of the artificial viruses that affects the minor α -helix region exhibited by rather unstructured peptides.
- The resulting artificial viruses are pseudo-spherical stable particles of approximately 80 nm, fully sustained by DNA–protein interactions rather than by protein–protein cross-molecular β -sheet interactions, which at difference from protein-only aggregates, are undetectable

Bibliography

Papers of special note have been highlighted as:

* of interest

** of considerable interest

- 1 Smaglik P. Clinical trials end at gene-therapy institute. *Nature* 405(6786), 497 (2000).
- 2 Edelstein ML, Abedi MR, Wixon J. Gene therapy clinical trials worldwide to 2007: an update. *J. Gene Med.* 9(10), 833–842 (2007).
- 3 Marshall E. Gene therapy. Second child in French trial is found to have leukemia. *Science* 299(5605), 320 (2003).
- 4 Marshall E. Gene therapy. What to do when clear success comes with an unclear risk? *Science* 298(5593), 510–511 (2002).
- 5 Smaglik P. Tighter watch urged on adenoviral vectors ... with proposal to report all 'adverse events'. *Nature* 402(6763), 707 (1999).
- 6 Douglas KL. Toward development of artificial viruses for gene therapy: a comparative evaluation of viral and non-viral transfection. *Biotechnol. Prog.* 24(4), 871–883 (2008).
- 7 Mastrobattista E, van der Aa MA, Hennink WE, Crommelin DJ. Artificial viruses: a nanotechnological approach to gene delivery. *Nat. Rev. Drug Discov.* 5(2), 115–121 (2006).
- ** The basic principles of artificial virus design and construction are reviewed, describing the diversity of structural approaches and chemical composition of the building blocks.
- 8 Wagner E. Strategies to improve DNA polyplexes for *in vivo* gene transfer: will "artificial viruses" be the answer? *Pharm. Res.* 21(1), 8–14 (2004).
- 9 Maham A, Tang Z, Wu H, Wang J, Lin Y. Protein-based nanomedicine platforms for drug delivery. *Small* 5(15), 1706–1721 (2009).
- * The spectrum of self-assembling protein materials with potential as platforms for drug delivery is extensively reviewed.
- 10 Petry H, Goldmann C, Axt O, Luke W. The use of virus-like particles for gene transfer. *Curr. Opin. Mol. Ther.* 5(5), 524–528 (2005).
- 11 Wu M, Sherwin T, Brown WL, Stockley PG. Delivery of antisense oligonucleotides to leukemia cells by RNA bacteriophage capsids. *Nanomedicine (Lond.)* 1(1), 67–76 (2005).
- 12 Aris A, Villaverde A. Modular protein engineering for non-viral gene therapy. *Trends Biotechnol.* 22(7), 371–377 (2004).
- 13 Vazquez E, Ferrer-Miralles N, Villaverde A. Peptide-assisted traffic engineering for nonviral gene therapy. *Drug Discov. Today* 13(23–24), 1067–1074 (2008).
- 14 Ferrer-Miralles N, Vazquez E, Villaverde A. Membrane-active peptides for non-viral gene therapy: making the safest easier. *Trends Biotechnol.* 26(5), 267–275 (2008).
- 15 Vazquez E, Roldán M, Díez-Gil C *et al.* Protein nanodisk assembling and intracellular trafficking powered by an arginine-rich (R9) peptide. *Nanomedicine (Lond.)* 5, 259–268 (2010).
- 16 Vazquez E, Cubarsi R, Unzueta U *et al.* Internalization and kinetics of nuclear migration of protein-only, arginine-rich nanoparticles. *Biomaterials* 31(35), 9333–9339 (2010).
- ** The internalization pattern and nuclear migration routes of a self-assembling, protein-only nanoparticle based on arginine-rich peptides are finely dissected.
- 17 Xavier J, Singh S, Dean DA, Rao NM, Gopal V. Designed multi-domain protein as a carrier of nucleic acids into cells. *J. Control Release* 133(2), 154–160 (2009).
- * The potential of a protein-only, Tat-derived modular construct for gene therapy is clearly shown through elegant experiments.
- 18 Peluffo H, Acarín L, Aris A *et al.* Neuroprotection from NMDA excitotoxic lesion by Cu/Zn superoxide dismutase gene delivery to the postnatal rat brain by a modular protein vector. *BMC Neurosci.* 7, 35 (2006).
- 19 Peluffo H, Aris A, Acarín L, Gonzalez B, Villaverde A, Castellano B. Nonviral gene delivery to the central nervous system based on a novel integrin-targeting multifunctional protein. *Hum. Gene Ther.* 14(13), 1215–1223 (2003).
- 20 Benito A, Mateu MG, Villaverde A. Improved mimicry of a foot-and-mouth disease virus antigenic site by a viral peptide displayed on β -galactosidase surface. *Biotechnol. NY* 13(8), 801–804 (1995).
- 21 Feliu JX, Benito A, Oliva B, Aviles FX, Villaverde A. Conformational flexibility in a highly mobile protein loop of foot-and-mouth disease virus: distinct structural requirements for integrin and antibody binding. *J. Mol. Biol.* 283(2), 331–338 (1998).
- 22 Villaverde A, Feliu JX, Harbottle RP, Benito A, Coustelle C. A recombinant, arginine-glycine-aspartic acid (RGD)

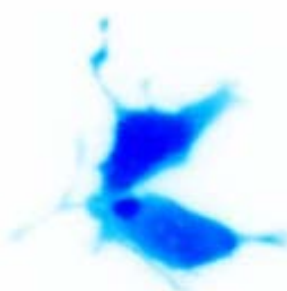
- motif from foot-and-mouth disease virus binds mammalian cells through vitronectin and, to a lower extent, fibronectin receptors. *Gene* 180(1-2), 101-106 (1996).
- 23 Yoneda Y. How proteins are transported from cytoplasm to the nucleus. *J. Biochem.* 121(5), 811-817 (1997).
- 24 Collins E, Birchall JC, Williams JL, Gumbleton M. Nuclear localisation and pDNA condensation in non-viral gene delivery. *J. Gene Med.* 9(4), 265-274 (2007).
- 25 Saccardo P, Villaverde A, Gonzalez-Montalban N. Peptide-mediated DNA condensation for non-viral gene therapy. *Biotechnol. Adv.* 27(4), 432-438 (2009).
- 26 Block H, Maertens B, Spriestersbach A *et al.* Immobilized-metal affinity chromatography (IMAC): a review. *Methods Enzymol.* 463, 439-473 (2009).
- 27 Garcia-Fruitos E, Seras-Franzoso J, Vazquez E, Villaverde A. Tunable geometry of bacterial inclusion bodies as substrate materials for tissue engineering. *Nanotechnology* 21(20), 205101 (2010).
- 28 Eswar N, Marti-Renom MA, Webb B *et al.* Comparative protein structure modeling with MODELLER. John Wiley & Sons, Inc., NJ, USA (Suppl. 15), 5.6.1-5.6.30 (2009).
- 29 Fontes MR, Teh T, Toth G *et al.* Role of flanking sequences and phosphorylation in the recognition of the simian-virus-40 large T-antigen nuclear localization sequences by importin- α . *Biochem. J.* 375(Pt 2), 339-349 (2003).
- 30 Hewat EA, Vendaguer N, Fita I *et al.* Structure of the complex of an Fab fragment of a neutralizing antibody with foot-and-mouth disease virus: positioning of a highly mobile antigenic loop. *EMBO J.* 16(7), 1492-1500 (1997).
- 31 Davidson B, Fasman GD. The conformational transitions of uncharged poly-L-lysine. α helix-random coil- β structure. *Biochemistry* 6(6), 1616-1629 (1967).
- 32 Pakhomova ON, Deep S, Huang Q, Zwiab C, Hinck AP. Solution structure of protein SRP19 of *Archaeoglobus fulgidus* signal recognition particle. *J. Mol. Biol.* 317(1), 145-158 (2002).
- 33 Chen J, Lee KH, Steinhauer DA, Stevens DJ, Skehel JJ, Wiley DC. Structure of the hemagglutinin precursor cleavage site, a determinant of influenza pathogenicity and the origin of the labile conformation. *Cell* 95(3), 409-417 (1998).
- 34 Petegnief V, Friguls B, Sanfeliu C, Sunol C, Planas AM. Transforming growth factor- α attenuates *N*-methyl-D-aspartic acid toxicity in cortical cultures by preventing protein synthesis inhibition through an Erk1/2-dependent mechanism. *J. Biol. Chem.* 278(52), 29552-29559 (2003).
- 35 Garcia-Fruitos E, Rodriguez-Carmona E, Diez-Gil C *et al.* Surface cell growth engineering assisted by a novel bacterial nanomaterial. *Adv. Mater.* 21(42), 4249-4253 (2009).
- 36 de Marco A, Schroedel A. Characterization of the aggregates formed during recombinant protein expression in bacteria. *BMC Biochem.* 6(1), 10 (2005).
- 37 Martinez-Alonso M, Gonzalez-Montalban N, Garcia-Fruitos E, Villaverde A. The functional quality of soluble recombinant polypeptides produced in *Escherichia coli* is defined by a wide conformational spectrum. *Appl. Environ. Microbiol.* 101(6), 1353-1358 (2008).
- 38 Doglia SM, Ami D, Natalello A, Gatti-Lafranconi P, Lotti M. Fourier transform infrared spectroscopy analysis of the conformational quality of recombinant proteins within inclusion bodies. *Biotechnol. J.* 3(2), 193-201 (2008).
- 39 Gonzalez-Montalban N, Natalello A, Garcia-Fruitos E, Villaverde A, Doglia SM. *In situ* protein folding and activation in bacterial inclusion bodies. *Biotechnol. Bioeng.* 100(4), 797-802 (2008).
- 40 Ami D, Natalello A, Taylor G, Tonon G, Maria DS. Structural analysis of protein inclusion bodies by Fourier transform infrared microspectroscopy. *Biochim. Biophys. Acta* 1764(4), 793-799 (2006).
- 41 Wang L, Maji SK, Sawaya MR, Eisenberg D, Rick R. Bacterial inclusion bodies contain amyloid-like structure. *PLoS Biol.* 6(8), e195 (2008).
- 42 Carrio M, Gonzalez-Montalban N, Vera A, Villaverde A, Ventura S. Amyloid-like properties of bacterial inclusion bodies. *J. Mol. Biol.* 347(5), 1025-1037 (2005).
- 43 Natalello A, Ami D, Brocca S, Lotti M, Doglia SM. Secondary structure, conformational stability and glycosylation of a recombinant *Candida rugosa* lipase studied by Fourier-transform infrared spectroscopy. *Biochem. J.* 385(Pt 2), 511-517 (2005).
- 44 Greenfield NJ. Using circular dichroism collected as a function of temperature to determine the thermodynamics of protein unfolding and binding interactions. *Nat. Protoc.* 1(6), 2527-2535 (2006).
- 45 Jiang W, Kim BY, Rutka JT, Chan WC. Nanoparticle-mediated cellular response is size-dependent. *Nat. Nanotechnol.* 3(3), 145-150 (2008).
- ** The size effect of nanoparticles on the mammalian cell biology is demonstrated in biological interfaces.
- 46 Chithrani BD, Ghazani AA, Chan WC. Determining the size and shape dependence of gold nanoparticle uptake into mammalian cells. *Nano Lett.* 6(4), 662-668 (2006).
- 47 Jiang W, Kim BY, Rutka JT, Chan WC. Advances and challenges of nanotechnology-based drug delivery systems. *Expert. Opin. Drug Deliv.* 4(6), 621-633 (2007).
- 48 Corchero JL, Villaverde A. Biomedical applications of distally controlled magnetic nanoparticles. *Trends Biotechnol.* 27(8), 468-476 (2009).
- 49 Vazquez E, Ferrer-Miralles N, Mangues R, Corchero JL, Schwartz S Jr, Villaverde A. Modular protein engineering in emerging cancer therapies. *Curr. Pharm. Des.* 15(8), 893-916 (2009).
- 50 Ferrer-Miralles N, Domingo-Espín J, Corchero JL, Vazquez E, Villaverde A. Microbial factories for recombinant pharmaceuticals. *Microb. Cell Fact.* 8(1), 17 (2009).
- 51 Rodriguez-Carmona E, Villaverde A. Nanostructured bacterial materials for innovative medicines. *Trends Microbiol.* 18(9), 423-430 (2010).
- 52 Uchida M, Klem MT, Allen M *et al.* Biological containers: protein cages as multifunctional nanoplateforms. *Adv. Mater.* 19, 1025-1042 (2007).
- 53 Aris A, Felix JX, Knight A, Coutelle C, Villaverde A. Exploiting viral cell-targeting abilities in a single polypeptide, non-infectious, recombinant vehicle for integrin-mediated DNA delivery and gene expression. *Biotechnol. Bioeng.* 68(6), 689-696 (2000).
- 54 Aris A, Villaverde A. Engineering nuclear localization signals in modular protein vehicles for gene therapy. *Biochem. Biophys. Res. Commun.* 304(4), 625-631 (2003).
- 55 Jacobson RH, Zhang XJ, DuBose RF, Matthews BW. Three-dimensional structure of β -galactosidase from *E. coli*. *Nature* 369(6483), 761-766 (1994).
- 56 Aris A, Villaverde A. Molecular organization of protein-DNA complexes for cell-targeted DNA delivery. *Biochem. Biophys. Res. Commun.* 278(2), 455-461 (2000).
- 57 Peluffo H, Gonzalez P, Aris A *et al.* RGD domains neuroprotect the immature brain by a glial-dependent mechanism. *Ann. Neurol.* 62(3), 251-261 (2007).
- 58 Tagawa T, Manvell M, Brown N *et al.* Characterisation of LMD virus-like nanoparticles self-assembled from cationic liposomes, adenovirus core peptide mu and plasmid DNA. *Gene Ther.* 9(9), 564-576 (2002).
- 59 Keller M, Tagawa T, Preuss M, Miller AD. Biophysical characterization of the DNA

- binding and condensing properties of adenoviral core peptide μ . *Biochemistry* 41(2), 652–659 (2002).
- 60 Midoux P, LeCam E, Coulaud D, Delain E, Pichon C. Histidine containing peptides and polypeptides as nucleic acid vectors. *Somat. Cell Mol. Genet.* 27(1–6), 27–47 (2002).
- 61 Ramsay E, Hadgraft J, Birchall J, Gumbleton M. Examination of the biophysical interaction between plasmid DNA and the polycations, polylysine and polyornithine, as a basis for their differential gene transfection *in-vitro*. *Int. J. Pharm.* 210(1–2), 97–107 (2000).
- 62 Teclé M, Preuss M, Miller AD. Kinetic study of DNA condensation by cationic peptides used in nonviral gene therapy: analogy of DNA condensation to protein folding. *Biochemistry* 42(35), 10343–10347 (2003).
- * The states of DNA condensation during interaction with cationic peptides have been analyzed, revealing the obstacles posed to DNA transcription at high peptide–DNA ratios.

Annex 7

Other publications

1. Mónica Martínez-Alonso , Verónica Toledo-Rubio, Rob Noad , Ugutz Unzueta, Neus Ferrer-Miralles , Polly Roy , Antonio Villaverde ; **Re-hosting bacterial chaperones for high-quality protein production**; Applied and Environmental Microbiology; 75(24): 7850–7854; 2009.
2. Verónica Toledo-Rubio, Esther Vazquez , Gemma Platas , Joan Domingo-Espín , Ugutz Unzueta, Elena García-Fruitós, Neus Ferrer-Miralles, Antonio P Villaverde; **Protein aggregation and soluble aggregate formation screened by a fast microdialysis assay** ; Journal of Biomolecular Screening; 15 (4):453-457 2010
3. Joan Domingo Espín, Ugutz Unzueta, Paolo Saccardo, Escarlata Rodríguez-Carmona, Jose Luis Corchero, Esther Vazquez and Neus Ferrer-Miralles; **Biological Entities for Drug Delivery and Gene Therapy: Protein Nanoparticles**; Progress in Molecular Biology and Translational Science: Nanoparticles in translational science and medicine; 104 247-298; 2011
4. Joan Domingo-Espín, Valérie Petegnief, Núria de Vera, Oscar Conchillo-Solé, Paolo Saccardo, Ugutz Unzueta, Esther Vazquez, Juan Cedano, Luciana Negro, Xavier Daur, Hugo Peluffo , Anna M. Planas , Antonio Villaverde, Neus Ferrer-Miralles; **RGD-based cell ligands for cell-targeted drug delivery act as potent trophic factors**; Nanomedicine, 8 (8) 1263:6; 2012.
5. Seras-Franzoso J, Peebo K, Corchero JL, Tsimbouri P.M., Unzueta U, Rinas U, Dalby MJ, Vazquez E, García-Fruitós E, Villaverde A. **A nanostructured bacterial bio-scaffold for the sustained bottom-up delivery of protein drugs**. Nanomedicine. [Epub ahead of print]. 2013.
6. Seras-Franzoso J, Peebo K, Corchero JL, Tsimbouri PM, Unzueta U, Rinas U, Dalby MJ, Vazquez E, García-Fruitós E, Villaverde A. **Topographically targeted osteogenesis of mesenchymal stem cells stimulated by inclusion bodies attached to polycaprolactone surfaces**. Nanomedicine (lond) [Epub ahead of print], 2013.



References

Reference List

1. Walker,H.K. The Origins of the History and Physical Examination.(1990).
2. Blevins,S.M. & Bronze,M.S. Robert Koch and the 'golden age' of bacteriology. *Int. J. Infect. Dis.* **14**, e744-e751 (2010).
3. Pasteur,L., Chamberland, & Roux Summary report of the experiments conducted at Pouilly-le-Fort, near Melun, on the anthrax vaccination, 1881. *Yale J. Biol. Med.* **75**, 59-62 (2002).
4. Diggins,F.W. The true history of the discovery of penicillin, with refutation of the misinformation in the literature. *Br. J. Biomed. Sci.* **56**, 83-93 (1999).
5. WATSON,J.D. & CRICK,F.H. Molecular structure of nucleic acids; a structure for deoxyribose nucleic acid. *Nature* **171**, 737-738 (1953).
6. Cohen,S.N., Chang,A.C., Boyer,H.W., & Helling,R.B. Construction of biologically functional bacterial plasmids in vitro. *Proc. Natl. Acad. Sci. U. S. A* **70**, 3240-3244 (1973).
7. Gobin,A.M. *et al.* Near infrared laser-tissue welding using nanoshells as an exogenous absorber. *Lasers Surg. Med.* **37**, 123-129 (2005).
8. Gazouli,M. *et al.* Development of a quantum-dot-labelled magnetic immunoassay method for circulating colorectal cancer cell detection. *World J. Gastroenterol.* **18**, 4419-4426 (2012).
9. Nie,S., Xing,Y., Kim,G.J., & Simons,J.W. Nanotechnology applications in cancer. *Annu. Rev. Biomed. Eng* **9**, 257-288 (2007).
10. Hanahan,D. & Weinberg,R.A. The hallmarks of cancer. *Cell* **100**, 57-70 (2000).
11. Knudson,A.G. Cancer genetics. *Am. J. Med. Genet.* **111**, 96-102 (2002).
12. Danaei,G., Vander,H.S., Lopez,A.D., Murray,C.J., & Ezzati,M. Causes of cancer in the world: comparative risk assessment of nine behavioural and environmental risk factors. *Lancet* **366**, 1784-1793 (2005).
13. Vogelstein,B. & Kinzler,K.W. Cancer genes and the pathways they control. *Nat. Med.* **10**, 789-799 (2004).
14. Pegram,M.D., Konecny,G., & Slamon,D.J. The molecular and cellular biology of HER2/neu gene amplification/overexpression and the clinical development of herceptin (trastuzumab) therapy for breast cancer. *Cancer Treat. Res.* **103**, 57-75 (2000).
15. Slamon,D.J. *et al.* Use of chemotherapy plus a monoclonal antibody against HER2 for metastatic breast cancer that overexpresses HER2. *N. Engl. J Med.* **344**, 783-792 (2001).

References

16. Piccart-Gebhart, M.J. *et al.* Trastuzumab after adjuvant chemotherapy in HER2-positive breast cancer. *N. Engl. J. Med.* **353**, 1659-1672 (2005).
17. Hughes, T.P. *et al.* Frequency of major molecular responses to imatinib or interferon alfa plus cytarabine in newly diagnosed chronic myeloid leukemia. *N. Engl. J. Med.* **349**, 1423-1432 (2003).
18. Druker, B.J. *et al.* Chronic myelogenous leukemia. *Hematology. Am. Soc. Hematol. Educ. Program.* 87-112 (2001).
19. Demetri, G.D. *et al.* Efficacy and safety of imatinib mesylate in advanced gastrointestinal stromal tumors. *N. Engl. J. Med.* **347**, 472-480 (2002).
20. Mechtersheimer, G. *et al.* Gastrointestinal stromal tumours and their response to treatment with the tyrosine kinase inhibitor imatinib. *Virchows Arch.* **444**, 108-118 (2004).
21. Langer, C.J. Emerging role of epidermal growth factor receptor inhibition in therapy for advanced malignancy: focus on NSCLC. *Int. J. Radiat. Oncol. Biol. Phys.* **58**, 991-1002 (2004).
22. Moore, M.J. Brief communication: a new combination in the treatment of advanced pancreatic cancer. *Semin. Oncol.* **32**, 5-6 (2005).
23. Taron, M. *et al.* Activating mutations in the tyrosine kinase domain of the epidermal growth factor receptor are associated with improved survival in gefitinib-treated chemorefractory lung adenocarcinomas. *Clin. Cancer Res.* **11**, 5878-5885 (2005).
24. Lynch, T.J. *et al.* Activating mutations in the epidermal growth factor receptor underlying responsiveness of non-small-cell lung cancer to gefitinib. *N. Engl. J. Med.* **350**, 2129-2139 (2004).
25. Pao, W. *et al.* EGF receptor gene mutations are common in lung cancers from "never smokers" and are associated with sensitivity of tumors to gefitinib and erlotinib. *Proc. Natl. Acad. Sci. U. S. A* **101**, 13306-13311 (2004).
26. Mellinghoff, I.K. *et al.* Molecular determinants of the response of glioblastomas to EGFR kinase inhibitors. *N. Engl. J. Med.* **353**, 2012-2024 (2005).
27. Shepherd, F.A. *et al.* Erlotinib in previously treated non-small-cell lung cancer. *N. Engl. J. Med.* **353**, 123-132 (2005).
28. Baselga, J. *et al.* Phase II multicenter study of the anti-epidermal growth factor receptor monoclonal antibody cetuximab in combination with platinum-based chemotherapy in patients with platinum-refractory metastatic and/or recurrent squamous cell carcinoma of the head and neck. *J. Clin. Oncol.* **23**, 5568-5577 (2005).
29. Cunningham, D. *et al.* Cetuximab monotherapy and cetuximab plus irinotecan in irinotecan-refractory metastatic colorectal cancer. *N. Engl. J. Med.* **351**, 337-345 (2004).

30. Kerbel,R. & Folkman,J. Clinical translation of angiogenesis inhibitors. *Nat. Rev. Cancer* **2**, 727-739 (2002).
31. Folkman,J. Role of angiogenesis in tumor growth and metastasis. *Semin. Oncol.* **29**, 15-18 (2002).
32. Ferrara,N., Hillan,K.J., Gerber,H.P., & Novotny,W. Discovery and development of bevacizumab, an anti-VEGF antibody for treating cancer. *Nat. Rev. Drug Discov.* **3**, 391-400 (2004).
33. Schmitt,C.A. & Lowe,S.W. Apoptosis and therapy. *J. Pathol.* **187**, 127-137 (1999).
34. Okada,H. & Mak,T.W. Pathways of apoptotic and non-apoptotic death in tumour cells. *Nat. Rev. Cancer* **4**, 592-603 (2004).
35. Borst,P. & Rottenberg,S. Cancer cell death by programmed necrosis? *Drug Resist. Updat.* **7**, 321-324 (2004).
36. Weitz,J. *et al.* Colorectal cancer. *Lancet* **365**, 153-165 (2005).
37. Eccles,S.A. & Welch,D.R. Metastasis: recent discoveries and novel treatment strategies. *Lancet* **369**, 1742-1757 (2007).
38. Iizumi,M., Liu,W., Pai,S.K., Furuta,E., & Watabe,K. Drug development against metastasis-related genes and their pathways: a rationale for cancer therapy. *Biochim. Biophys. Acta* **1786**, 87-104 (2008).
39. Kinzler,K.W. & Vogelstein,B. Lessons from hereditary colorectal cancer. *Cell* **87**, 159-170 (1996).
40. Nagasaka,T. *et al.* Hypermethylation of O6-methylguanine-DNA methyltransferase promoter may predict nonrecurrence after chemotherapy in colorectal cancer cases. *Clin. Cancer Res.* **9**, 5306-5312 (2003).
41. Haydon,A.M. & Jass,J.R. Emerging pathways in colorectal-cancer development. *Lancet Oncol.* **3**, 83-88 (2002).
42. Grady,W.M. Genetic testing for high-risk colon cancer patients. *Gastroenterology* **124**, 1574-1594 (2003).
43. Samowitz,W.S. *et al.* The colon cancer burden of genetically defined hereditary nonpolyposis colon cancer. *Gastroenterology* **121**, 830-838 (2001).
44. Venesio,T. *et al.* High frequency of MYH gene mutations in a subset of patients with familial adenomatous polyposis. *Gastroenterology* **126**, 1681-1685 (2004).
45. Sieber,O.M. *et al.* Multiple colorectal adenomas, classic adenomatous polyposis, and germ-line mutations in MYH. *N. Engl. J. Med.* **348**, 791-799 (2003).
46. Yamada,S., Yashiro,M., Maeda,K., Nishiguchi,Y., & Hirakawa,K. A novel high-specificity approach for colorectal neoplasia: Detection of K-ras2 oncogene mutation in normal mucosa. *Int. J Cancer* **113**, 1015-1021 (2005).

References

47. Kumar,R., Sukumar,S., & Barbacid,M. Activation of ras oncogenes preceding the onset of neoplasia. *Science* **248**, 1101-1104 (1990).
48. Ross,P.J. *et al.* Inhibition of Kirsten-ras expression in human colorectal cancer using rationally selected Kirsten-ras antisense oligonucleotides. *Mol. Cancer Ther.* **1**, 29-41 (2001).
49. Benvenuti,S. *et al.* Oncogenic activation of the RAS/RAF signaling pathway impairs the response of metastatic colorectal cancers to anti-epidermal growth factor receptor antibody therapies. *Cancer Res.* **67**, 2643-2648 (2007).
50. Brummelkamp,T.R., Bernards,R., & Agami,R. Stable suppression of tumorigenicity by virus-mediated RNA interference. *Cancer Cell* **2**, 243-247 (2002).
51. Lu,P.Y., Xie,F.Y., & Woodle,M.C. Modulation of angiogenesis with siRNA inhibitors for novel therapeutics. *Trends Mol. Med.* **11**, 104-113 (2005).
52. Matos,P. *et al.* B-Raf(V600E) cooperates with alternative spliced Rac1b to sustain colorectal cancer cell survival. *Gastroenterology* **135**, 899-906 (2008).
53. Oliveira,C. *et al.* KRAS and BRAF oncogenic mutations in MSS colorectal carcinoma progression. *Oncogene* **26**, 158-163 (2007).
54. Davies,H. *et al.* Mutations of the BRAF gene in human cancer. *Nature* **417**, 949-954 (2002).
55. Zeelenberg,I.S., Ruuls-Van,S.L., & Roos,E. The chemokine receptor CXCR4 is required for outgrowth of colon carcinoma micrometastases. *Cancer Res.* **63**, 3833-3839 (2003).
56. Schimanski,C.C., Galle,P.R., & Moehler,M. Chemokine receptor CXCR4-prognostic factor for gastrointestinal tumors. *World J. Gastroenterol.* **14**, 4721-4724 (2008).
57. Gassmann,P. *et al.* CXCR4 regulates the early extravasation of metastatic tumor cells in vivo. *Neoplasia.* **11**, 651-661 (2009).
58. Meyerhardt,J.A. & Mayer,R.J. Systemic therapy for colorectal cancer. *N. Engl. J Med.* **352**, 476-487 (2005).
59. Cercek,A. & Saltz,L.B. First-line treatment of patients with metastatic colorectal cancer: an overview of recent data on chemotherapy plus targeted agents. *Clin. Colorectal Cancer* **7 Suppl 2**, S47-S51 (2008).
60. Tang,M.F., Lei,L., Guo,S.R., & Huang,W.L. Recent progress in nanotechnology for cancer therapy. *Chin J. Cancer* **29**, 775-780 (2010).
61. Park,J.H. *et al.* Cooperative nanoparticles for tumor detection and photothermally triggered drug delivery. *Adv. Mater.* **22**, 880-885 (2010).
62. Gabizon,A., Shmeeda,H., & Barenholz,Y. Pharmacokinetics of pegylated liposomal Doxorubicin: review of animal and human studies. *Clin. Pharmacokinet.* **42**, 419-436 (2003).

63. Cho,K., Wang,X., Nie,S., Chen,Z.G., & Shin,D.M. Therapeutic nanoparticles for drug delivery in cancer. *Clin. Cancer Res.* **14**, 1310-1316 (2008).
64. Maeda,H. Macromolecular therapeutics in cancer treatment: The EPR effect and beyond. *J. Control Release*(2012).
65. Iyer,A.K., Khaled,G., Fang,J., & Maeda,H. Exploiting the enhanced permeability and retention effect for tumor targeting. *Drug Discov. Today* **11**, 812-818 (2006).
66. Petros,R.A. & DeSimone,J.M. Strategies in the design of nanoparticles for therapeutic applications. *Nat. Rev. Drug Discov.* **9**, 615-627 (2010).
67. Vasir,J.K. & Labhasetwar,V. Biodegradable nanoparticles for cytosolic delivery of therapeutics. *Adv. Drug Deliv. Rev.* **59**, 718-728 (2007).
68. Zhang,Z. *et al.* Biomimetic nanocarrier for direct cytosolic drug delivery. *Angew. Chem. Int. Ed Engl.* **48**, 9171-9175 (2009).
69. Pouton,C.W., Wagstaff,K.M., Roth,D.M., Moseley,G.W., & Jans,D.A. Targeted delivery to the nucleus. *Adv. Drug Deliv. Rev.* **59**, 698-717 (2007).
70. Hodoniczky,J., Sims,C.G., Best,W.M., Bentel,J.M., & Wilce,J.A. The intracellular and nuclear-targeted delivery of an antiandrogen drug by carrier peptides. *Biopolymers* **90**, 595-603 (2008).
71. Misra,R. & Sahoo,S.K. Intracellular trafficking of nuclear localization signal conjugated nanoparticles for cancer therapy. *Eur. J. Pharm. Sci.* **39**, 152-163 (2010).
72. Mukhopadhyay,A. & Weiner,H. Delivery of drugs and macromolecules to mitochondria. *Adv. Drug Deliv. Rev.* **59**, 729-738 (2007).
73. Yamada,Y. & Harashima,H. Mitochondrial drug delivery systems for macromolecule and their therapeutic application to mitochondrial diseases. *Adv. Drug Deliv. Rev.* **60**, 1439-1462 (2008).
74. Terlecky,S.R. & Koepke,J.I. Drug delivery to peroxisomes: employing unique trafficking mechanisms to target protein therapeutics. *Adv. Drug Deliv. Rev.* **59**, 739-747 (2007).
75. Bareford,L.M. & Swaan,P.W. Endocytic mechanisms for targeted drug delivery. *Adv. Drug Deliv. Rev.* **59**, 748-758 (2007).
76. Jain,M., Venkatraman,G., & Batra,S.K. Optimization of radioimmunotherapy of solid tumors: biological impediments and their modulation. *Clin. Cancer Res.* **13**, 1374-1382 (2007).
77. Dreaden,E.C., Austin,L.A., Mackey,M.A., & El-Sayed,M.A. Size matters: gold nanoparticles in targeted cancer drug delivery. *Ther. Deliv.* **3**, 457-478 (2012).
78. Schroeder,A. *et al.* Treating metastatic cancer with nanotechnology. *Nat. Rev. Cancer* **12**, 39-50 (2012).

References

79. Champion,J.A., Katare,Y.K., & Mitragotri,S. Particle shape: a new design parameter for micro- and nanoscale drug delivery carriers. *J. Control Release* **121**, 3-9 (2007).
80. Moghimi,S.M., Hunter,A.C., & Murray,J.C. Long-circulating and target-specific nanoparticles: theory to practice. *Pharmacol. Rev.* **53**, 283-318 (2001).
81. Choi,H.S. *et al.* Renal clearance of quantum dots. *Nat. Biotechnol.* **25**, 1165-1170 (2007).
82. Choi,H.S. *et al.* Rapid translocation of nanoparticles from the lung airspaces to the body. *Nat. Biotechnol.* **28**, 1300-1303 (2010).
83. Reddy,S.T. *et al.* Exploiting lymphatic transport and complement activation in nanoparticle vaccines. *Nat. Biotechnol.* **25**, 1159-1164 (2007).
84. Raz,A., Bucana,C., Fogler,W.E., Poste,G., & Fidler,I.J. Biochemical, morphological, and ultrastructural studies on the uptake of liposomes by murine macrophages. *Cancer Res.* **41**, 487-494 (1981).
85. Sadauskas,E. *et al.* Kupffer cells are central in the removal of nanoparticles from the organism. *Part Fibre. Toxicol.* **4**, 10 (2007).
86. Azarmi,S., Roa,W.H., & Lobenberg,R. Targeted delivery of nanoparticles for the treatment of lung diseases. *Adv. Drug Deliv. Rev.* **60**, 863-875 (2008).
87. Edwards,D.A. *et al.* Large porous particles for pulmonary drug delivery. *Science* **276**, 1868-1871 (1997).
88. Jiang,W., Kim,B.Y., Rutka,J.T., & Chan,W.C. Nanoparticle-mediated cellular response is size-dependent. *Nat. Nanotechnol.* **3**, 145-150 (2008).
89. Chithrani,B.D., Ghazani,A.A., & Chan,W.C. Determining the size and shape dependence of gold nanoparticle uptake into mammalian cells. *Nano. Lett.* **6**, 662-668 (2006).
90. Gao,H., Shi,W., & Freund,L.B. Mechanics of receptor-mediated endocytosis. *Proc. Natl. Acad. Sci. U. S. A* **102**, 9469-9474 (2005).
91. Mukherjee,S., Ghosh,R.N., & Maxfield,F.R. Endocytosis. *Physiol Rev.* **77**, 759-803 (1997).
92. Medina-Kauwe,L.K., Xie,J., & Hamm-Alvarez,S. Intracellular trafficking of nonviral vectors. *Gene Ther.* **12**, 1734-1751 (2005).
93. Doherty,G.J. & McMahon,H.T. Mechanisms of endocytosis. *Annu. Rev. Biochem.* **78**, 857-902 (2009).
94. Rejman,J., Oberle,V., Zuhorn,I.S., & Hoekstra,D. Size-dependent internalization of particles via the pathways of clathrin- and caveolae-mediated endocytosis. *Biochem J* **377**, 159-169 (2004).

95. Tkachenko,A.G. *et al.* Multifunctional gold nanoparticle-peptide complexes for nuclear targeting. *J. Am. Chem. Soc.* **125**, 4700-4701 (2003).
96. Harashima,H., Sakata,K., Funato,K., & Kiwada,H. Enhanced hepatic uptake of liposomes through complement activation depending on the size of liposomes. *Pharm. Res.* **11**, 402-406 (1994).
97. Hardman,R. A toxicologic review of quantum dots: toxicity depends on physicochemical and environmental factors. *Environ. Health Perspect.* **114**, 165-172 (2006).
98. Duncan,R. & Gaspar,R. Nanomedicine(s) under the microscope. *Mol. Pharm.* **8**, 2101-2141 (2011).
99. Muller,R.H. & Keck,C.M. Drug delivery to the brain--realization by novel drug carriers. *J. Nanosci. Nanotechnol.* **4**, 471-483 (2004).
100. Blasi,P., Schoubben,A., Giovagnoli,S., Rossi,C., & Ricci,M. Lipid nanoparticles for drug delivery to the brain: in vivo veritas. *J. Biomed. Nanotechnol.* **5**, 344-350 (2009).
101. Wood,B.J. *et al.* Phase I study of heat-deployed liposomal doxorubicin during radiofrequency ablation for hepatic malignancies. *J. Vasc. Interv. Radiol.* **23**, 248-255 (2012).
102. Turner,D.C., Moshkelani,D., Shemesh,C.S., Luc,D., & Zhang,H. Near-infrared image-guided delivery and controlled release using optimized thermosensitive liposomes. *Pharm. Res.* **29**, 2092-2103 (2012).
103. Leite,E.A. *et al.* Encapsulation of cisplatin in long-circulating and pH-sensitive liposomes improves its antitumor effect and reduces acute toxicity. *Int. J. Nanomedicine.* **7**, 5259-5269 (2012).
104. Pearson,R.M., Sunoqrot,S., Hsu,H.J., Bae,J.W., & Hong,S. Dendritic nanoparticles: the next generation of nanocarriers? *Ther. Deliv.* **3**, 941-959 (2012).
105. Murphy,E.A. *et al.* Targeted nanogels: a versatile platform for drug delivery to tumors. *Mol. Cancer Ther.* **10**, 972-982 (2011).
106. Astete,C.E. & Sabliov,C.M. Synthesis and characterization of PLGA nanoparticles. *J. Biomater. Sci. Polym. Ed* **17**, 247-289 (2006).
107. Kukowska-Latallo,J.F. *et al.* Nanoparticle targeting of anticancer drug improves therapeutic response in animal model of human epithelial cancer. *Cancer Res.* **65**, 5317-5324 (2005).
108. El-Sayed,M., Kiani,M.F., Naimark,M.D., Hikal,A.H., & Ghandehari,H. Extravasation of poly(amidoamine) (PAMAM) dendrimers across microvascular network endothelium. *Pharm. Res.* **18**, 23-28 (2001).
109. Davis,M.E. The first targeted delivery of siRNA in humans via a self-assembling, cyclodextrin polymer-based nanoparticle: from concept to clinic. *Mol. Pharm.* **6**, 659-668 (2009).

References

110. Libutti,S.K. *et al.* Phase I and pharmacokinetic studies of CYT-6091, a novel PEGylated colloidal gold-rhTNF nanomedicine. *Clin. Cancer Res.* **16**, 6139-6149 (2010).
111. Lal,S., Clare,S.E., & Halas,N.J. Nanoshell-enabled photothermal cancer therapy: impending clinical impact. *Acc. Chem. Res.* **41**, 1842-1851 (2008).
112. Atkinson,R.L. *et al.* Thermal enhancement with optically activated gold nanoshells sensitizes breast cancer stem cells to radiation therapy. *Sci. Transl. Med.* **2**, 55ra79 (2010).
113. Maier-Hauff,K. *et al.* Efficacy and safety of intratumoral thermotherapy using magnetic iron-oxide nanoparticles combined with external beam radiotherapy on patients with recurrent glioblastoma multiforme. *J. Neurooncol.* **103**, 317-324 (2011).
114. Lubbe,A.S. *et al.* Clinical experiences with magnetic drug targeting: a phase I study with 4'-epidoxorubicin in 14 patients with advanced solid tumors. *Cancer Res.* **56**, 4686-4693 (1996).
115. Scarberry,K.E., Dickerson,E.B., Zhang,Z.J., Benigno,B.B., & McDonald,J.F. Selective removal of ovarian cancer cells from human ascites fluid using magnetic nanoparticles. *Nanomedicine.* **6**, 399-408 (2010).
116. Slowing,I.I., Trewyn,B.G., & Lin,V.S. Mesoporous silica nanoparticles for intracellular delivery of membrane-impermeable proteins. *J. Am. Chem. Soc.* **129**, 8845-8849 (2007).
117. Alivisatos,A.P., Gu,W., & Larabell,C. Quantum dots as cellular probes. *Annu. Rev. Biomed. Eng* **7**, 55-76 (2005).
118. Gao,X., Cui,Y., Levenson,R.M., Chung,L.W., & Nie,S. In vivo cancer targeting and imaging with semiconductor quantum dots. *Nat. Biotechnol.* **22**, 969-976 (2004).
119. Partha,R., Lackey,M., Hirsch,A., Casscells,S.W., & Conyers,J.L. Self assembly of amphiphilic C60 fullerene derivatives into nanoscale supramolecular structures. *J. Nanobiotechnology.* **5**, 6 (2007).
120. Sinha,N. & Yeow,J.T. Carbon nanotubes for biomedical applications. *IEEE Trans. Nanobioscience.* **4**, 180-195 (2005).
121. Chow,E.K. *et al.* Nanodiamond therapeutic delivery agents mediate enhanced chemoresistant tumor treatment. *Sci. Transl. Med.* **3**, 73ra21 (2011).
122. Kam,N.W., Liu,Z., & Dai,H. Functionalization of carbon nanotubes via cleavable disulfide bonds for efficient intracellular delivery of siRNA and potent gene silencing. *J. Am. Chem. Soc.* **127**, 12492-12493 (2005).
123. Pogodin,S. & Baulin,V.A. Can a carbon nanotube pierce through a phospholipid bilayer? *ACS Nano.* **4**, 5293-5300 (2010).
124. Kostarelos,K. *et al.* Cellular uptake of functionalized carbon nanotubes is independent of functional group and cell type. *Nat. Nanotechnol.* **2**, 108-113 (2007).

125. Maham,A., Tang,Z., Wu,H., Wang,J., & Lin,Y. Protein-based nanomedicine platforms for drug delivery. *Small* **5**, 1706-1721 (2009).
126. Ludwig,C. & Wagner,R. Virus-like particles-universal molecular toolboxes. *Curr. Opin. Biotechnol.* **18**, 537-545 (2007).
127. Roldao,A., Mellado,M.C., Castilho,L.R., Carrondo,M.J., & Alves,P.M. Virus-like particles in vaccine development. *Expert. Rev. Vaccines.* **9**, 1149-1176 (2010).
128. Mastrobattista,E., van der Aa,M.A., Hennink,W.E., & Crommelin,D.J. Artificial viruses: a nanotechnological approach to gene delivery. *Nat. Rev. Drug Discov.* **5**, 115-121 (2006).
129. Aris,A. & Villaverde,A. Modular protein engineering for non-viral gene therapy. *Trends Biotechnol.* **22**, 371-377 (2004).
130. Douglas,K.L. Toward development of artificial viruses for gene therapy: a comparative evaluation of viral and non-viral transfection. *Biotechnol. Prog.* **24**, 871-883 (2008).
131. Gradishar,W.J. *et al.* Phase III trial of nanoparticle albumin-bound paclitaxel compared with polyethylated castor oil-based paclitaxel in women with breast cancer. *J. Clin. Oncol.* **23**, 7794-7803 (2005).
132. Aaron,J., Travis,K., Harrison,N., & Sokolov,K. Dynamic imaging of molecular assemblies in live cells based on nanoparticle plasmon resonance coupling. *Nano. Lett.* **9**, 3612-3618 (2009).
133. Thomas,M. & Klibanov,A.M. Conjugation to gold nanoparticles enhances polyethylenimine's transfer of plasmid DNA into mammalian cells. *Proc. Natl. Acad. Sci. U. S. A* **100**, 9138-9143 (2003).
134. Li,P., Li,D., Zhang,L., Li,G., & Wang,E. Cationic lipid bilayer coated gold nanoparticles-mediated transfection of mammalian cells. *Biomaterials* **29**, 3617-3624 (2008).
135. Masuda,T. *et al.* Envelope-type lipid nanoparticles incorporating a short PEG-lipid conjugate for improved control of intracellular trafficking and transgene transcription. *Biomaterials* **30**, 4806-4814 (2009).
136. Lin,M.M., Kim,d.K., El Haj,A.J., & Dobson,J. Development of superparamagnetic iron oxide nanoparticles (SPIONS) for translation to clinical applications. *IEEE Trans. Nanobioscience.* **7**, 298-305 (2008).
137. Yu,M. *et al.* A simple approach to prepare monodisperse mesoporous silica nanospheres with adjustable sizes. *J. Colloid Interface Sci.* **376**, 67-75 (2012).
138. Merkel,T.J. *et al.* Scalable, shape-specific, top-down fabrication methods for the synthesis of engineered colloidal particles. *Langmuir* **26**, 13086-13096 (2010).
139. Dunn,S.S. *et al.* Reductively responsive siRNA-conjugated hydrogel nanoparticles for gene silencing. *J. Am. Chem. Soc.* **134**, 7423-7430 (2012).

References

140. Elizondo,E., Veciana,J., & Ventosa,N. Nanostructuring molecular materials as particles and vesicles for drug delivery, using compressed and supercritical fluids. *Nanomedicine. (Lond)* **7**, 1391-1408 (2012).
141. Corchero,J.L. & Cedano,J. Self-assembling, protein-based intracellular bacterial organelles: emerging vehicles for encapsulating, targeting and delivering therapeutical cargoes. *Microb. Cell Fact.* **10**, 92 (2011).
142. Tolcher,A.W. *et al.* Randomized phase II study of BR96-doxorubicin conjugate in patients with metastatic breast cancer. *J. Clin. Oncol.* **17**, 478-484 (1999).
143. Alberts,D.S. & Garcia,D.J. Safety aspects of pegylated liposomal doxorubicin in patients with cancer. *Drugs* **54 Suppl 4**, 30-35 (1997).
144. Plank,C., Mechtler,K., Szoka,F.C., Jr., & Wagner,E. Activation of the complement system by synthetic DNA complexes: a potential barrier for intravenous gene delivery. *Hum. Gene Ther.* **7**, 1437-1446 (1996).
145. Szebeni,J. & Moghimi,S.M. Liposome triggering of innate immune responses: a perspective on benefits and adverse reactions. *J. Liposome Res.* **19**, 85-90 (2009).
146. Hamad,I., Hunter,A.C., Szebeni,J., & Moghimi,S.M. Poly(ethylene glycol)s generate complement activation products in human serum through increased alternative pathway turnover and a MASP-2-dependent process. *Mol. Immunol.* **46**, 225-232 (2008).
147. Nielsen,G.D., Roursgaard,M., Jensen,K.A., Poulsen,S.S., & Larsen,S.T. In vivo biology and toxicology of fullerenes and their derivatives. *Basic Clin. Pharmacol. Toxicol.* **103**, 197-208 (2008).
148. Aschberger,K. *et al.* Review of carbon nanotubes toxicity and exposure--appraisal of human health risk assessment based on open literature. *Crit Rev. Toxicol.* **40**, 759-790 (2010).
149. Kunzmann,A. *et al.* Toxicology of engineered nanomaterials: focus on biocompatibility, biodistribution and biodegradation. *Biochim. Biophys. Acta* **1810**, 361-373 (2011).
150. Pan,Y. *et al.* Gold nanoparticles of diameter 1.4 nm trigger necrosis by oxidative stress and mitochondrial damage. *Small* **5**, 2067-2076 (2009).
151. Poon,V.K. & Burd,A. In vitro cytotoxicity of silver: implication for clinical wound care. *Burns* **30**, 140-147 (2004).
152. Muller,K. *et al.* Effect of ultrasmall superparamagnetic iron oxide nanoparticles (Ferumoxtran-10) on human monocyte-macrophages in vitro. *Biomaterials* **28**, 1629-1642 (2007).
153. Mahmoudi,M. *et al.* A new approach for the in vitro identification of the cytotoxicity of superparamagnetic iron oxide nanoparticles. *Colloids Surf. B Biointerfaces.* **75**, 300-309 (2010).

154. Bostanci,M.O. & Bagirici,F. Nitric oxide synthesis inhibition attenuates iron-induced neurotoxicity: a stereological study. *Neurotoxicology* **29**, 130-135 (2008).
155. Fadeel,B. & Garcia-Bennett,A.E. Better safe than sorry: Understanding the toxicological properties of inorganic nanoparticles manufactured for biomedical applications. *Adv. Drug Deliv. Rev.* **62**, 362-374 (2010).
156. Lin,Y.S. & Haynes,C.L. Impacts of mesoporous silica nanoparticle size, pore ordering, and pore integrity on hemolytic activity. *J. Am. Chem. Soc.* **132**, 4834-4842 (2010).
157. Templeton,D.M. & Liu,Y. Multiple roles of cadmium in cell death and survival. *Chem. Biol. Interact.* **188**, 267-275 (2010).
158. Tsoi,K.M., Dai,Q., Alman,B.A., & Chan,W.C. Are Quantum Dots Toxic? Exploring the Discrepancy Between Cell Culture and Animal Studies. *Acc. Chem. Res.*(2012).
159. Lovric,J., Cho,S.J., Winnik,F.M., & Maysinger,D. Unmodified cadmium telluride quantum dots induce reactive oxygen species formation leading to multiple organelle damage and cell death. *Chem. Biol.* **12**, 1227-1234 (2005).
160. Maysinger,D., Lovric,J., Eisenberg,A., & Savic,R. Fate of micelles and quantum dots in cells. *Eur. J. Pharm. Biopharm.* **65**, 270-281 (2007).
161. Leroueil,P.R. *et al.* Wide varieties of cationic nanoparticles induce defects in supported lipid bilayers. *Nano. Lett.* **8**, 420-424 (2008).
162. Lee,J.H. *et al.* Nanosized polyamidoamine (PAMAM) dendrimer-induced apoptosis mediated by mitochondrial dysfunction. *Toxicol. Lett.* **190**, 202-207 (2009).
163. Malik,N. *et al.* Dendrimers: relationship between structure and biocompatibility in vitro, and preliminary studies on the biodistribution of 125I-labelled polyamidoamine dendrimers in vivo. *J. Control Release* **65**, 133-148 (2000).
164. Baneyx,F. Recombinant protein expression in Escherichia coli. *Curr. Opin. Biotechnol.* **10**, 411-421 (1999).
165. Human insulin receives FDA approval. *FDA. Drug Bull.* **12**, 18-19 (1982).
166. Schmidt,F.R. Recombinant expression systems in the pharmaceutical industry. *Appl. Microbiol. Biotechnol.* **65**, 363-372 (2004).
167. Ikonomou,L., Schneider,Y.J., & Agathos,S.N. Insect cell culture for industrial production of recombinant proteins. *Appl. Microbiol. Biotechnol.* **62**, 1-20 (2003).
168. Birch,J.R. & Froud,S.J. Mammalian cell culture systems for recombinant protein production. *Biologicals* **22**, 127-133 (1994).
169. Ferrer-Miralles,N., Domingo-Espin,J., Corchero,J.L., Vazquez,E., & Villaverde,A. Microbial factories for recombinant pharmaceuticals. *Microb. Cell Fact.* **8**, 17 (2009).
170. He,M. Cell-free protein synthesis: applications in proteomics and biotechnology. *N. Biotechnol.* **25**, 126-132 (2008).

References

171. Scheffel,U., Rhodes,B.A., Natarajan,T.K., & Wagner,H.N., Jr. Albumin microspheres for study of the reticuloendothelial system. *J. Nucl. Med.* **13**, 498-503 (1972).
172. Vazquez,E. *et al.* Modular protein engineering in emerging cancer therapies. *Curr. Pharm. Des* **15**, 893-916 (2009).
173. Vazquez,E., Ferrer-Miralles,N., & Villaverde,A. Peptide-assisted traffic engineering for nonviral gene therapy. *Drug Discov. Today* **13**, 1067-1074 (2008).
174. Tu,R.S. & Tirrell,M. Bottom-up design of biomimetic assemblies. *Adv. Drug Deliv. Rev.* **56**, 1537-1563 (2004).
175. Leckband,D. Measuring the forces that control protein interactions. *Annu. Rev. Biophys. Biomol. Struct.* **29**, 1-26 (2000).
176. Meyer,E.E., Rosenberg,K.J., & Israelachvili,J. Recent progress in understanding hydrophobic interactions. *Proc. Natl. Acad. Sci. U. S. A* **103**, 15739-15746 (2006).
177. Domingo-Espin,J. *et al.* Nanoparticulate architecture of protein-based artificial viruses is supported by protein-DNA interactions. *Nanomedicine. (Lond)* **6**, 1047-1061 (2011).
178. Domingo-Espin,J. *et al.* Engineered biological entities for drug delivery and gene therapy protein nanoparticles. *Prog. Mol. Biol. Transl. Sci.* **104**, 247-298 (2011).
179. Ramqvist,T., Andreasson,K., & Dalianis,T. Vaccination, immune and gene therapy based on virus-like particles against viral infections and cancer. *Expert. Opin. Biol. Ther.* **7**, 997-1007 (2007).
180. Slilaty,S.N. & Aposhian,H.V. Gene transfer by polyoma-like particles assembled in a cell-free system. *Science* **220**, 725-727 (1983).
181. Lenz,P. *et al.* Papillomavirus-like particles induce acute activation of dendritic cells. *J. Immunol.* **166**, 5346-5355 (2001).
182. Brandenburg,B. *et al.* A novel system for efficient gene transfer into primary human hepatocytes via cell-permeable hepatitis B virus-like particle. *Hepatology* **42**, 1300-1309 (2005).
183. Li,T.C. *et al.* Essential elements of the capsid protein for self-assembly into empty virus-like particles of hepatitis E virus. *J. Virol.* **79**, 12999-13006 (2005).
184. Xiang,J. *et al.* Recombinant hepatitis C virus-like particles expressed by baculovirus: utility in cell-binding and antibody detection assays. *J. Med. Virol.* **68**, 537-543 (2002).
185. Andreasson,K. *et al.* Murine pneumotropic virus chimeric Her2/neu virus-like particles as prophylactic and therapeutic vaccines against Her2/neu expressing tumors. *Int. J. Cancer* **124**, 150-156 (2009).
186. Murtatori,C., Bona,R., & Federico,M. Lentivirus-based virus-like particles as a new protein delivery tool. *Methods Mol. Biol.* **614**, 111-124 (2010).

187. Singh,P., Destito,G., Schneemann,A., & Manchester,M. Canine parvovirus-like particles, a novel nanomaterial for tumor targeting. *J. Nanobiotechnology.* **4**, 2 (2006).
188. Herbst-Kralovetz,M., Mason,H.S., & Chen,Q. Norwalk virus-like particles as vaccines. *Expert. Rev. Vaccines.* **9**, 299-307 (2010).
189. Seow,Y. & Wood,M.J. Biological gene delivery vehicles: beyond viral vectors. *Mol. Ther.* **17**, 767-777 (2009).
190. Krebs,M.R., Domike,K.R., Cannon,D., & Donald,A.M. Common motifs in protein self-assembly. *Faraday Discuss.* **139**, 265-274 (2008).
191. Krebs,M.R., Domike,K.R., & Donald,A.M. Protein aggregation: more than just fibrils. *Biochem. Soc. Trans.* **37**, 682-686 (2009).
192. Peluffo,H. *et al.* Nonviral gene delivery to the central nervous system based on a novel integrin-targeting multifunctional protein. *Hum Gene Ther.* **14**, 1215-1223 (2003).
193. Peluffo,H. *et al.* Neuroprotection from NMDA excitotoxic lesion by Cu/Zn superoxide dismutase gene delivery to the postnatal rat brain by a modular protein vector. *BMC. Neurosci.* **7**, 35 (2006).
194. Domingo-Espin,J. *et al.* RGD-based cell ligands for cell-targeted drug delivery act as potent trophic factors. *Nanomedicine.*(2012).
195. Garcia-Fruitos,E. *et al.* Bacterial inclusion bodies: making gold from waste. *Trends Biotechnol.* **30**, 65-70 (2012).
196. Vazquez,E. *et al.* Functional inclusion bodies produced in bacteria as naturally occurring nanopills for advanced cell therapies. *Adv. Mater.* **24**, 1742-1747 (2012).
197. Villaverde,A. *et al.* Packaging protein drugs as bacterial inclusion bodies for therapeutic applications. *Microb. Cell Fact.* **11**, 76 (2012).
198. Bora,R.S., Gupta,D., Mukkur,T.K., & Saini,K.S. RNA interference therapeutics for cancer: challenges and opportunities (review). *Mol. Med. Report.* **6**, 9-15 (2012).
199. Gavrilov,K. & Saltzman,W.M. Therapeutic siRNA: principles, challenges, and strategies. *Yale J. Biol. Med.* **85**, 187-200 (2012).
200. Shen,H., Sun,T., & Ferrari,M. Nanovector delivery of siRNA for cancer therapy. *Cancer Gene Ther.* **19**, 367-373 (2012).
201. Downward,J. Targeting RAS signalling pathways in cancer therapy. *Nat. Rev. Cancer* **3**, 11-22 (2003).
202. Meng,R.D. & El-Deiry,W.S. Tumor suppressor gene therapy for cancer: from the bench to the clinic. *Drug Resist. Updat.* **1**, 205-210 (1998).

References

203. Greenblatt,M.S., Bennett,W.P., Hollstein,M., & Harris,C.C. Mutations in the p53 tumor suppressor gene: clues to cancer etiology and molecular pathogenesis. *Cancer Res.* **54**, 4855-4878 (1994).
204. Nielsen,L.L. & Maneval,D.C. P53 tumor suppressor gene therapy for cancer. *Cancer Gene Ther.* **5**, 52-63 (1998).
205. Clayman,G.L., Frank,D.K., Bruso,P.A., & Goepfert,H. Adenovirus-mediated wild-type p53 gene transfer as a surgical adjuvant in advanced head and neck cancers. *Clin. Cancer Res.* **5**, 1715-1722 (1999).
206. Bossi,G. & Sacchi,A. Restoration of wild-type p53 function in human cancer: relevance for tumor therapy. *Head Neck* **29**, 272-284 (2007).
207. Shinoura,N. *et al.* Adenovirus-mediated transfer of caspase-8 augments cell death in gliomas: implication for gene therapy. *Hum. Gene Ther.* **11**, 1123-1137 (2000).
208. Kerr,D.J., Young,L.S., Searle,P.F., & McNeish,I.A. Gene directed enzyme prodrug therapy for cancer. *Adv. Drug Deliv. Rev.* **26**, 173-184 (1997).
209. Portsmouth,D., Hlavaty,J., & Renner,M. Suicide genes for cancer therapy. *Mol. Aspects Med.* **28**, 4-41 (2007).
210. Link,C.J., Jr., Levy,J.P., McCann,L.Z., & Moorman,D.W. Gene therapy for colon cancer with the herpes simplex thymidine kinase gene. *J. Surg. Oncol.* **64**, 289-294 (1997).
211. Koyama,F. *et al.* Enzyme/prodrug gene therapy for human colon cancer cells using adenovirus-mediated transfer of the Escherichia coli cytosine deaminase gene driven by a CAG promoter associated with 5-fluorocytosine administration. *J. Exp. Clin. Cancer Res.* **19**, 75-80 (2000).
212. Koyama,F. *et al.* Combined suicide gene therapy for human colon cancer cells using adenovirus-mediated transfer of escherichia coli cytosine deaminase gene and Escherichia coli uracil phosphoribosyltransferase gene with 5-fluorocytosine. *Cancer Gene Ther.* **7**, 1015-1022 (2000).
213. Topfer,K. *et al.* Tumor evasion from T cell surveillance. *J. Biomed. Biotechnol.* **2011**, 918471 (2011).
214. Senzer,N. *et al.* TNFerade biologic, an adenovector with a radiation-inducible promoter, carrying the human tumor necrosis factor alpha gene: a phase I study in patients with solid tumors. *J. Clin. Oncol.* **22**, 592-601 (2004).
215. MacGill,R.S. *et al.* Local gene delivery of tumor necrosis factor alpha can impact primary tumor growth and metastases through a host-mediated response. *Clin. Exp. Metastasis* **24**, 521-531 (2007).
216. Mazzolini,G. *et al.* Regression of colon cancer and induction of antitumor immunity by intratumoral injection of adenovirus expressing interleukin-12. *Cancer Gene Ther.* **6**, 514-522 (1999).

217. Sun,Y. *et al.* In vivo gene transfer of CD40 ligand into colon cancer cells induces local production of cytokines and chemokines, tumor eradication and protective antitumor immunity. *Gene Ther.* **7**, 1467-1476 (2000).
218. Durai,R., Yang,S.Y., Seifalian,A.M., & Winslet,M.C. Principles and applications of gene therapy in colon cancer. *J Gastrointestin. Liver Dis* **17**, 59-67 (2008).
219. Ueda,K. *et al.* The *mdr1* gene, responsible for multidrug-resistance, codes for P-glycoprotein. *Biochem. Biophys. Res. Commun.* **141**, 956-962 (1986).
220. Roninson,I.B. The role of the MDR1 (P-glycoprotein) gene in multidrug resistance in vitro and in vivo. *Biochem. Pharmacol.* **43**, 95-102 (1992).
221. Ishii,M. *et al.* Soluble TRAIL gene and actinomycin D synergistically suppressed multiple metastasis of TRAIL-resistant colon cancer in the liver. *Cancer Lett.* **245**, 134-143 (2007).
222. Yang,B., Eshleman,J.R., Berger,N.A., & Markowitz,S.D. Wild-type p53 protein potentiates cytotoxicity of therapeutic agents in human colon cancer cells. *Clin. Cancer Res.* **2**, 1649-1657 (1996).
223. Ogawa,N. *et al.* Novel combination therapy for human colon cancer with adenovirus-mediated wild-type p53 gene transfer and DNA-damaging chemotherapeutic agent. *Int. J. Cancer* **73**, 367-370 (1997).
224. Wildner,O., Blaese,R.M., & Candotti,F. Enzyme prodrug gene therapy: synergistic use of the herpes simplex virus-cellular thymidine kinase/ganciclovir system and thymidylate synthase inhibitors for the treatment of colon cancer. *Cancer Res.* **59**, 5233-5238 (1999).
225. Hou,S. *et al.* Eradication of hepatoma and colon cancer in mice with Flt3L gene therapy in combination with 5-FU. *Cancer Immunol. Immunother.* **56**, 1605-1613 (2007).
226. Rosenberg,S.A. *et al.* Gene transfer into humans--immunotherapy of patients with advanced melanoma, using tumor-infiltrating lymphocytes modified by retroviral gene transduction. *N. Engl. J. Med.* **323**, 570-578 (1990).
227. Lundstrom,K. Latest development in viral vectors for gene therapy. *Trends Biotechnol.* **21**, 117-122 (2003).
228. Baum,C. Insertional mutagenesis in gene therapy and stem cell biology. *Curr. Opin. Hematol.* **14**, 337-342 (2007).
229. Nienhuis,A.W., Dunbar,C.E., & Sorrentino,B.P. Genotoxicity of retroviral integration in hematopoietic cells. *Mol. Ther.* **13**, 1031-1049 (2006).
230. Tomanin,R. & Scarpa,M. Why do we need new gene therapy viral vectors? Characteristics, limitations and future perspectives of viral vector transduction. *Curr. Gene Ther.* **4**, 357-372 (2004).
231. Smaglik,P. Tighter watch urged on adenoviral vectors...with proposal to report all 'adverse events'. *Nature* **402**, 707 (1999).

References

232. Dewey,R.A. *et al.* Chronic brain inflammation and persistent herpes simplex virus 1 thymidine kinase expression in survivors of syngeneic glioma treated by adenovirus-mediated gene therapy: implications for clinical trials. *Nat. Med.* **5**, 1256-1263 (1999).
233. Cowsill,C. *et al.* Central nervous system toxicity of two adenoviral vectors encoding variants of the herpes simplex virus type 1 thymidine kinase: reduced cytotoxicity of a truncated HSV1-TK. *Gene Ther.* **7**, 679-685 (2000).
234. Marshall,E. Gene therapy. Second child in French trial is found to have leukemia. *Science* **299**, 320 (2003).
235. Marshall,E. Gene therapy. What to do when clear success comes with an unclear risk? *Science* **298**, 510-511 (2002).
236. Yla-Herttuala,S. Endgame: glybera finally recommended for approval as the first gene therapy drug in the European union. *Mol. Ther.* **20**, 1831-1832 (2012).
237. De Laporte,L., Cruz,R.J., & Shea,L.D. Design of modular non-viral gene therapy vectors. *Biomaterials* **27**, 947-954 (2006).
238. Li,S. & Huang,L. Nonviral gene therapy: promises and challenges. *Gene Ther.* **7**, 31-34 (2000).
239. Tachibana,R. *et al.* Quantitative analysis of correlation between number of nuclear plasmids and gene expression activity after transfection with cationic liposomes. *Pharm. Res.* **19**, 377-381 (2002).
240. Wiethoff,C.M. & Middaugh,C.R. Barriers to nonviral gene delivery. *J Pharm. Sci* **92**, 203-217 (2003).
241. Hart,S.L. *et al.* Gene delivery and expression mediated by an integrin-binding peptide. *Gene Ther.* **2**, 552-554 (1995).
242. Edelstein,M.L., Abedi,M.R., & Wixon,J. Gene therapy clinical trials worldwide to 2007--an update. *J. Gene Med.* **9**, 833-842 (2007).
243. Pearson,S., Jia,H., & Kandachi,K. China approves first gene therapy. *Nat. Biotechnol.* **22**, 3-4 (2004).
244. Orr,R.M. Technology evaluation: fomivirsen, Isis Pharmaceuticals Inc/CIBA vision. *Curr. Opin. Mol. Ther.* **3**, 288-294 (2001).
245. Maberley,D. Pegaptanib for neovascular age-related macular degeneration. *Issues Emerg. Health Technol.* 1-4 (2005).
246. Que-Gewirth,N.S. & Sullenger,B.A. Gene therapy progress and prospects: RNA aptamers. *Gene Ther.* **14**, 283-291 (2007).
247. Petry,H., Goldmann,C., Ast,O., & Luke,W. The use of virus-like particles for gene transfer. *Curr. Opin. Mol. Ther.* **5**, 524-528 (2003).

248. Uherek,C., Fominaya,J., & Wels,W. A modular DNA carrier protein based on the structure of diphtheria toxin mediates target cell-specific gene delivery. *J. Biol. Chem.* **273**, 8835-8841 (1998).
249. Fominaya,J., Uherek,C., & Wels,W. A chimeric fusion protein containing transforming growth factor-alpha mediates gene transfer via binding to the EGF receptor. *Gene Ther.* **5**, 521-530 (1998).
250. Sloots,A. & Wels,W.S. Recombinant derivatives of the human high-mobility group protein HMGB2 mediate efficient nonviral gene delivery. *FEBS J.* **272**, 4221-4236 (2005).
251. Rajagopalan,R., Xavier,J., Rangaraj,N., Rao,N.M., & Gopal,V. Recombinant fusion proteins TAT-Mu, Mu and Mu-Mu mediate efficient non-viral gene delivery. *J. Gene Med.* **9**, 275-286 (2007).
252. Vaysse,L. *et al.* Development of a self-assembling nuclear targeting vector system based on the tetracycline repressor protein. *J. Biol. Chem.* **279**, 5555-5564 (2004).
253. Ferrer-Miralles,N., Vazquez,E., & Villaverde,A. Membrane-active peptides for non-viral gene therapy: making the safest easier. *Trends Biotechnol.* **26**, 267-275 (2008).
254. Aris,A., Feliu,J.X., Knight,A., Coutelle,C., & Villaverde,A. Exploiting viral cell-targeting abilities in a single polypeptide, non-infectious, recombinant vehicle for integrin-mediated DNA delivery and gene expression. *Biotechnol. Bioeng.* **68**, 689-696 (2000).
255. Aris,A. & Villaverde,A. Molecular organization of protein-DNA complexes for cell-targeted DNA delivery. *Biochem Biophys. Res. Commun.* **278**, 455-461 (2000).
256. Aris,A. & Villaverde,A. Engineering nuclear localization signals in modular protein vehicles for gene therapy. *Biochem Biophys. Res. Commun.* **304**, 625-631 (2003).
257. Villaverde,A. *et al.* A cell adhesion peptide from foot-and-mouth disease virus can direct cell targeted delivery of a functional enzyme. *Biotechnol. Bioeng.* **59**, 294-301 (1998).
258. Peluffo,H. *et al.* RGD domains neuroprotect the immature brain by a glial-dependent mechanism. *Ann. Neurol.* **62**, 251-261 (2007).
259. Zhang,S.S. *et al.* CD133(+)CXCR4(+) colon cancer cells exhibit metastatic potential and predict poor prognosis of patients. *BMC. Med.* **10**, 85 (2012).
260. Brand,S. *et al.* CXCR4 and CXCL12 are inversely expressed in colorectal cancer cells and modulate cancer cell migration, invasion and MMP-9 activation. *Exp. Cell Res.* **310**, 117-130 (2005).
261. Liang,X. CXCR4, inhibitors and mechanisms of action. *Chem. Biol Drug Des* **72**, 97-110 (2008).

References

262. Shirozu, M. *et al.* Structure and chromosomal localization of the human stromal cell-derived factor 1 (SDF1) gene. *Genomics* **28**, 495-500 (1995).
263. Kofuku, Y. *et al.* Structural basis of the interaction between chemokine stromal cell-derived factor-1/CXCL12 and its G-protein-coupled receptor CXCR4. *J Biol Chem.* (2009).
264. Huang, X. *et al.* Molecular dynamics simulations on SDF-1 α : binding with CXCR4 receptor. *Biophys. J* **84**, 171-184 (2003).
265. Amara, A. *et al.* HIV coreceptor downregulation as antiviral principle: SDF-1 α -dependent internalization of the chemokine receptor CXCR4 contributes to inhibition of HIV replication. *J Exp. Med.* **186**, 139-146 (1997).
266. Li, K. *et al.* Small peptide analogue of SDF-1 α supports survival of cord blood CD34 $^{+}$ cells in synergy with other cytokines and enhances their ex vivo expansion and engraftment into nonobese diabetic/severe combined immunodeficient mice. *Stem Cells* **24**, 55-64 (2006).
267. Yang, O.O. *et al.* Enhanced inhibition of human immunodeficiency virus type 1 by Met-stromal-derived factor 1 β correlates with down-modulation of CXCR4. *J Virol.* **73**, 4582-4589 (1999).
268. Sakaida, H. *et al.* T-tropic human immunodeficiency virus type 1 (HIV-1)-derived V3 loop peptides directly bind to CXCR-4 and inhibit T-tropic HIV-1 infection. *J Virol.* **72**, 9763-9770 (1998).
269. Kledal, T.N. *et al.* A broad-spectrum chemokine antagonist encoded by Kaposi's sarcoma-associated herpesvirus. *Science* **277**, 1656-1659 (1997).
270. Zhou, N., Luo, Z., Luo, J., Hall, J.W., & Huang, Z. A novel peptide antagonist of CXCR4 derived from the N-terminus of viral chemokine vMIP-II. *Biochemistry* **39**, 3782-3787 (2000).
271. Murakami, T. *et al.* Inhibitory mechanism of the CXCR4 antagonist T22 against human immunodeficiency virus type 1 infection. *J Virol.* **73**, 7489-7496 (1999).
272. Wender, P.A. *et al.* The design, synthesis, and evaluation of molecules that enable or enhance cellular uptake: peptoid molecular transporters. *Proc. Natl. Acad. Sci. U. S. A* **97**, 13003-13008 (2000).
273. Park, J. *et al.* Mutational analysis of a human immunodeficiency virus type 1 Tat protein transduction domain which is required for delivery of an exogenous protein into mammalian cells. *J Gen. Virol.* **83**, 1173-1181 (2002).
274. Nash, G.M. *et al.* KRAS Mutation and Microsatellite Instability: Two Genetic Markers of Early Tumor Development That Influence the Prognosis of Colorectal Cancer. *Ann. Surg. Oncol.* (2009).
275. Nash, G.M. *et al.* KRAS Mutation Correlates With Accelerated Metastatic Progression in Patients With Colorectal Liver Metastases. *Ann. Surg. Oncol.* (2009).

276. Wagner,E. Strategies to improve DNA polyplexes for in vivo gene transfer: will "artificial viruses" be the answer? *Pharm. Res.* **21**, 8-14 (2004).
277. Mastrobattista,E., van der Aa,M.A., Hennink,W.E., & Crommelin,D.J. Artificial viruses: a nanotechnological approach to gene delivery. *Nat. Rev. Drug Discov.* **5**, 115-121 (2006).
278. Tu,R.S. & Tirrell,M. Bottom-up design of biomimetic assemblies. *Adv. Drug Deliv. Rev.* **56**, 1537-1563 (2004).
279. Giacca,M. & Zacchigna,S. Virus-mediated gene delivery for human gene therapy. *J. Control Release* **161**, 377-388 (2012).
280. Ma,Y., Nolte,R.J., & Cornelissen,J.J. Virus-based nanocarriers for drug delivery. *Adv. Drug Deliv. Rev.* **64**, 811-825 (2012).
281. Han,M., Kickhoefer,V.A., Nemerow,G.R., & Rome,L.H. Targeted vault nanoparticles engineered with an endosomolytic peptide deliver biomolecules to the cytoplasm. *ACS Nano.* **5**, 6128-6137 (2011).
282. Corchero,J.L. & Cedano,J. Self-assembling, protein-based intracellular bacterial organelles: emerging vehicles for encapsulating, targeting and delivering therapeutical cargoes. *Microb Cell Fact.* **10**, 92 (2011).
283. Doll,T.A., Raman,S., Dey,R., & Burkhard,P. Nanoscale assemblies and their biomedical applications. *J. R. Soc. Interface* **10**, 20120740 (2013).
284. Aris,A. & Villaverde,A. Engineering nuclear localization signals in modular protein vehicles for gene therapy. *Biochem. Biophys. Res. Commun.* **304**, 625-631 (2003).
285. Aris,A. & Villaverde,A. Molecular organization of protein-DNA complexes for cell-targeted DNA delivery. *Biochem. Biophys. Res. Commun.* **278**, 455-461 (2000).
286. Domingo-Espin,J. *et al.* Nanoparticulate architecture of protein-based artificial viruses is supported by protein-DNA interactions. *Nanomedicine (Lond)* **6**, 1047-1061 (2011).
287. Lakshmanan,A., Zhang,S., & Hauser,C.A. Short self-assembling peptides as building blocks for modern nanodevices. *Trends Biotechnol* **30**, 155-165 (2012).
288. Zhou,B., Xing,L., Wu,W., Zhang,X.E., & Lin,Z. Small surfactant-like peptides can drive soluble proteins into active aggregates. *Microb. Cell Fact.* **11**, 10 (2012).
289. Wu,W., Xing,L., Zhou,B., & Lin,Z. Active protein aggregates induced by terminally attached self-assembling peptide ELK16 in Escherichia coli. *Microb. Cell Fact.* **10**, 9 (2011).
290. Unzueta,U. *et al.* Non-amyloidogenic peptide tags for the regulatable self-assembling of protein-only nanoparticles. *Biomaterials* **33**, 8714-8722 (2012).
291. Vazquez,E. *et al.* Internalization and kinetics of nuclear migration of protein-only, arginine-rich nanoparticles. *Biomaterials* **31**, 9333-9339 (2010).

References

292. Unzueta,U. *et al.* Intracellular CXCR4⁺ cell targeting with T22-empowered protein-only nanoparticles. *Int. J. Nanomedicine* **7**, 4533-4544 (2012).
293. Vazquez,E. *et al.* Protein nanodisk assembling and intracellular trafficking powered by an arginine-rich (R9) peptide. *Nanomedicine (Lond)* **5**, 259-268 (2010).
294. N.Eswar *et al.* Comparative Protein Structure Modeling With MODELLER. *Current Protocols in Bioinformatics*, John Wiley & Sons, Inc. [Supplement 15], 5.6.1-5.6.30, 200. 2009. Ref Type: Generic
295. de Vries,S.J. *et al.* HADDOCK versus HADDOCK: new features and performance of HADDOCK2.0 on the CAPRI targets. *Proteins* **69**, 726-733 (2007).
296. Guerois,R., Nielsen,J.E., & Serrano,L. Predicting changes in the stability of proteins and protein complexes: a study of more than 1000 mutations. *J. Mol. Biol.* **320**, 369-387 (2002).
297. Guex,N. & Peitsch,M.C. SWISS-MODEL and the Swiss-PdbViewer: an environment for comparative protein modeling. *Electrophoresis* **18**, 2714-2723 (1997).
298. Guex,N., Diemand,A., & Peitsch,M.C. Protein modelling for all. *Trends Biochem. Sci.* **24**, 364-367 (1999).
299. Pettersen,E.F. *et al.* UCSF Chimera--a visualization system for exploratory research and analysis. *J. Comput. Chem.* **25**, 1605-1612 (2004).
300. Ferrer-Miralles,N. *et al.* Biological activities of histidine-rich peptides; merging Biotechnology and Nanomedicine. *Microb Cell Fact.* **10**, 101 (2011).
301. Domingo-Espin,J. *et al.* RGD-based cell ligands for cell-targeted drug delivery act as potent trophic factors. *Nanomedicine* **8**, 1263-1266 (2012).
302. Edelstein,M.L., Abedi,M.R., & Wixon,J. Gene therapy clinical trials worldwide to 2007--an update. *J. Gene Med.* **9**, 833-842 (2007).
303. Abbott,A. Questions linger about unexplained gene-therapy trial death. *Nat. Med.* **12**, 597 (2006).
304. Williams,D.A. & Baum,C. Medicine. Gene therapy--new challenges ahead. *Science* **302**, 400-401 (2003).
305. Aris,A. & Villaverde,A. Modular protein engineering for non-viral gene therapy. *Trends Biotechnol.* **22**, 371-377 (2004).
306. Villaverde A *Nanoparticles in translational science and medicine*(Academic Press (Elsevier), London, 2011).
307. Sanvicens,N. & Marco,M.P. Multifunctional nanoparticles--properties and prospects for their use in human medicine. *Trends Biotechnol.* **26**, 425-433 (2008).
308. Rodriguez-Carmona,E. & Villaverde,A. Nanostructured bacterial materials for innovative medicines. *Trends Microbiol.* **18**, 423-430 (2010).

309. Vazquez,E. *et al.* Modular protein engineering in emerging cancer therapies. *Curr. Pharm. Des* **15**, 893-916 (2009).
310. Vazquez,E., Ferrer-Miralles,N., & Villaverde,A. Peptide-assisted traffic engineering for nonviral gene therapy. *Drug Discov. Today* **13**, 1067-1074 (2008).
311. Ferrer-Miralles,N., Vazquez,E., & Villaverde,A. Membrane-active peptides for non-viral gene therapy: making the safest easier. *Trends Biotechnol.* **26**, 267-275 (2008).
312. Zlotnick,A. Are weak protein-protein interactions the general rule in capsid assembly? *Virology* **315**, 269-274 (2003).
313. Guo,J. & Xin,H. Chinese gene therapy. Splicing out the West? *Science* **314**, 1232-1235 (2006).
314. Li,S. & Huang,L. Nonviral gene therapy: promises and challenges. *Gene Ther.* **7**, 31-34 (2000).
315. Wiethoff,C.M. & Middaugh,C.R. Barriers to nonviral gene delivery. *J. Pharm. Sci.* **92**, 203-217 (2003).
316. Jafari,M., Soltani,M., Naahidi,S., Karunaratne,D.N., & Chen,P. Nonviral approach for targeted nucleic acid delivery. *Curr. Med. Chem.* **19**, 197-208 (2012).
317. Vazquez,E. & Villaverde,A. Engineering building blocks for self-assembling protein nanoparticles. *Microb. Cell Fact.* **9**, 101 (2010).
318. Petry,H., Goldmann,C., Ast,O., & Luke,W. The use of virus-like particles for gene transfer. *Curr. Opin. Mol. Ther.* **5**, 524-528 (2003).
319. Georgens,C., Weyermann,J., & Zimmer,A. Recombinant virus like particles as drug delivery system. *Curr. Pharm. Biotechnol.* **6**, 49-55 (2005).
320. Cheng,S., Liu,Y., Crowley,C.S., Yeates,T.O., & Bobik,T.A. Bacterial microcompartments: their properties and paradoxes. *Bioessays* **30**, 1084-1095 (2008).
321. Fan,C. *et al.* Short N-terminal sequences package proteins into bacterial microcompartments1. *Proc. Natl. Acad. Sci. U. S. A* **107**, 7509-7514 (2010).
322. Rome,L.H. & Kickhoefer,V.A. Development of the Vault Particle as a Platform Technology. *ACS Nano.*(2012).
323. Peluffo,H. *et al.* Neuroprotection from NMDA excitotoxic lesion by Cu/Zn superoxide dismutase gene delivery to the postnatal rat brain by a modular protein vector. *BMC. Neurosci.* **7**, 35 (2006).
324. Vazquez,E. *et al.* Protein nanodisk assembling and intracellular trafficking powered by an arginine-rich (R9) peptide. *Nanomedicine. (Lond)* **5**, 259-268 (2010).

References

325. Domingo-Espin, J. *et al.* Nanoparticulate architecture of protein-based artificial viruses is supported by protein-DNA interactions. *Nanomedicine (Lond)* **6**, 1047-1061 (2011).
326. Yang, Y. & Burkhard, P. Encapsulation of gold nanoparticles into self-assembling protein nanoparticles. *J. Nanobiotechnology*. **10**, 42 (2012).
327. Ferrer-Mirallas, N., Domingo-Espin, J., Corchero, J.L., Vazquez, E., & Villaverde, A. Microbial factories for recombinant pharmaceuticals. *Microb. Cell Fact.* **8**, 17 (2009).
328. Corchero, J.L. *et al.* Unconventional microbial systems for the cost-efficient production of high-quality protein therapeutics. *Biotechnol. Adv.* (2012).
329. Saccardo, P., Villaverde, A., & Gonzalez-Montalban, N. Peptide-mediated DNA condensation for non-viral gene therapy. *Biotechnol. Adv.* **27**, 432-438 (2009).
330. Aris, A., Feliu, J.X., Knight, A., Coutelle, C., & Villaverde, A. Exploiting viral cell-targeting abilities in a single polypeptide, non-infectious, recombinant vehicle for integrin-mediated DNA delivery and gene expression. *Biotechnol Bioeng* **68**, 689-696 (2000).
331. Demain, A.L. & Vaishnav, P. Production of recombinant proteins by microbes and higher organisms. *Biotechnol. Adv.* **27**, 297-306 (2009).
332. Vazquez, E. & Villaverde, A. Engineering building blocks for self-assembling protein nanoparticles. *Microb. Cell Fact.* **9**, 101 (2010).
333. Zhang, L., Pornpattananangku, D., Hu, C.M., & Huang, C.M. Development of nanoparticles for antimicrobial drug delivery. *Curr. Med. Chem.* **17**, 585-594 (2010).
334. Sarker, D.K. Engineering of nanoemulsions for drug delivery. *Curr. Drug Deliv.* **2**, 297-310 (2005).
335. Sarker, D.K. Sculpted amphiphilic liposomal particles for modifiable medicinal applications. *Curr. Drug Discov. Technol.* **6**, 52-58 (2009).
336. Huynh, N.T., Passirani, C., Saulnier, P., & Benoit, J.P. Lipid nanocapsules: a new platform for nanomedicine. *Int. J. Pharm.* **379**, 201-209 (2009).
337. Patel, D. & Sawant, K.K. Self micro-emulsifying drug delivery system: formulation development and biopharmaceutical evaluation of lipophilic drugs. *Curr. Drug Deliv.* **6**, 419-424 (2009).
338. Betancourt, T. & Brannon-Peppas, L. Micro- and nanofabrication methods in nanotechnological medical and pharmaceutical devices. *Int. J. Nanomedicine.* **1**, 483-495 (2006).
339. Caldorera-Moore, M., Guimard, N., Shi, L., & Roy, K. Designer nanoparticles: incorporating size, shape and triggered release into nanoscale drug carriers. *Expert. Opin. Drug Deliv.* **7**, 479-495 (2010).
340. Mao, C. *et al.* Viral assembly of oriented quantum dot nanowires. *Proc. Natl. Acad. Sci. U. S. A* **100**, 6946-6951 (2003).

341. Mao,C. *et al.* Virus-based toolkit for the directed synthesis of magnetic and semiconducting nanowires. *Science* **303**, 213-217 (2004).
342. Nam,K.T. *et al.* Virus-enabled synthesis and assembly of nanowires for lithium ion battery electrodes. *Science* **312**, 885-888 (2006).
343. Goldmann,C. *et al.* Packaging of small molecules into VP1-virus-like particles of the human polyomavirus JC virus. *J. Virol. Methods* **90**, 85-90 (2000).
344. Georgens,C., Weyermann,J., & Zimmer,A. Recombinant virus like particles as drug delivery system. *Curr. Pharm. Biotechnol.* **6**, 49-55 (2005).
345. Malboeuf,C.M. *et al.* Human papillomavirus-like particles mediate functional delivery of plasmid DNA to antigen presenting cells in vivo. *Vaccine* **25**, 3270-3276 (2007).
346. Lee,T.J., Schwartz,C., & Guo,P. Construction of bacteriophage phi29 DNA packaging motor and its applications in nanotechnology and therapy. *Ann. Biomed. Eng* **37**, 2064-2081 (2009).
347. Hiratsuka,Y., Miyata,M., Tada,T., & Uyeda,T.Q. A microrotary motor powered by bacteria. *Proc. Natl. Acad. Sci. U. S. A* **103**, 13618-13623 (2006).
348. Kumara,M.T., Muralidharan,S., & Tripp,B.C. Generation and characterization of inorganic and organic nanotubes on bioengineered flagella of mesophilic bacteria. *J. Nanosci. Nanotechnol.* **7**, 2260-2272 (2007).
349. Deplanche,K., Woods,R.D., Mikheenko,I.P., Sockett,R.E., & Macaskie,L.E. Manufacture of stable palladium and gold nanoparticles on native and genetically engineered flagella scaffolds. *Biotechnol. Bioeng.* **101**, 873-880 (2008).
350. Hassane,F.S. *et al.* A peptide-based dendrimer that enhances the splice-redirecting activity of PNA conjugates in cells. *Bioconjug. Chem.* **20**, 1523-1530 (2009).
351. Rodriguez-Carmona,E. & Villaverde,A. Nanostructured bacterial materials for innovative medicines. *Trends Microbiol.* **18**, 423-430 (2010).
352. Villaverde,A. Nanotechnology, bionanotechnology and microbial cell factories. *Microb. Cell Fact.* **9**, 53 (2010).
353. Straub,J.E. & Thirumalai,D. Principles governing oligomer formation in amyloidogenic peptides. *Curr. Opin. Struct. Biol.* **20**, 187-195 (2010).
354. Reddy,G., Straub,J.E., & Thirumalai,D. Dynamics of locking of peptides onto growing amyloid fibrils. *Proc. Natl. Acad. Sci. U. S. A* **106**, 11948-11953 (2009).
355. Espargaro,A., Villar-Pique,A., Sabate,R., & Ventura,S. Yeast prions form infectious amyloid inclusion bodies in bacteria. *Microb. Cell Fact.* **11**, 89 (2012).
356. Villar-Pique,A., Espargaro,A., Sabate,R., de Groot,N.S., & Ventura,S. Using bacterial inclusion bodies to screen for amyloid aggregation inhibitors. *Microb. Cell Fact.* **11**, 55 (2012).

References

357. Garcia-Fruitos,E., Sabate,R., de Groot,N.S., Villaverde,A., & Ventura,S. Biological role of bacterial inclusion bodies: a model for amyloid aggregation. *FEBS J.* **278**, 2419-2427 (2011).
358. Koutsopoulos,S., Unsworth,L.D., Nagai,Y., & Zhang,S. Controlled release of functional proteins through designer self-assembling peptide nanofiber hydrogel scaffold. *Proc. Natl. Acad. Sci. U. S. A* **106**, 4623-4628 (2009).
359. Zhang,S., Holmes,T., Lockshin,C., & Rich,A. Spontaneous assembly of a self-complementary oligopeptide to form a stable macroscopic membrane. *Proc. Natl. Acad. Sci. U. S. A* **90**, 3334-3338 (1993).
360. Wu,W., Xing,L., Zhou,B., & Lin,Z. Active protein aggregates induced by terminally attached self-assembling peptide ELK16 in Escherichia coli. *Microb. Cell Fact.* **10**, 9 (2011).
361. Zhou,B., Xing,L., Wu,W., Zhang,X.E., & Lin,Z. Small surfactant-like peptides can drive soluble proteins into active aggregates. *Microb. Cell Fact.* **11**, 10 (2012).
362. Collins,L. *et al.* Self-assembly of peptides into spherical nanoparticles for delivery of hydrophilic moieties to the cytosol. *ACS Nano.* **4**, 2856-2864 (2010).
363. Wright,E.R. & Conticello,V.P. Self-assembly of block copolymers derived from elastin-mimetic polypeptide sequences. *Adv. Drug Deliv. Rev.* **54**, 1057-1073 (2002).
364. Lamm,M.H. & Ke,P.C. Cell trafficking of carbon nanotubes based on fluorescence detection. *Methods Mol. Biol.* **625**, 135-151 (2010).
365. Peng,L., Liu,M., Xue,Y.N., Huang,S.W., & Zhuo,R.X. Transfection and intracellular trafficking characteristics for poly(amidoamine)s with pendant primary amine in the delivery of plasmid DNA to bone marrow stromal cells. *Biomaterials* **30**, 5825-5833 (2009).
366. Perumal,O.P., Inapagolla,R., Kannan,S., & Kannan,R.M. The effect of surface functionality on cellular trafficking of dendrimers. *Biomaterials* **29**, 3469-3476 (2008).
367. Barua,S. & Rege,K. The influence of mediators of intracellular trafficking on transgene expression efficacy of polymer-plasmid DNA complexes. *Biomaterials* **31**, 5894-5902 (2010).
368. Karve,S., Alaouie,A., Zhou,Y., Rotolo,J., & Sofou,S. The use of pH-triggered leaky heterogeneities on rigid lipid bilayers to improve intracellular trafficking and therapeutic potential of targeted liposomal immunochemotherapy. *Biomaterials* **30**, 6055-6064 (2009).
369. Vasir,J.K. & Labhasetwar,V. Quantification of the force of nanoparticle-cell membrane interactions and its influence on intracellular trafficking of nanoparticles. *Biomaterials* **29**, 4244-4252 (2008).
370. Vazquez,E. *et al.* Protein nanodisk assembling and intracellular trafficking powered by an arginine-rich (R9) peptide. *Nanomedicine. (Lond)* **5**, 259-268 (2010).

371. Kumar,P. *et al.* Transvascular delivery of small interfering RNA to the central nervous system. *Nature* **448**, 39-43 (2007).
372. Serda,R.E., Godin,B., Blanco,E., Chiappini,C., & Ferrari,M. Multi-stage delivery nano-particle systems for therapeutic applications. *Biochim. Biophys. Acta* **1810**, 317-329 (2011).
373. Suh,J., Wirtz,D., & Hanes,J. Efficient active transport of gene nanocarriers to the cell nucleus. *Proc. Natl. Acad. Sci. U. S. A* **100**, 3878-3882 (2003).
374. Ng,C.P., Goodman,T.T., Park,I.K., & Pun,S.H. Bio-mimetic surface engineering of plasmid-loaded nanoparticles for active intracellular trafficking by actin comet-tail motility. *Biomaterials* **30**, 951-958 (2009).
375. Bergen,J.M. & Pun,S.H. Analysis of the intracellular barriers encountered by nonviral gene carriers in a model of spatially controlled delivery to neurons. *J. Gene Med.* **10**, 187-197 (2008).
376. Riehemann,K. *et al.* Nanomedicine--challenge and perspectives. *Angew. Chem. Int. Ed Engl.* **48**, 872-897 (2009).
377. Dietz,G.P. & Bahr,M. Delivery of bioactive molecules into the cell: the Trojan horse approach. *Mol. Cell Neurosci.* **27**, 85-131 (2004).
378. Thurber,G.M., Schmidt,M.M., & Wittrup,K.D. Factors determining antibody distribution in tumors. *Trends Pharmacol. Sci.* **29**, 57-61 (2008).
379. Ellis,L.M. & Hicklin,D.J. Resistance to Targeted Therapies: Refining Anticancer Therapy in the Era of Molecular Oncology. *Clin. Cancer Res.* **15**, 7471-7478 (2009).
380. Laakkonen,P. & Vuorinen,K. Homing peptides as targeted delivery vehicles. *Integr. Biol. (Camb.)* **2**, 326-337 (2010).
381. Enback,J. & Laakkonen,P. Tumour-homing peptides: tools for targeting, imaging and destruction. *Biochem. Soc. Trans.* **35**, 780-783 (2007).
382. Mocellin,S., Lise,M., & Nitti,D. Targeted therapy for colorectal cancer: mapping the way. *Trends Mol. Med.* **11**, 327-335 (2005).
383. Wilen,C.B., Tilton,J.C., & Doms,R.W. Molecular mechanisms of HIV entry. *Adv. Exp. Med. Biol.* **726**, 223-242 (2012).
384. Klonisch,T. *et al.* Cancer stem cell markers in common cancers - therapeutic implications. *Trends Mol. Med.* **14**, 450-460 (2008).
385. Sun,X. *et al.* CXCL12 / CXCR4 / CXCR7 chemokine axis and cancer progression. *Cancer Metastasis Rev.* **29**, 709-722 (2010).
386. Kim,J. *et al.* Chemokine receptor CXCR4 expression in patients with melanoma and colorectal cancer liver metastases and the association with disease outcome. *Ann. Surg.* **244**, 113-120 (2006).

References

387. Liang,Z. *et al.* Silencing of CXCR4 blocks breast cancer metastasis. *Cancer Res.* **65**, 967-971 (2005).
388. Rusconi,S., Scozzafava,A., Mastrolorenzo,A., & Supuran,C.T. An update in the development of HIV entry inhibitors. *Curr. Top. Med. Chem.* **7**, 1273-1289 (2007).
389. Ferrer-Miralles,N. *et al.* Biological activities of histidine-rich peptides; merging biotechnology and nanomedicine. *Microb. Cell Fact.* **10**, 101 (2011).
390. Sleeman,J. & Steeg,P.S. Cancer metastasis as a therapeutic target. *Eur. J. Cancer* **46**, 1177-1180 (2010).
391. Wagner,E. Strategies to improve DNA polyplexes for in vivo gene transfer: will "artificial viruses" be the answer? *Pharm. Res.* **21**, 8-14 (2004).
392. Doll,T.A., Raman,S., Dey,R., & Burkhard,P. Nanoscale assemblies and their biomedical applications. *J. R. Soc. Interface* **10**, 20120740 (2013).
393. Gallagher,S.R. & Desjardins,P.R. Quantitation of DNA and RNA with absorption and fluorescence spectroscopy. *Curr. Protoc. Mol. Biol.* **Appendix 3**, Appendix (2006).

A decorative graphic consisting of a blue ink splatter on the left side, with a horizontal line extending to the right, ending in a smaller blue mark.

Acknowledgements

Acknowledgements

Es difícil saber que decir en un momento como este, sobre todo porque no soy muy dado a los discursos y además, todo este tiempo escribiendo la tesis me ha dejado las neuronas literalmente fritas. Sin embargo, no tengo ninguna duda de que tengo muchísimas cosas que agradecer ya que hay muchísima gente que de alguna forma u otra, ha contribuido a que todo esto haya sido posible.

Cuando empecé hace cuatro años, veía muy lejos este día, y parecía que nunca iba a llegar pero la verdad es que al final ha llegado. Y lo cierto es que lo digo con cierta pena porque a pesar de todos los altibajos que haya podido pasar durante el transcurso de este periodo de mi vida el balance general ha sido muy positivo y no me cabe ninguna duda de que si pudiera volvería a empezar otra vez.

En estos momentos, sentado aquí pensando en todo, me vienen muchas cosas a la cabeza y se me ocurren muchísimas personas a las que debo dar las gracias por algún motivo u otro, pero como manda el protocolo empezare por mis directores de tesis.

Toni, has sido la primera persona que confió en mí para iniciar esta aventura dándome la oportunidad de trabajar en este grupo y aprender todo lo que se. Soy muy consciente de que todavía me quedan muchísimas cosas por aprender pero suelen decir que las primeras oportunidades son las que más cuestan y eso te lo debo a ti. Ojala algún día todas las personas a las que un día nos diste una oportunidad llegemos a estar a tu altura en este a veces tan difícil mundo de la ciencia. Por todo eso y por otras muchas cosas más, gracias!

Neus, ha sido muy enriquecedor trabajar a tu lado, me has enseñado muchas cosas y has sido un apoyo imprescindible en el desarrollo de todo este trabajo. Gracias por todos tus consejos científicos y por los buenos momentos que hemos pasado en el laboratorio.

Esther, solo puedo decir que durante estos años has sido mucho más que mi directora de tesis. Que ha sido un placer trabajar a tu lado y que he aprendido muchísimas cosas de ti. Has sido un apoyo incondicional para mí tanto en los buenos como en los malos momentos. Te has preocupado por mí en momentos personales muy delicados y he recibido muy buenos consejos por tu parte. Por todos esos consejos, por el gran trabajo realizado, por todas las confianzas compartidas, por saber poner ese punto de cordura a mi caos y por ser a veces más que mi directora, mi psicoterapeuta personal mil gracias!

Pepe, ha sido muy divertido trabajar junto a ti. Creo que el sentido del humor es una parte esencial de nuestras vidas y algo que nunca jamás deberíamos perder. Gracias por hacer las largas horas del laboratorio más divertidas.

Acknowledgements

Rosa M., gracias por evitar que el laboratorio estuviera sumido en el caos. Sin tu ayuda estaríamos perdidos muchas veces. Ha sido muy agradable trabajar contigo.

Nuria y Rosa F., ha sido corto el periodo de tiempo que hemos podido compartir en el laboratorio pero no por eso peor. Ha sido un placer trabajar con vosotras y me quedo con todas las cosas que he aprendido con vosotras. Gracias.

Vero, el día que te fuiste de laboratorio te llevaste una parte de nosotros contigo. Has sido el alma del laboratorio y la persona con la que podíamos contar para absolutamente todo. Tú eres la prueba de que el talento de las personas no se mide con los títulos. En este laboratorio muchas veces no habríamos sido nada sin ti. Muchas gracias por todos los momentos compartidos, por lo que hemos aprendido juntos y por tener siempre esa sonrisa imborrable en la cara. Tus abrazos y las largas horas de compañía en el confocal, DLS han sido insustituibles. We miss you so so so pero que so so much!

Fela, guardo muchísimos buenos recuerdos de los momentos compartidos en el laboratorio. Gracias por poner ese toque de humor tan necesario, también por entender tan bien mi extraño sentido del humor, por ser mi vecina de ordenador, por lo mucho que nos hemos divertido y por preocuparte tanto siempre por mí no solo en lo profesional sino sobre todo en lo personal. Este laboratorio perdió parte de su alma el día que tú te fuiste.

Escar, gracias a ti también por todos los momentos compartidos en el laboratorio. Ha sido un placer trabajar contigo. El laboratorio tampoco será lo mismo sin ti.

Joan, gracias por todas las cosas que he aprendido durante estos años junto a ti. Mi estancia en este laboratorio tampoco hubiera sido lo mismo sin ti.

Delia, que pena que tu paso por el laboratorio fuera tan corto. Hemos pasado muchos momentos divertidos juntos. Ha sido corto pero muy intenso. Todos los momentos de buen humor, risas y diversión son impagables. Muchas gracias. Se te echa de menos!

Joan Mark (Johnny), que momentos más divertidos hemos pasados. Para mí has sido la gran sorpresa del laboratorio. Hemos pasado poco tiempo junto en el laboratorio pero ha sido muy intenso. Gracias por los momentos compartidos, por los cafés antes del inglés, por las viejas del Artbo, por las risas, por las copas show cabaret y por todos los momentos que están por venir.

Elena, parece mentira que hayan pasado tantos años verdad? Aún recuerdo el día de tu tesis y mira ahora... Ha sido muy enriquecedor trabajar a tu lado, y espero que podamos seguir trabajando aunque sea por unos meses más. Solo decir que gracias por los momentos vividos y que estamos todos deseando conocer a Martí!

Mireia, has sido de las últimas en llegar al laboratorio pero no por eso menos importante. No hemos tenido mucho tiempo pero los momentos vividos han sido estupendos. Muchas gracias por toda la ayuda que me has dado cuando lo he necesitado. Espero que tengamos más tiempo para seguir conociéndonos.

Olivia, gracias a ti también por todos los momentos divertidos vividos. Algún día descubrirás que el autoclave era la solución para todo tus problemas :P . Mientras tanto espero que sigamos compartiendo muchos momentos divertidos.

Xu, we have not spent so much time in the lab together but it has been nice to know you, know about your culture and share special moments with you. I hope we can continue working together, learn some more Chinese and teach you some Spanish words. I hope you will someday bring us with you to china to visit your country and culture.

Joaquin! Muchas gracias por toda la ayuda y los momentos vividos. Te ha tocado ser mi guía en todo este largo proceso burocrático llamado tesis. Si he conseguido entregar los millones de papeles con sus respectivas, firmas, sellos, bendición del papa y aprobación de Esperanza Gracia ha sido gracias a ti. Solo me falta sacrificar una cabra a media noche un día de luna llena en el que Júpiter este alineado con Saturno y ya lo tendré todo; pero no sin antes haber rellenar el archivo "Tes195" donde la cabra da su consentimiento para participar en el ritual y renuncia expresamente a formar parte de cualquier otro ritual de futuras tesis doctorales y entregarlo debidamente firmado y sellado por los ángeles del infierno antes del primer lunes de cada mes a las 14:00 del mediodía, la 13:00 si es año bisiesto. En definitiva muchas gracias por el compañerismo, el soporte moral y los momentos vividos.

Paolo! Que decir, cuantas cosas vividas, compartidas. No tendríamos páginas suficientes para explicar todas las vivencias compartidas. Ha sido un largo proceso pero después de todos estos años no me llevo un compañero de trabajo sino un amigo. Muchas gracias por todas las horas en el laboratorio, pero muchísimo más por todas las cosas extralaborables que hemos vivido. Esas excursiones, días de playa, aquopolis, port aventura... a no eso no, cenas, cine, mojitos y un largo etc. Pero sobre todo muchas gracias por todas esos momentos que nunca jamás contaremos :P.

Fabián, lamentablemente hemos tenido muy poco tiempo para conocernos pero ha sido un placer compartir el tiempo que hemos coincidido en el laboratorio. Gracias por echarme un cable cuando lo he necesitado y espero poder tener la oportunidad de conocernos más.

Eugenia, ha sido un placer conocerte también y pasar tiempo junto a ti. Espero que tengas suerte, que puedas quedarte en el laboratorio y que con un poco de suerte tengamos tiempo de compartir más cosas. Gracias por todos los momentos, por apuntarte a todos los lab parties y por estar siempre de buen humor.

Acknowledgements

Gracias también a todos los estudiantes, niñas Argo etc.. que han hecho que nuestra vida en el laboratorio fuera más divertida e interesante. Agradecer especialmente a Veronica Monforte por ser tan natural, atenta, humilde e inundarnos siempre con su positivismo y buen humor.

Por último no me olvido de vosotros:

Frantxu! Muchas gracias por enseñarme todo lo que se de cultivos celulares, por hacer todo lo posible porque mis proyectos salieran adelante y por dejarte la piel en cada cosa que hacías con tal de ayudarme. Pero especialmente muchísimas gracias por todos los momentos personales vividos, las largas charlas, confidencias.... TODO aquí sin ti hubiera sido mucho más difícil.

Y Monica, que decir... poco se puede decir que tú y yo ya no sepamos. Cuando yo era nuevo en esto y me sentía completamente perdido, tú estuviste ahí, ayudándome y apoyándome. Mi estancia en este laboratorio sin ti no hubiera sido lo mismo. Tu eres de las mejores cosas que me llevo de toda esta experiencia; me llevo una amiga con la que espero pueda vivir muchas cosas más en el futuro. Muchas gracias por todos tus consejos científicos pero sobre todo, mil gracias a ti por todos los momentos vividos, por esos días de playa, los Martinis con limón, por esas sesiones de fitness, por darme una colleja cuando lo necesitaba y sobre todo por haber estado ahí siempre que lo he necesitado. El trabajo viene y va pero las personas que te encuentras por el camino son para siempre.

Muchas gracias también a Ramón, Virtudes e Isolda por la colaboración, por el magnífico trabajo realizado, y por haber hecho posible que me sienta tan orgulloso de los resultados que entre todos hemos conseguido a lo largo de este proyecto.

Thank you Luisa for receiving me in you laboratory. It has been a great experience to spend this period of time in Napoli. Thanks also to Gilda, Michella, Valentina, Annabel, Sara, Eugenio and all the people from the lab, but especially to Laura, Umberto and Gennaro. You all have made my internship period unforgettable!

Mena!!!! A special girl needs a special mention. I have no words to describe my feelings. You are the most special person I have ever met. I will never be able to give you back all the things you have given to me! You have made my stage in Napoli one of the most special periods of my live. Thank you so much for everything! I only hope we will meet again in a near future either here in Barcelona or in Napoli. Ti voglio bene!

Como suelen decir, no todo puede ser trabajo no? Hay muchas personas que fuera del ámbito laboral han sido parte indispensable de todo este proceso y no puedo olvidarme de ellos.

Acknowledgements

un agradecimiento especial a mi Laia, por ser la primera amiga que hice cuando llegue a la uni y no conocía a nadie. Por ser mi traductora personal “catalán-castellano, castellano-catalan” cuando no entendía nada de las clases y por ser la primera en hacernos sentir esa extraña sensación de que se te case una amiga y te des cuenta de lo mucho que hemos crecido todos juntos!

También quiero agradecer a Mireia, Jose, Mark, Sergie, Cristina, Raul, Esther, Silvia... y toda la tropa por los buenos momentos vividos, todas las cenas de cumpleaños, las barbacoas y un largo etc. Quiero agradecer especialmente a Mireia, por haber compartido junto a mí, tantos y tantos momentos especiales. Nuestro viaje a Londres, a Euskadi, las risas, las confianzas, las largas horas en la biblioteca y nuestras aventuras con Rachid! Y sobre todo por ser mi amiga!

Gracias también a Merçe, Helen y Eli por hacer tan divertidas todos los meses que nos pasábamos encerrados en la biblioteca, por las comidas en el CAU, y por ese día tan inolvidable en L' Estartit!

No me puedo olvidar tampoco de mis Maris! Carlos, Igor y Antonio. Cuando llegue por primera vez al JALG, nunca pensé que de ahí saldría lo que a día de hoy son uno de mis mejores amigos. Las cosas que hemos vivido juntos durante estos años han sido inolvidables. Gracias por todas las locuras, las fiestas en el arena, las largas charlas, por los días de eurovisión, por Idaira y sobre todo por ese viaje tan inolvidable a Tenerife! Igor, ha sido genial compartir piso contigo aunque a veces fuera un poco difícil, espero que todo te vaya bien por Alemania y podamos asistir de aquí a algún añito a la presentación de tu tesis. Carlos, cuantas cosas nos ha tocado vivir, hemos pasado algunos de los mejores y peores momentos de nuestra vida juntos pero lo importante es que siempre hemos estado ahí. Gracias siempre por tus consejos, por ser nuestra bruja personal, nuestro psicoterapeuta, un pilar fundamental de este grupo y por qué algún día presumiremos de ser el amigo del autor del mejor best-seller de la historia. Recuerda las cosas que hablamos y nunca pierdas la ilusión por cumplir tus sueños. Y finalmente mi Toñi! Tengo tantas cosas que agradecerte a ti también. Gracias por ser la persona más borde con cariño que he conocido, por no dejarnos opinar de arte, por las visitas guiadas, las sesiones de estudio a altas horas de la madrugada, la portera de la biblio, las fiestas de pijama, por las visitas a Barcelona, por dejarme abrazarte, por el viaje a Tenerife, el viaje a Valencia, el loroparque, el Seat Ibiza de tu madre, por tus canciones, por tu gran apoyo en los momentos que más lo he necesitado y por habernos permitido conocer a tu abuela! Todos sabemos que no soportas que lea la tesis antes que tú pero no te preocupes, algún día lo superarás.

Gracias también a Karen por iniciar nuestra aventura en Barcelona juntos y haber compartido tantos momentos aquí. A Tamara por ser esa amiga incondicional que siempre está ahí, por las cenas en tu casa, por preocuparte tanto por mi tesis y por

hacer que sienta que nunca me he ido cuando estamos juntos. Quiero agradecer a Oihana por todos los momentos que hemos vivido juntos y especialmente a Mari, por todos esos mensajes nocturnos, las confianzas los ánimos, las clases de solfeo, la ilusión por superarse y seguir adelante y sobre todo por todos esos mensajes en blanco que aunque no dijeran nada, me hacían saber que estabas ahí.

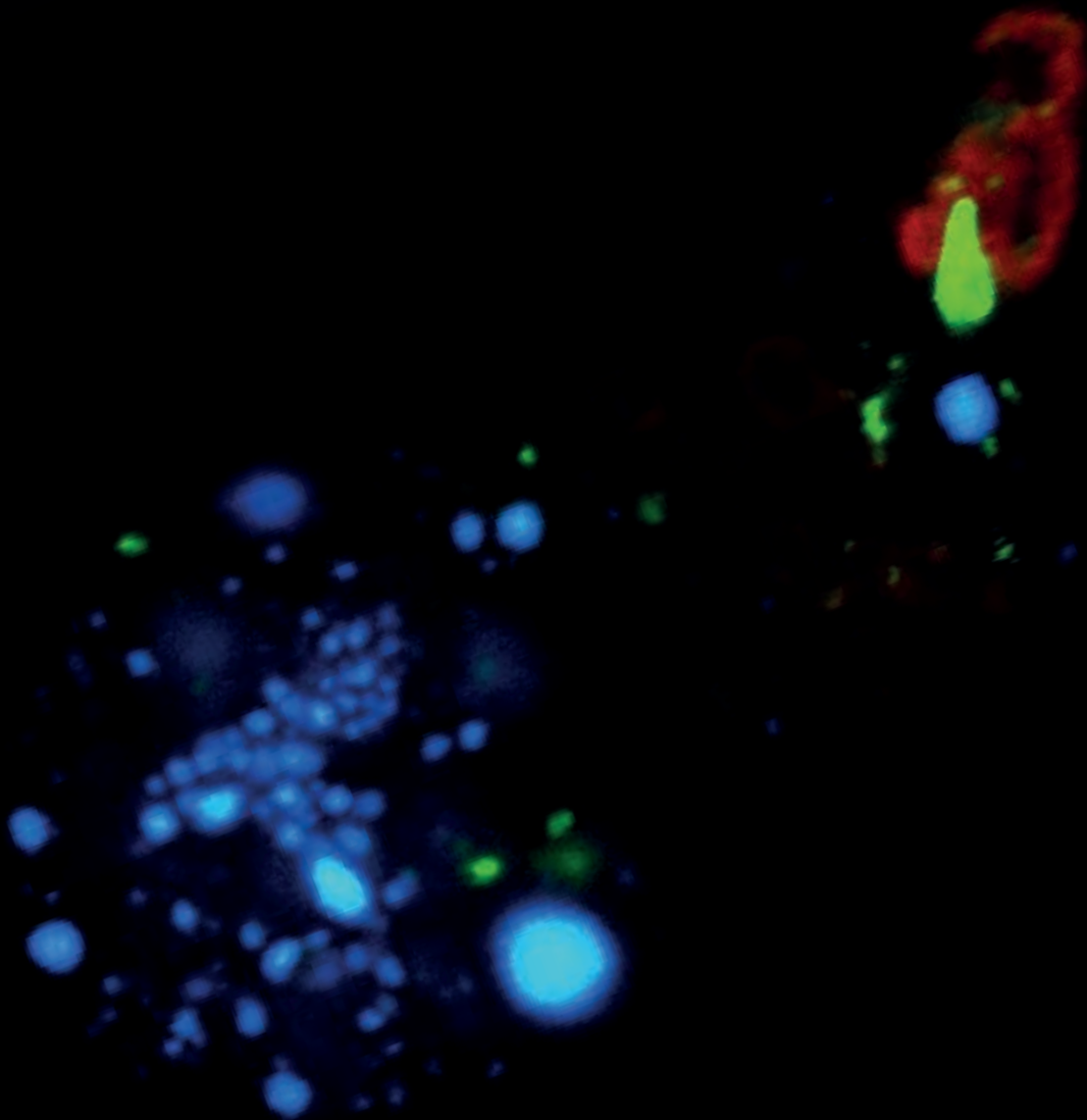
Gracias a mis compañeros de piso (Urtzi, Carlos, Dalia...) por hacer mi vida aquí más divertida fácil y sobre todo por hacerme sentir que aquí también tenía mi pequeña familia. Especialmente gracias a Dalia, por ser la compañera de piso más desequilibrada que he tenido, por todas las locuras, las risas, confianzas, excursiones, por respetar tanto el equilibrio del hogar cuando tenía que estudiar, por las situaciones surrealistas y por haberse convertido en una hermana para mí aquí.

Para acabar solamente me falta agradecer a algunas personas que han tenido un papel clave en todo este proceso y que han tenido que sufrirlo.

Iñaki, gracias por ser un pilar fundamental y mi apoyo al principio de toda esta aventura. Si no fuera por ti, es más que probable que hubiese tirado la toalla y que nunca hubiera llegado hasta este punto. Me has enseñado muchas cosas. Gracias por todas las cosas vividas y por poder contar con un amigo como tú a día de hoy.

David, tú también has jugado un papel fundamental durante el desarrollo de mi tesis doctoral. Me enseñaste que nunca debo dejar de lado las cosas que más quiero por el trabajo y que hay cosas más importantes que triunfar profesionalmente. Espero que todo lo aprendido a tu lado me sirva de algo en el futuro.

Y finalmente, no tengo líneas suficientes en esta tesis doctoral para dar las gracias a Sergio. Compartir mi vida contigo durante estos últimos años es lo mejor que me ha pasado. Gracias por aguantarme cuando a lo largo de la escritura de esta tesis estaba al borde de un ataque de nervios, por todas las explicaciones científicas que has tenido que soportar, por los ensayos de presentaciones, por permitir que todo el tiempo dedicado al trabajo te lo restara a ti y por estar siempre ahí. Gracias también por ser mi compañero de viaje en mi estancia en Nápoles y por haberme permitido vivir esa experiencia junto a ti. Pero sobre todo gracias por ser mi compañero de viaje en esta aventura personal que hemos iniciamos tú y yo. Llegados al final de mi tesis, no tengo ni idea de que es lo siguiente que me depara el destino, pero sea lo que sea, solo espero poder vivirlo junto a ti.



Departament de Genètica i Microbiologia
Facultat de Biociències

Ugutx Unzueta Elorza

PhD Thesis
2013